

Overview of the genus *Briareum* (Cnidaria, Octocorallia, Briareidae) in the Indo-Pacific, with the description of a new species

Kaveh Samimi-Namin¹, Leen P. van Ofwegen¹

¹ Department of Marine Zoology, Naturalis Biodiversity Center, PO Box 9517, 2300 RA Leiden, the Netherlands

Corresponding author: Kaveh Samimi-Namin (kaveh_s_n@yahoo.com; kaveh.samimi@naturalis.nl)

Academic editor: B. W. Hoeksema | Received 31 August 2015 | Accepted 9 November 2015 | Published 28 January 2016

<http://zoobank.org/D01314A3-CC0F-40EF-BED0-1C0CAD991372>

Citation: Samimi-Namin K, van Ofwegen LP (2016) Overview of the genus *Briareum* (Cnidaria, Octocorallia, Briareidae) in the Indo-Pacific, with the description of a new species. ZooKeys 557: 1–44. doi: 10.3897/zookeys.557.6298

Abstract

The status of Indo-Pacific *Briareum* species (Cnidaria, Octocorallia, Briareidae) is reviewed by presenting their sclerite features and habitus descriptions. Following the re-examination of type material, museum specimens and newly collected specimens, a species identification key is provided. The species distributions are discussed and updated distribution ranges are depicted. Moreover, a new taxon, *B. cylindrum* **sp. n.** is described and depicted, whereas *B. excavatum* (Nutting, 1911) is synonymised with *B. stechei* (Kükenthal, 1908). *Briareum hamrum* (Gohar, 1948) is recorded from the Persian Gulf and Oman Sea for the first time. Consequently, in total four *Briareum* species are recognized in the Indo-Pacific; *B. hamrum* from the western Indian Ocean, and *B. cylindrum* **sp. n.**, *B. stechei*, and *B. violaceum* from the central and eastern Indo-Pacific region.

Keywords

Alcyonacea, Anthozoa, identification key, Oman Sea, Persian Gulf, sclerite variability, species range, synonymy

Introduction

Briareum Blainville, 1830 is the only genus in the family Briareidae with a wide distribution, occurring in both the Atlantic and the Indo-West Pacific (Fabricius and Alderslade 2001). It is zooxanthellate and therefore restricted to shallow, well-illuminated waters. It

can be found in a wide range of habitats forming different colony shapes. The single Atlantic species, *Briareum asbestinum* (Pallas, 1766) has two main colony forms, encrusting and digitate (Bayer 1961; Bilewitch 2010). The Indo-Pacific species can form encrusting colonies, finger like lobes, or cylindrical branches, which may be hollow.

Briareum has unique morphological characteristics among octocoral genera. Corals of this genus are reasonably easy to recognize due to the characteristic shape and colour of their colonies and sclerites. The majority of the sclerites are spindles, some of them branched, with low or tall, spiny tubercles arranged in relative distinct girdles. The most basal layer generally includes multiple branched, reticulate and fused forms with very tall, complex tubercles. The medulla has magenta-coloured sclerites; the cortex may have magenta or colourless sclerites (Fabricius and Alderslade 2001). Only one species, *B. violaceum* (Quoy & Gaimard, 1833) has been recorded with magenta-coloured sclerites in both layers of the coenenchyme. In the literature, specimens with tall, deep magenta coloured calyces have usually been referred to *Pachyclavularia* Roule, 1908. Fabricius and Alderslade (2001) synonymized that genus with *Briareum*. The Indo-Pacific membranous and hollow-branched forms were referred to *Solenopodium* Kükenthal, 1916a. Bayer (1961) proposed *Solenopodium* as a junior synonym of *Briareum*. For details about the status of *Briareum* species refer to van Ofwegen (2015).

These morphological characters in *Briareum* species can show high variation in response to environmental factors such as depth, water motion, light, and predator damage (West 1997). For instance, high variation in colony and sclerite sizes, polyp density, egg size, and number of eggs has been reported for *B. asbestinum* along depth gradients in the Atlantic (West et al. 1993). These morphological variation and plasticity known from this genus together with inadequacy of descriptions in the literature has resulted in obscurity of the species characters, leading to misidentifications. This uncertainty in identification becomes obvious in the biochemistry and pharmacological studies in which the identification of source organisms is of great interest. It has been proven that *Briareum* offers extensive bioactive chemical compounds with antiviral, and antimicrobial properties (Chen et al. 2006; Wang et al. 2012; Yeh et al. 2012), and it is the most important source of briarane-type metabolites among the diterpenoids isolated from octocorals (Sung et al. 2002; Hong et al. 2012). In spite of *Briareum* being a valuable and an important source of biochemical compounds, the identifications of these species usually remains unsatisfactory and uncertain. In addition to their variation in shape and the lack of accurate morphological descriptions, the extent of molecular knowledge about different species is also limited. Although molecular records from the Indo-Pacific are rare, *Briareum* is distinctly recognized as one of the basal genera in the Octocorallia phylogeny (McFadden et al. 2006). The current records suggest the existence of at least three different species of *Briareum* across the Indo-Pacific region (McFadden et al. 2011, 2014; Miyazaki and Reimer 2014; GenBank (<http://www.ncbi.nlm.nih.gov/genbank/>)). These data emphasize the need for further morphological and molecular knowledge about *Briareum* species across wider geographical areas.

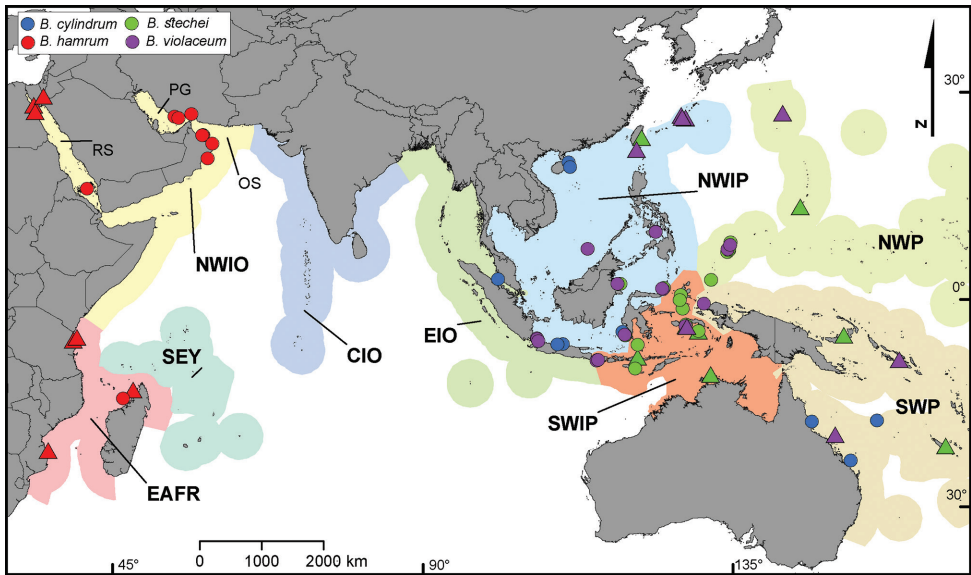


Figure 1. Distribution map of Indo-Pacific *Briareum* species based on: ● = examined material; ▲ = literature records. Colour shades on the background represent different marine regions. PG = Persian Gulf; OS = Oman Sea; RS = Red Sea; NWIO = North Western Indian Ocean; SEY = Seychelles; EAFR = East Africa; CIO = Central Indian Ocean; EIO = East Indian Ocean; SWIP = South West Indo-Pacific; NWIP = North West Indo-Pacific; NWP = North West Pacific; SWP = South West Pacific.

Here, the sclerite features and descriptions of *Briareum* species are presented based on the re-examination of type specimens, museum material, and newly collected material from the Indian Ocean and Indo-Pacific region, much of which is from the centre of maximum marine species richness, the Coral Triangle (Hoeksema 2007). An identification key to the presently recognized Indo-Pacific species is provided, a new taxon is described and two species are synonymised. Moreover, we show the variability of the sclerites among examined material and point out the difficulties, uncertainties and potential topics for further research. A distribution map of the examined material is also provided, together with all published species for the Indian Ocean and Indo-Pacific region (Figure 1). This study can be used in molecular and biochemical studies and may help coral researchers to identify *Briareum* material.

Abbreviations

NBC	Naturalis Biodiversity Center, Leiden, The Netherlands; previously National Museum of Natural History (NNM); formerly Rijksmuseum van Natuurlijke Historie (RMNH)
OCDN/OPHG	Numbers used by the Coral Reef Research Foundation, Palau
RMNH	Rijksmuseum van Natuurlijke Historie, currently NBC

UNESCO-IOC	United Nations Educational, Scientific and Cultural Organization- Intergovernmental Oceanographic Commission
UNHAS	Universitas Hasanuddin, Makassar, Indonesia
ZMA	Zoological Museum Amsterdam, Amsterdam, The Netherlands
ZMB	Zoologisches Museum Berlin, Berlin, Germany

Material and methods

All studied material is deposited in the Naturalis Biodiversity Center. All *Briareum* specimens deposited in the RMNH coelenterate collection were examined, including misidentified material. Additional specimens collected by the Coral Reef Research Foundation, Palau, were also examined.

In order to identify the material, sclerites were obtained by dissolving the tissues in 10% sodium hypochlorite, followed by rinsing in fresh water. Due to variation in size and shape of the sclerites, it is recommended to use all parts of the colony. For example, missing calyces might result in finding shorter sclerites. For scanning electron microscopy (SEM), the sclerites were carefully rinsed with double-distilled water, dried at room temperature, were mounted on a stub with double-sided carbon tape, then coated with gold-palladium (AuPd), and examined using a Jeol 6480LV SEM operated at 10 kV.

Morphological descriptions and systematic account

Class Anthozoa Ehrenberg, 1831

Subclass Octocorallia Haeckel, 1866

Order Alcyonacea Lamouroux, 1812

Family Briareidae Blainville, 1830

Genus *Briareum* Blainville, 1830

Briareum Blainville, 1830: 484

Asbestia Nardo, 1845: 106

Pachyclavularia Roule, 1908: 165

Solenopodium Kükenthal, 1916a: 174

Diagnosis. Colonies lobate, digitate or encrusting, normally with a whitish outer layer and magenta inner layer, but completely magenta or white colonies also occur. Polyps monomorphic, retractile, and without sclerites. Protruding false calyces appear in varying degrees of prominence or are not present at all. Surface layer with straight or curved spindles. Medulla with sclerites shaped like those of the surface layer but larger and coarser, and with additional branching sclerites, which can be fused. Zooxanthellate.

Distribution. The genus has been recorded from the Caribbean and the Indo-Pacific (Red Sea, Persian Gulf, Oman Sea, Arabian Sea, Australia, Indonesia, Micronesia, Taiwan, and Bonin Islands).

Type species

Briareum asbestinum (Pallas, 1766)

Alcyonium asbestinum Pallas, 1766: 344.

Briareum gorgonoideum Blainville, 1830: 484.

Ammothea polyanthes Duchassaing & Michelotti, 1860: 15, pl. 1 fig. 6.

Erythropodium marquesarum Kükenthal, 1916a: 173; 1919: 34 (Marquesas-Islands, Caribbean)

Briareum asbestinum Kükenthal, 1916b: 469, figs F–H, pl. 23 figs 1–7; Verseveldt 1940: 9, figs 2–4; Bayer 1961: 62, fig. 11; Bilewitch et al. 2010: 93.

Distribution. Caribbean, Gulf of Mexico.

Key to the Indo-Pacific *Briareum* species

- 1 Coenenchymal spindles up to 0.45 mm long with prominent, sparsely set tubercles *B. hamrum*
- Coenenchymal spindles longer than 0.45 mm long with low, closely set tubercles..... **2**
- 2 Many cylinders present in coenenchyme, with dense tuberculation *B. cylindrum* sp. n.
- Only spindles present in coenenchyme **3**
- 3 Many spindles with pointed ends in coenenchyme, all sclerites magenta..... *B. violaceum*
- Many spindles with blunt ends in coenenchyme, sclerites magenta and colourless..... *B. stechei*

Briareum cylindrum sp. n.

<http://zoobank.org/CDFC1779-62C2-4F27-943C-329D9F28BC3C>

Figures 2A–D, 3–7

Material examined. *Holotype*: RMNH Coel. 34193, Malaysia, northwest of channel running due west out of SMART resort, about 100 m away, lobster wall, depth 11 m, 8 July 2004, coll. Nicolas J. Pilcher (OPHG1352–C) (id. *B. excavatum*).

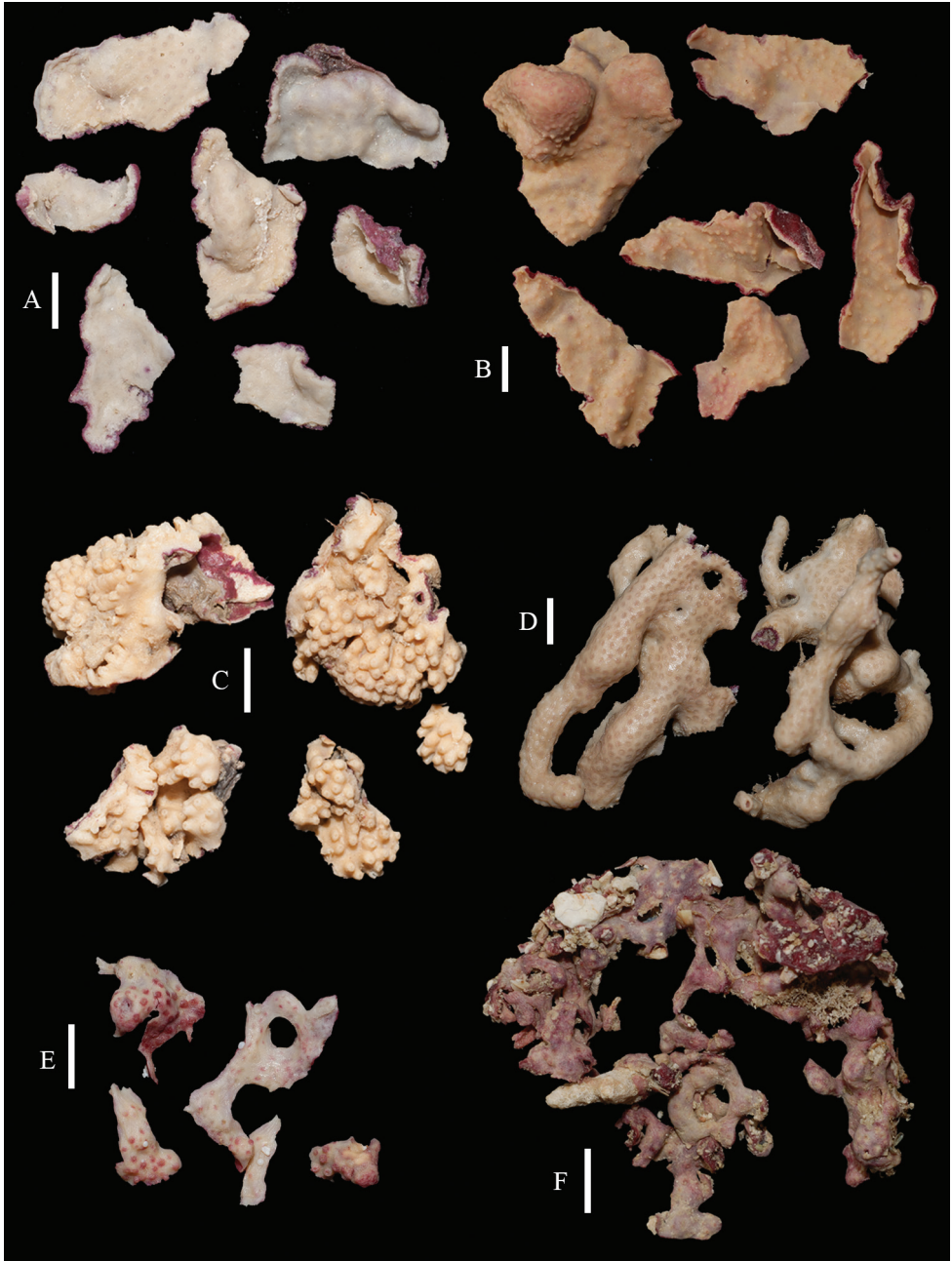


Figure 2. Colonies of *Briareum*: **A–D** *B. cylindrum* **A** RMNH Coel. 34193 (holotype) **B** RMNH Coel. 13747 **C** RMNH Coel. 32569 **D** RMNH Coel. 41443 **E–F** *B. hamrum* **E** RMNH Coel. 6809 **F** RMNH Coel. 41407. Scale bars: 1 cm.

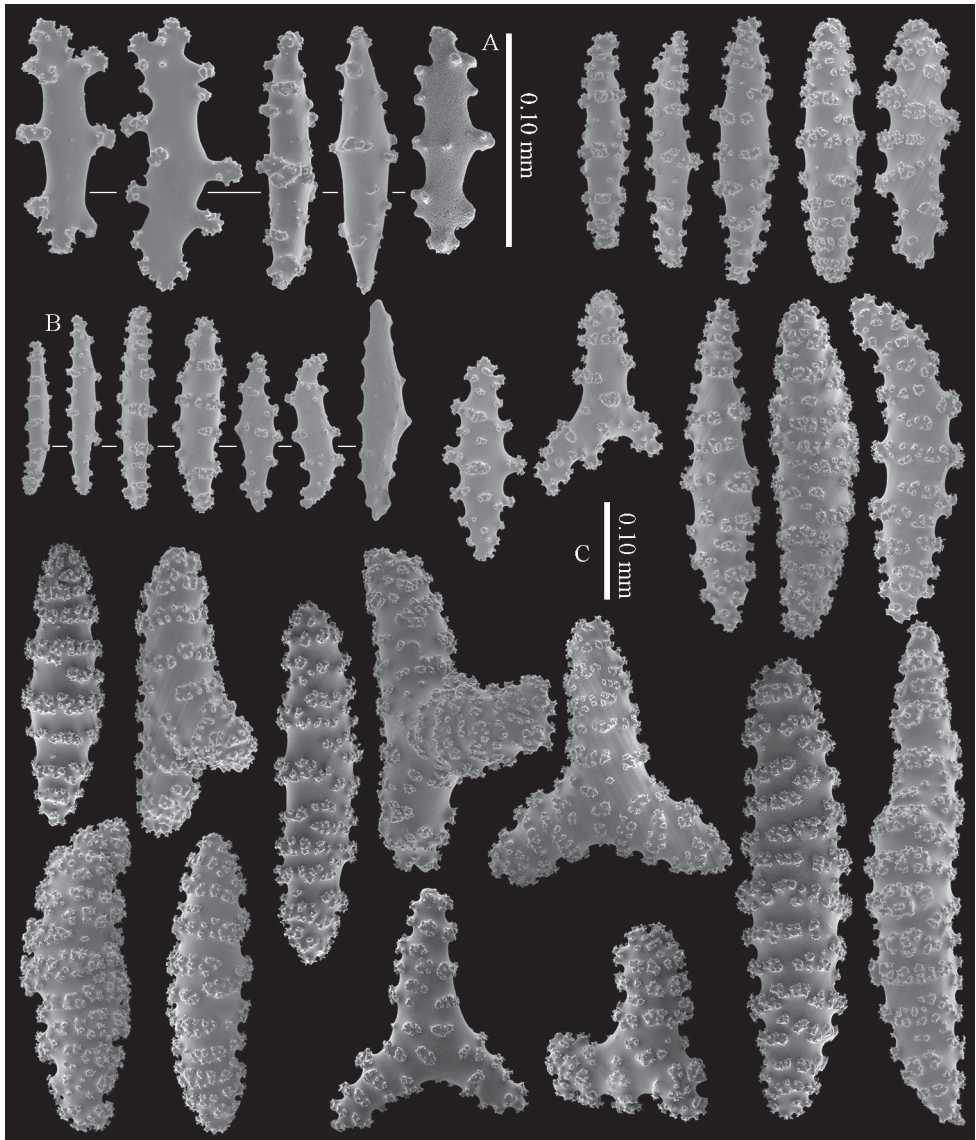


Figure 3. *Briareum cylindrum* sp. n., holotype, RMNH Coel. 34193 **A–B** sclerites of top calyx **C** cortex sclerites. Scale bar of **C** also applies to **B**.

Paratypes: RMNH Coel. 2241, Indonesia, Java, coll. C.G.C. Reinwardt (id. *B. stechei*); RMNH Coel. 2242, 1 microscope slide, Indonesia, Java, coll. C.G.C. Reinwardt, (id. *B. stechei*); RMNH Coel. 11655, Australia, Feather Reef, seaward slope, 17°33'S, 146°23'E, depth 0–10 m, 6 July 1975, coll. R.N. Garrett (id. *B. stechei*); RMNH Coel. 11797, Australia, Queensland, Great Barrier Reef, Heron Island, on side of Bommie, 15 m depth, 20 July 1973, coll. N. Coleman (id. *B. stechei*); RMNH Coel. 13747, Australia, Coral

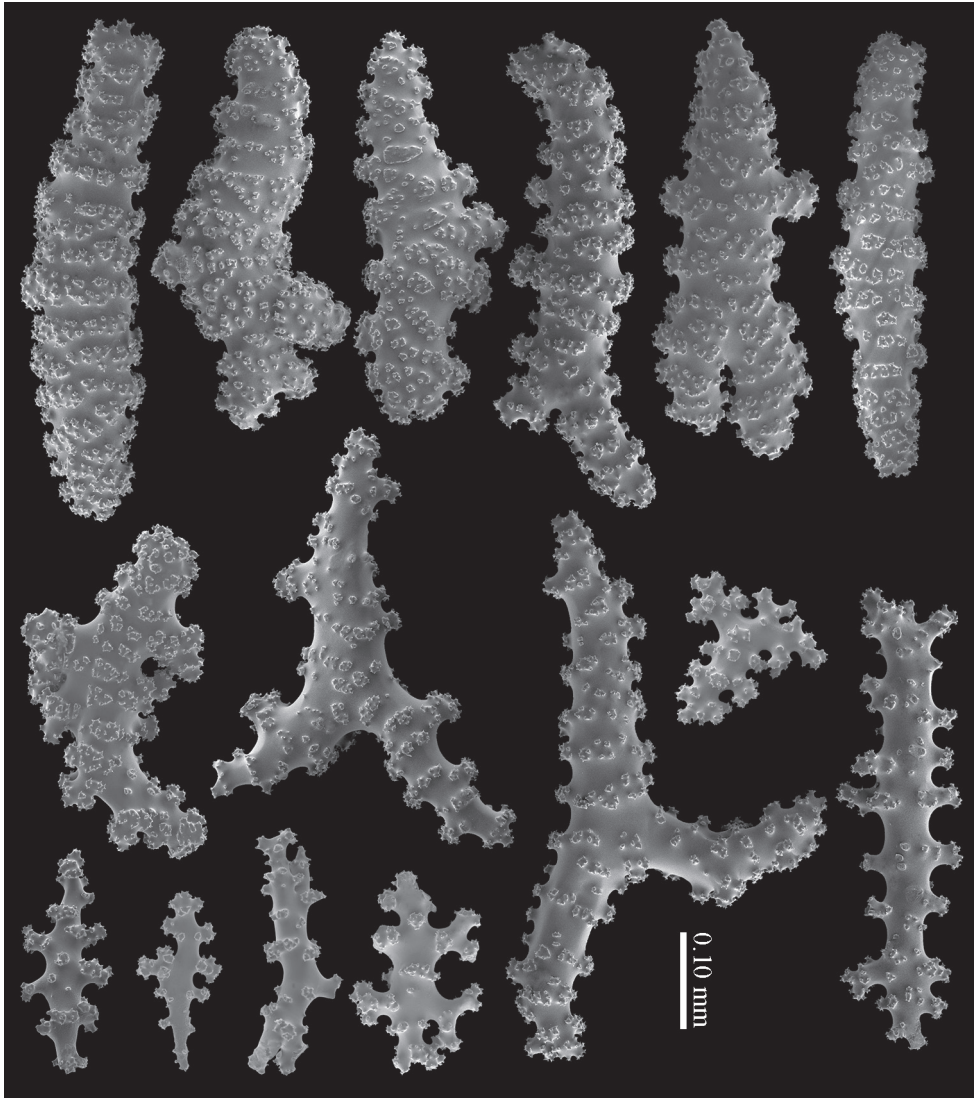


Figure 4. *Briareum cylindrum* sp. n., holotype, RMNH Coel. 34193, medullar sclerites.

Sea, Mellish Reef, depth 8 m, encrusting on coral block, 1 May 1979, coll. N.L. Bruce, aboard R/V *Lady Basten* (id. *B. stechei*); RMNH Coel. 32569, China, Hainan Island, Xidao, 50 km from Haikou City; depth 15 m. October 2003, coll. Wenhan Lin (HSD 9); RMNH Coel. 32570, China, Hainan Island, Xidao, 50 km from Haikou City; depth 15 m. October 2003, coll. Wenhan Lin (HSE 25); RMNH Coel. 41443, Buginesia Progr. UNHAS-NNM 1994/1995, SUL.BCW, Indonesia, southwest Sulawesi, Spermonde Archipelago, west of Barang Caddi (=11 km Northwest of Ujung Pandang = Makassar), 5°05'S, 119°19'E, coral reef, SCUBA diving, 4 May 1994, coll. B.W. Hoeksema; RMNH

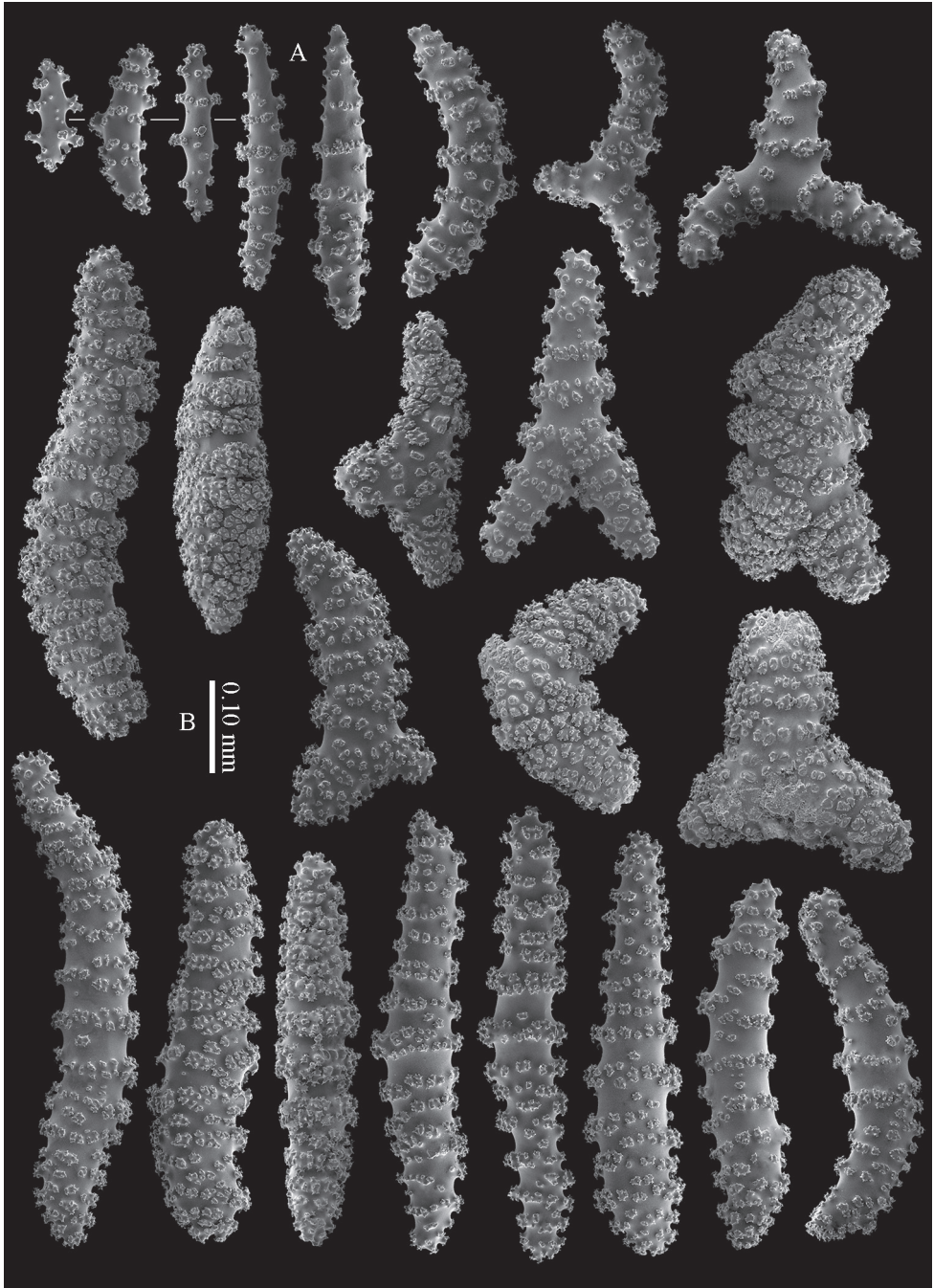


Figure 5. *Briareum cylindrum* sp. n., paratype, RMNH Coel. 41443; **A** sclerites of coenenchyme next to polyp openings **B** cortex sclerites.

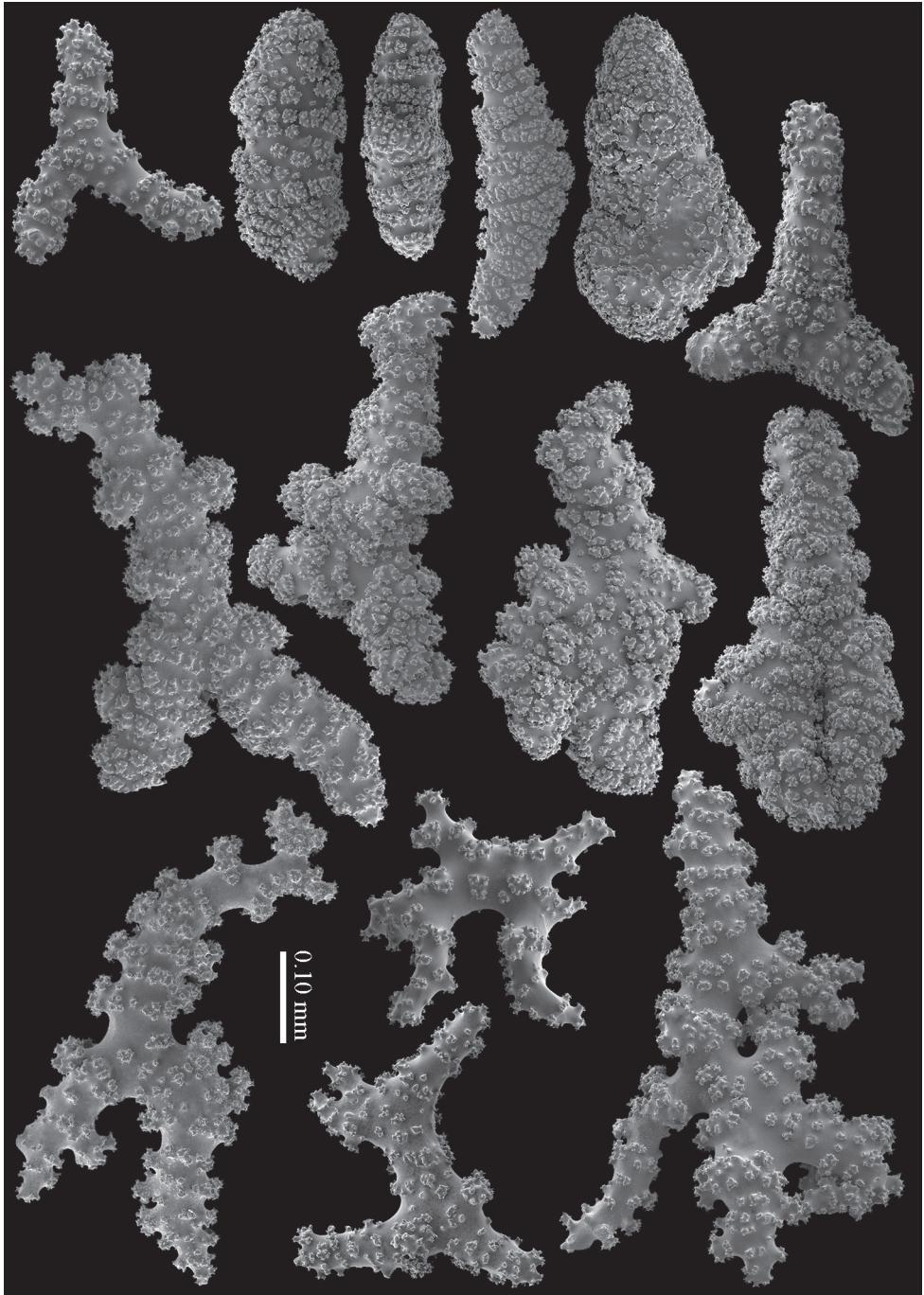


Figure 6. *Briareum cylindrum* sp. n., paratype, RMNH Coel. 41443, medullar sclerites.

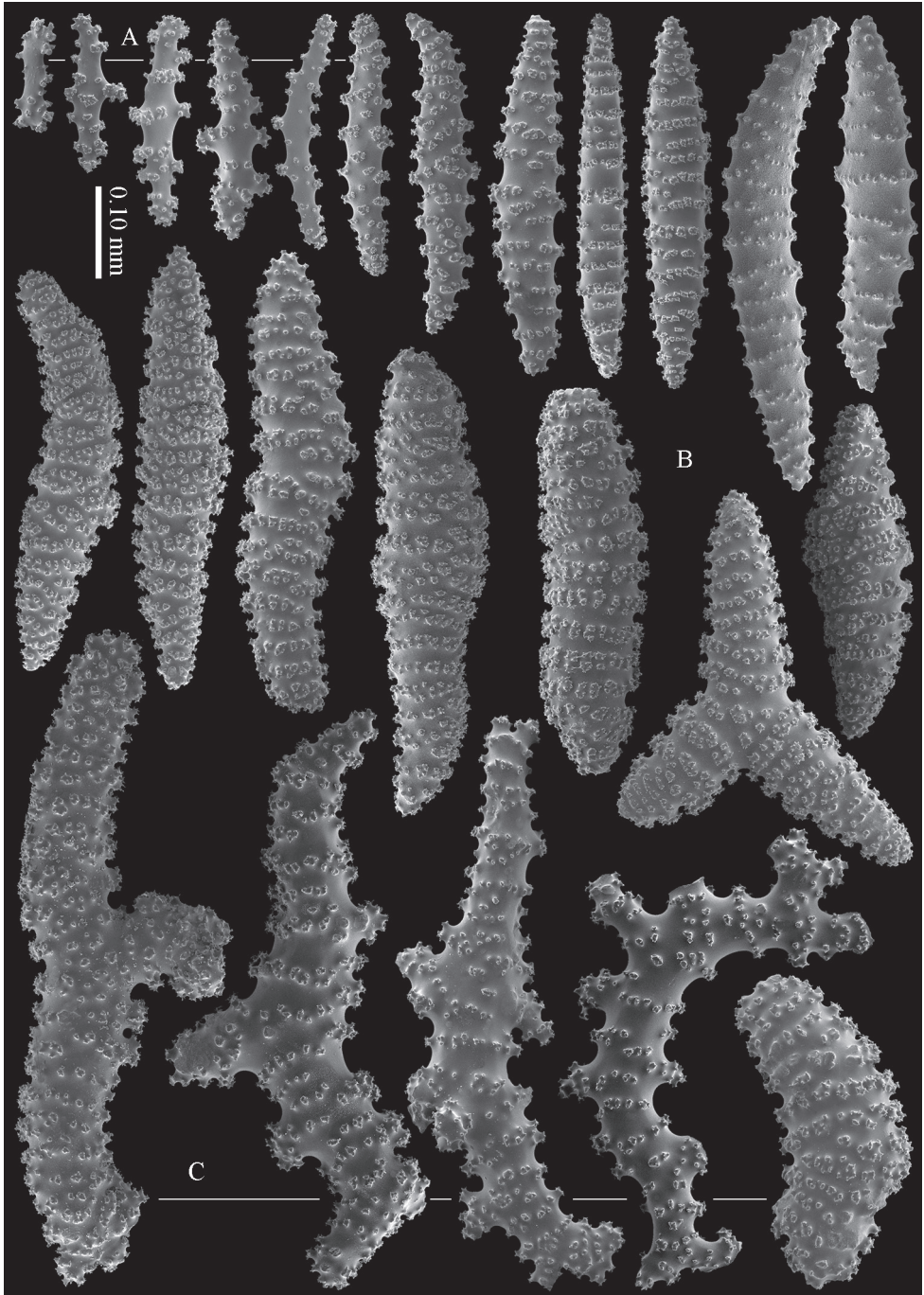


Figure 7. *Briareum cylindrum* sp. n., paratype, RMNH Coel. 32569; **A** sclerites of top calyx **B** cortex sclerites **C** medullar sclerites.

Coel. 41444, Buginesia Progr. UNHAS-NNM 1994/1995, SUL.KAPN, Indonesia, southwest Sulawesi, Spermonde Archipelago, north of Kapoposang Isl (= 66 km NW of Ujung Pandang = Makassar), 4°40'S, 118°57'E, coral reef, SCUBA diving, coll. B.W. Hoeksema; RMNH Coel. 41446, CEB.05, Philippines, Cebu Strait, west of Bohol, west side of Cabilao Island, south side fish sanctuary, 9°52.60'N 123°45.61'E, dense algae-covered reef flat to 4 m depth, vertical wall with caves to 45 m, SCUBA diving, 8 November 1999, coll. L.P. van Ofwegen; RMNH Coel. 41447, CEB.11, Philippines, Cebu Strait, west of Bohol, east side of Cabilao Island, south of Cambacis, 9°52.92'N 123°47.37'E, to 6 m patchy reef with algae, below steep slope with caves, snorkelling and SCUBA diving, 14 November 1999, coll. L.P. van Ofwegen.

Description. The holotype consists of several fragments of an encrusting colony, the largest being 4 by 1.5 cm in diameter (Figure 2A) with white surface and magenta underside. Calyces hardly projecting.

The calyces contain colourless, flattened rods with prominent simple tubercles (Figure 3A, B). These rods are up to 0.20 mm long. The cortex contains colourless spindles, cylinders, and tripoids (Figure 3C). All these forms have complex tubercles, often arranged in girdles. These sclerites can be up to 0.60 mm long but most are only 0.30 mm long. The medulla contains magenta spindles and branched spindles with simple or complex tubercles (Figure 4). These sclerites are 0.20–0.60 mm long. They can be fused into small clumps.

Etymology. The Latin “cylindrum”, cylinder, refers to the shape of the sclerites.

Morphological variation. RMNH Coel. 13747, RMNH Coel. 32569, RMNH Coel. 41443 and RMNH Coel. 41444 have distinctly longer sclerites with more complex tubercles (Figs 5–7). RMNH Coel. 13747 has slightly raised calyces (Figure 2B); RMNH Coel. 32569 has distinct calyces (Figure 2C), RMNH Coel. 41443 has no calyces at all (Figure 2D).

Remarks. *Briareum cylindrum* mostly resembles *B. stechei* but differs in having many cylinders with complex tubercles in the coenenchyme.

Distribution. Australia, Coral Triangle, China. Depth 0–15 m.

Briareum hamrum (Gohar, 1948)

Figures 8–10, 2E–F, 11A–B, 26A–B

? *Symphodium punctatum* May, 1898: 11 (Tumbatu, Zanzibar); Thomson and Henderson 1906: 408, pl. 29 fig. 9 (Chuaka, Tanzania); Tixier-Durivault 1966: 104, figs 96–97 (Madagascar).

? *Symphodium splendens* Thomson & Henderson, 1906: 409, pl. 29 fig. 8 (Chuaka, Tanzania).

? *Alcyonium (Erythropodium) contortum* Kükenthal, 1906: 50, pl. 7 figs 34–36, pl. 8 figs 37–38 (Red Sea, Tor, Jimschi).

? *Solenopodium contortum* Kükenthal, 1919: 41; Stiasny 1937: 10, fig. B (re-examination type).

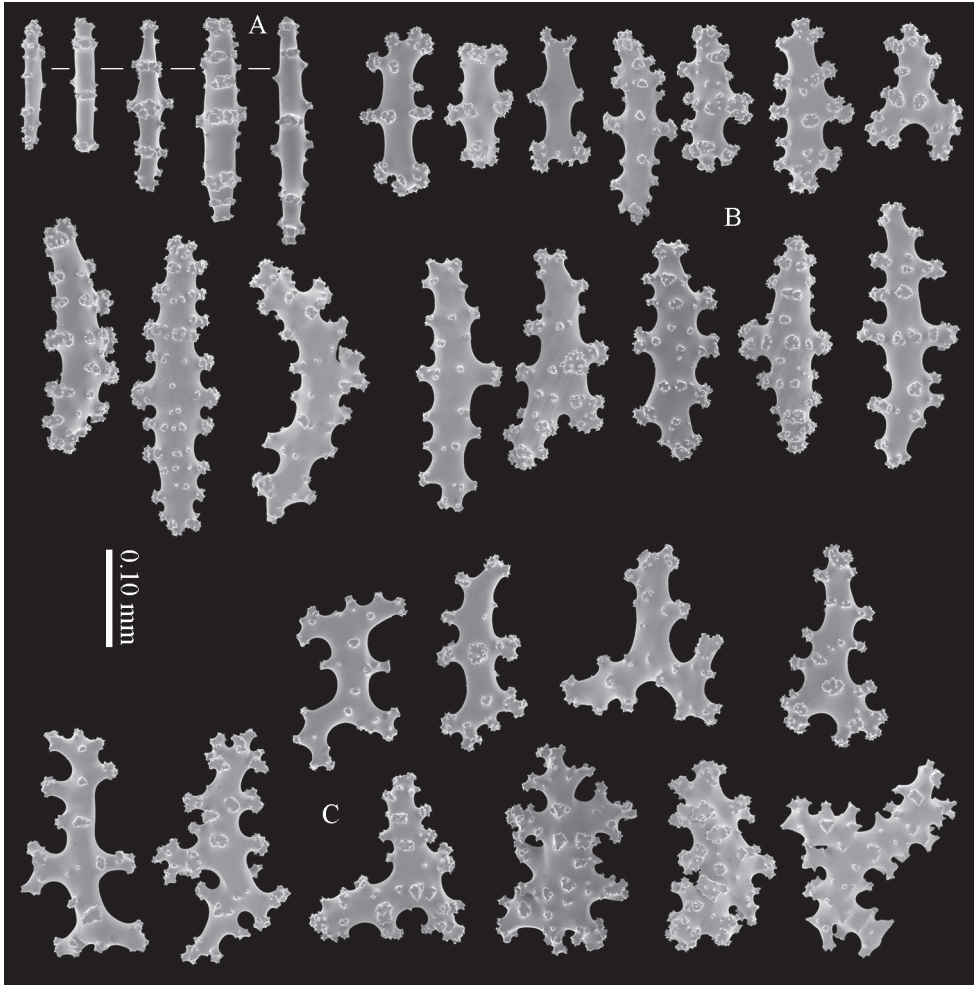


Figure 8. *Briareum hamrum* (Gohar, 1948), RMNH Coel. 6809; **A** sclerites of top calyx **B** cortex sclerites **C** medullar sclerites.

Clavularia hamra Gohar, 1948: 4, figs 1–5 (Hurghada, Red Sea); Verseveldt 1970: 209 (Eilat).

Solenopodium violaceum Broch & Horridge, 1956: 157 (Hurghada, Red Sea).

Briareum hamrum; Alderslade 2000: 246; Benayahu et al. 2003: 51 (Bazaruto Island, Mozambique).

Briareum hamra [sic]; Alderslade and McFadden 2007: 42.

Material examined. RMNH Coel. 6809, Red Sea, coll. L.F. Fishelson, NS 6468, det. J. Verseveldt; RMNH Coel. 41406, Madagascar, Tuléar, coll. Nicole Gravier-Bonnet (179), 1967–69, don. H. Zibrowius, Centre d’Oceanologie de Marseille, Station Marine d’Endoume; RMNH Coel. 41407, Iran, Persian Gulf, north of Kish

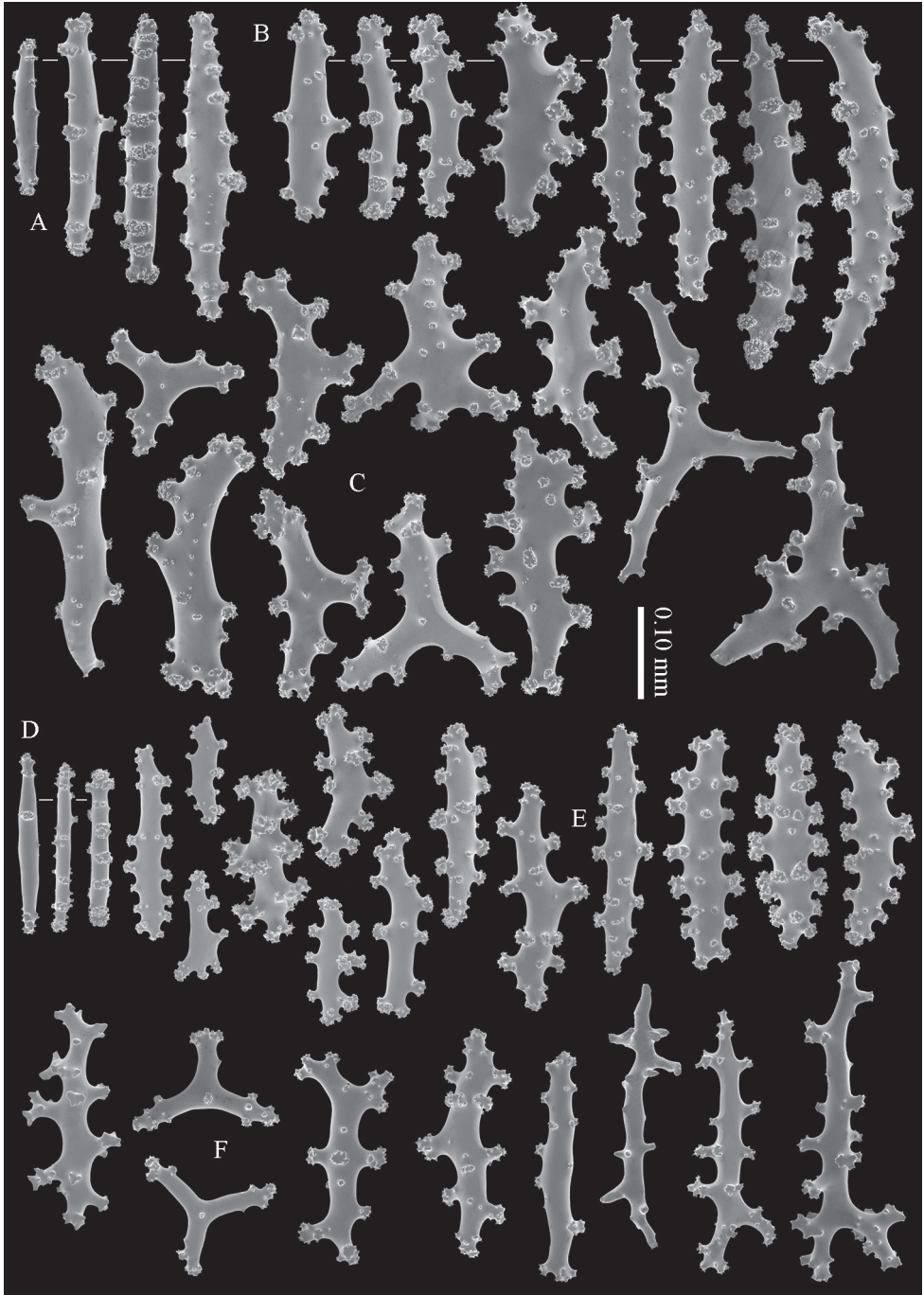


Figure 9. *Briareum hamrum* (Gohar, 1948), RMNH Coel. 41407; **A** sclerites of top calyx **B** cortex sclerites **C** medullar sclerites; RMNH Coel. 41409 **D** sclerites of top calyx **E** cortex sclerites **F** medullar sclerites.

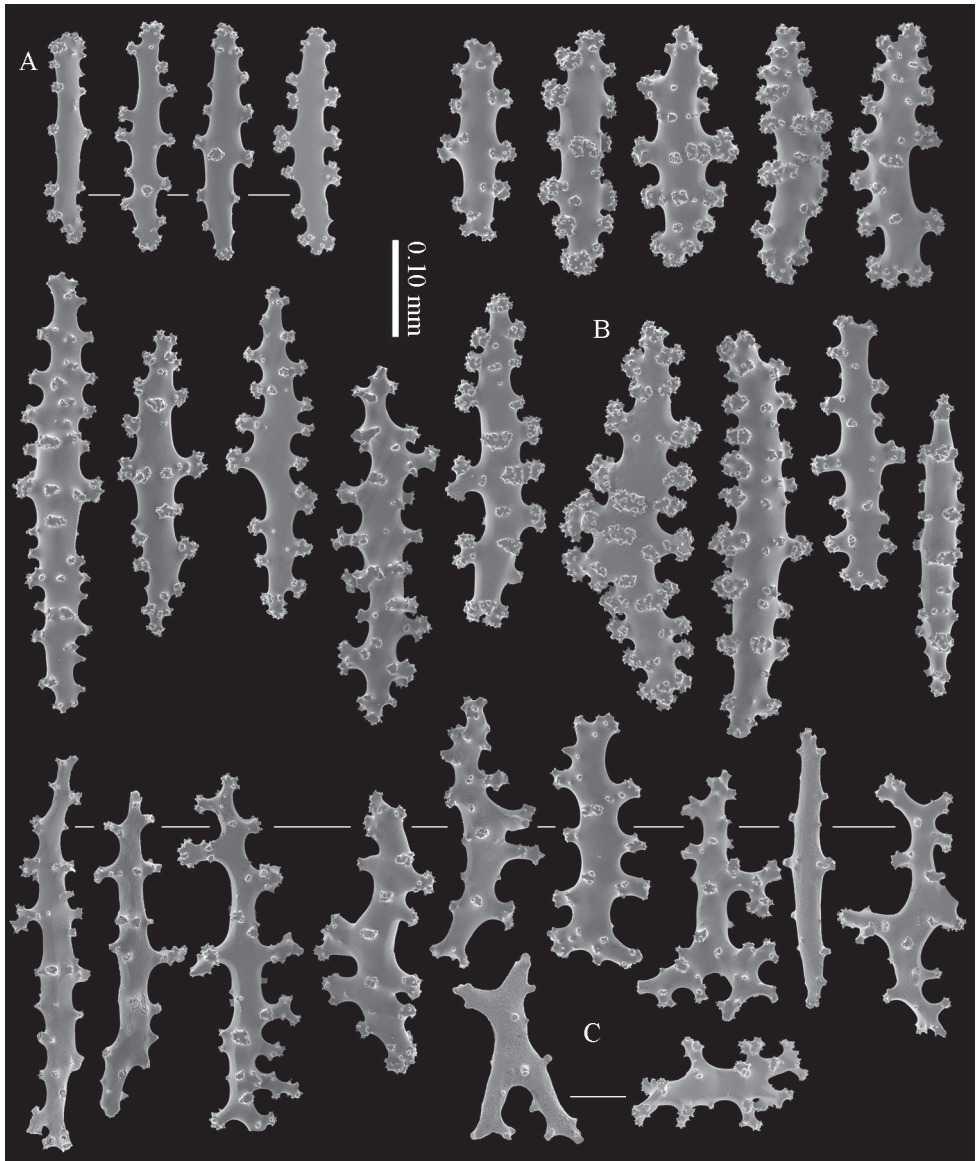


Figure 10. *Briareum hamrum* (Gohar, 1948), RMNH Coel. 41410; **A** sclerites of top calyx **B** cortex sclerites **C** medullar sclerites.

Island, 26°34.512'N 53°59.320'E, 10 m depth, coll. K. Samimi-Namin, 1 October 2009; RMNH Coel. 41408, Iran, Strait of Hormuz, Persian Gulf, north of Larak Island, 26°53.304'N 56°23.769'E, depth 12 m, coll. K. Samimi-Namin, 17 February 2009; RMNH Coel. 41409–41411, Oman, Daymaniyat Islands, 23°51.965'N 58°5.606'E, coll. K. Samimi-Namin; RMNH Coel. 41412, Persian Gulf, north of Farur Island, depth 12–15 m, 10 February 2010, coll. K. Samimi-Namin; RMNH

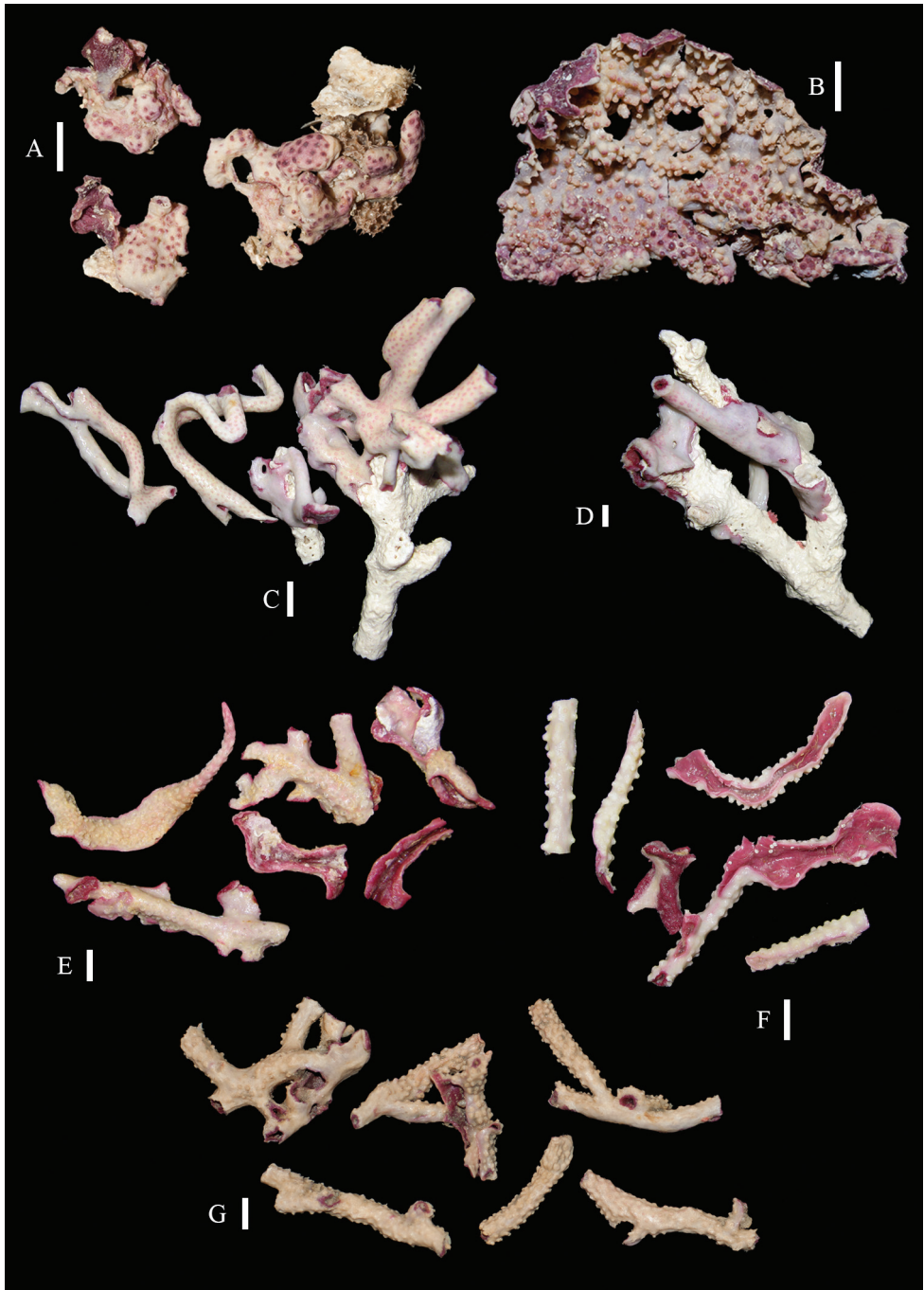


Figure 11. **A–B** Colonies of *Briareum hamrum*; **A** RMNH Coel. 41409 **B** RMNH Coel. 41410 **C–D** *Briareum stechei* **C** ZMB 5828, holotype of *Erythropodium stechei* **D** ZMB 5816 **E–F** *Solenopodium stechei* var. *novaepomeraniae* **E** ZMB 5016 **F** ZMB 5854 **G** ZMA 3410, syntype of *B. excavatum*. Scale bars: 1 cm.

Coel. 41413, Oman, Daymaniyat Islands, 23°51.720'N 58°6.253'E, depth 18 m, coll. K. Samimi-Namin, 23 April 2011; RMNH Coel. 41414, Oman, Daymaniyat Islands, 23°51.720'N 58°6.253'E, depth 18 m, coll. K. Samimi-Namin, 23 April 2011; RMNH Coel. 41415, Oman, Daymaniyat Islands, 23°51.720'N 58°6.253'E, depth 18 m, coll. K. Samimi-Namin, 23 April 2011.

Diagnosis. Calyx with straight spindles containing small tubercles arranged in transverse rows and flattened spindles (Figure 8A). Cortex with straight or bent spindles with complex tubercles (Figure 8B). Coenenchymal sclerites 0.10–0.35 mm long. Medulla additionally has branched sclerites with simple or complex tubercles (Figure 8C). These sclerites are slightly shorter, up to 0.30 mm long. Sclerites of the surface layer are colourless; interior sclerites are magenta.

Remarks. Alderslade (2000) referred *Clavularia hamra* Gohar, 1948 to *Briareum*, consequently the species name had to be changed to *hamrum*.

Gohar (1948: 10) compared his *Clavularia hamra* with both *Sympodium punctatum* May, 1898 and *S. splendens* Thomson & Henderson, 1906, and noticed their close resemblance. According to Gohar (1848), *S. punctatum* differs in having sclerites up to 0.266 mm long while they are up to 0.35 mm long in *C. hamra*. *Sympodium splendens* differs in having two rows of pinnules on either side of the tentacles, each row consisting of 20–24 pinnules, while in *C. hamra* there is only one row of 16–22 pinnules, which are much longer. However, an odd second row of 1–3 pinnules can be present in *C. hamra*. Furthermore, *C. hamra* has no triradiate or tetradiate sclerites, described for *S. splendens*. Next to the radiates Thomson and Henderson (1906) described the sclerites to be straight and curved spindles, up to 0.4 mm long. From our material and findings of Prof. Y. Benayahu (see Alderslade 2000: 246) it seems only one *Briareum* species is present in the Red Sea and the western Indian Ocean. Consequently, the correct name should be the oldest available, *Briareum punctatum* May, 1898, but the type material of *B. punctatum* is missing. As we had no material from its type locality, Zanzibar, we could not designate a proper neotype yet. As the species was never again found in Zanzibar we still have some doubts about its identity and thus defer to *B. hamrum* for the moment. Notably, also the type material of *Sympodium splendens*, *Alcyonium (Erythropodium) contortum* and *Briareum hamrum* seems to be missing.

This is the first record of a *Briareum* species from the Persian Gulf, and Oman Sea (see Samimi-Namin and van Ofwegen 2009, 2012).

Morphological variation. RMNH Coel. 41407 (Figure 2F) from the Persian Gulf differs from the above described Red Sea specimen. It has longer sclerites (up to 0.40 mm long; Figure 9B) and more slender interior branched bodies (Figure 9C). RMNH Coel. 41410 (Figure 11A) from Oman has even longer sclerites than the Persian Gulf specimen (up to 0.45 mm long; Figure 10); it is the only specimen having long calyces. RMNH Coel. 41409 (Figure 11B), also from Oman, has sclerites (Figure 9D–F) with the same size as the Red Sea specimen, but the slender interior branched bodies as the Persian Gulf and other Oman specimen. RMNH Coel. 41412 has completely colourless sclerites, however, the colour of live specimens was similar to others.

The shape of the colonies in the examined material showed variation, from completely encrusting to somewhat having branches and an undulated surface.

Colour. The living colonies were cream with magenta tints in some parts of the colony. Polyps were dark green to brown, brown pinnules, white oral disk and white line that continues along the tentacles (Figure 26A–B)

Distribution. Red Sea, East Africa, Oman Sea, Arabian Sea, Persian Gulf.

***Briareum stechei* (Kükenthal, 1908)**

Figures 11C–G, 12–18, 26C–D

Erythropodium stechei Kükenthal, 1908: 19 (Banda); 1919: 38.

Suberia excavata Nutting, 1911: 14, pl. 3 fig. 2, 2a, pl. 11 fig. 4 (Ambon).

Solenopodium excavatum; Kükenthal 1919: 42; 1924: 13; Stiasny 1937: 12, Pl. 1 figs 4–5, fig. C (re-examination type); Verseveldt 1940: 32–37.

Solenopodium stechei var. *novaepommeraniae* Kükenthal, 1919: 901 (New Britain); 1924: 13.

Solenopodium stechei; Aurivillius 1931: 9 (Timor); Stiasny 1937: 17, pl. 1 figs 1–3, fig. E (re-examination syntype ZMB 5828); Macfadyen 1936: 67 (Australia); Tixier-Durivault 1970: 325 (New Caledonia).

Briareum excavatum; Benayahu 1997: 238 (Guam); Erhardt and Baensch 2000: 220 (life image, RMNH Coel. 24018); Benayahu et al. 2004: 551, fig. 3 (Taiwan).

Briareum stechei; Grasshoff 1999: 6, fig. 5 (New Caledonia).

Briareum [sic] *excavatum* Benayahu 2002: 20 (Ryukyu Archipelago, Japan).

Briareum cf. *stechei*; Alderslade and McFadden 2007: 41, fig. 10B.

Material examined. ZMB 5828, holotype *Erythropodium stechei*: Banda Island (Moluccas), litoral, leg. Steche; ZMB 5816, Ambon (Moluccas), litoral, leg. Steche; ZMB 5016, 5854, holotype *Solenopodium stechei* var. *novaepommeraniae*, Neupommern, litoral, leg. Schoede; ZMA 3410, syntype *B. excavatum*; Siboga Exped. stat. 142, Maluku, anchorage off Laiwui, depth 23 m, Hensen vertical net, tow net, dredge; ZMA 3489, same data as ZMA 3410; RMNH Coel. 5837, Indonesia, Laiwui, Obi Major St. 142 Siboga expedition (id. *Solenopodium excavatum*); RMNH Coel. 18416, Indonesia, Celebes, Westside Samalona, 18 m depth, 18 September 1980, coll. H. Moll (id. *B. excavatum*); RMNH Coel. 41416, Indonesian-Dutch Snellius II Exp., Sta. 4.052, NE coast of Sumba, E of Melolo, 09°55'S, 120°45'E, edge of extensive, gently sloping reef flat, SCUBA diving, snorkelling, depth 10–15 m, 13/14 September 1984; RMNH Coel. 41417, Indonesian-Dutch Snellius II Exp., Sta. 4.222, northeast Taka Bone Rate (tiger islands), south of Pulau Tarupa Kecil, rectangular dredge, depth 58 m, 06°31.5'S, 121°08.0'E, sandy bottom with gorgonians antipatharians, sponges, 14 October 1984; RMNH Coel. 41418, Buginesia Progr. UNHAS-NNM 1994/1995, Sta. SUL.SAM S, Indonesia, southwest Sulawesi, Spermonde Archipelago, south of Samalona Isl. (= 7.5 km W of Ujung Pandang = Makassar), 5°07'S, 119°20'E; coral reef; SCUBA diving, 31 May 1994, coll. B.W. Hoeksema; RMNH Coel. 41419, BUN.06, Indonesia, North Sulawesi, Tanjung Totowitan main coast, steep slope fringing

reef, 01°45'N 124°58.500'E, SCUBA diving, 6 May 1998, coll. B.W. Hoeksema and L.P. van Ofwegen; RMNH Coel. 24018, Indonesia, Banda Island, depth 12 m, 30 September 1998, coll. H. Erhardt, dry material, det. L.P. van Ofwegen (id. *B. excavatum*); RMNH Coel. 41420–21, RUM.20, Indonesia, Moluccas, Ambon, Hitu, north coast, Hitulama; 20 November 1990, coll. C.J.H.M Fransen; RMNH Coel. 41422, BUN.14, Sta.14: Indonesia, N. Sulawesi, Bunaken Park, NE Bunaken Island, steep slope, 124°46'30"E 01°36'30"N, SCUBA diving, 10. May 1998; Coll. B.W. Hoeksema; RMNH Coel. 41423, CEB.08, Philippines, Cebu Strait, west of Bohol, north side of Cabilao Island, Cabacungan Point, 9°51.55'N 123°45.95'E, reef edge with dense coral cover, overhanging wall with caves, snorkelling and SCUBA diving, 11 November 1999, coll. L.P. van Ofwegen; RMNH Coel. 41424, BER.16, Indonesia, northeast Kalimantan, Berau Islands, Maratua Island, NE-side, 2°17.487'N 118°35.483'E, SCUBA diving, 10 October 2003, depth 28 m, coll. L.P. van Ofwegen and M. Slierings; RMNH Coel. 38607, Sabah, Layang Layang atoll, outer reef on east end of atoll, 07°22.69'N 113°52.23'E, depth 10 m, 13 October 2006 (0CDN 9322–R); RMNH Coel. 39998, Palau, Angaur, northeast side of island, reef sloping 30° to sandy slope below 200 ft., reef top, rock, depth 8 m, 06°55.36'N 134°08.68'E, 21 June 2008 (0CDN9600–T); RMNH Coel. 40023; Palau, SW Islands, Helen Reef lagoon, reef of conservation area main lagoon marker, lagoon patch reef, large with shallower reef area, sand/rubble/coral patches, 16 September 2008, depth 14 m, lagoon Pinnacle, Rock, 02°52.860'N 131°46.510'E (0CDN9778–N); RMNH Coel. 40078, Palau, Velasco Reef north of Kayangel, central 'lagoon' area; pinnacle/large patch reef 15 m depth in mid 'lagoon' of Velasco reef Lagoon pinnacle, rock depth 15 m, 08°17.290'N 134°38.200'E; 26 June 2009 (0CDN9988–Q); RMNH Coel. 41425, Exp. Indonesia, Ternate – Halmahera. 2009, TER.15, Indonesia, Halmahera, Tidore, Cobo, 0°45.312'N 127°24.397'E, 01 November 2009; RMNH Coel. 40884, PAL.168, Republic of Palau, Koror, Wonder Channel, 7°10.869'N 134°21.612'E, depth 19.6 m, 21 May 2010, coll. C.S. McFadden; RMNH Coel. 40885, PAL.173, Republic of Palau, Koror, Wonder Channel, 7°10.869'N, 134°21.612'E, depth 18.8 m, 21 May 2010, coll. C.S. McFadden; RMNH Coel. 40886, PAL.218, Republic of Palau, Koror, Pinchers, 7°20.402'N 134°25.682'E, depth 7.3 m, 22 May 2010, coll. C.S. McFadden; RMNH Coel. 40887, PAL.314, Republic of Palau, Koror, Turtle Cove, 7°05.078'N 134°15.730'E, depth 52 m, 24 May 2010, coll. C.S. McFadden; RMNH Coel. 41445, CEB.05, Philippines, Cebu Strait, W of Bohol, west side of Cabilao Island, south side fish sanctuary, 9°52.60'N 123°45.61'E, dense algae-covered reef flat to 4 m, vertical wall with caves to 45 m, SCUBA diving, 8 November 1999, coll. L.P. van Ofwegen; RMNH Coel. 41448, BER.03, Indonesia, northeast Kalimantan, Berau Islands, Derawan Island, southern side (jetty Derawan Dive Resort), 2°17.055'N 118°14.813'E, SCUBA diving, 22 October 2003, depth 20 m, coll. L.P. van Ofwegen and M. Slierings; RMNH Coel. 41615, TER.32, Indonesia, Pulau Pulau Gura Ici, east Pulau Gura Ici, 0°1.288'S, 127°14.287'E, 10 November 2009, depth 18 m, coll. B.T. Reijnen.

Diagnosis. Cortex with straight or bent spindles with simple or complex tubercles mostly arranged in transverse rows (Figure 12A). These cortex sclerites are 0.10–0.75 mm long. The medulla additionally has branched bodies with simple or complex tubercles (Figure 12B). These sclerites are slightly shorter, up to 0.60 mm long. Sclerites of surface layer colourless, interior sclerites magenta.

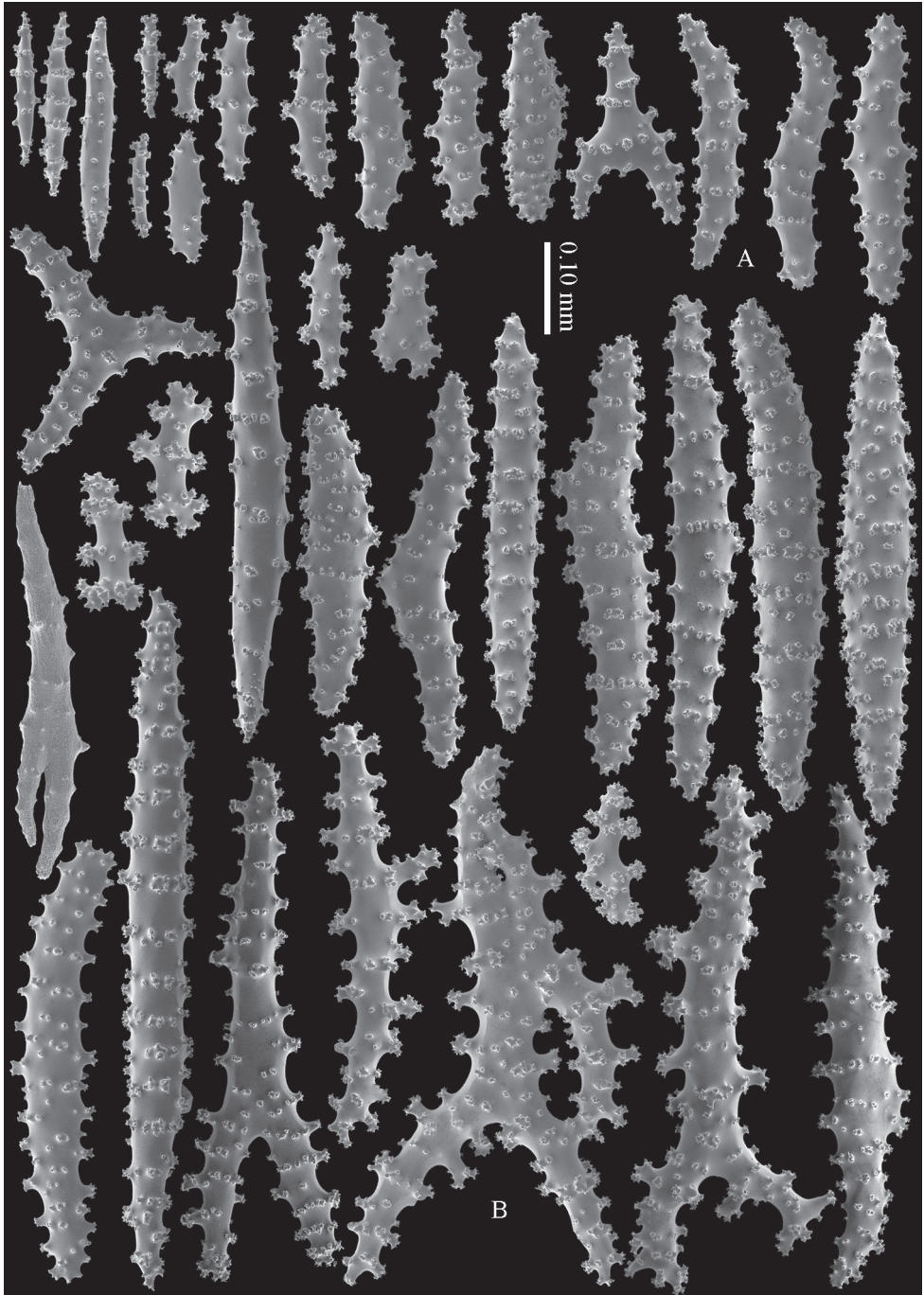


Figure 12. *Briareum stechei* (Kükenthal, 1908), ZMB 5828, holotype; **A** cortex sclerites **B** medullar sclerites.

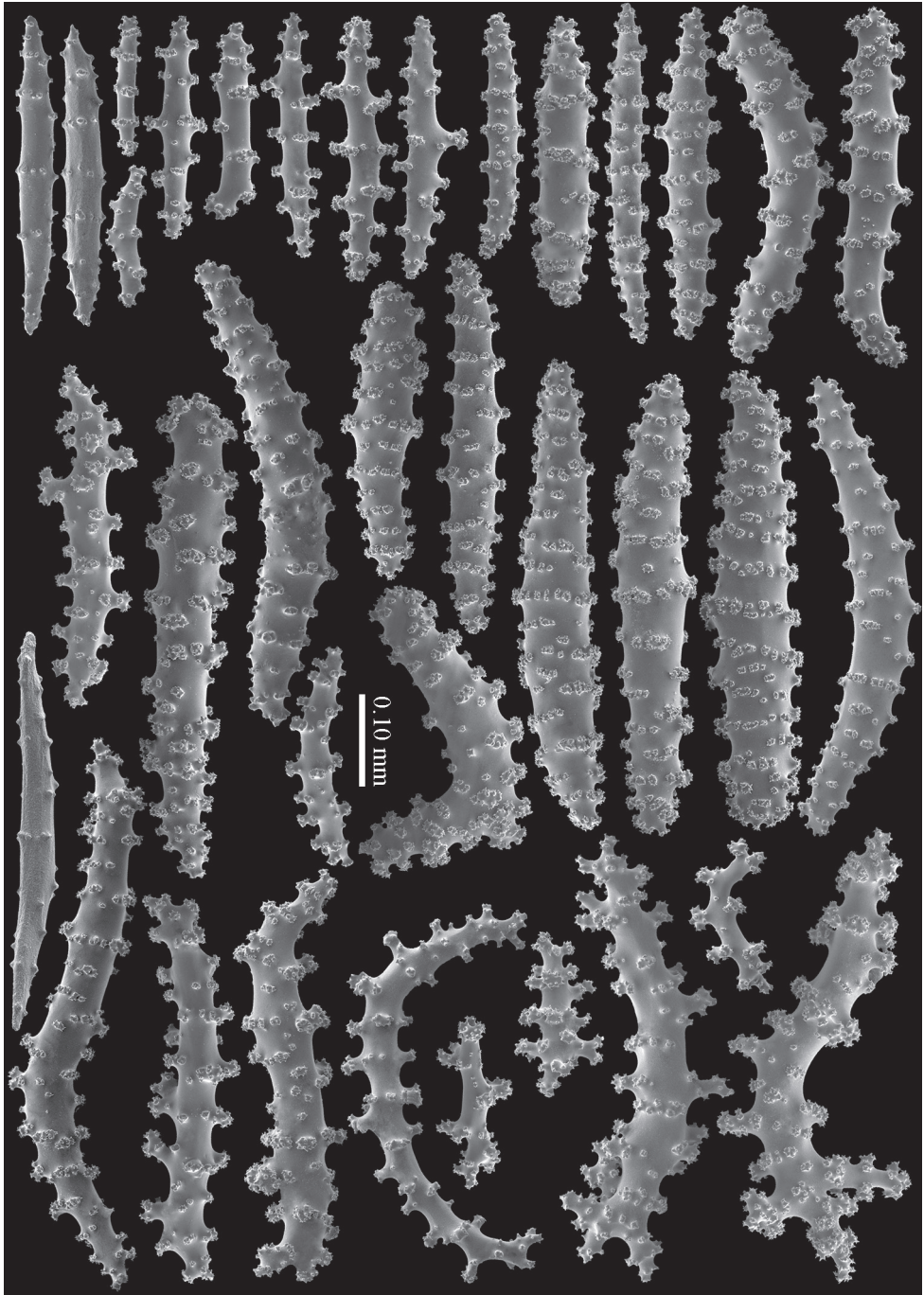


Figure 13. *Briareum stechei* (Kükenthal, 1908), ZMA 3410, syntype of *B. excavatum*; **A** cortex sclerites
B medullar sclerites.

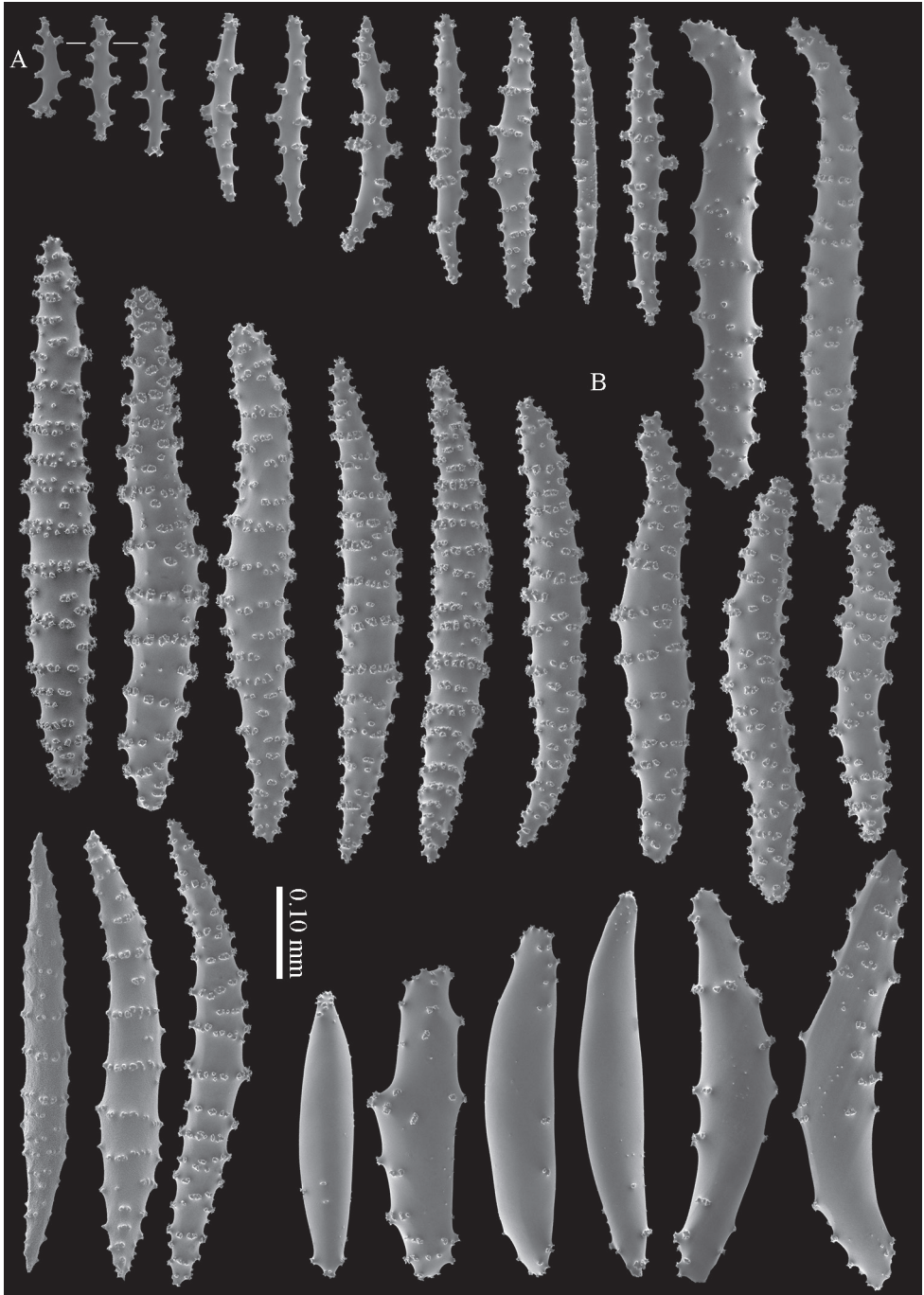


Figure 14. *Briareum stechei* (Kükenthal, 1908), RMNH Coel. 40023; **A** sclerites of top calyx **B** cortex sclerites.

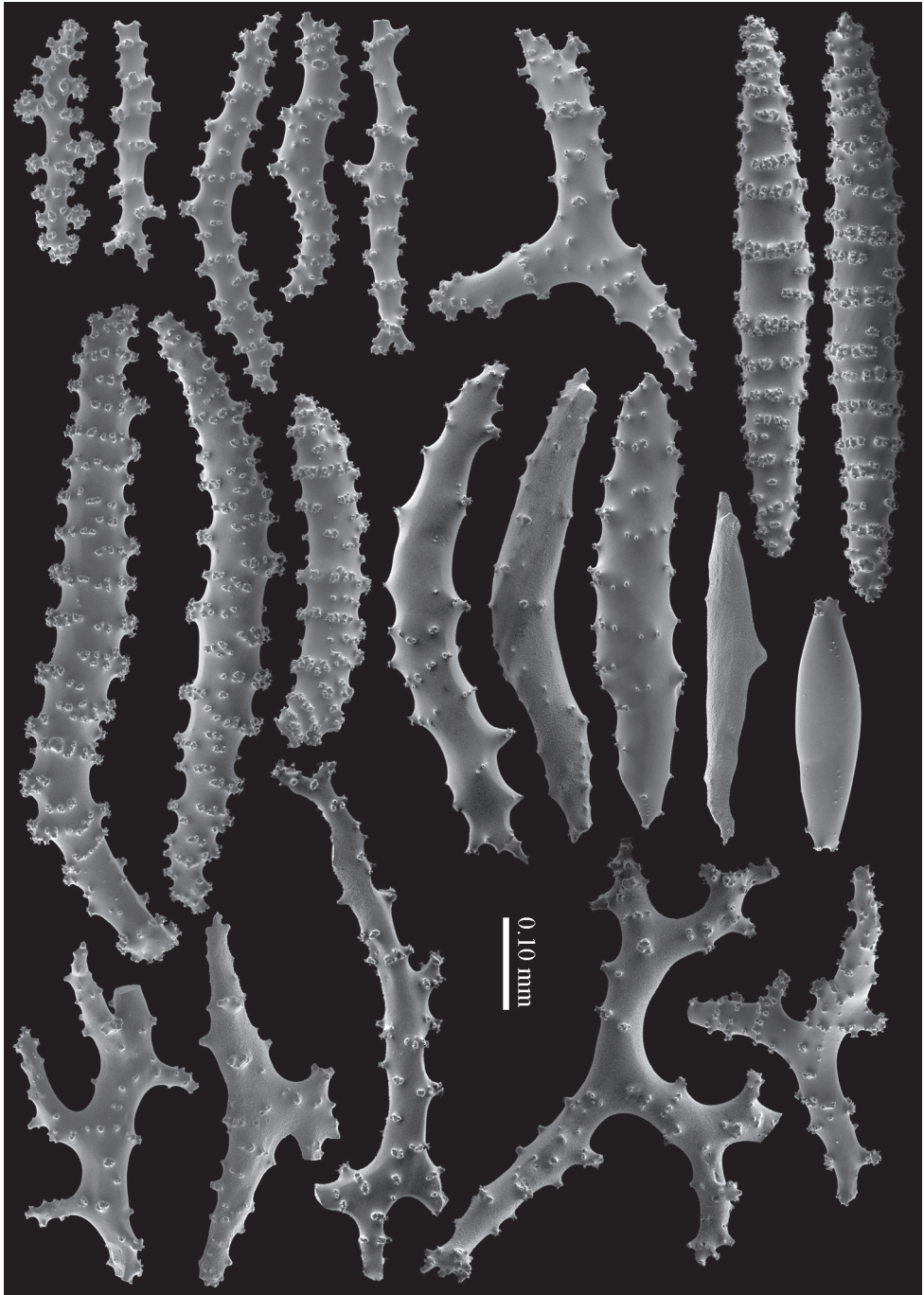


Figure 15. *Briareum stechei* (Kükenthal, 1908), RMNH Coel. 40023; medullar sclerites.

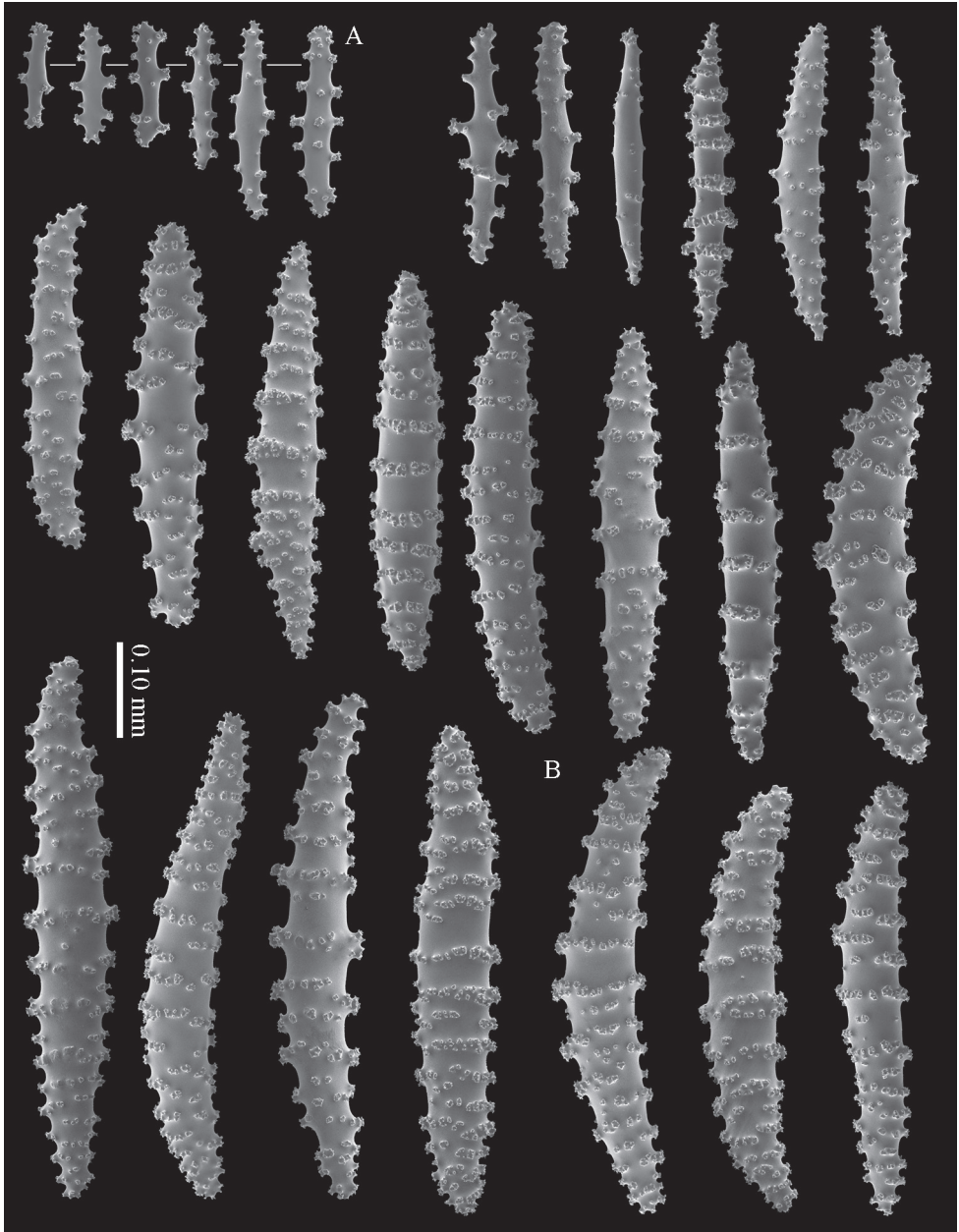


Figure 16. *Briareum stechei* (Kükenthal, 1908), RMNH Coel. 40023; **A** sclerites of top calyx **B** cortex sclerites.

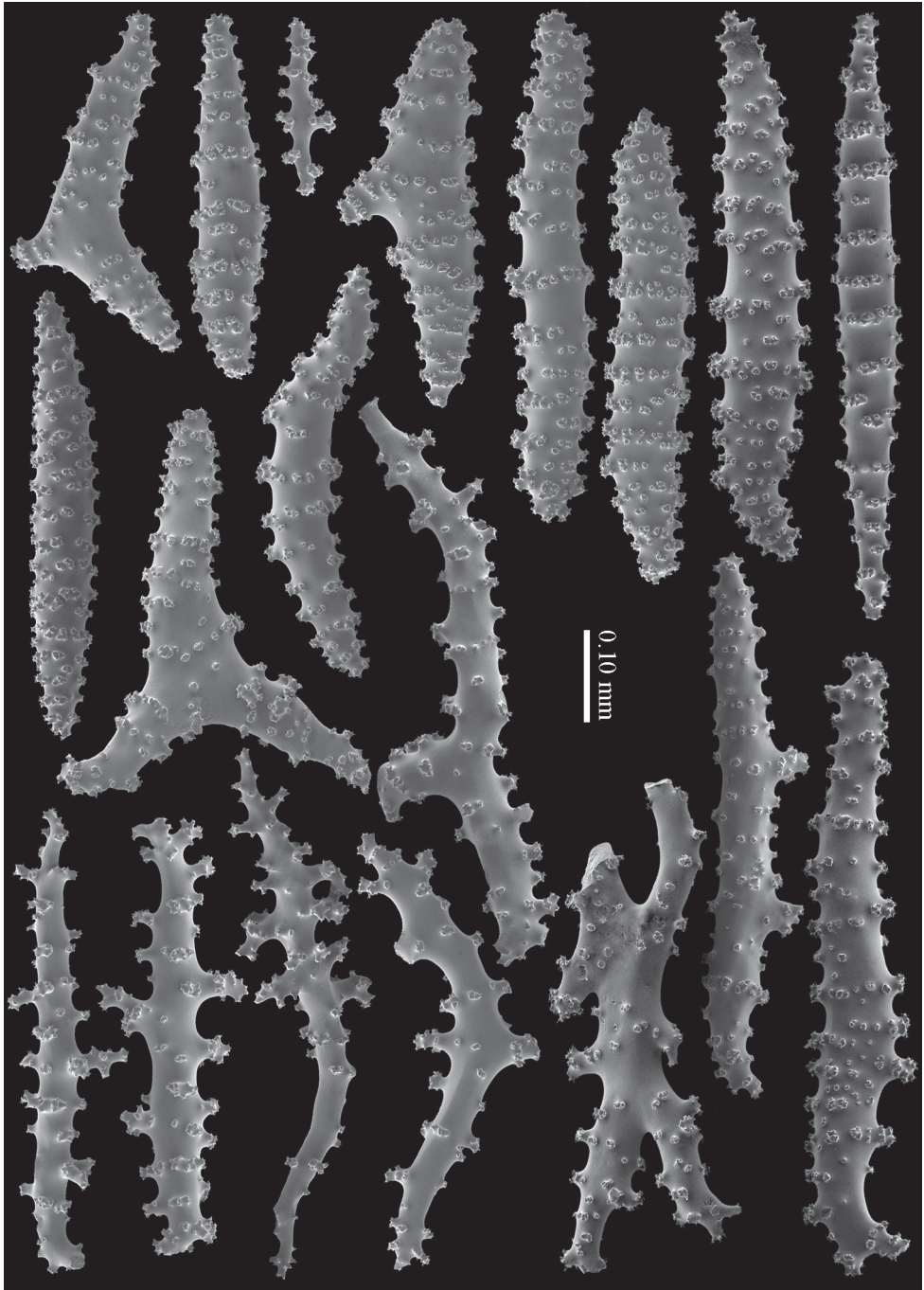


Figure 17. *Briareum stechei* (Kükenthal, 1908), RMNH Coel. 40023; medullar sclerites.

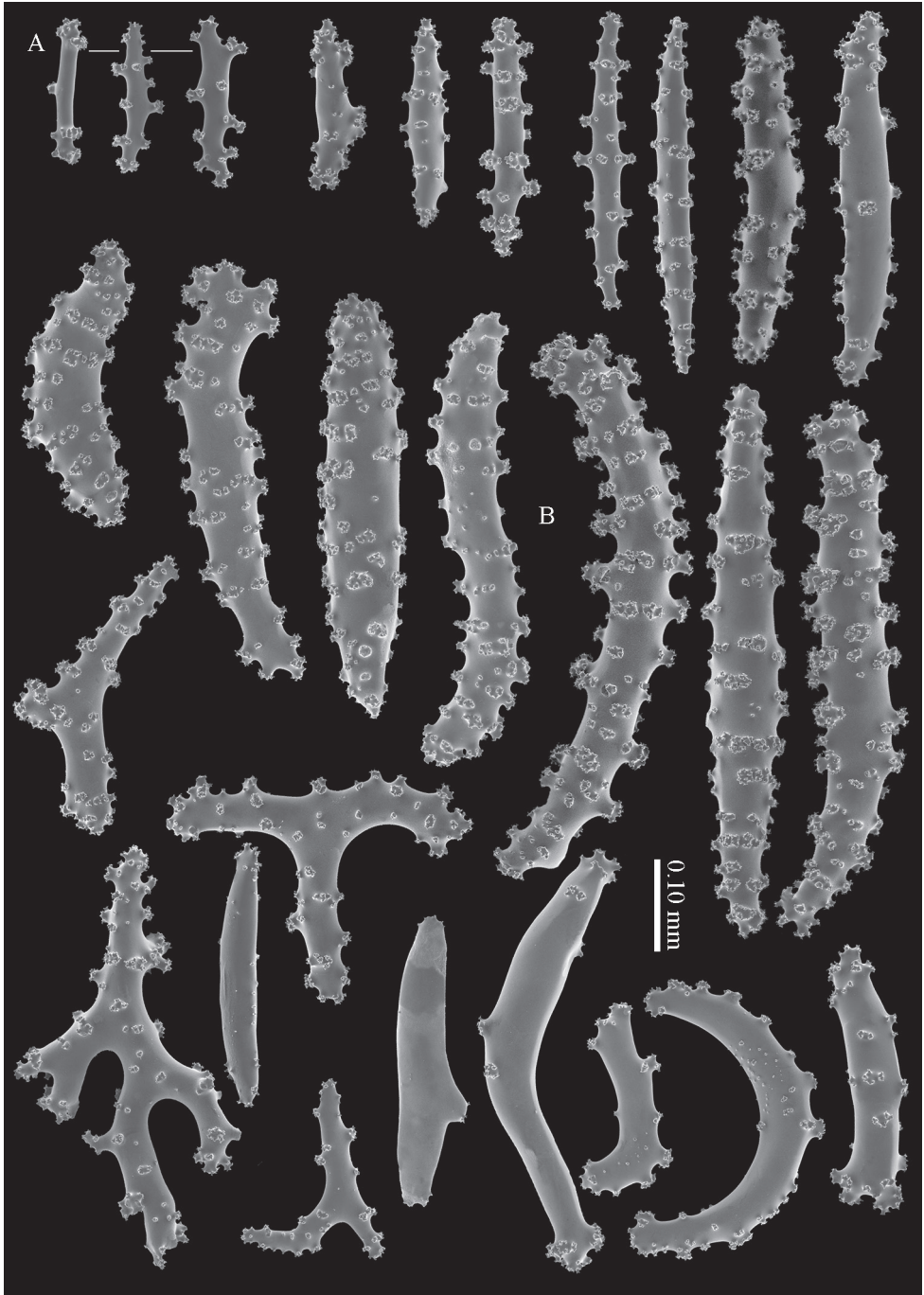


Figure 18. *Briareum stechei* (Kükenthal, 1908), RMNH 41421; **A** sclerites of top calyx **B** sclerites of coenenchyme.

Remarks. The sclerites are most like those of *B. violaceum* but in that species many spindles are longer than the longest of *B. stechei*.

Nutting (1911) apparently was not aware of Kükenthal's earlier (1908) description of *Erythropodium stechei*; actually, at first he did not compare his new species with any previously described one. Later, Kükenthal (1919) noticed the resemblance with his *E. stechei*, now in the genus *Solenopodium* Kükenthal, 1916a, and put it in the synonymy of that species with a question mark as he did not re-examine Nutting's material. Stiasny (1937) re-examined type material of both *S. stechei* and *S. excavatum* and kept them as separate species. According to him, *S. excavatum* differs in having higher calyces (Figure 11G), and by lacking calyx sclerites and "dendritic" sclerites in the interior. Verseveldt (1940: 37) was the last to compare these two species and noted no less than six aspects of difference between them, however, he did not re-examine the type material of *B. stechei*. We present sclerites images of the types of the two species (Figures 12–13). We consider the differences mentioned by previous authors as intraspecific variation, similar to that as observed in *B. hamrum*, and therefore we synonymize *B. excavatum* with *B. stechei*.

Kükenthal (1908) described *Erythropodium stechei* from Banda only. In the Berlin Museum, ZMB 5828 (Fig 11C), material from Banda, and ZMB 5816 (Figure 11D), material from Ambon, are present, both labelled type. It looks like these specimens represent the same material. It is puzzling to us why Ambon is now mentioned as the locality of ZMB 5816.

Solenopodium stechei var. *novaepommeraniae* is also represented by two collection numbers in Berlin, ZMB 5016 (Figure 11E) and ZMB 5854 (Figure 11F), here obviously the original material was split into two.

Morphological variation. To show the enormous variation in sclerites we have made SEM images of two specimens from Palau (RMNH Coel. 40023) collected at the same locality. One of them shows almost smooth spindles (Figs 14–15) while the other, like the type, has none at all (Figs 16–17). RMNH Coel. 41421 has peculiar bent and smooth sclerites (Figure 18).

Distribution. Coral Triangle, Australia (Low Isles), Guam, Taiwan.

Briareum violaceum (Quoy & Gaimard, 1833)

Figures 19–25, 26E–F

Clavularia violacea Quoy & Gaimard, 1833: 262, pl. 21 figs 13–16 (Solomon Islands).

Pachyclavularia erecta Roule, 1908: 165, pl. 6 figs 4–5 (Ambon); Thomson and Dean 1931: 19, pl. 2 figs 4, 8–9, pl. 5 figs 6–7, 9, pl. 16 figs 1–2 (Indonesia); Macfadyen 1936: 20 (Great Barrier Reef); Imahara 1996: 19 (Japan).

Pachyclavularia violacea; Gohar 1940: 20; Utinomi 1956: 223 (Bonin Islands), 1959 (Taiwan); Verseveldt 1960: 211 (Indonesia), 1972: 457 (Marshall Islands); Utinomi 1976: 3; Benayahu 1995: 106 (Sesoko Island, Japan); van Ofwegen 1996: 207 (Bismarck Sea); Imahara 1996: 19 (Okinawa, Japan).

Briareum violacea; Benayahu 2002: 20 (Ryukyu Archipelago, Japan); Benayahu et al. 2004 (South Taiwan).

Briareum violaceum; Alderslade and McFadden 2007: 42.

Not *Solenopodium violaceum* Broch & Horridge, 1956: 157 (= *B. hamrum*; Red Sea).

Material examined. RMNH Coel. 38608, Sabah, Layang Layang Atoll, outer reef on east-end of atoll, 07°22.69'N 113°52.23'E, depth 5 m, 13 October 2006 (0CDN 9323–S); RMNH Coel. 40883, PAL.100, 21 May 2010 Palau, Koror, Siaies Tunnel, 7°18.686'N, 134°13.596'E, 31 m depth, coll. C.S. McFadden; RMNH Coel. 40001, Palau, Northern Reefs, northwest corner, just east of reef tip, slope, rock, 29 June 2008, depth 20 m, 07°58.96'N, 134°34.39'E (0CDN9611–H); RMNH Coel. 41426, MAL.04 Indonesia, Ambon, Outer bay, south coast northeast of Cape Hahurong, 03°47'S, 128°06'E, calcareous platforms in littoral and shallow sublittoral, rather steep slope with more than 50% coral cover; snorkelling and diving, depth 10–27 m; 6 November 1996, coll. L.P. van Ofwegen; RMNH Coel. 41427, BUN.15, Indonesia, N. Sulawesi, Bunaken Park (main coast), Tanjung Pisok, reef flat, 124°48'E 01°34'N, SCUBA diving, 11 May 1998, coll. B.W. Hoeksema and L.P. van Ofwegen; RMNH Coel. 41428, CEB.08, Philippines, Cebu Strait, west of Bohol, north side of Cabilao Island, Cabacungan Point, 9°51.55'N 123°45.95'E, reef edge with dense coral cover, overhanging wall with caves; snorkelling and SCUBA diving, 11 November 1999, coll. L.P. van Ofwegen; RMNH Coel. 41429, CEB.09, Philippines, Cebu Strait, W of Bohol, north side of Cabilao Island, NE of Looc, 9°53.59'N 123°46.92'E, reef edge with dense coral cover, overhanging wall with caves; snorkelling and SCUBA diving, 12, 13 November 1999, coll. L.P. van Ofwegen; RMNH Coel. 41430, Bali Lombok Strait Exp. 2001, NNM-LIPI-WWF, BAL.04, Indonesia, Bali, Sanur, Jeladi Willis, south of channel entrance; 8°40.983'S, 115°16.050'E, slowly declining shallow reef slope, sandy base; SCUBA-diving to 10 m depth; 1 April 2001, coll. L.P. van Ofwegen and M. Slierings; RMNH Coel. 41431, Indonesia Ambon. Bali Lombok Strait Exp. 2001, NNM-LIPI-WWF, BAL.06, Indonesia, Bali, Sanur, Bangsal Point; 8°40.233'S, 115°15.867'E, slowly declining shallow reef slope, sandy base; SCUBA diving to 9 m depth; 2 April 2001, coll. L.P. van Ofwegen and M. Slierings; RMNH Coel. 41432, Kepulauan Seribu Exped. 2005, SER.23, Indonesia, Java Sea, Kepulauan Seribu (Thousand Islands), off Jakarta, Jukung Island, northwest side, 5°34.017'S, 106°31.633'E, SCUBA diving and snorkelling, 15 September 2005, coll. L.P. van Ofwegen and M. Slierings; RMNH Coel. 41433, Kepulauan Seribu Exped. 2005, SER.25, Indonesia, Java Sea, Kepulauan Seribu (Thousand Islands), off Jakarta, Kotok Kecil Island, northwest side, 5°41.933'S, 106°32.383'E, SCUBA diving and snorkelling, 16 September 2005; RMNH Coel. 41434, Buginesia Progr. UNHAS-NNM 1994/1995, SUL. BTN, Indonesia, SW Sulawesi, Spermonde Archipelago, north of Bone Tambung (= 17 km NW of Ujung Pandang = Makassar), 5°02'S, 119°16'E, coral reef; SCUBA diving, 14 May 1994, coll. B.W. Hoeksema; RMNH Coel. 41435, CEB.13, Philippines, Cebu Strait, W of Bohol, N side of Sandingan Island, 9°51.87'N 123°47.76'E, 0–7 m sandy, patchy coral cover, 7–24 m rubble slope, snorkelling and SCUBA diving.

ing; 13 November 1999, coll. L.P. van Ofwegen; RMNH Coel. 41436, Kepulauan Seribu Exped. 2005, SER.06, Indonesia, Java Sea, Kepulauan Seribu (Thousand Islands), off Jakarta, Dapur Island, northwest side, 5°56.733'S, 106°43.450'E, SCUBA diving and snorkelling, 9 September 2005; RMNH Coel. 41437, Indonesia Ambon. Bali Lombok Strait Exp. 2001, NNM-LIPI-WWF, BAL.25, Indonesia, Bali, northwest of Nusa Lembongan, Lembongan Bay, Bali Hai pontoon, off Desa Jungutbatu, 8°40.417'S, 115°26.300'E; shallow bay with few patches of coral; SCUBA-diving to 12 m depth; 17 April 2001, coll. L.P. van Ofwegen and M. Slierings; RMNH Coel. 41438, MAL.04 Indonesia, Ambon, Outer bay, south coast northeast of Cape Hahurong, 03°47'S, 128°06'E; calcareous platforms in littoral and shallow sublittoral, rather steep slope with more than 50% coral cover; snorkelling and diving, depth 2–28 m, 6 November 1996, coll. L.P. van Ofwegen; RMNH Coel. 41439, RAJ.12, Indonesia, Raja Ampat Islands, W Papua, east Kri, Sorido Wall, 00°33.220'S, 130°41.282'E, 22 November 2007, depth 30 m, coll. L.P. van Ofwegen; RMNH Coel. 41440, BUN.08, Indonesia, north Sulawesi, Bunaken Park, south Manado Tua Island, vertical wall in front of church, 1°37.000'N 124°41.500'E, SCUBA diving 15 m, 7 May 1998, coll. B.W. Hoeksema and L.P. van Ofwegen; RMNH Coel. 41441, BER.15, Indonesia, northeast Kalimantan, Berau Islands, Panjang Island, west side, 2°19.285'N 118°13.425'E, SCUBA diving, 9 October 2003, depth 20 m, coll. L.P. van Ofwegen and M. Slierings; RMNH Coel. 41442, Bali Lombok Strait Exp. 2001, NNM-LIPI-WWF, BAL.12, Indonesia, Bali, east side Nusa Dua, off Club Med Hotel, north of channel, 8°47.100'S, 115°13.950'E; slowly declining reef slope, sandy base; SCUBA diving to 20 m depth; 4 April 2001, coll. L.P. van Ofwegen and M. Slierings.

Diagnosis. Top of the calyces with some rods, 0.10–0.15 mm long (Figure 20A). Cortex with straight and bent spindles with simple or complex tubercles arranged in rows (Figure 20B). Cortex sclerites up to 1 mm long. Interior additionally has branched bodies with simple or complex tubercles (Figure 20C), some fused into small clumps. These sclerites slightly shorter, up to 0.70 mm long. All sclerites magenta.

Remarks. Gohar (1940: 20) synonymized *Pachyclavularia erecta* with *P. violacea*. The type of *Briareum violaceum* is stored in Paris. It was not re-examined by us.

Morphological variation. RMNH Coel. 41435 (Figure 19B) showed sclerites with very small and simple tubercles (Figure 21).

RMNH Coel. 41434 (Figure 19C) and RMNH Coel. 41436 (Figure 19D) have unusually small spindles (Figs 22–23) approaching those found in *B. stechei*. This is probably due to the very short calyces in these specimens (Figs 19C–D).

Several specimens, RMNH Coel. 41441 (Figure 19E); RMNH Coel. 41439, RMNH Coel. 41437 (Figure 19F), RMNH Coel. 41438, and RMNH Coel. 41440 showed shorter more slender spindles, but with prominent tuberculation (Figs 24–25). RMNH Coel. 41441 (Figure 19E) has widely spaced big calyces; RMNH Coel. 41437 looks more like the type specimen. (Figure 19F). As all sclerites are magenta we provisionally include them in *B. violaceum*.

Distribution. Vanuatu, Japan (Ryukyu Archipelago, Bonin Islands), Taiwan, Coral Triangle, Australia (Great Barrier Reef).

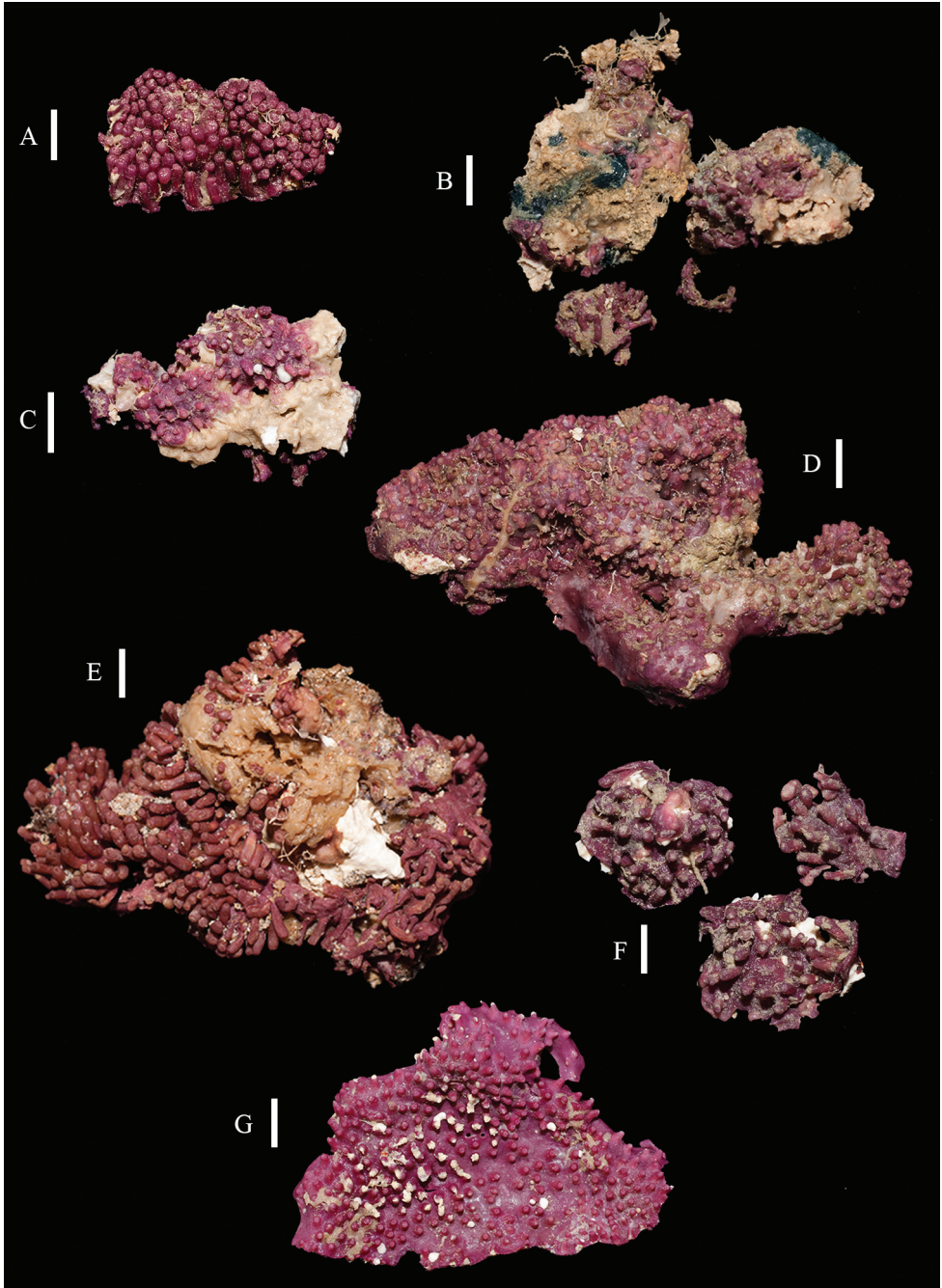


Figure 19. Colonies of *Briareum violaceum*; **A** RMNH Coel. 38608 **B** RMNH Coel. 41435 **C** RMNH Coel. 41434 **D** RMNH Coel. 41436 **E** RMNH Coel. 41437 **F** RMNH Coel. 41441 **G** RMNH Coel. 41428. Scale bars: 1 cm.

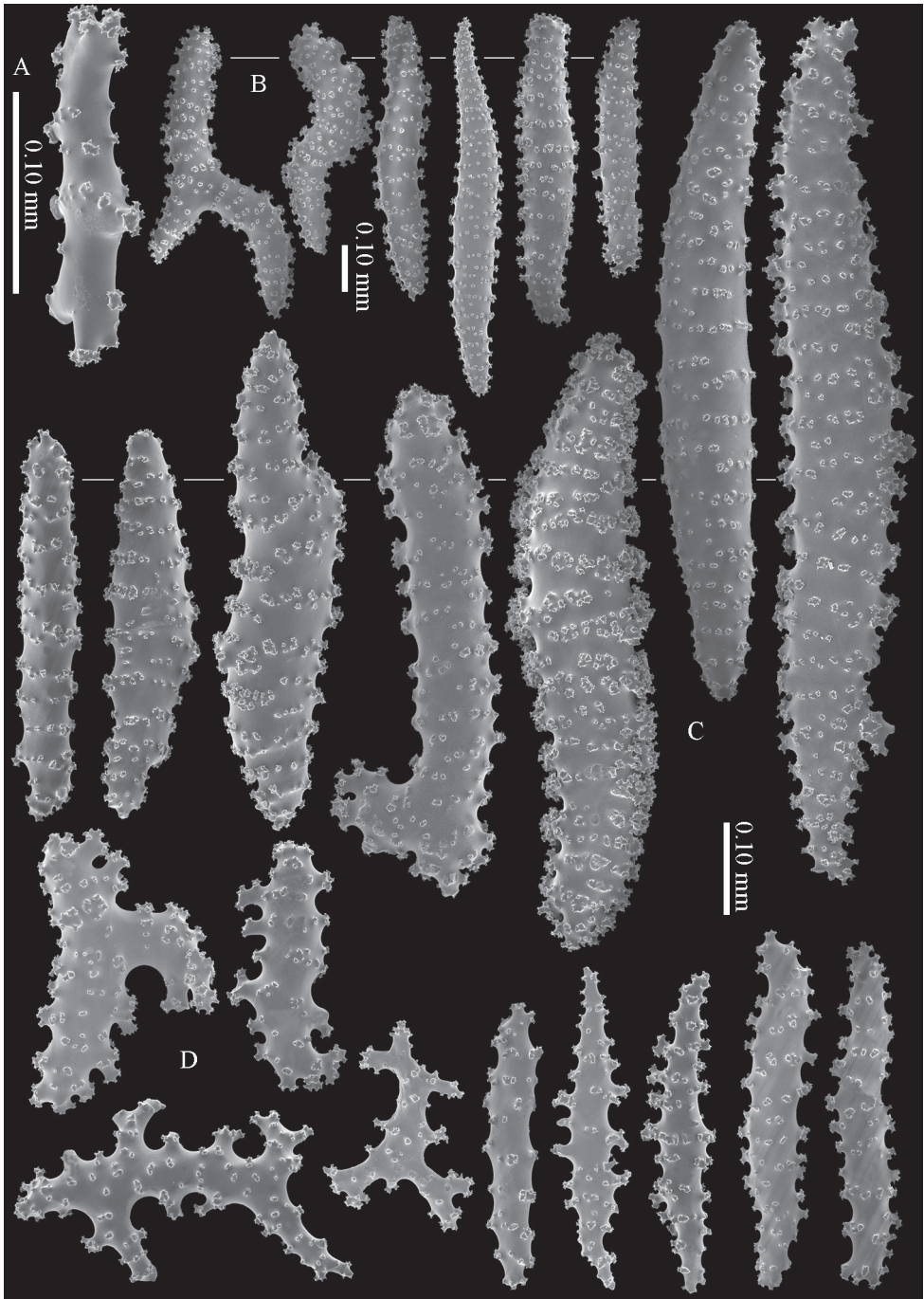


Figure 20. *Briareum violaceum* (Quoy & Gaimard, 1833), RMNH 38608; **A** sclerite of top calyx **B–C** cortex sclerites **D** medullar sclerites.



Figure 21. *Briareum violaceum* (Quoy & Gaimard, 1833), RMNH Coel. 41435; **A** sclerite of top calyx
B sclerites of coenenchyme.

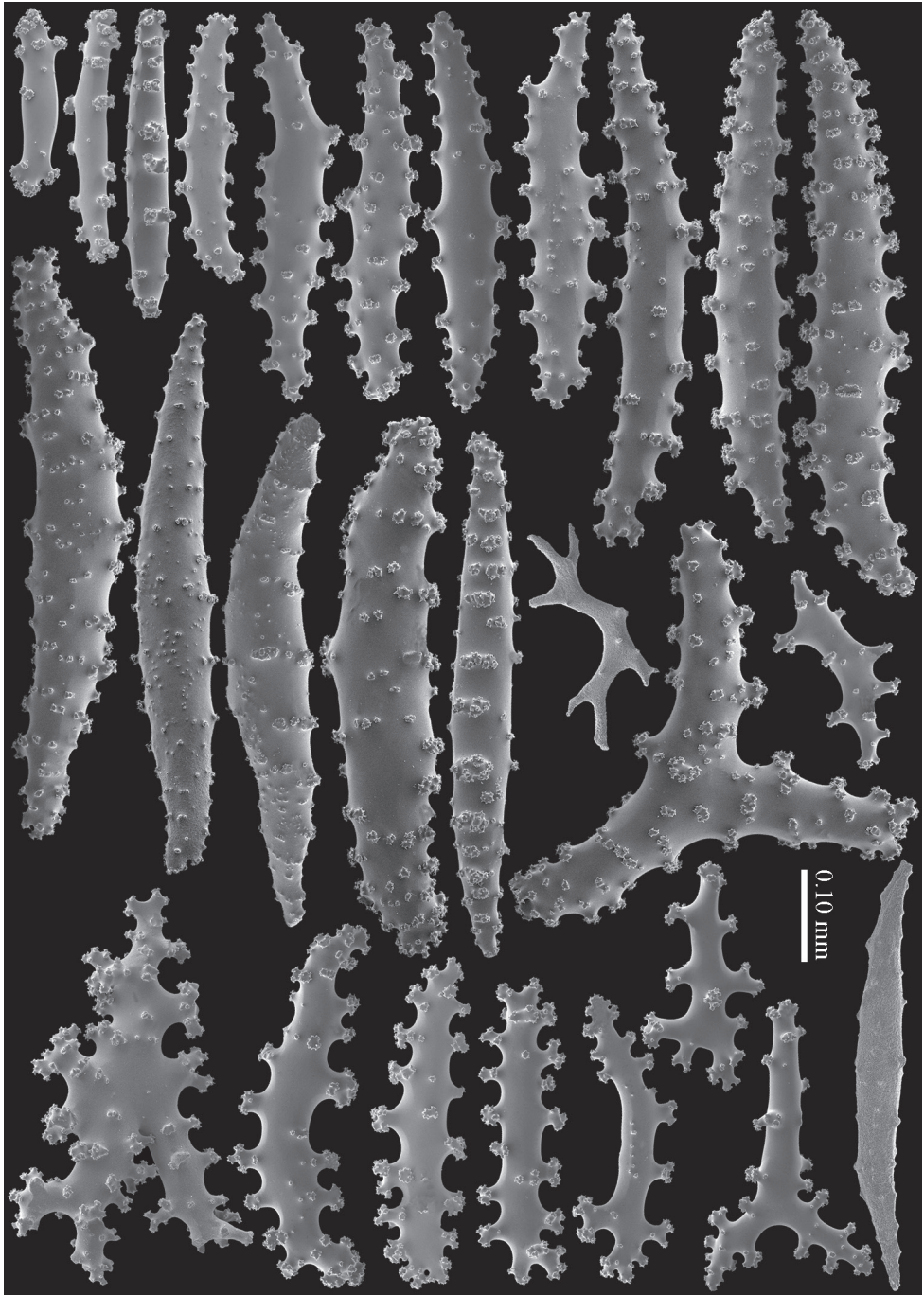


Figure 22. *Briareum violaceum* (Quoy & Gaimard, 1833), RMNH Coel. 41434, sclerites of coenenchyme.

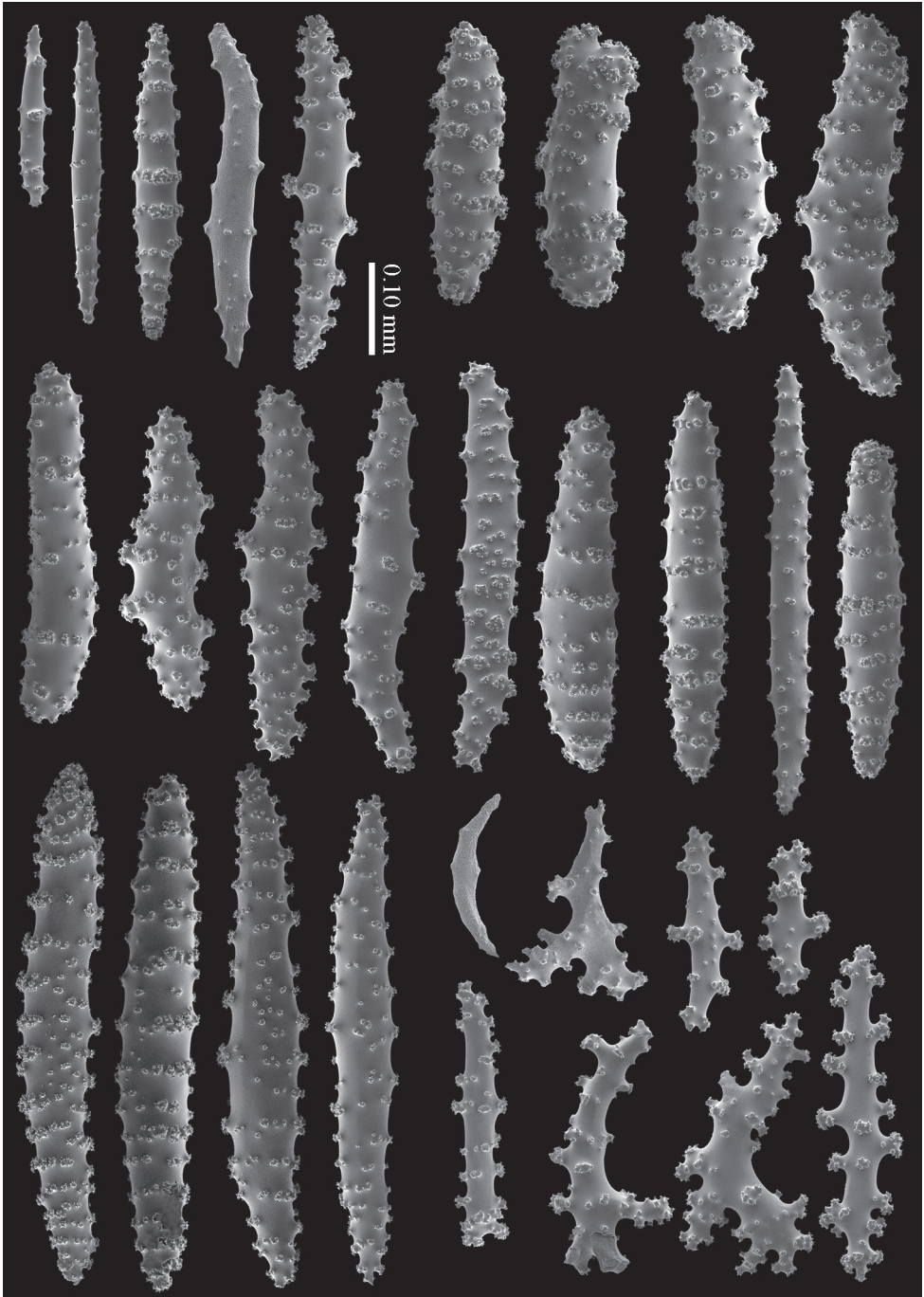


Figure 23. *Briareum violaceum* (Quoy & Gaimard, 1833), RMNH Coel. 41436, sclerites of coenenchyme.

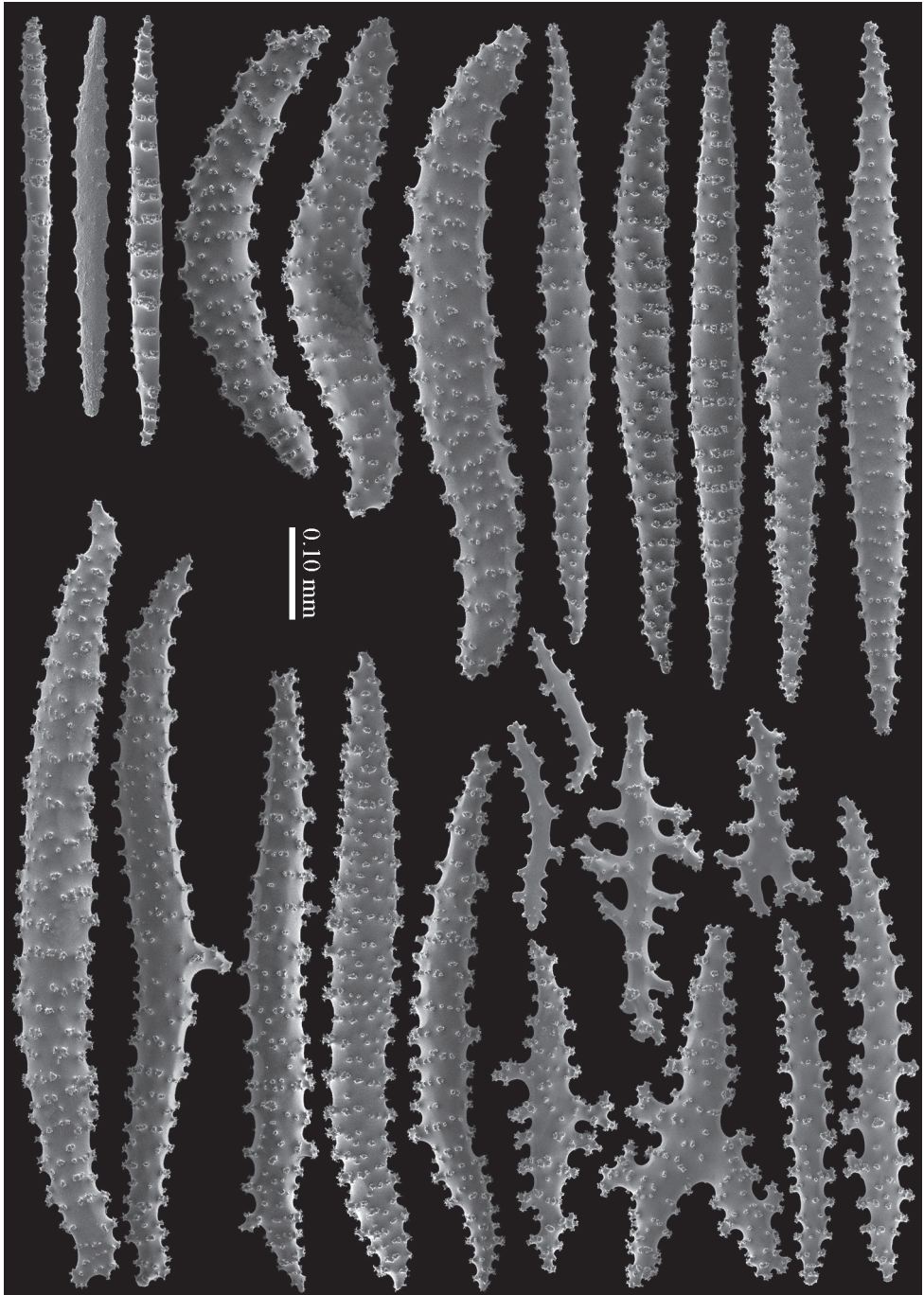


Figure 24. *Briareum violaceum* (Quoy & Gaimard, 1833), RMNH Coel. 41441, sclerites of coenenchyme.

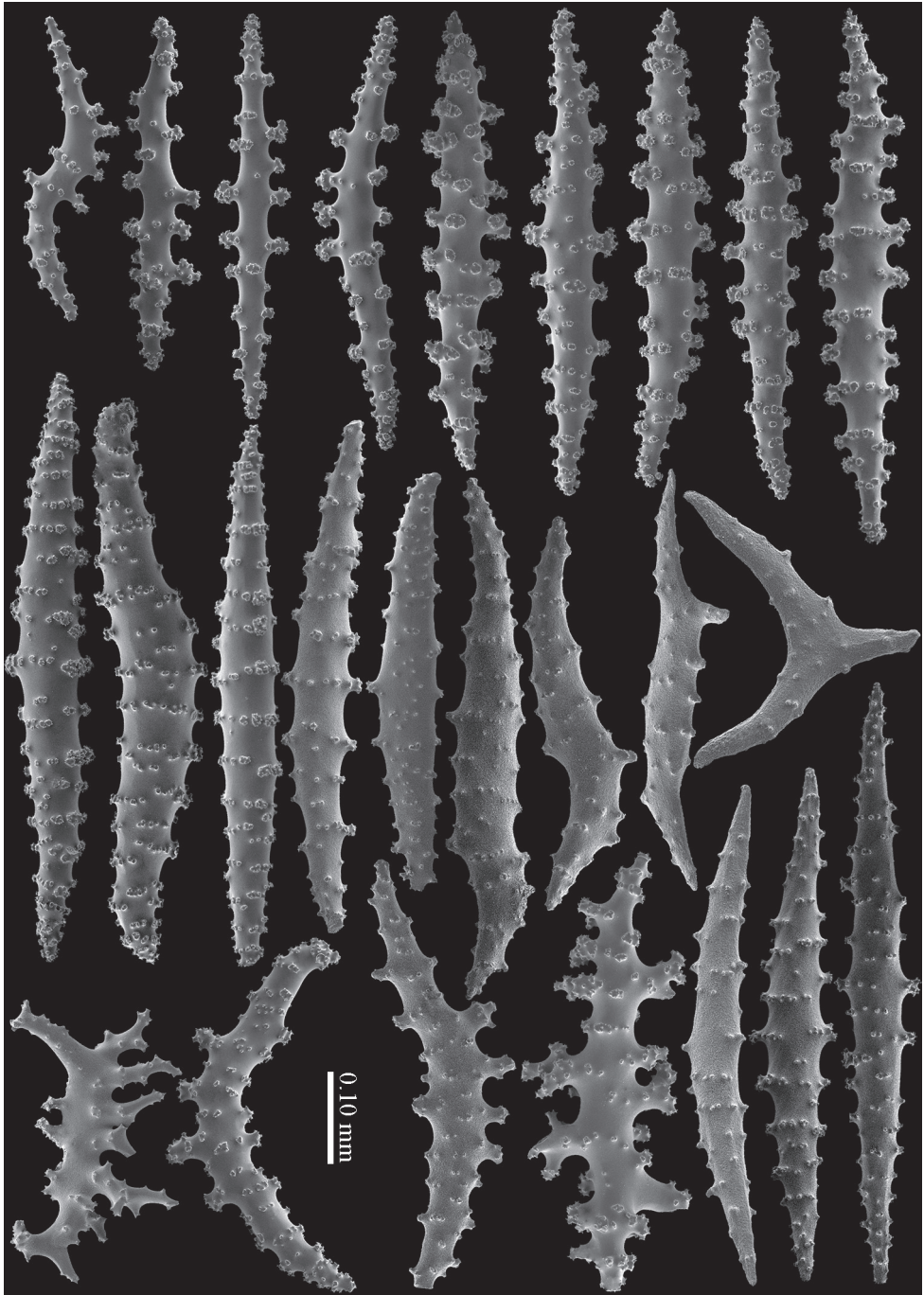


Figure 25. *Briareum violaceum* (Quoy & Gaimard, 1833), RMNH Coel. 41437, sclerites of coenenchyme.

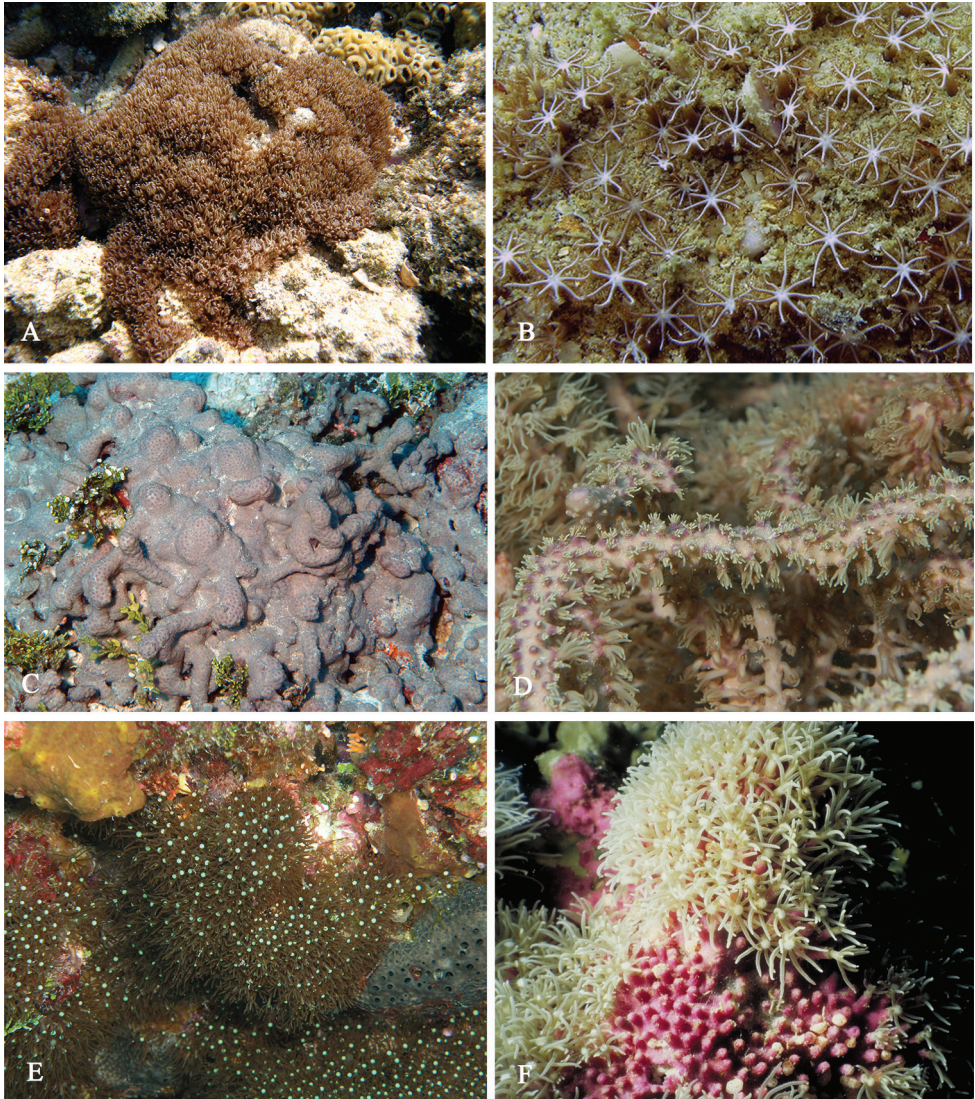


Figure 26. **A–B** *Briareum hamrum* (Gohar, 1948) **A** Colony **B** close-up of tentacles **C–D** *Briareum stechei* (Kükenthal, 1908) **C** Colony **D** close-up of tentacles **E–F** *Briareum violaceum* (Quoy & Gaimard, 1833) **E** Colony **F** close-up of tentacles.

Discussion

All *Briareum* specimens deposited at the RMNH coelenterate collection were examined, from more than 50 localities around the world. The status of the Indo-Pacific *Briareum* species is reviewed and additional information provided. Moreover, a new taxon, *B. cylindrum* is described, and *B. excavatum* (Nutting, 1911) synonymised with *B. stechei* (Kükenthal, 1908). In total four *Briareum* species are recognized in the Indo-Pacific region; one recorded from the western Indo-Pacific, and the rest from the central and eastern Indo-Pacific.

The development in molecular and chemical studies, which reliably discriminate species, has been a challenge in cnidarians. Mitochondrial genes evolve slower than nuclear genes in anthozoans (Chen et al. 2009), therefore mitochondrial markers are invariant within and among genera (Shearer and Cofforth 2008). In octocorals, an extended mitochondrial barcode of COI plus the octocoral-specific mitochondrial gene mtMutS is usually diagnostic at the genus level and narrows species down to a small number of candidate sister taxa (McFadden et al. 2014). McFadden et al. (2011, 2014) included five *Briareum* specimens from Palau (RMNH Coel. 40883–40887) and one specimen from the Red Sea (ZMTAU CO34187) in their molecular studies using this marker. They distinguished three different species, two from Palau and one from the Red Sea. All Palau specimens were examined by us and proved to be indeed two species, *B. stechei* and *B. violaceum*. The one from the Red Sea identified by Prof. Benayahu represents *B. hamrum*. Miyazaki and Reimer (2014), who used other DNA markers and examined specimens from southern Japan, found three different morphological types of *Briareum* which seemed to be similar genetically and the authors suggested further analysis to reveal the phylogenetic relationships of these three types. Probably their material now can be identified with the morphological findings presented here.

This study shows variability in sclerite morphology among the examined material which is in agreement with the previous studies. Considering this fact, we decided not to complicate the situation with introducing more new species than necessary. Instead we grouped the species together based on major differences in sclerite shape and variability. Several examples in our examined specimens have somewhat different sclerite shapes, and they are considered as intraspecific variation.

Based on the examined underwater photographs, the polyp shape and colour pattern in the examined material of *B. hamrum* were consistent, having distinguishable pinnules with dark green to brown colour, white oral disk and white line along the tentacles (Figure 26A–B). The pinnules in this species were also noticed by Gohar (1948). In *B. stechei*, the pinnules were not distinguishable and in *B. violaceum* they were very small. There was no underwater *in situ* photograph of *B. cylindrum* available to us. These characters were not reported before, therefore their importance and consistency is yet to be understood.

Briareum shows a wide distribution range with one Atlantic and four Indo-West Pacific species. Our results showed that *B. hamrum* occurs only in the western and north-

western Indian Ocean (Figure 1). This area consists of several sub-regions including East Africa, Seychelles, central Indian Ocean (Maldives and Chagos Archipelago), northwestern Indian Ocean (Arabian Sea, Oman Sea), Red Sea, and the Persian Gulf. The recent larval dispersal modelling suggests that the Red Sea and the Persian Gulf have the highest isolation in larval sources (Wood et al. 2014). This perhaps could explain the high number of endemic species described from these areas (Sheppard and Sheppard 1991; Sheppard et al. 2010; Samimi-Namin and van Ofwegen 2009), and suggests that the majority of the coral population maintained by high levels of self-seeding. *B. hamrum* clearly can tolerate high environmental fluctuations that exist in the Persian Gulf (Sheppard et al. 2010), and the Red Sea. *Briareum* species have not yet been recorded from the central Indian Ocean, Chagos Archipelago (Reinicke and van Ofwegen 1999), Maldives (Vennam and van Ofwegen 1996), and south west India (Herdman 1905; Thomson and Simpson 1909); however, it is expected to be found in these areas. The rest of the *Briareum* species have overlapping distribution in the central Indo-Pacific, which is expected due to its high levels of larval connectivity (Wood et al. 2014). More sampling efforts and examination of more material is necessary to clarify the distribution boundaries.

At present there are still uncertainties about the total number of *Briareum* species and their distribution boundaries, especially in the central Indo-Pacific. Further examination of newly collected material, together with *in situ* photographs (see e.g. Hoeksema and van Ofwegen 2004) and genetic material will eventually reveal the species characters and their variation along environmental gradients.

Acknowledgements

We would like to thank Dr. Carsten Lüter at the Museum für Naturkunde in Berlin for loan of the type material of *Briareum stechei*, and Dr. George Heiss and Prof. Wolfgang Kiessling for supporting the first author's visit to Berlin. Koos van Egmond (NBC) for curatorial assistance. Dr. Helmut Sattmann at the Naturhistorische Museum Wien for providing the permission to access the collection. Dr. H. Rezai is appreciated for support and accompanying in some field trips. Dr. H. Alizadeh, and Dr. V. Chegini (Iranian National Institute for Oceanography) are acknowledged for their support and for facilitating field surveys in Iran. We are grateful to the Ministry of Environment and Climate Affairs, Oman, for support. The first author is grateful to Dr. S.C. Wilson, O. Taylor, A. Wilson, I. Benson, F. Al-Abdali, J. Hillman (Five Oceans Environmental Services LLC, Muscat) for their support. Collection in Musandam, Oman, was possible thanks to Dr. T. Alpermann, and Dr. F. Krupp (Forschungsinstitut und Naturmuseum Senckenberg, Frankfurt am Main, Germany). The research at NBC and partial field work was supported by Schure-Beijerinck-Poppingfonds (KNAW), Alida Buitendijkfonds, Jan Joost ter Pelkwijkfonds, and Martin-Fellowship (NBC) to the first author; Dr. B.W. Hoeksema is appreciated for his advice and support herein. The Alfred P. Sloan Foundation and the Census of

Marine Life are gratefully acknowledged for the research grant provided to the first author; in this regard, Dr. M. R. Claereboudt (Sultan Qaboos University, Oman), Dr. N. D'Adamo (UNESCO, IOC, Perth), Dr. J.H. Ausubel (Rockefeller University), and Dr. P. Miloslavich (Universidad Simón Bolívar) are greatly appreciated for their continued support and encouragement. Dr. S.D. Cairns (National Museum of Natural History, United States), and two anonymous reviewers are appreciated for their constructive comments and suggestions, which helped improve the manuscript.

References

- Alderslade P (2000) Four new genera of soft corals (Coelenterata: Octocorallia), with notes on the classification of some established taxa. *Zoologische Mededelingen, Leiden* 74(16): 237–249.
- Alderslade P, McFadden CS (2007) Pinnule-less polyps: a new genus and new species of Indo-Pacific Clavulariidae and validation of the soft coral genus *Acrossota* and the family Acrossotidae (Coelenterata: Octocorallia). *Zootaxa* 1400: 27–44.
- Aurivillius M (1931) The Gorgonarians from Dr. Sixten Bock's expedition to Japan and Bonin Islands 1914. *Kungliga Svenska Vetenskapsakademien Handlingar* 3(9) 4: 1–337.
- Bayer FM (1961) The shallow-water Octocorallia of the West Indian region. A manual for marine biologists. *Studies on the Fauna of Curaçao and other Caribbean Islands* 12: 1–373.
- Benayahu Y (1995) Species composition of soft corals (Octocorallia, Alcyonacea) on the coral reefs of Sesoko Island, Ryukyu Archipelago, Japan. *Galaxea* 12: 103–124.
- Benayahu Y (1997) A review of three alcyonacean families (Octocorallia) from Guam. *Micronesia* 30(2): 207–244.
- Benayahu Y (2002) Soft corals (Octocorallia: Alcyonacea) of the southern Ryukyu Archipelago: The families Tubiporidae, Clavulariidae, Alcyoniidae and Briareidae. *Galaxea* 4: 11–32. doi: 10.3755/jcrs.2002.11
- Benayahu Y, Shlagman A, Schleyer MH (2003) Corals of the South-west Indian Ocean: VI. The Alcyonacea (Octocorallia) of Mozambique, with a discussion on soft coral distribution on south equatorial East African reefs. *Zoologische Verhandlungen Leiden* 345: 49–57.
- Benayahu Y, Jeng M-S, Perkol-Finkel S, Dai C-F (2004) Soft corals (Octocorallia: Alcyonacea) from southern Taiwan. II. Species diversity and distributional Patterns. *Zoological Studies* 43(3): 548–560.
- Bilewicz JP, Coates KA, Currie DC, Trapido-Rosenthal HG (2010) Molecular and morphological variation supports monotypy of the octocoral *Briareum* Blainville, 1830 (Octocorallia: Alcyonacea) in the Western Atlantic. *Proceedings of the Biological Society of Washington* 123(2): 93–112. doi: 10.2988/09-22.1
- Blainville HMD de (1830) *Dictionnaire des Sciences Naturelles* 60. Paris, 631 pp.
- Broch H, Horridge A (1956) A new species of *Solenopodium* (Stolonifera: Octocorallia) from the Red Sea. *Proceedings of the Zoological Society of London* 128(2): 149–160. doi: 10.1111/j.1096-3642.1957.tb00263.x

- Chen Y-P, Wu S-L, Su J-H, Lin M-R, Hu W-P, Hwang T-L, Sheu J-H (2006) Briarexcativins G and H, Two new Briaranes from the octocoral *Briareum excavatum*. Bulletin of the Chemical Society of Japan 79(12): 1900–1905. doi: 10.1246/bcsj.79.1900
- Chen I-P, Tang C-Y, Chiou C-Y, Hsa J-H, Wei NW, Wallace CC, Muir P, Wu H, Chen CA (2009) Comparative analyses of coding and non-coding DNA regions indicate that *Acropora* (Anthozoa: Scleractinia) possesses a similar evolutionary tempo of nuclear vs. mitochondrial genomes as in plants. Journal of Marine Biotechnology 11: 141–152. doi: 10.1007/s10126-008-9129-2
- Duchassaing P, Michelotti J (1860) Mémoire sur les coralliaires des Antilles. Mémoires de l'Académie des Sciences de Turin (2) 19: 279–365. [reprint paged 1–89]
- Erhardt H, Baensch HA (2000) Meerwasser atlas 5: Wirbellose, 1–1150. Mergus, Melle, Germany.
- Fabricius K, Alderslade P (2001) Soft corals and sea fans: a comprehensive guide to the tropical shallow-water genera of the Central-West Pacific, the Indian Ocean and the Red Sea. Australian Institute of Marine Science, Townsville, 264 pp.
- Gohar HAF (1940) A revision of some genera of the Stolonifera (with an emended system of classification and the description of two new species). Publications of the Marine Biological Station of Al-Ghardaqa (Red Sea) 3: 1–25.
- Gohar HAF (1948) A description and some biological studies of a new alcyonarian species *Clavularia hamra* Gohar. Publications of the Marine Biological Station of Al-Ghardaqa (Red Sea) 6: 3–33.
- Grasshoff M (1999) The shallow water gorgonians of New Caledonia and adjacent islands (Coelenterata: Octocorallia). Senckenbergiana Biologica 78(1/2): 1–245.
- Herdman WA (1905) Report to the Government of Ceylon on the Pearl Oyster Fisheries of the Gulf of Manaar (Vol. 3). Published at the request of the colonial government by the Royal Society.
- Hoeksema BW (2007) Delineation of the Indo-Malayan Centre of maximum marine biodiversity: the Coral Triangle. In: Renema W (Ed.) Biogeography, Time and Place: Distributions, Barriers and Islands. Springer, Dordrecht, 117–178. doi: 10.1007/978-1-4020-6374-9_5
- Hoeksema BW, van Ofwegen LP (2004) Fauna Malesiana: Indo-Malayan reef corals: a generic overview. World Biodiversity Database CD-ROM Series.
- Hong P-H, Su Y-D, Su J-H, Chen Y-H, Hwang T-L, Weng C-F, Lee C-H, Wen Z-H, Sheu J-H, Lin N-C, Kuo Y-H, Sung P-J (2012) Briarenolides F and G, new briarane diterpenoids from a *Briareum* sp. octocoral. Marine Drugs 10: 1156–1168. doi: 10.3390/md10051156
- Imahara Y (1996) Previously recorded octocorals from Japan and adjacent seas. Precious Corals & Octocoral Research 4–5: 17–44.
- Kükenthal W (1906) Alcyonacea. Wissenschaftliche Ergebnisse der Deutschen Tiefsee-Expedition auf dem Dampfer “Valdivia” 1898–1899, 13(1) Lieferung 1, 1–111.
- Kükenthal W (1908) Diagnosen neuer Gorgoniden (4. Mitteilung). Zoologischer Anzeiger 33(1): 9–20.
- Kükenthal W (1916a) System und Stammesgeschichte der Scleraxonier und der Ursprung der Holaxonier. Zoologischer Anzeiger 47(6): 170–183.

- Kükenthal W (1916b) Die Gorgonarien Westindiens. Kap. 1, Die Scleraxonier; 2, Über den Venusfächer; 3, die Gattung *Xiphigorgia* H.M. Edw. Zoologische Jahrbücher Supplement 11(4): 443–504.
- Kükenthal W (1919) Gorgonaria. Wissenschaftliche Ergebnisse der Deutschen Tiefsee-Expedition auf dem Dampfer “Valdivia” 1898–1899 13(2): 1–946.
- Kükenthal W (1924) Gorgonaria. Das Tierreich 47. Berlin and Leipzig, 478 pp.
- MacFadyen LMI (1936) Alcyonaria (Stolonifera, Alcyonacea, Telestacea and Gorgonacea). Great Barrier Reef Expedition Scientific Reports 5(2): 19–72.
- May W (1898) Die von Dr. Stuhlmann im Jahre 1889 gesammelten ostafrikanischen Alcyonaceen des Hamburger Museums. Jahrbuch der Hamburgischen Wissenschaftlichen Anstalten 15(2): 1–38.
- McFadden CS, France SC, Sánchez JA, Alderslade P (2006) A molecular phylogenetic analysis of the Octocorallia (Cnidaria: Anthozoa) based on mitochondrial protein-coding sequences. Molecular Phylogenetics and Evolution 41: 513–527. doi: 10.1016/j.ympev.2006.06.010
- McFadden CS, Benayahu Y, Pante E, Thoma JN, Nevarez PA, France SC (2011) Limitations of mitochondrial gene barcoding in Octocorallia. Molecular Ecology Resources 11: 19–31. doi: 10.1111/j.1755-0998.2010.02875.x
- McFadden CS, Brown AS, Brayton C, Hunt CB, van Ofwegen LP (2014) Application of DNA barcoding in biodiversity studies of shallow water octocorals: molecular proxies agree with morphological estimates of species richness in Palau. Coral Reefs 33(2): 275–286. doi: 10.1007/s00338-013-1123-0
- Miyazaki Y, Reimer JD (2014) Morphological and genetic diversity of *Briareum* (Anthozoa: Octocorallia) from the Ryukyu Archipelago, Japan. Zoological Science 31: 692–702. doi: 10.2108/zs130171
- Nardo GD (1845) Distribuzione naturale in ordine, famiglie e generi della classe dei zoofiti (Blainville). Nuovi annali delle scienze naturali Bologna (2) 3: 104–109.
- Nutting CC (1911) The Gorgonacea of the Siboga Expedition VIII. The Scleraxonia. Siboga Expedition Monograph 13(5): 1–62.
- van Ofwegen LP (1996) Octocorallia from the Bismarck Sea (part II). Zoologische Mededelingen 70(13): 207–215.
- van Ofwegen LP (2015) *Briareum* Blainville, 1834. World Register of Marine Species (WoRMS). <http://www.marinespecies.org/aphia.php?p=taxdetails&id=267277> [on 2015-10-31]
- Pallas PS (1766) Elenchus zoophytorum sistens generum adumbrationes generaliores et specierum cognitarum succinctas descriptiones cum selectis auctorum synonymis. Hagae Comitum, [i]–xvi + [17]–28 + 1–451 pp. doi: 10.5962/bhl.title.6595
- Quoy JRC, Gaimard P (1833) Zoophytes. In: Voyage de découvertes de l’Astrolabe exécuté par ordre du Roi, pendant les années 1826–1827–1828–1829, sous le commandement de M.J. Dumont d’Urville. Zoologie 4: 1–390.
- Reinicke GB, van Ofwegen LP (1999) Soft corals alcyonacea: octocorallia from shallow water in the Chagos Archipelago: species assemblages and their distribution. Ecology of the Chagos Archipelago. Linnean Society Occasional Publications 2: 351.
- Roule L (1908) Alcyonaires d’Amboine. Revue Suisse de Zoologie 16: 161–194.

- Samimi-Namin K, van Ofwegen LP (2009) Some shallow water octocorals (Coelenterata: Anthozoa) of the Persian Gulf. *Zootaxa* 2058: 1–52.
- Samimi-Namin K, van Ofwegen L (2012) The Octocoral Fauna of the Gulf. In: Riegl BM, Purkis SJ (Eds) *Coral Reefs of the Gulf: adaptation to climatic extremes*. Springer Netherlands, 225–252. doi: 10.1007/978-94-007-3008-3_12
- Shearer TL, Coffroth MA (2008) Barcoding corals: limited by interspecific divergence not intraspecific variation. *Molecular Ecology Resources* 8: 247–255. doi: 10.1111/j.1471-8286.2007.01996.x
- Sheppard C, Al-Husiani M, Al-Jamali F, Al-Yamani F, Baldwin R, Bishop J, Benzoni F, Durtieux E, Dulvy NK, Durvasula SRV, Jones DA, Loughland R, Medio D, Nithyanandan M, Pilling GM, Polikarpov I, Price ARG, Purkis S, Riegl B, Saburova M, Samimi-Namin K, Taylor O, Wilson S, Zainal K (2010) The Gulf: A young sea in decline. *Marine Pollution Bulletin* 60(1): 13–38. doi: 10.1016/j.marpolbul.2009.10.017
- Sheppard CRC, Sheppard ALS (1991) Corals and coral communities of Arabia. *Fauna of Saudi Arabia* 12: 3–170.
- Sτίαςny G (1937) Die Gorgonacea der Siboga Expedition. Supplement II. Revision der Scleraxonia mit Ausschluss der Melitodidae und Coralliidae. *Siboga Expedition Monograph* 13d(8): 1–138.
- Sung P-J, Sheu J-H, Xu J-P (2002) Survey of briarane-type diterpenoids of marine origin. *Heterocycles* 57: 535–579. doi: 10.3987/REV-01-546
- Thomson JA, Dean LM (1931) The Alcyonacea of the Siboga Expedition with an addendum to the Gorgonacea. *Siboga Expedition Monograph* 13d: 1–227.
- Thomson JA, Henderson WD (1906) The marine fauna of Zanzibar British East Africa, from collections made by Cyril Crossland, M.A., B.Sc., F.Z.S., in the years 1901 and 1902. *Alcyonaria*. *Proceedings of the Zoological Society of London* 1: 393–443.
- Thomson JA, Simpson JJ (1909) An account of the Alcyonarians collected by the RIM SS Investigator in the Indian Ocean. II. The Alcyonarians of the littoral area: XII, 319.
- Tixier-Durivault A (1966) Octocoralliaires de Madagascar et des îles avoisinantes. *Faune Madagascar* 21: 1–456.
- Tixier-Durivault A (1970) Les octocoralliaires de Nouvelle-Calédonie. *L'Expedition française sur les récifs coralliens de la Nouvelle-Calédonie* 4: 171–350.
- Utinomi H (1956) On some alcyonarians from the west-Pacific islands (Palau, Ponape and Bonins). *Publications of the Seto Marine Biological Laboratory* 5(2): 221–242.
- Utinomi H (1976) Shallow-water octocorals of the Ryukyu Archipelago (Part I). *Sesoko Marine Science Laboratory Technical Report* 4: 1–5.
- Verseveldt J (1940) Studies on Octocorallia of the families Briareidae, Paragorgiidae and Anthothelidae. *Temminckia* 5: 1–142.
- Verseveldt J (1960) Octocorallia from the Malay Archipelago (Part I.) *Biological Results of the Snellius Expedition XX*. *Temminckia* 10: 209–251.
- Verseveldt J (1970) Report on some Octocorallia (alcyonacea) from the northern Red Sea. *Israel Journal of Zoology* 19: 209–229.
- Verseveldt J (1972) Report on a few octocorals from Eniwetok Atoll, Marshall Islands. *Zoologische Mededelingen Leiden* 47(36): 457–464.

- Vennam J, van Ofwegen LP van (1996) Soft corals (Coelenterata: Octocorallia: Alcyonacea) from the Laccadives (SW India), with a re-examination of *Sinularia gravis* Tixier-Durivault, 1970. Zoologische Mededelingen Leiden 70(29): 437–452.
- Wang S-K, Yeh T-T, Duh C-Y (2012) Briacavatulides D-F, New Briaranes from the Taiwanese Octocoral *Briareum excavatum*. Marine Drugs 10(9): 2103–2110. doi: 10.3390/md10092103
- West JM, Harvell CD, Walls AM (1993) Morphological plasticity in a gorgonian coral (*Briareum asbestinum*) over a depth cline. Marine Ecology Progress Series 94: 61–69. doi: 10.3354/meps094061
- West JM (1997) Plasticity in the sclerites of a gorgonian coral: tests of water motion, light level, and damage cues. The Biological Bulletin 192(2): 279–289. doi: 10.2307/1542721
- Wood S, Paris C, Ridgwell AJ, Hendy E (2014) Modelling dispersal and connectivity of broadcast spawning corals at the global scale. Global Ecology and Biogeography 23(1): 1–11. doi: 10.1111/geb.12101
- Yeh T-T, Wang S-K, Dai C-F, Duh C-Y (2012) Briacavatulides A–C, New Briaranes from the Taiwanese Octocoral *Briareum excavatum*. Marine Drugs 10(5): 1019–1026. doi: 10.3390/md10051019

A new species of the genus *Timalinyssus* Mironov, 2001 (Acarina, Psoroptidia) with a key to known species

Ioana Cristina Constantinescu¹, Gabriel Chişamera¹,
D. Khlur B. Mukhim², Costică Adam¹

1 “Grigore Antipa” National Museum of Natural History, Sos. Kiseleff no.1, 011341 Bucharest, Romania

2 Zoology Department, Lady Keane College, 793001 Shillong, Meghalaya, India

Corresponding author: Ioana Cristina Constantinescu (cristinactinescu@yahoo.com)

Academic editor: A. Bochkov | Received 5 November 2015 | Accepted 15 December 2015 | Published 28 January 2016

<http://zoobank.org/205A55C9-626B-4975-8A35-0057E417D4F7>

Citation: Constantinescu IC, Chişamera G, Mukhim DKB, Adam C (2016) A new species of the genus *Timalinyssus* Mironov, 2001 (Acarina, Psoroptidia) with a key to known species. *ZooKeys* 557: 45–57. doi: 10.3897/zookeys.557.7098

Abstract

The article describes a new species of the feather mite family Pteronyssidae (Acarina: Psoroptidia) from the Gray Sibia *Heterophasia gracilis* (McClelland) (Passeriformes, Leiothrichidae) in India (Meghalaya, Jaintia Hills, Shnongrim village). Males of *Timalinyssus wablangi* **sp. n.** differ from those of all *Timalinyssus* species by having the horseshoe-shaped epiandrum with a short anterior extension. Females of the new species differ from those of all previously known species of the genus in having the hysteronotal shield with deep lateral incisions between *e*2 and *f*2 setae. A key to all species of the genus *Timalinyssus* is presented.

Keywords

Pteronyssidae, *Timalinyssus wablangi*, new species, systematics

Introduction

The feather mite family Pteronyssidae currently includes about 180 species in 23 genera (Gaud and Mouchet 1959; Faccini and Atyeo 1981, Mironov 2001, 2005; Mironov and Wauthy 2005a, 2005b, 2008; Mironov and Proctor 2011; Constantinescu et al. 2014a, 2014b). Within this family, the genus *Timalinyssus* Mironov encompasses

six species of large-sized mites that can be found on birds of the families Leiothrichidae and Paradoxornithidae (Passeriformes) from Asia (China, Taiwan, Vietnam and India). The type species is *Timalinyssus formosanus* Mironov, 2001 from *Actinodura morisoniana* (Ogilvie-Grant). Initial diagnostic characters given to the genus (Mironov 2001) proved to be insufficient as new species were subsequently described (Wang and Wang 2008; Mironov and Proctor 2011; Constantinescu et al. 2014a). Mironov and Proctor (2011) described the distinctive feature differentiating it from the closely related genus *Mouchetia*, namely the structure of tarsus III in males. In *Timalinyssus*, tarsus III is usually elongated and curved, with a claw-like or bidentate apical process and the dorsal surface of this segment bearing a smooth or indented longitudinal crest (in the case of *T. oliferae*, the longitudinal crest is absent but one rounded dorsal tooth is present). Males of *Mouchetia* have tarsus III with a large spine on apex and subapical spine on the outer margin of this segment. Females of *Timalinyssus* differ from those of the genus *Mouchetia* in having the hysteronotal shield not narrowed in the anterior half. In the present paper a new *Timalinyssus* species found on the Gray Sibia *Heterophasia gracilis* (McClelland) is described and a key to all known species of the genus is also provided.

Materials and methods

The material used in the present paper was collected in Meghalaya (India) in January 2014. The birds were captured using mist-nets, identified and visually checked for the presence of mites and after collecting them released back into the wild. Mite specimens were taken from birds manually with a needle and placed in vials with ethanol. Later, in the laboratory, the mite specimens were cleared in lactic acid and mounted on microscope slides in Hoyer's medium. Drawings were made using an Olympus CX21 microscope, with a camera lucida drawing device. The bird specimens were identified according to Rasmussen and Anderton (2012) and Grimmett et al. (2011), and the taxonomy of the birds follows Clements et al. (2013). The setation of mite's body follows that of Griffiths et al. (1990) with modifications of Norton (1998) concerning coxal setae, while the setation of legs follows Gaud and Atyeo (1996). The description of *Timalinyssus wahlangi* sp. n. is given according to the current format used for species of the pteronyssid taxa (Faccini and Atyeo 1981; Hernandez 2012; Mironov 1992, 2001). The measuring techniques of particular structures used in the present paper were described by Mironov and Proctor (2011). We give the full set of measurements for a holotype (male) and range of measurements for corresponding paratypes. All measurements are in micrometres (μm). The holotypes and all paratypes of the new species are deposited in the Acarological Collection of the "Grigore Antipa" National Museum of Natural History, Bucharest, Romania.

Results

Family Pteronyssidae Oudemans, 1941

Genus *Timalinyssus* Mironov, 2001

Timalinyssus wablangi sp. n.

<http://zoobank.org/7E0C381A-DEC3-47D8-90F8-7FB83F2FC293>

Figs 1–5

Type material. Male holotype (ANA450), 3 male (ANA448, ANA449, ANA451) and 1 female (ANA452) paratypes 25.01.2014, 3 female (ANA445, ANA446, ANA447) paratypes 20.01.2014, from the Gray Sibia *Heterophasia gracilis* (McClelland) (Passeriformes, Leiothrichidae); **INDIA:** Meghalaya, Jaintia Hills, Shnongrim village, (25°21'12.36"N, 92°31'3.06"E); 1151 m; subtropical forest; collector D. Khlur B. Mukhim.

Description. MALE (Figs 1; 2; 5A–C; holotype, range for 3 paratypes in parentheses): Idiosoma 370 long (370–380), 250 wide (240–260). Prodorsal shield length 100 (100–110), width 92 (92–98), not fused with scapular shields. Distance between bases of setae *se* 80 (80–82), distance between bases of setae *si* 62 (60–63), posterior margin almost straight, lateral margins with small incisions at level of setae *se*. Setae *c*2 short, filiform, about 20 (15–20) in length, situated on medial margins of humeral shields. Setae *c*3 enlarged in basal part and filiform in apical part, 130 (125–140) in length. Hysteronotal shield with slightly concave anterior margin, anterior angles rounded, length 220 (215–230), width at anterior margin 100 (98–105). Distance along midline between prodorsal and hysteronotal shields 44 (44–56). Width of opisthosoma at level of setae *f*2 58 (58–66). Opisthosomal lobes short, with acute

Table 1. *Timalinyssus* species and their host associations.

Mite species	Host species	Host family	Location	References
<i>Timalinyssus oliferae</i> (Mironov, 1990)	<i>Leiothrix argentauris</i> (Hodgson)	Leiothrichidae	Vietnam	Mironov 1990; Mironov 2001
<i>Timalinyssus formosanus</i> Mironov, 2001	<i>Actinodura morrisoniana</i> Ogilvie-Grant	Leiothrichidae	Taiwan	Mironov 2001
<i>Timalinyssus longitarsus</i> Wang & Wang, 2008	<i>Garrulax canorus canorus</i> (Linnaeus)	Leiothrichidae	China	Wang and Wang 2008
	<i>Garrulax pectoralis</i> (Gould)	Leiothrichidae	China	Mironov and Proctor 2011
<i>Timalinyssus curvilobus</i> Mironov & Proctor, 2011	<i>Ianthocinclia sannio</i> (Swinhoe)	Paradoxornithidae	China	Mironov and Proctor 2011
<i>Timalinyssus gallator</i> Mironov & Proctor, 2011	<i>Lioparus chrysotis</i> (Blyth)	Leiothrichidae	China	Mironov and Proctor 2011
<i>Timalinyssus actinodurae</i> Constantinescu, 2014	<i>Actinodura cyanouroptera</i> (Hodgson)	Leiothrichidae	India	Constantinescu et al. 2014a
<i>Timalinyssus wablangi</i> sp. n.	<i>Heterophasia gracilis</i> (McClelland)	Leiothrichidae	India	Present paper

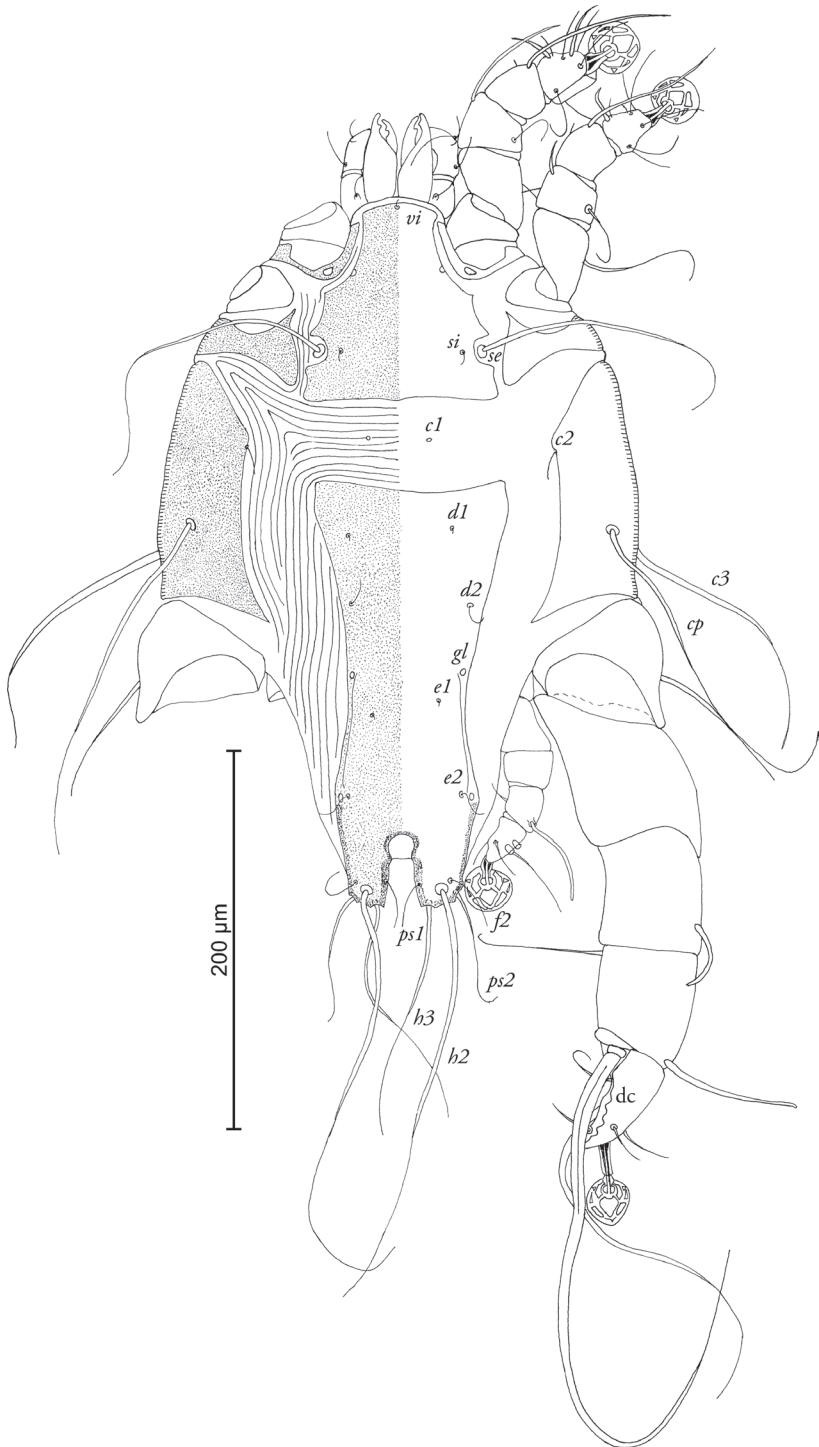


Figure 1. *Timalinyssus wahlangi* sp. n., male holotype: dorsal view of idiosoma. Abbreviations: dc – dorsal crest.

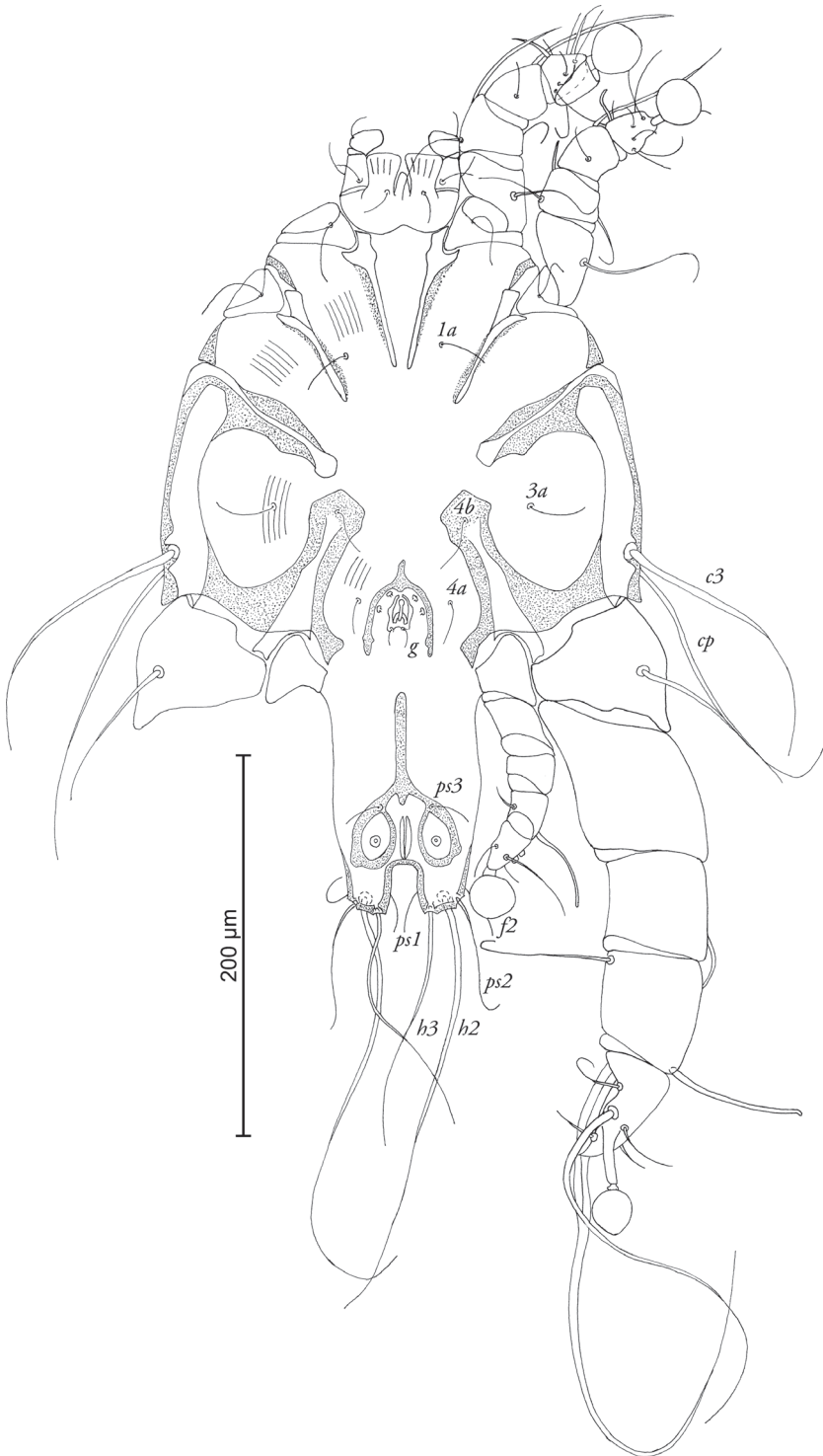


Figure 2. *Timalinyssus wablangi* sp. n., male holotype: ventral view of idiosoma.

inner and lateral angles and bidentate posterior margin. Terminal cleft U-shaped, length 20 (18–21), supranal concavity opens posteriorly. Position of setae *e1* posterior to gland openings *gl*. Lengths of dorsal setae: *c2-d2* 94 (94–105), *d2-e2* 98 (98–110), *d2-gl* 36 (36–37), *e2-h2* 46 (36–46), *h2-h2* 42 (42–54), *h3-h3* 28 (28–30), *ps1-h3* 8 (6–8). Transventral sclerite absent, epiandrum horseshoe-shaped with short anterior extension, posterior tips extending considerably beyond base of genital apparatus (Fig. 2). Length of genital apparatus 18 (18–20), width at base 12 (12–14), aedeagus length 12 (9–12). Setae *g* situated on base of genital arch. Anal suckers ovate, their size excluding surrounding membrane: longer diameter 18 (14–18), shorter diameter 12 (12–14). Adanal shield shaped as an inverted Y, narrow, almost completely encircling anal field. Ventral measurements: *4b-3a* 38 (38–40), *4a-g* 24 (22–26), *3a-4a* 68 (68–76), *ps3-ps3* 26 (20–26), *ps3-h3* 44 (42–44). Tarsus III 60 (58–74) in length, with acute apical process and 5 denticles on dorsal longitudinal crest, macrochaeta *r* with very thick basal part, macrochaeta *s* about 1/3 of macrochaeta *r*, other tarsal setae filiform, shorter than segment (Fig. 5 B).

FEMALE (Figs 3; 4; range for 4 paratypes): Idiosoma 345–380 long, 185–200 wide. Prodorsal shield not fused with scapular shields, posterior margin slightly concave, length of shield 98–100, width 100–110, setae *se* separated by 82–92. Setae *c2* hair-like, about 12–14 long, situated on striated tegument. Hysteronotal shield almost rectangular, with anterior margin slightly concave, anterior part of this shield with rounded lateral extensions, lateral margins with deep incisions between bases of setae *e2* and *f2*, length 220–230, width at anterior margin 96–110. Distance along midline between prodorsal and hysteronotal shields 28–36. Posterior end of opisthosoma with 1 pair of widely separated opisthosomal lobes bearing bases of setae *h3*. Opisthosomal lobes small, with oblique posterior margin, without membrane. Length of terminal cleft 18–24, width at lobar bases 52–68. Position of setae *e1* posterior to gland openings *gl*. Dorsal measurements *c2-d2* 74–82, *d2-e2* 80–90, *e2-h3* 72–74, *d2-gl* 40–44, *e1-gl* 30–40, *h2-ps1* 34–38, *h2-h2* 110–120, *h3-h3* 70–88. Epigynium approximately semicircular, 28–30 long, 66–72 wide. Apodemes of egg-laying opening extending to midlevel of trochanters III. Epimerites IVa present, rudimentary. Legs IV extending to level of setae *h2*.

Etymology. The new species is named in a memory of Mr. Dran Wahlang, a father of the junior coauthor, D. Khlur B. Mukhim.

Remarks. Of the six previously known species, *Timalinyssus wahlangi* sp. n. is closest to *T. actinodurae* Constantinescu, 2014 from *Actinodura cyanouroptera* (Hodgson) (Leiothrichidae) (Constantinescu et al. 2014a). Males in both species have the prodorsal shield not fused with scapular shields, setae *c2* situated on medial margins of the humeral shields, the adanal shield shaped as an inverted Y, a similar shape of tarsus III with an acute apical process and small denticles on the dorsal longitudinal crest, and setae *r* and *s* represented by macrochaetae. Males of the new species clearly differ from those of *T. actinodurae* in having the following features: setae *se* are situated on the striated tegument, setae *e1* are situated posterior to the level of gland openings *gl*, the hysteronotal shield has a concave anterior margin, setae *ps1* are situ-

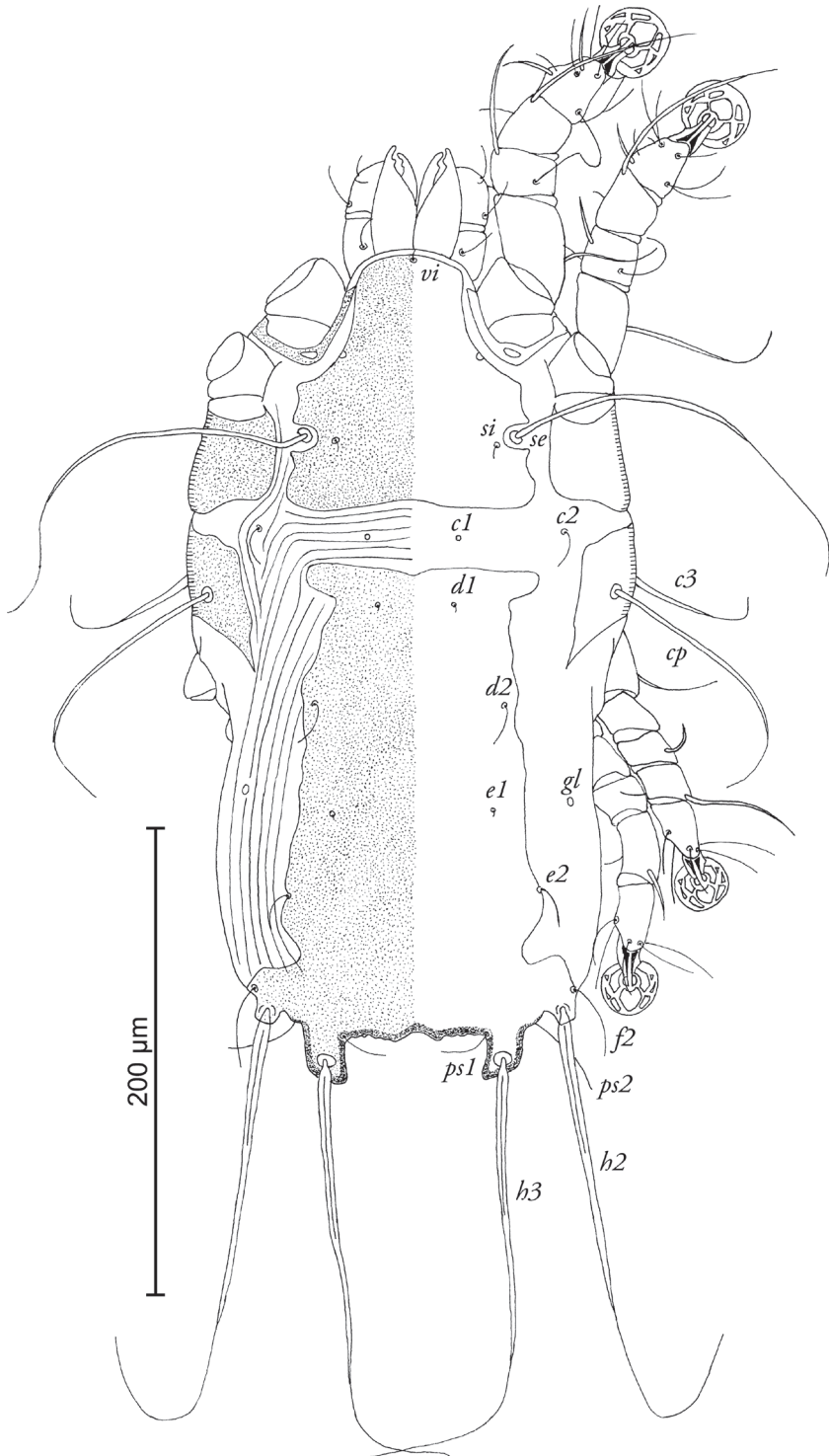


Figure 3. *Timalinyssus wahlangi* sp. n., female paratype: dorsal view of idiosoma.

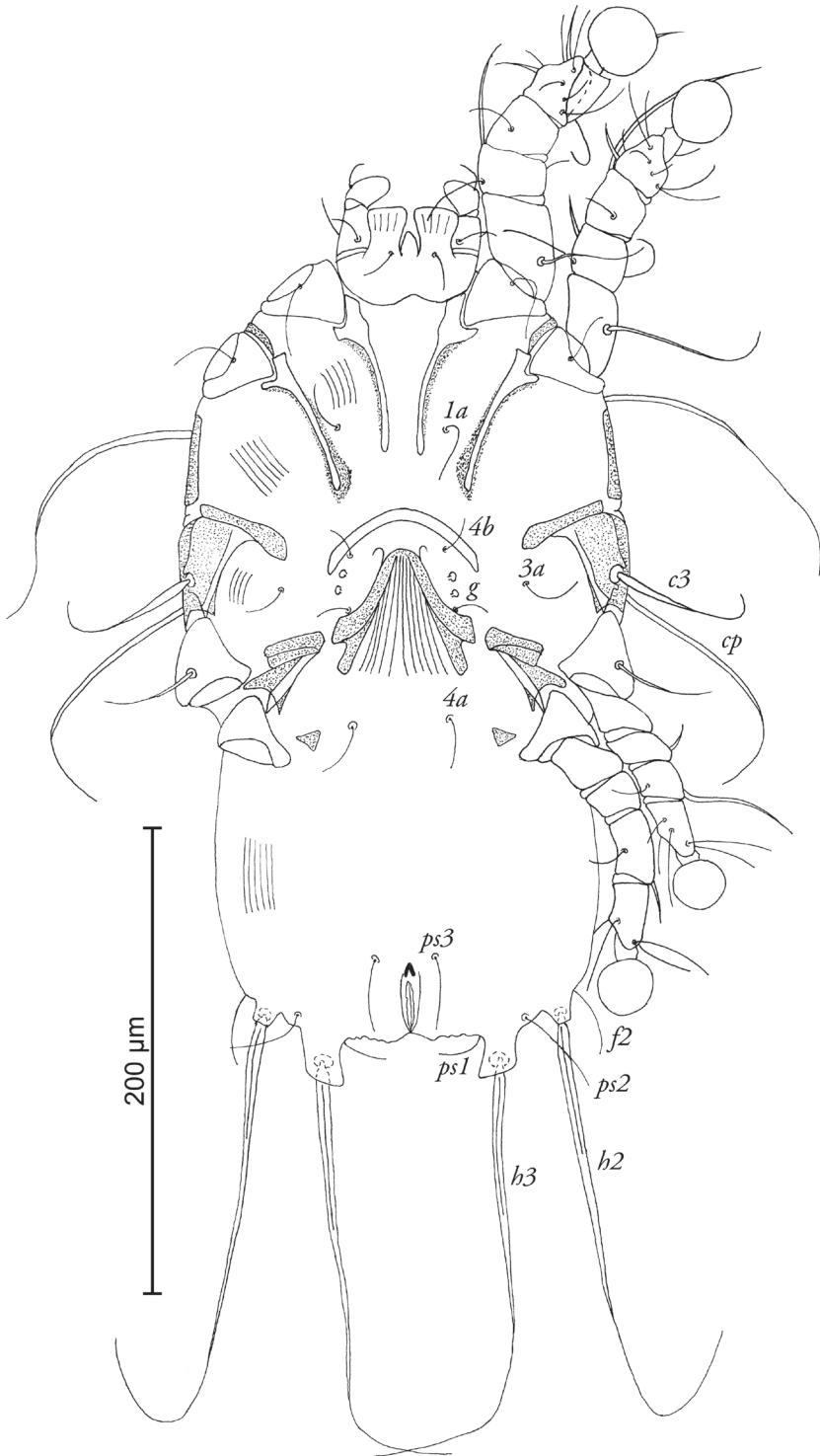


Figure 4. *Timalinyssus wablengi* sp. n., female paratype: ventral view of idiosoma.

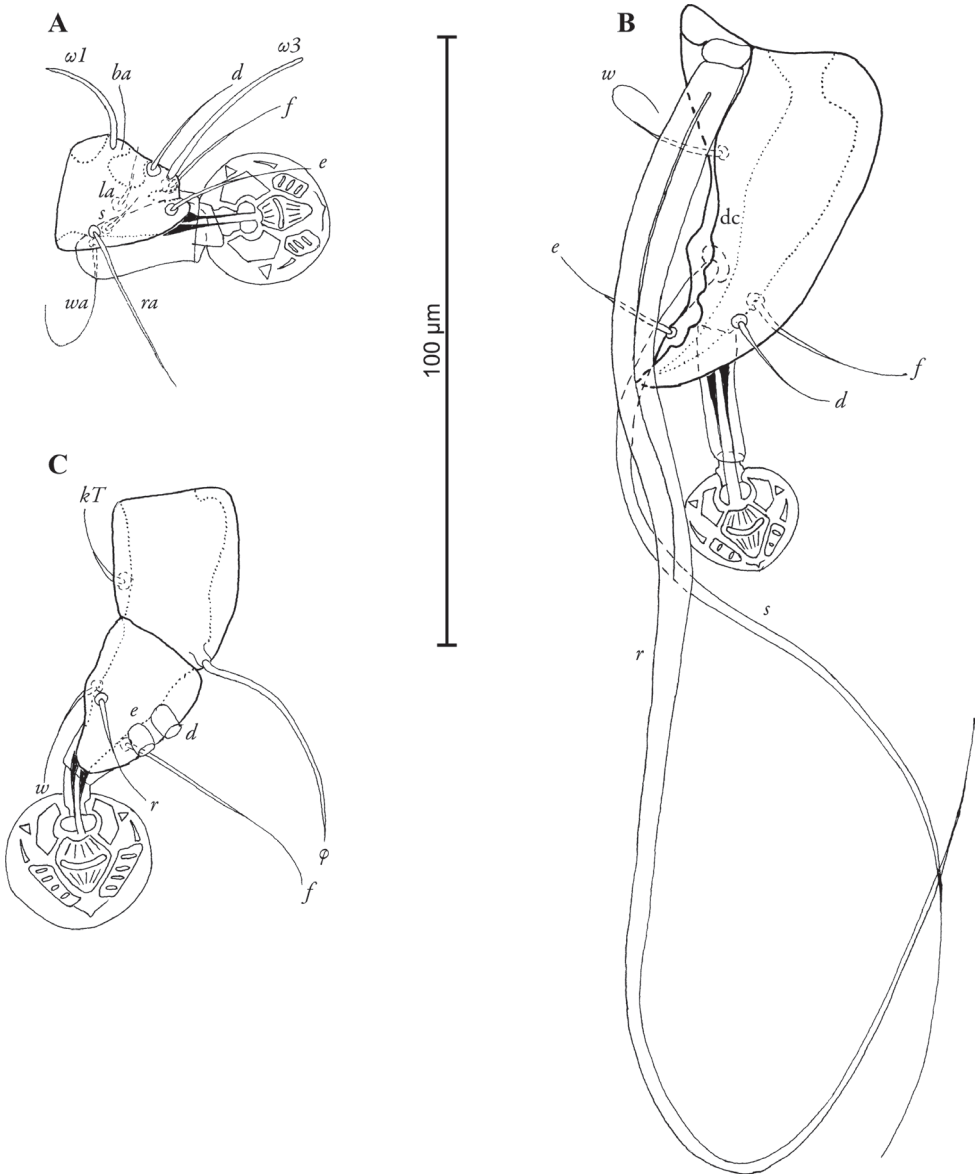


Figure 5. *Timalinyssus wahlangi* sp. n., details of male legs, dorsal view: **A** tarsus of leg I **B** tarsus of leg III **C** tibia and tarsus of leg IV; Abbreviations: dc – dorsal crest.

ated clearly distant from the inner angle of the opisthosomal lobes, the transventral sclerite is absent, the epiandrum is horseshoe-shaped with short anterior extension, and dorsal longitudinal crest of tarsus III has 4-5 denticles. In males of *T. actinoduræ*, setae *se* are situated on the prodorsal shield, setae *e1* are situated approximately at the same transverse level with the gland openings *gl*, the hysteronotal shield has a straight anterior margin, the setae *ps1* are situated almost apically, the transventral sclerite is

present, epiandrum is shaped as an inverted U and fused with the posterior end of the transventral sclerite, and the dorsal longitudinal crest of tarsus III has 2 denticles. Females in both species have opisthosomal lobes short and separated by wide terminal cleft and the hysteronotal shield with lateral extensions in anterior part. Females of *T. wahlangi* sp. n. differ from those of *T. actinodurae* (and also of the other five known species) by the shape of the hysteronotal shield that has lateral margins with deep incisions between setae *e2* and *f2*. Furthermore, females of the new species differ from those of *T. actinodurae* in having the prodorsal shield not fused with scapular shields, setae *se* situated on the striated tegument, the opisthosomal lobes without lateral membranes, and legs IV extending to the level of setae *h2*. Females of *T. actinodurae* have the prodorsal shield fused with the scapular shields, setae *se* are situated on the prodorsal shield, the opisthosomal lobes have lateral membranes, and legs IV do not extend to the level of setae *h2*.

Key to males of *Timalinyssus*

- 1 Prodorsal shield fused with scapular shields 2
- Prodorsal shield not fused with scapular shields 3
- 2 Setae *se* situated on prodorsal shield, transventral sclerite present, setae *ps2* narrowly lanceolate, setae *h3* longer than *h2*, tarsus III with one macrochaeta *r* *T. oliferae*
- Setae *se* situated on striated tegument, transventral sclerite absent, setae *ps2* filiform, setae *h2* longer than *h3*, tarsus III with two macrochaetae, *r* and *d*.. *T. formosanus*
- 3 Setae *c2* situated on medial margin of humeral shields 4
- Setae *c2* situated on striated tegument or on anterior margin of humeral shields 5
- 4 Transventral sclerite present, setae *e1* and gland openings *gl* at the same transverse level, dorsal longitudinal crest of tarsus III with 2 poorly distinct denticles *T. actinodurae*
- Transventral sclerite absent, setae *e1* situated posterior to level of gland openings *gl*, dorsal longitudinal crest of tarsus III with 4-5 denticles *T. wahlangi* sp. n.
- 5 Setae *c2* situated on anterior margin of humeral shields, opisthosomal lobes strongly elongated and bifurcate apically, legs III longer than length of idiosoma *T. grillator*
- Setae *c2* situated on striated tegument, opisthosomal lobes short and without apical bifurcation, legs III shorter than length of idiosoma 6
- 6 Opisthosomal lobes straight, epiandrum present; tarsus III with acute apical process, two macrochaetae *r* and *s*, and indented dorsal crest .. *T. longitarsus*
- Opisthosomal lobes bent towards, epiandrum absent; tarsus III with bidentate apical process, one macrochaeta *r*, and smooth dorsal crest *T. curvilobus*

Key to females of *Timalinyssus*(Female of *T. grallator* unknown)

- 1 Dorsal setae *f2* and *h2* situated on hysteronotal shield 2
 – Dorsal setae *f2* and *h2* situated on striated tegument ***T. longitarsus***
- 2 Opisthosomal lobes present, external copulatory tube absent 3
 – Without distinct opisthosomal lobes, external copulatory tube present
 ***T. curvilobus***
- 3 Opisthosomal lobes longer than wide and separated by narrow terminal cleft 4
 – Opisthosomal lobes small and separated by terminal cleft much wider than lobes 5
- 4 Anterior part of hysteronotal shield with rounded lateral extensions, setae *e1* anterior to level of gland openings *gl*, setae *se* situated on prodorsal shield... ***T. oliferae***
 – Anterior part of hysteronotal shield without rounded lateral extensions, setae *e1* posterior to level of gland openings *gl*, setae *se* situated on striated tegument ***T. formosanus***
- 5 Prodorsal shield fused with scapular shields, setae *se* on prodorsal shield, lateral margins of hysteronotal shield without incisions, opisthosomal lobes with lateral membrane, legs IV not extending to level of setae *h2*. ***T. actinoduruae***
 – Prodorsal shield not fused with scapular shields, setae *se* on striated tegument, lateral margins with deep incisions between *e2* and *f2* setae, opisthosomal lobes without lateral membrane, legs IV with ambulacral discs extending to level of setae *h2*..... ***T. wablangi* sp. n.**

Acknowledgments

We are grateful to the Additional Principal Chief Conservator of Forests, Wildlife & Chief Wildlife Warden from Shillong (Meghalaya, India) for the permission to catch birds (permission No. FWC.G/173/Pt.). We would like to thank our proofreader, PhD. Ana Wetzl (Assistant Professor of English, Kent State University at Trumbull, USA).

References

- Clements JF, Schulenberg TS, Iliff MJ, Sullivan BL, Wood CL, Roberson D (2013) The eBird/Clements checklist of birds of the world. Version 6.9. <http://www.birds.cornell.edu/clementschecklist/download/> [accessed August 2015]
- Constantinescu IC, Chişamera G, Mukhim KB, Adam C (2014a) Two new feather mite species of the family Pteronyssidae (Acarina: Analgoidea) from Meghalaya (Northeast India). *Zootaxa* 3774(4): 351–366. doi: 10.11646/zootaxa.3774.4.4

- Constantinescu IC, Chişamera G, Mukhim KB, Adam C (2014b) Two new species of feather mites (Acarina: Psoroptidia) from the Great Barbet, *Psilopogon virens* (Piciformes: Megalaimidae). *Zootaxa* 3893(1): 127–142. doi: 10.11646/zootaxa.3893.1.6
- Faccini JL, Atyeo WT (1981) Generic Revision of the Pteronyssinae and Hyonyssinae (Analgoidea: Avenzoariidae). *Proceedings of the Academy of Natural Sciences of Philadelphia* 133: 20–72.
- Gaud J, Atyeo WT (1996) Feather mites of the world (Acarina, Astigmata): the supraspecific taxa. *Musée Royal de l’Afrique Centrale, Annales Sciences Zoologiques* 277: 1–191.
- Gaud J, Mouchet J (1959) Acariens plumicoles des oiseux du Cameroun. V. Pterolichidae. *Annales de Parasitologie humaine et comparée* 34: 493–545.
- Griffiths DA, Atyeo WT, Norton RA, Lynch CA (1990) The idiosomal chaetotaxy of astigmatid mites. *Journal of Zoology* 220: 1–32. doi: 10.1111/j.1469-7998.1990.tb04291.x
- Grimmett R, Inskipp C, Inskipp T (2011) *Helm Field Guides: Birds of the Indian Subcontinent*. Christopher Helm, London, 528 pp.
- Hernandes FA (2012) Two new feather mite species (Acari, Pteronyssidae) from the white-barred piculet, *Picumnus cirratus* (Aves, Piciformes). *Folia Parasitologica* 59: 301–307. doi: 10.14411/fp.2012.042
- Mironov SV (1990) New species of the feather mites of the genus *Mouchetia* (Analgoidea: Avenzoariidae) from Passeriformes in Vietnam. *Parazitologiya* 24: 268–278. [In Russian]
- Mironov SV (1992) Five new species of the feather mite genus *Pteroherpus* Gaud (Analgoidea: Avenzoariidae) from passerine birds of Vietnam. *International Journal of Acarology* 18: 257–268. doi: 10.1080/01647959208683958
- Mironov SV (2001) Description of four new genera of the feather mite family Pteronyssidae Oudemans 1941 (Astigmata: Analgoidea) with notes on systematic of the family. *Acarina* 9(1): 3–22.
- Mironov SV (2005) A new feather mite genus, *Megalaimobius* gen. n. (Astigmata: Pteronyssidae), from the Asian Barbets (Piciformes: Ramphastidae: Megalaiminae) in Vietnam. *Acarina* 13(2): 117–126.
- Mironov SV, Proctor HC (2011) Four new feather mite species of the family Pteronyssidae (Astigmata: Analgoidea) from Laughing-Thrushes (Passeriformes: Timaliidae) in China. *Acarina* 19: 35–51.
- Mironov SV, Wauthy G (2005a) A review of the feather mite genus *Pteronyssoides* Hull, 1931 (Astigmata: Pteronyssidae) from African and European passerines (Aves: Passeriformes) with analysis of mite phylogeny and host associations. *Bulletin de L’Institut Royal des Sciences Naturelles de Belgique, Entomologie* 75: 155–214.
- Mironov SV, Wauthy G (2005b) A new species of the feather mite genus *Mouchetia* Gaud, 1961 (Astigmata: Pteronyssidae) from the greencap eremomela *Eremomela scotops* (Passeriformes: Sylviidae) and taxonomic notes to species of the genus. *Acarina* 13: 3–14.
- Mironov SV, Wauthy G (2008) A systematic review of the feather mite genus *Pteroherpus* Gaud, 1981 (Astigmata: Pteronyssidae). *Bulletin de L’Institut Royal des Sciences Naturelles de Belgique, Entomologie* 78: 155–200.
- Norton AR (1998) Morphological evidence for the evolutionary origin of Astigmata (Acari: Acariformes). *Experimental & Applied Acarology* 22: 559–594. doi: 10.1023/A:1006135509248

- Oudemans AC (1941) Neue Funde auf dem Gebiete der Systematik und der Nomenklatur der Acari. Zoologischer Anzeiger 136: 177–186.
- Rasmussen PC, Anderton JC (2012) Birds of South Asia – The Ripley Guide (Volumes 1 and 2; second edition). National Museum of Natural History – Smithsonian Institution, Michigan State University and Lynx Edicions, Washington, DC, Michigan and Barcelona, 684 pp. [vol. 1], 378 pp. [vol. 2].
- Wang ZY, Wan JJ (2008) A new species of feather mite: *Timalinyssus* Mironov, 2001 (Astigmata: Pteronyssidae) from *Garrulax canorus canorus* (Linnaeus) (Passeriformes: Timaliidae) in China. Zootaxa 1962: 65–68.

A revision of *Megalocraerus* Lewis, 1902 (Coleoptera, Histeridae: Exosternini)

Michael S. Caterino¹, Alexey K. Tishechkin²

1 Department of Agricultural & Environmental Sciences, Clemson University, Clemson, SC 29634-0310 USA **2** USDA Systematic Entomology Laboratory, c/o Smithsonian Institution, National Museum of Natural History, Washington, DC 20013-7012

Corresponding author: Michael S. Caterino (mcateri@clemson.edu)

Academic editor: J. Klimaszewski | Received 4 November 2015 | Accepted 19 January 2016 | Published 28 January 2016

<http://zoobank.org/F77F8AA3-BCF6-4367-A6EA-997CD9076F26>

Citation: Caterino MS, Tishechkin AK (2016) A revision of *Megalocraerus* Lewis, 1902 (Coleoptera, Histeridae: Exosternini). *ZooKeys* 557: 59–78. doi: 10.3897/zookeys.557.7087

Abstract

The formerly monotypic Neotropical genus *Megalocraerus* Lewis is revised to include five species, known from southeastern Brazil to Costa Rica: *M. rubricatus* Lewis, *M. mandibularis* **sp. n.**, *M. chico* **sp. n.**, *M. madrededios* **sp. n.**, and *M. tiputini* **sp. n.** We describe the species, map their distributions, and provide a key for their identification. Their subcylindrical body form and emarginate mesosternum have previously hindered placement to tribe, although their current assignment to Exosternini now appears well supported by morphological evidence. Nothing is known of the natural history of the species.

Keywords

Histeridae, Histerinae, Exosternini, subcortical predator, Neotropical region

Introduction

Megalocraerus Lewis is a rarely-collected, hitherto monotypic genus of Histerinae, occurring only in the Neotropical realm, of historically uncertain placement. When Lewis (1902) established the genus, uncertainty about its relationships was already evident in his comparison to various genera: “The genus established here is represented by a species having the superficies of *Pachycraerus* [Marseul], but the mesosternum is not produced anteriorly and the tarsal grooves in the anterior tibiae are straight. The

antennal fossettes are similar to those of *Exosternus*” (Lewis 1902). Lewis’s ‘superfices of *Pachycraerus*’ most likely referred to the elongate, subcylindrical body shape shared by these two genera. When Bickhardt (1917) established tribes in Histerinae, *Megalocraerus* was placed in Histerini, while the other two genera were placed in Exosternini, defined by the projecting mesoventrite *Megalocraerus* had been noted to lack. The genus has received little further attention, and has remained in Histerini since, through several recent catalogs (Mazur 1984, 1997, 2011).

There have been few attempts to refine tribes in Histerinae, and none have attempted to distinguish symplesiomorphies from synapomorphies. Diagnoses based on single characters, such as presence or absence of a projecting mesoventrite, exemplify this ambiguity. According to recent treatments, Histerini includes those Histerinae with the anterior margin of the mesoventrite emarginate or straight (Bickhardt 1917), the protarsal grooves straight (Bickhardt 1917), and two complete antennal annuli present (Mazur 1990). While *Megalocraerus* satisfies the first two of these, no more than a single complete antennal annulus can be seen. However, the elongate subcylindrical shape of *Megalocraerus* is otherwise unknown in Histerini. *Megalocraerus* is excluded from either Platysomatini or Omalodini by its lack of distinctly ‘V’-shaped antennal annuli (Mazur 1990). Mazur’s (1990) definition of Exosternini relied only on reduced antennal annuli and a ‘simple, tubular’ penis, implicitly discarding the shape of the anterior mesoventral margin as significant. Despite the fact that this loose definition of Exosternini could have included *Megalocraerus*, it has never been reassigned.

Recent attempts to resolve phylogenetic relationships in Exosternini and Histerinae (Caterino and Tishechkin 2015, Leivas et al. 2015) have mostly served to show that none of the tribes of Histerinae are monophyletic as currently constituted (perhaps true even of the subfamily). However, *Megalocraerus* is closely related to most other Neotropical Exosternini, with particularly close relationships to *Hypobletus* Schmidt. Among their putative synapomorphies, some of the most reliable would be elongate body form, emarginate mesoventrite, emarginate epistoma, antennal club with reduced annuli, and apices of elytra with increasingly distinct punctures (reconstructed as a parallelism with *Baconia*, in which this condition is also distinct). Noteably, the Afro-tropical genera suggested by Lewis (1902) to show some commonalities, *Pachycraerus* and *Exosternus*, are far removed (all results from Caterino and Tishechkin 2015).

In addition to hereby formally reassigning *Megalocraerus* to Exosternini (at least pending further work on tribal definitions of Histerinae), we herein describe several newly discovered species in the genus, which serve to broaden its scope and morphological diversity considerably.

Materials and methods

The morphological terminology used follows Caterino and Tishechkin (2014), based on Wenzel and Dybas (1941), Helava et al. (1985), Ôhara (1994) and Lawrence et al. (2011). Total body length is measured from the anterior margin of the pronotum to the

posterior margin of the elytra (to exclude preservation variability in head and pygidial extension); width is measured at the widest point, generally near the elytral humeri. Conventional imaging was done using a Visionary Digital's 'Passport' portable imaging system, which incorporates a Canon 7D with MP-E 65mm 1–5× macro zoom lens. Images were stacked using Helicon Focus software (www.heliconsoft.com). SEM imaging was done on a Zeiss EVO 40 scope, and the specimen was sputter coated with gold.

Collections are abbreviated as follows:

BMNH	Natural History Museum, London, UK
CHND	The Nicolas Dégallier collection, Paris, France
FMNH	The Field Museum, Chicago, USA
FSCA	Florida State Collection of Arthropods, Gainesville, USA
INBIO	Instituto Nacional de Biodiversidad, San Jose, Costa Rica
SEMC	Snow Entomology Museum, University of Kansas, Lawrence, USA
UFPR	Universidade Federal do Paraná, Curitiba, Brazil

Taxonomy

Megalocraerus Lewis, 1902

Megalocraerus Lewis, 1902: 231

Type species. *Megalocraerus rubricatus* Lewis, by monotypy.

Diagnosis. The genus is readily separated from other Histerinae in the Neotropics, where few other large cylindrical species have been described. In addition to this general body shape, the depressed epistoma and reduced, subtriangular labrum will distinguish any member of the genus easily.

Description. **Size range:** Length 2.8–4.1 mm; width 2.0–2.6 mm; **Body:** elongate, parallel-sided, subcylindrical, slightly depressed; body castaneous to piceous, rarely bi-colored with the elytral bases rufescent. **Head:** Frons broad, prominent, slightly bulging in front of eyes, becoming depressed and narrowing toward concave epistoma; frontal disc coarsely punctate; frontal stria deeply impressed along inner edges of eyes, angled anteromediad at front, interrupted across width of epistoma, free ends may be bent mediad or dorsad; supraorbital stria largely obsolete, fragments may be present at middle; labrum reduced, short and subtriangular, apex rounded to subangulate; mandibles rather short, more or less evenly curved to subacute apices, usually with prominent tooth on each incisor edge, lacking inner submarginal ridge; antennal scape moderately expanded to apex, with carina along outer posterior edge, funicle gradually expanded, antennomere 8 broadly cupuliform; antennal club rounded, not elongate, apex rounded to subtruncate, with apical and subapical annuli crowded into apical third, subapical annulus weakly expanded at middle of dorsal and ventral surfaces, basal annulus absent; gena

narrowly depressed posterad cardo; gular sutures visible but not impressed; submentum short, with apical row of ~15 setae; mentum narrowing anterad, apex emarginate, with sparse setae; labial and maxillary palpi basically fusiform, narrowed apically. **Pronotum:** Pronotal sides subparallel, weakly rounded, narrowed anteriorly, apical emargination broad; vaguely but indistinctly depressed in prescutellar region; anterior gland openings very fine, present on sides of anterior emargination; marginal stria complete along sides, variably fragmented to obsolete along anterior margin; marginal pronotal stria very fine, continuous around lateral and anterior margins. **Elytra:** two (rarely three) complete epipleural striae present, innermost continued variably mediad along part of anterior elytral margin; inner and outer subhumeral striae at most weakly indicated, generally absent; striae 1–4 complete, 5th stria complete or basally abbreviated; sutural stria complete, connected to base of 5th or rarely 4th stria; elytral disc with coarser punctation toward apex, ground punctation usually very fine and sparse but may be coarser and more conspicuous; elytral striae tending to become prolonged mediad along the basal elytral margin, sometimes forming a distinct stria. **Prosternum:** Prosternal lobe broad, about two-thirds length of keel; with marginal stria variably obsolete at sides; prosternal keel weakly produced posteriorly, with two complete carinal striae free or joined at apices; lateral striae of keel widely divergent anterad along presternal suture. **Mesoventrite:** Anterior mesoventral margin broadly, not too deeply emarginate, with complete marginal stria, often with secondary fragments in anterolateral corners; mesometaventral stria absent. **Metaventrite:** Postmesocoxal stria short or indistinct; inner lateral metaventral stria variably abbreviated apically, not reaching metacoxa; disc with only fine ground punctation. **Abdomen:** Abdominal ventrite 1 usually with one more or less complete lateral stria, anterior margin lacking stria; propygidium short, 4–5× broader than long, disc lacking obvious gland openings; pygidium with apical margin broadly rounded, lacking marginal stria. **Legs:** Protrochanter lacking setae; meso- and metatrochanters each with two very short setae (often abraded or lost); protibia acutely multidentate, with 5–6 lateral marginal spines and 2–3 fine apical marginal spines; two protibial spurs present, short; tarsal groove on anterior surface only well developed in apical fourth; protarsi not sexually dimorphic, with single pair of apical setae on most tarsomeres; mesotibial margin distinctly multidentate, with 3–6 marginal denticles; metatibial margin not toothed, but with several fine marginal spines, tarsal claws simple; apical tarsomere on all tarsi elongate, curved; ventral tarsal setae variable, simple to flattened and sublaminar. **Male:** accessory sclerites absent; 8th tergite subparallel-sided to narrowed apically, basal apodemes of 8th tergite with thin, acute ventral extensions curving distad, convergent medially, separated from body of tergite by deep lateral emarginations parallel to basal margin; ventrolateral lobes rounded to subacute, variably separated along ventral midline; 8th sternite divided along midline with inner edges parallel, more or less approximate, outer upper edges produced apically into narrow, convergent processes or broad lobes, apices with thin velar membrane between, lacking distinct setae; 9th tergite with apices narrow, roundly convergent, lacking setae, ventrolateral apodemes weak to distinctly dentate; spiculum gastrale (S9) generally wide-stemmed, relatively weakly sclerotized along midline, apices divergent but not strongly produced or hooked; 10th

tergite entire or variously partially divided, usually evenly sclerotized but sometimes appearing more strongly sclerotized toward apex; basal piece about one-fourth tegmen length, with apicoventral apodemes produced, more or less convergent beneath base of tegmen; tegmen rather narrow, moderately to strongly dorsoventrally flattened, usually lacking medioventral process, apices divided, sometimes distinctly separated at tips; median lobe half or greater length of tegmen, with proximal arms bent near midpoint.

Female: 8th tergite broad, relatively flat, deeply emarginate apically; 8th sternite undivided, with strongly sclerotized, straight basal apodemes; valviferae weakly expanded proximally; coxite simple, only weakly differentiated into upper and lower surfaces, lacking apical teeth, apex narrowed, subtruncate, with prominent, setose gonostyle; bursa copulatrix membranous; spermatheca forming a short, bulbous sac, inserted beneath apex of bursa, bearing single thin spermathecal gland near its base.

Distribution. This genus is known from Central and South America, from Costa Rica in the north to Rio de Janeiro state (Brazil) in the south. However, there are many gaps, with records only from Costa Rica, French Guiana, Ecuador, Peru, and Brazil, though it almost certainly occurs in the intervening areas.

Natural history. No specimen labels reveal any details of the natural history of the species of *Megalocraerus*, with all or nearly all specimens collected using flight interception ('window') traps. Given the subcylindrical, elongate morphology, an under-bark habit may be suggested, but there is no direct evidence for any such association.

Key to species

- 1 Elytra with rufescent maculations; prosternal carinal striae subparallel and relatively narrowly separated *M. rubricatus* Lewis
- Body unicolorous, black to castaneous; prosternal carinal striae divergent at least posteriorly 2
- 2 Ground punctation of elytra conspicuous, with coarse secondary punctures gradually becoming denser in apical half 4
- Ground punctation of elytra fine and largely inconspicuous; coarser apical punctures rather discretely limited to about apical one-fifth 3
- 3 Male with dorsobasal mandibular processes; ventral setae of tarsomeres simple; Guianas *M. mandibularis* sp. n.
- Male mandible unmodified; ventral setae of all tarsomeres flattened, sublaminar; Central America *M. chico* sp. n.*
- 4 Body broader, shorter and flatter, vaguely rufescent; 4th dorsal stria united with sutural stria at base, 5th stria slightly abbreviated at base; known from Peru *M. madredeios* sp. n.
- Body more elongate and more convex, piceous; 5th dorsal stria united with sutural stria at base; known from Ecuador *M. tiputini* sp. n.
- * A possibly distinct form known from French Guiana keys out here. However, we have no males to properly assess its distinctness and do not describe it here.

***Megalocraerus rubricatus* Lewis, 1902**

Figs 1–4, 8

Megalocraerus rubricatus Lewis, 1902: 231

Type material. **Lectotype**, here designated (BMNH): “Bresil”/”Jatahy, Prov. Goyas”. Although Lewis slightly differentiated the primary type locality in Goyas, his mention of a second specimen from ‘the Amazon Region’ leaves some room for ambiguity, which we address through this lectotype designation; cotype only “Bresil”.

Other material. **Brazil** (country record only; ‘Amazon Region’ as published; Lewis, 1902; BMNH). **French Guiana:** 1: Rés. des Nouragues, Régina, 4°2.27'N, 52°40.35'W, 10.x.2009, FIT, SEAG (CHND); 4: same locality and collectors, 3.xi.2009, (CHND); 1: Belvédère de Saül, 3°1'22"N, 53°12'34"W, FIT, 17.ix.2010, SEAG (CHND).

Diagnosis. The type species is the most easily recognizable in the genus, being at once the largest and most elongate, while also unique in its red basal elytral maculae. The basal sutural arch does not meet any of the other dorsal striae, whereas it is continuous with either the 4th or 5th dorsal stria in all other species.

Description. **Size:** Length 3.5–4.1 mm; width 2.3–2.6 mm; **Body:** elongate, parallel-sided, moderately depressed; castaneous with distinct red maculations on basal two-thirds of elytra. **Head:** Frons finely and doubly punctate, with medium punctures separated by about their diameters against fine ground punctation, decreasing in size but slightly increasing in density anteromediad; frontal stria present along inner margins of eyes, broadly interrupted across epistoma; supraorbital stria absent; epistoma depressed, narrowing anterad; labrum impunctate, but with fine microsculpture; mandibles each with inner marginal tooth. **Pronotum:** Pronotal sides weakly rounded, slightly narrowed anterad, marginal stria complete, lateral stria absent, fragments of anterior stria usually present; pronotal disk with small secondary punctures sparse basomedially, increasing in density toward front and sides, with fine ground punctation more or less uniform; larger punctures present along posterior margin. **Elytra:** Two complete epipleural stria present; subhumeral striae absent; dorsal striae 1–4 more or less complete, 5th stria obsolete near base, not meeting basal arch of complete sutural stria; bases of dorsal striae extending mediad along basal elytral margin, but only very rarely meeting base of next stria; ground punctation of elytral disk fine, small secondary punctures present in apical fourth. **Prosternum:** Prosternal lobe evenly rounded, complete to sides, with marginal stria usually obsolete at sides; prosternal keel with two complete carinal striae. **Mesoventrite:** Anterior mesoventral margin evenly emarginate, with complete, fine marginal stria; mesometaventral stria absent; disk with only fine ground punctation. **Metaventrite:** Metaventral disk finely punctate at middle, more coarsely so laterad lateral metaventral stria; postmesocoxal stria obscured by punctation. **Abdomen:** Abdominal ventrites rather coarsely but shallowly punctate throughout widths;

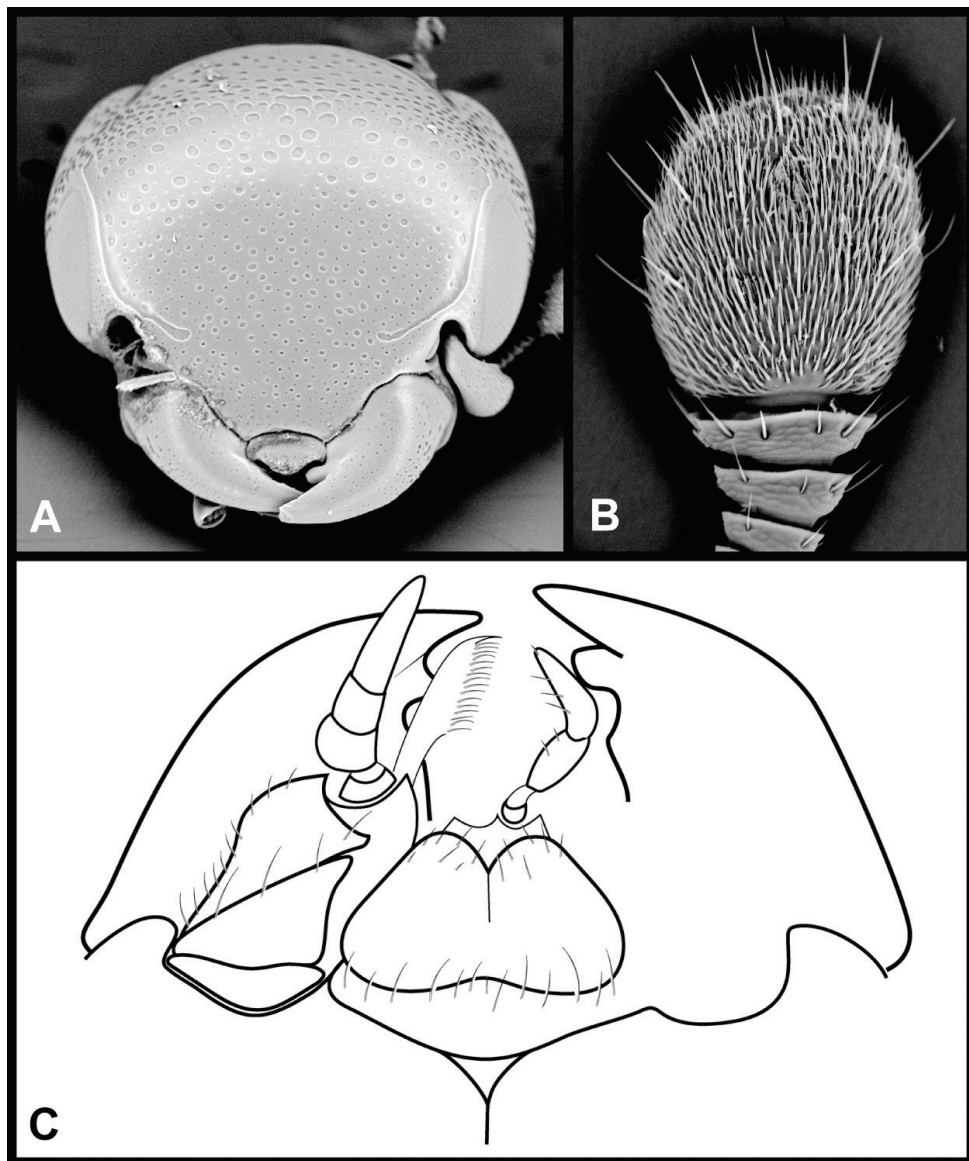


Figure 1. Generic characters of *Megalocraerus*. **A** Frons **B** Antenna **C** Mouthparts, ventral view (one maxilla and labial palpus omitted for clarity).

propygidium transverse, about three times as wide as long, coarsely punctate, with punctures separated by slightly less than their diameters; pygidium similarly coarsely punctate at base, more finely and sparsely apicad. **Male:** 8th tergite with deep, rather narrow basal emargination, ventrobasal processes nearly meeting, dorsally with fine median emargination; halves of 8th sternite approximate along much of midline,

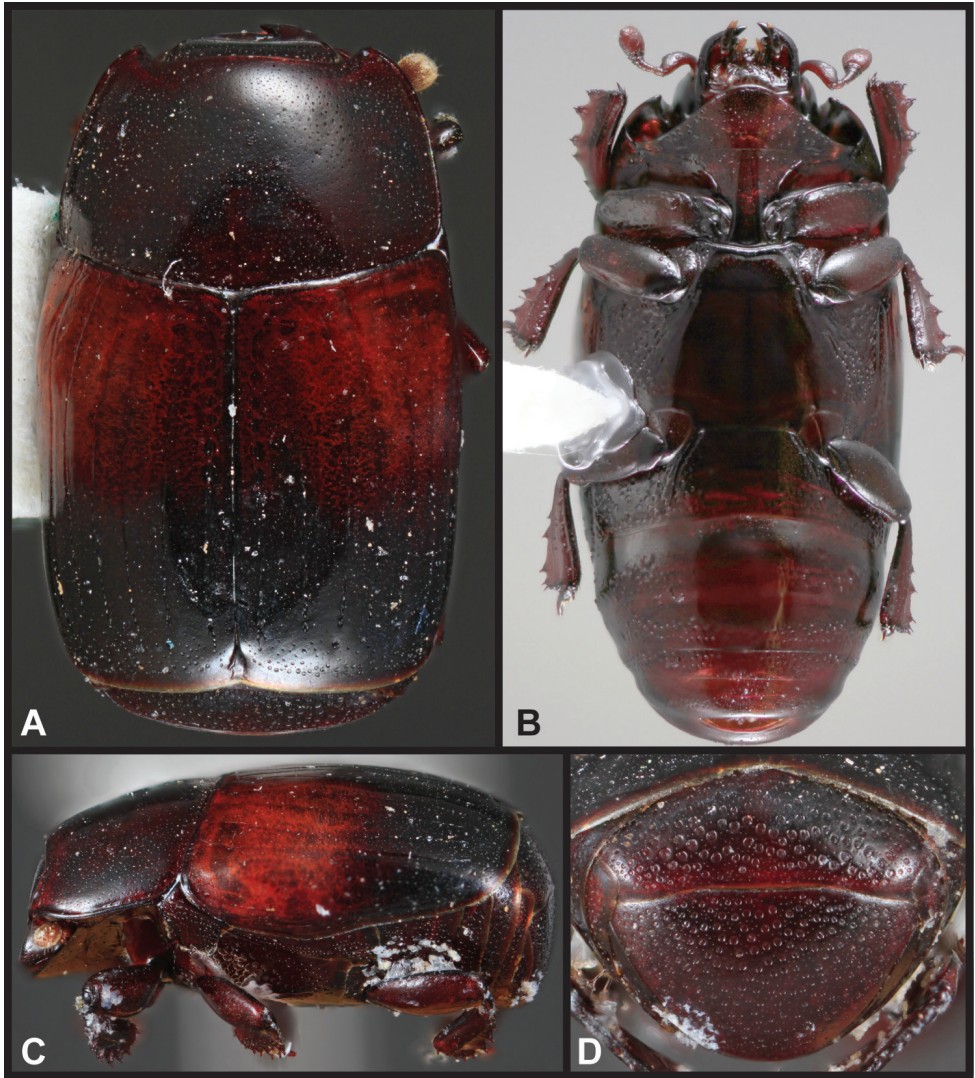


Figure 2. Lectotype of *M. rubricatus*. **A** Dorsal **B** Ventral **C** Lateral **D** Pygidial habitus.

apicomedial processes rather narrow, subacute; 9th tergite with acute, incurved apices; spiculum gastrale (S9) broad throughout, slightly narrowed at neck, apex shallowly emarginate; 10th tergite with median basal emargination; aedeagus flattened throughout, sides weakly rounded, apices slightly separated; median lobe slightly more than one-half tegmen length.

Remarks. While previously the only exemplar of the genus, *M. rubricatus* is atypical of the group in a number of ways, being significantly larger, flatter, and with distinctive coloration. It is easily recognized in the group.

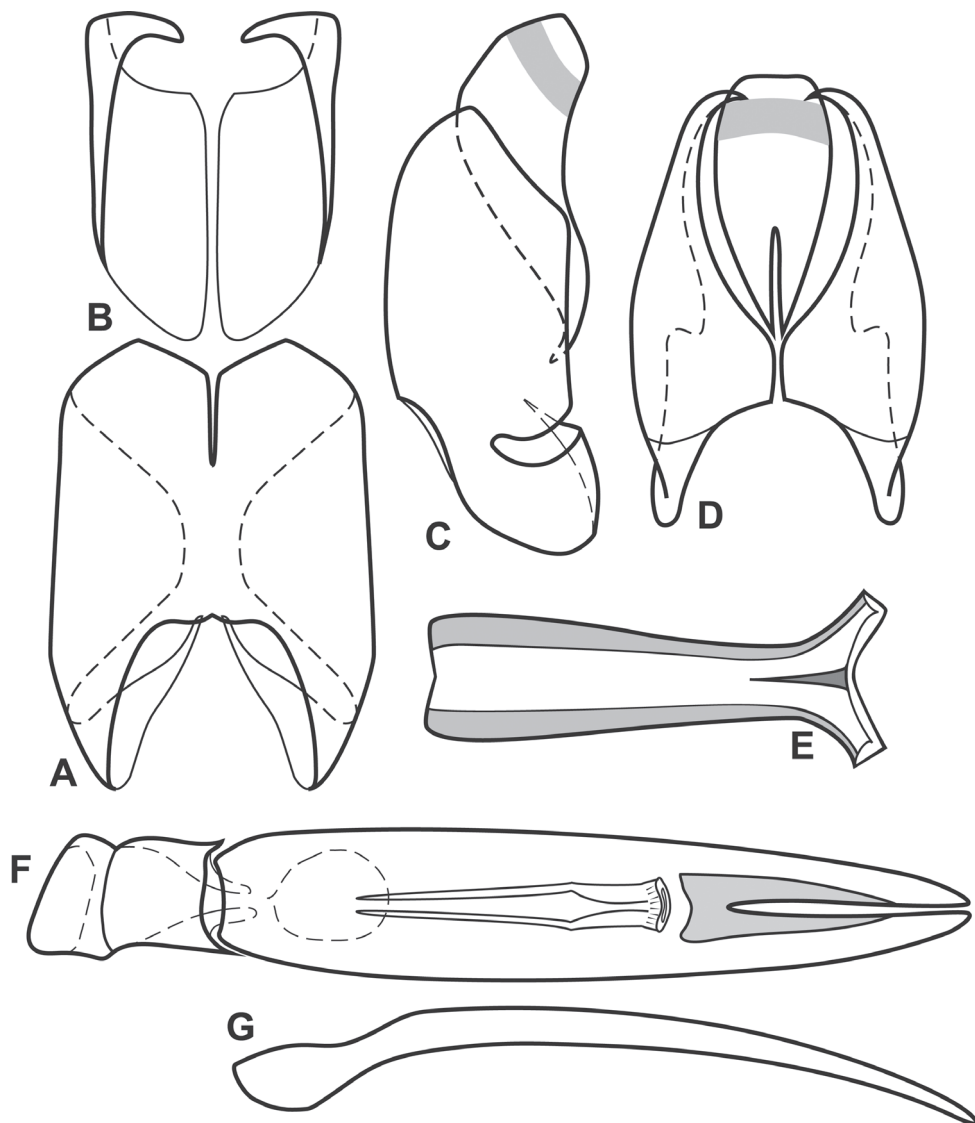


Figure 3. Male genitalia, *M. rubricatus*. **A** 8th tergite, dorsal view **B** 8th sternite, dorsal view **C** 8th tergite and sternite, lateral view, *in situ* **D** 9th and 10th tergites, dorsal view **E** 9th sternite, dorsal view **F** Aedeagus, dorsal view **G** Tegmen, lateral view.

***Megalocraerus mandibularis* sp. n.**

<http://zoobank.org/BA792625-172B-4467-ABD4-E693BAB30CD9>

Figs 5A–B, 6A–B, 8

Type material. Holotype male: “FRENCH GUIANA, KAW, xii 2014, leg: J.L.GUIGLARIS” (FMNH).

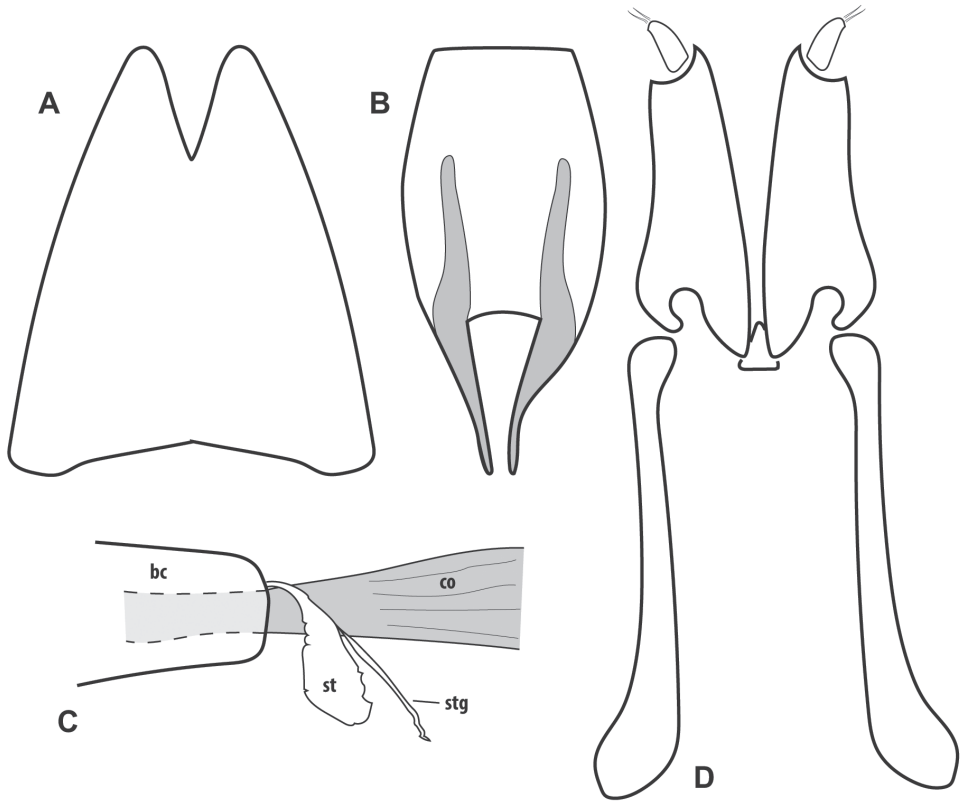


Figure 4. Female genitalia, *M. rubricatus*. **A** 8th tergite, dorsal view **B** 8th sternite, ventral view **C** Bursa copulatrix (bc), common oviduct (co), spermatheca (st) and attached spermathecal gland (stg) **D** Ovipositor.

Diagnosis. This species is very distinctive, at least in the male, exhibiting unique dorsobasal mandibular processes (Fig. 6). Because only the male is known, it is unclear if these are secondary sexual characters or not, though it seems likely. Otherwise the species is very similar to *M. chico* known from southern Central America. The two differ in tarsal setae, with *M. mandibularis* having simple ventral setae, while *M. chico* has sublaminar setae. In addition, *M. mandibularis* has rather more numerous and strongly dentate tibiae, than any other species, with the mesotibia in particular exhibiting 6 distinct spinose teeth. Other species generally show fewer and less deeply divided tibial teeth on all legs. Finally, the basal elytral stria, uniting the bases of the marginal epipleural through sutural dorsal striae, is more strongly and completely impressed here than in other species, although the extent of variation in this character in other species is difficult to assess with limited material. The male genitalia are highly distinct, showing strong dorsoventral curvature.

Description. **Size:** Length 2.8 mm; width 2.0 mm; **Body:** broad, subparallel-sided, elongate, weakly depressed; darkly castaneous. **Head:** Frons finely and doubly punctate, with medium punctures separated by slightly more than their diameters against fine ground

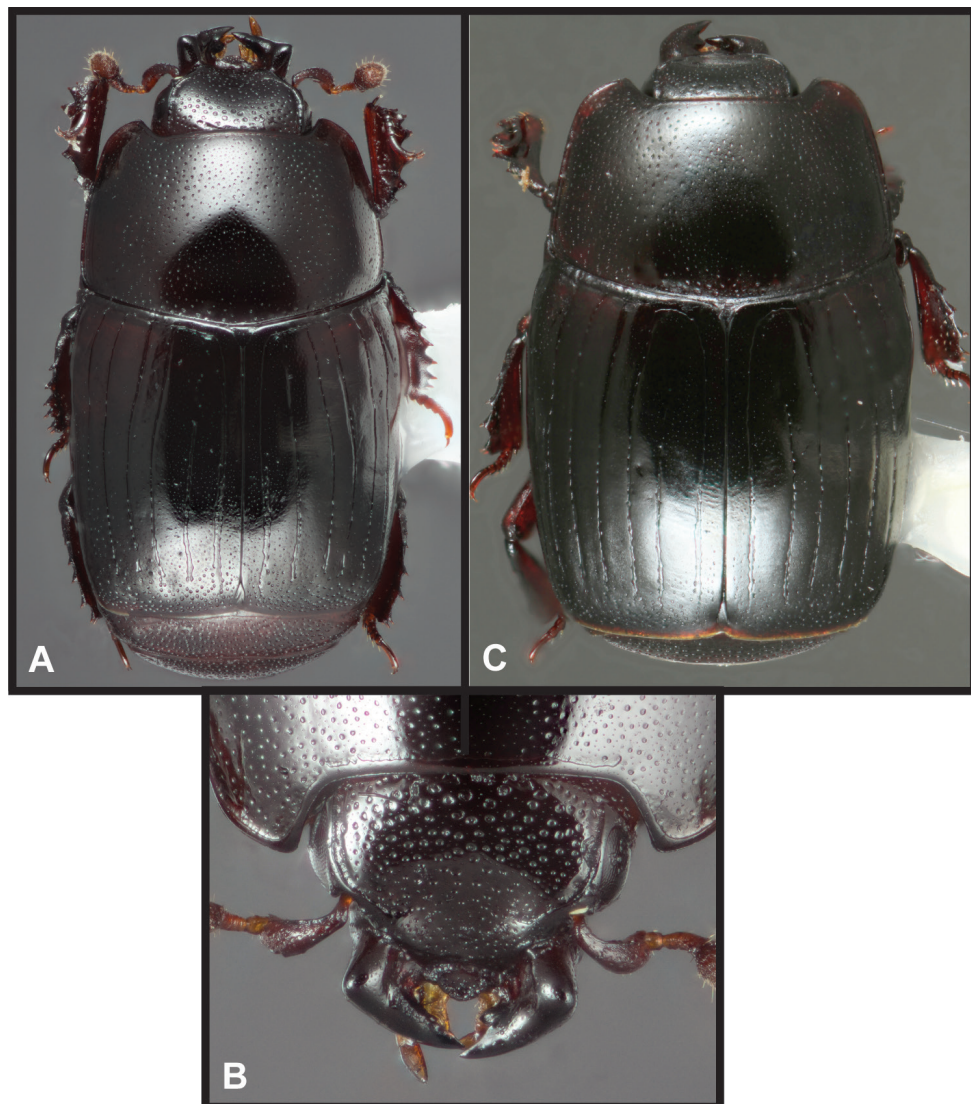


Figure 5. **A** Dorsal habitus *Megalocraerus mandibularis* **B** Mandibles male *M. mandibularis* **C** Dorsal habitus *M. chico*.

punctuation, decreasing in size but slightly increasing in density anteromedial, sparser toward the eyes; frontal stria present along inner margins of eyes, bent inward above antennal insertions, broadly interrupted across epistoma; faint fragments of supraorbital stria present; epistoma depressed, narrowing anterad; labrum minutely punctate; mandibles each with inner marginal tooth and (in male) with bluntly triangular dorsobasal process. **Pronotum:** Pronotal sides weakly convergent to anterior corners, marginal stria present along sides and front, very briefly interrupted behind eyes; pronotal disk rather finely and sparsely punctate, puncture density diminishing basomedially, with finer ground puncta-

tion throughout; basal margin with a few coarser punctures near margin. **Elytra:** Two complete and an outer partial epipleural striae present; fine fragments of inner subhumeral stria present at middle; dorsal striae 1–4 largely complete, weak or fragmented apically; 5th stria interrupted near basal third, obsolete in basal sixth; sutural stria complete; inner epipleural, 1st–4th and sutural striae connected by distinct basal marginal stria; elytral disks with fine but conspicuous ground punctation throughout, coarser secondary punctures present in apical sixth, with few secondary punctures scattered in apical interstriae, particularly along the elytral suture. **Prosternum:** Prosternal lobe evenly, somewhat narrow rounded, complete to sides, marginal stria present only at middle for approximately buccal cavity width; prosternal keel with complete carinal striae diverging slightly front and rear, indistinct around basal projection. **Mesoventrite:** Anterior mesoventral margin evenly emarginate, with complete, marginal stria; mesometaventral stria absent; disk with very fine, sparse ground punctation, with few secondary punctures at sides. **Metaventrite:** Lateral metaventral stria present, extending toward outer corner of metacoxa, slightly abbreviated apically; postmesocoxal stria indistinct. **Abdomen:** Abdominal ventrites finely punctate at middle, slightly more coarsely at sides; propygidium strongly transverse, about four times as wide as long, coarsely punctate, with punctures separated by slightly less than their diameters, rather uniformly throughout; pygidium similarly coarsely punctate at base, punctures becoming finer and denser toward apex. **Male:** 8th tergite with broad basal emargination, ventrobasal processes rather weak, not meeting beneath, dorsally with narrow median emargination; halves of 8th sternite slightly separated along midline, apico-medial processes rather narrow, subacute; 9th tergite with blunt, incurved apices; spiculum gastrale (S9) broad basally and apically, abruptly narrowed near midpoint, apex shallowly emarginate; 10th tergite entire; basal piece about one-third tegmen length, narrowly cylindrical; tegmen flattened throughout, abruptly bent ventrad one-third from base, sides weakly, sinuately divergent from base two-thirds to apex, narrowing to apices; median lobe narrow, slightly more than one-half tegmen length.

Remarks. We mention a ‘French Guiana form’ known only from females (or specimens who lost their genitalia prior to study) in the key and below. There is some slight possibility that it represents the female of this species, based not only on the distribution, but also on the shared character of relatively strongly spinose tibiae. However, the size difference is substantial, with the male *M. mandibularis* much smaller than the three known specimens of this other form. Additional material will be necessary to confidently address this question.

This species is named for its unique and prominent mandibular processes.

***Megalocraerus chico* sp. n.**

<http://zoobank.org/A7AB7A75-BEF8-4A4D-A902-7A89389FFD9E>

Figs 5C, 6C–D, 8

Type material. Holotype male: “Rancho Quemado, Península de Osa, 200 m, Prov. Punt., COSTA RICA. F.Quesada, Dic 1991, L-S 292500, 511000” / “INBIO

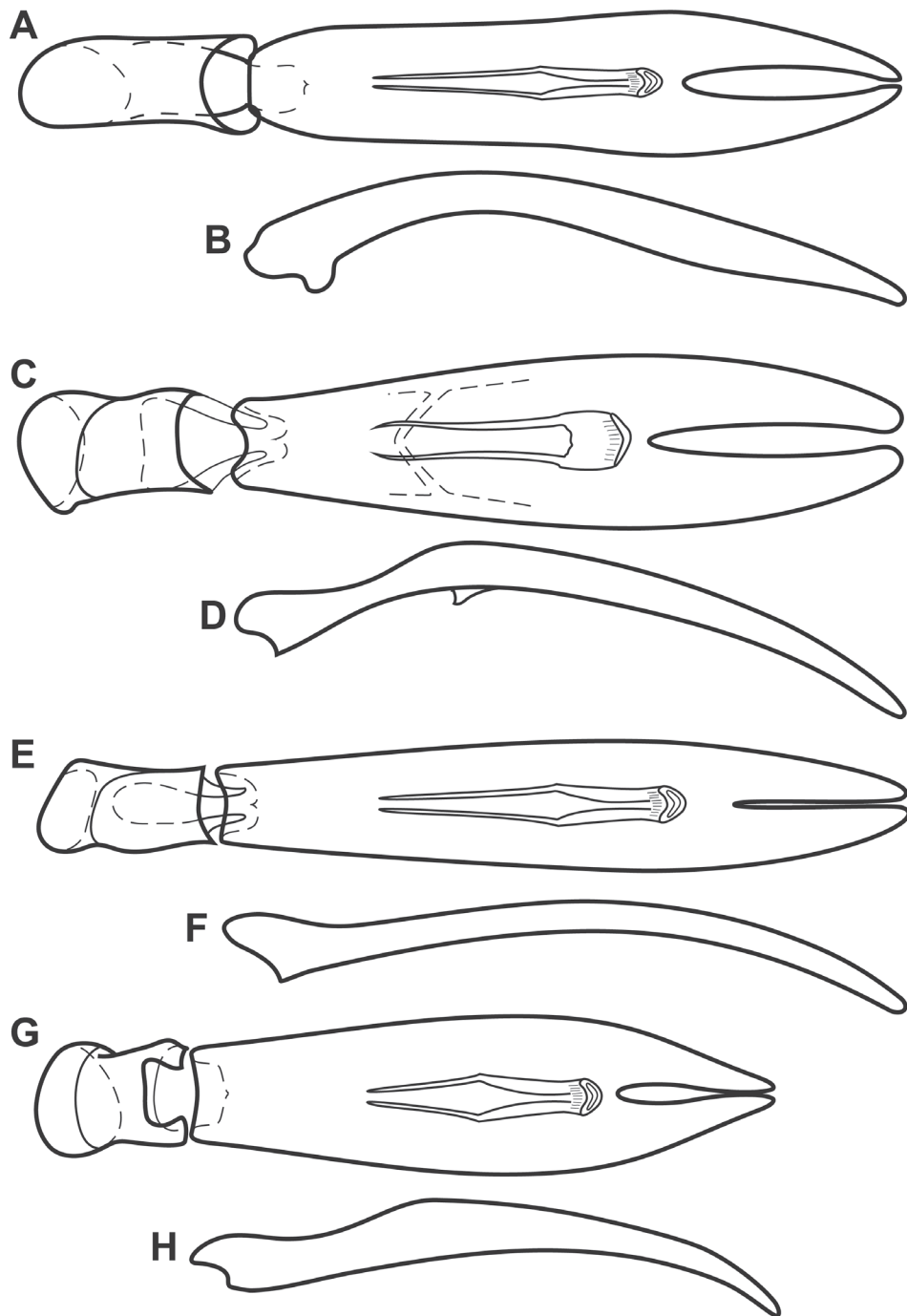


Figure 6. Aedeagi of *Megalocraerus* spp. **A** *Megalocraerus mandibularis*, dorsal view **B** *M. mandibularis*, lateral view **C** *M. chico*, dorsal view **D** *M. chico*, lateral view **E** *M. madredeios*, dorsal view **F** *M. madredeios*, lateral view **G** unnamed *Megalocraerus* sp. from Rio de Janeiro, dorsal view **H** unnamed *Megalocraerus* sp. from Rio de Janeiro, lateral view.

CRI000331213” (INBIO); **Paratype** female: Turrialba, CATIE [Centro Agronómico Tropical de Investigación y Enseñanza], 22.vi.-5.vii.1984, H.L.Dozier (FSCA).

Diagnosis. This species is relatively small and dorsoventrally depressed. It is similar overall to *M. mandibularis*, but lacks the modified male mandibles of that species. They also differ in tarsal setae, which are flattened and sublaminar in this species, but simple in *M. mandibularis*. An additional form that we do not describe from French Guiana keys out with this species, although that entity is significantly larger and has more conspicuous meso- and metaventral punctation. This species and *M. madreddios* both have the 4th dorsal stria connected to the sutural arch, but the latter species is more distinctly broad and flattened, as well as lighter in color. Finally, the distinct medioventral process of the aedeagus is unique.

Description. Size: Length 2.9–3.0 mm; width 2.0 mm; **Body:** broad, subparallel-sided, elongate, moderately depressed; piceous to weakly castaneous. **Head:** Frons finely and doubly punctate, with medium punctures separated by slightly more than their diameters against fine ground punctation, decreasing in size but slightly increasing in density anteromedially; frontal stria present along inner margins of eyes, bent inward above antennal insertions, broadly interrupted across epistoma; supraorbital stria absent; epistoma depressed, narrowing anterad; labrum minutely punctate; mandibles each with inner marginal tooth. **Pronotum:** Pronotal sides straight, subparallel in basal three-fourths, abruptly narrowed anteriorly, marginal stria complete, lateral stria absent, anterior marginal stria more or less complete; pronotal disk with numerous shallow, elongate secondary punctures at sides and front, diminishing basomedially, with fine ground punctation largely restricted to basal area; basal margin with coarser punctures. **Elytra:** Two complete epipleural striae present; subhumeral striae absent; dorsal striae 1–4 complete, 1–3 variously continued medially along basal margin, 4th meeting basal arch of sutural stria, 5th stria obsolete in anterior fourth; elytral disks with conspicuous ground punctation throughout, coarser secondary punctures present in apical sixth. **Prosternum:** Prosternal lobe evenly, somewhat narrowly rounded, complete to sides, marginal stria obsolete at sides; prosternal keel with two complete carinal striae diverging slightly front and rear, continued around basal projection of keel (may be fragmented). **Mesoventrite:** Anterior mesosternal margin evenly emarginate, with complete marginal stria; mesometasternal ventral absent; disk with only fine ground punctation. **Metaventrite:** Metaventral disk impunctate at middle, lateral metaventral stria present, extending toward outer corner of metacoxa, slightly abbreviated apically; postmesocoxal stria very short. **Abdomen:** Abdominal ventrites finely punctate at middle, slightly more coarsely at sides; propygidium strongly transverse, about four times as wide as long, coarsely punctate, with punctures separated by slightly less than their diameters, rather uniformly throughout; pygidium similarly coarsely punctate at base, punctures becoming finer, but also denser toward apex. **Male:** 8th tergite with deep but rather broad basal emargination, ventrobasal processes thin, distant beneath, dorsally with fine, deep median emargination, with desclerotized line extending nearly to base; halves of 8th sternite slightly separated along midline, apicomedial processes rather narrow, subacute; 9th tergite

with blunt, incurved apices; spiculum gastrale (S9) broad in basal third, abruptly narrowed, thence broadening to head, apex shallowly emarginate; 10th tergite entire; aedeagus flattened throughout, with distinct medioventral process, sides weakly rounded, widest near midpoint, apices slightly separated; median lobe slightly less than one-half tegmen length.

Remarks. The name of this species (Spanish for ‘small’) refers to its relatively small size. In this case it is used as a noun in apposition. This species was included in the phylogenetic analysis of Caterino and Tishechkin (2015) as ‘*Megalocraerus*2’.

***Megalocraerus madredeios* sp. n.**

<http://zoobank.org/DBC355ED-9B57-4039-92C0-76EE483848C8>

Figs 6E–F, 7A, 8

Type material. Holotype male: PERU: Madre de Dios: Pantiacolla Lodge, Alto Madre de Dios R., 12°39.3'S, 71°13.9'W, 420 m, 14–19.xi.2007, FIT, D. Brzoska (SEMC0874296); Paratype female: same data as type (SEMC0872118); SEMC.

Diagnosis. The body shape of this species is distinct, being broader and less elongate, and slightly more depressed than any of the others. Additionally the 4th stria meeting the basal sutural arch is shared only with *M. chico* (above).

Description. Size: Length 3.1–3.3 mm; width 2.3–2.4 mm; **Body:** broad, subparallel-sided, slightly elongate, moderately depressed; castaneous to slightly rufescent; the elytral bases, pronotum, and venter tending to be slightly lighter than the apical elytral two-thirds. **Head:** Frons finely and doubly punctate, with medium punctures separated by slightly more than their diameters against fine ground punctation, decreasing in size but slightly increasing in density anteromedial; frontal stria present along inner margins of eyes, bent inward above antennal insertions, broadly interrupted across epistoma; supraorbital stria absent; epistoma depressed, narrowing anterad; labrum minutely punctate; mandibles each with inner marginal tooth. **Pronotum:** Pronotal sides weakly rounded, slightly narrowed anterad, marginal stria complete, lateral stria absent, anterior marginal stria slightly fragmented; pronotal disk with small secondary punctures sparse basomedially, increasing in density toward front and sides, with fine ground punctation more or less uniform. **Elytra:** Two complete epipleural stria present; subhumeral striae absent; dorsal striae 1–4 complete, 4th meeting basal arch of sutural stria, 5th stria obsolete near base; bases of dorsal striae extending medially along basal elytral margin, but not meeting base of next stria; elytral disks with conspicuous ground punctation throughout, and increasingly dense secondary punctation toward apices. **Prosternum:** Prosternal lobe evenly, broadly rounded, complete to sides, with marginal stria obsolete at sides; prosternal keel with two complete carinal striae converging anteriorly. **Mesoventrite:** Anterior mesoventral margin evenly emarginate, with complete, marginal stria; mesometaventral stria absent; disk with only fine ground punctation. **Metaventrte:** Metaventral disk impunctate at middle, with few fine punctures in

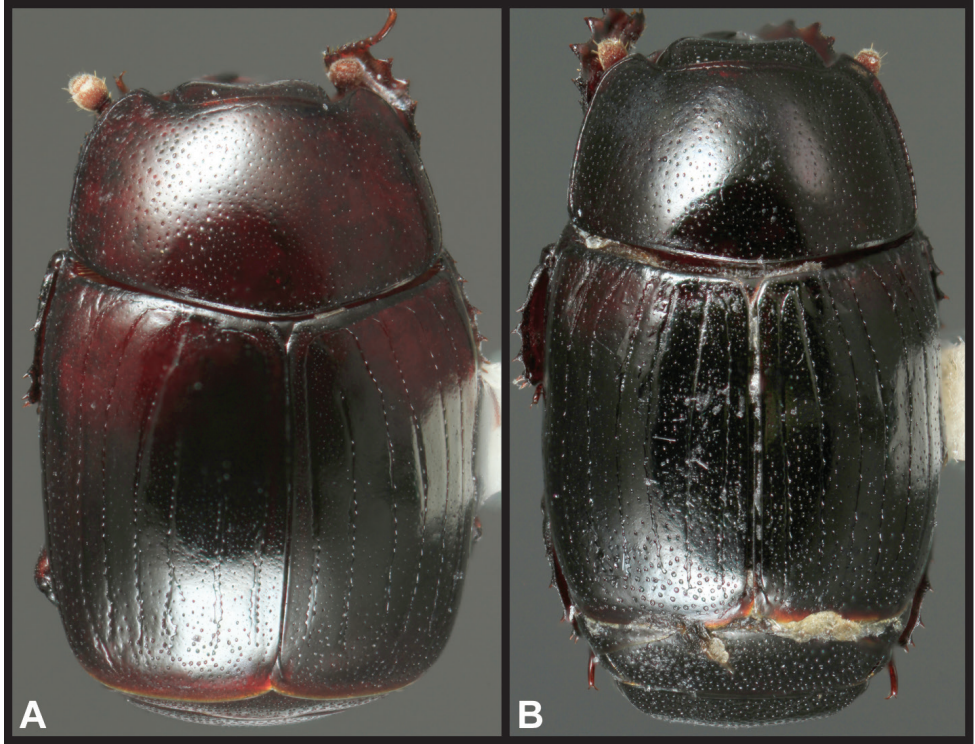


Figure 7. Dorsal habitus. **A** *Megalocraerus madredeios* **B** *M. tiputini*.

front of metacoxae, lateral metaventral stria present, extending toward outer corner of metacoxa, slightly obsolete apically; postmesocoxal stria very short. **Abdomen:** Abdominal ventrites finely punctate at middle, slightly more coarsely at sides; propygidium strongly transverse, about four times as wide as long, coarsely punctate, with punctures separated by slightly less than their diameters, a little denser toward sides; pygidium similarly coarsely punctate at base, punctures becoming finer, but also denser toward apex. **Male:** 8th tergite with deep basal emargination, ventrobasal processes nearly meeting, dorsally with fine, narrow median emargination; halves of 8th sternite slightly separated along midline, apicomедial processes broadly lobate; 9th tergite with acute, slightly recurved apices, ventrally with uniquely denticulate basal apodeme; spiculum gastrale (S9) broad in basal third, abruptly narrowed, broadening gradually toward head, apex broadly emarginate; 10th tergite entire but weakly desclerotized along much of midline; aedeagus flattened throughout, sides weakly rounded, widest just apicad midpoint, apices meeting; median lobe slightly more than one-half tegmen length.

Remarks. This species is named for the rich region of Peru in which it is found. This species was included in the phylogenetic analysis of Caterino and Tishechkin (2015) as ‘*Megalocraerus*1’.



Figure 8. Map showing all collecting records for *Megalocraerus* spp.

***Megalocraerus tiputini* sp. n.**

<http://zoobank.org/F0EF342E-532B-45AF-A602-E0CF3664511C>

Figs 7B, 8

Type material. Holotype female: ECUADOR: Orellana: Est. Biodiv. Tiputini, 0.6376°S, 76.1499°W, 2–9.vi.2011, FIT, M. Caterino & A. Tishechkin, DNA Extract MSC-2211, EXO-00738 (FMNH).

Diagnosis. This species' most distinctive character is its conspicuous metaventral punctation. It is also distinctly more densely punctate on the pygidia than other species. It is also unique (in the sole known specimen, at least) in having a complete 5th dorsal stria joined to the sutural stria.

Description. Size: Length 3.2 mm; width 2.3 mm; **Body:** subparallel-sided, elongate, weakly subcylindrical; piceous. **Head:** Frons finely and doubly punctate, with medium punctures separated by slightly more than their diameters against fine ground punctation, decreasing in size but slightly increasing in density anteromediad; frontal stria present along inner margins of eyes, bent inward above antennal insertions, broadly interrupted across epistoma; supraorbital stria absent; epistoma depressed, narrowing anterad; labrum minutely punctate; mandibles each with inner marginal tooth. **Pronotum:** Pronotal sides weakly convergent from base to apical fourth, thence abruptly narrowing, marginal stria complete, continuous with distinct anterior marginal stria, lateral stria absent; pronotal disk finely and shallowly but densely punctate, slightly sparser basomedially; basal margin with only few coarser punctures. **Elytra:** Two complete epipleural stria present; subhumeral striae absent; dorsal striae 1–5 complete, the 5th stria meeting basal arch of sutural stria; elytral disks with conspicuous ground punctation throughout, increasing in density apically. **Prosternum:** Prosternal lobe evenly, somewhat narrow rounded, complete to sides, marginal stria obsolete at sides; prosternal keel with two complete carinal striae diverging slightly front and rear. **Mesoventrite:** Anterior mesoventral margin evenly emarginate, with complete, marginal stria; mesometaventral stria absent; disk with fine secondary punctation. **Metaventrite:** Metaventral disk finely but densely punctate at middle, more coarsely to sides, lateral metaventral stria present, curving laterad toward middle of metepisternum, slightly obsolete apically; postmesocoxal parallel but shorter. **Abdomen:** Abdominal ventrites distinctly punctate throughout; propygidium transverse, about three times as wide as long, coarsely punctate, with punctures separated by about half their diameters, rather uniformly throughout; pygidium similarly coarsely punctate at base, diminished in size apically.

Remarks. Although known from a sole female, this species is more than adequately distinct to describe. We name the species to honor the staff and facilities of the Tiputini Biodiversity Station, who have assisted us and countless other researchers in studying the biota of the region. This species was included in the phylogenetic analysis of Caterino and Tishechkin (2015) as '*Megalocraerus*4'.

Unplaced specimens

Brasil: 1: [Rio de Janeiro] Corcovado-GB, 3.xii.1965, Moure-Seabra (UFPR).

Remarks. This specimen represents a distinct species based on male genitalia, with a broader and more dorsally 'humped' aedeagus than any other species (Fig. 6G, H) Unfortunately the body of this specimen was lost, aside from the male genitalia, so we refrain from describing it as new. We hope that additional collecting in the remain-

ing Atlantic Forest around Rio de Janeiro will one day turn up additional material of this species. This species was included in the phylogenetic analysis of Caterino and Tishechkin (2015) as '*Megalocraerus*3'.

French Guiana: 1: Mont Tabulaire Itoupé, 3.022°N, 53.084°W, 400 m, 17.iii.2010, FIT, SEAG (CHND); 2: Nouragues, Inselberg Camp, 4.08°N, 52.68°W, 30.ix.2012, SEAG (CHND).

Remarks. These three specimens key to *M. chico* described above, and share tibial characters with *M. mandibularis*, but they are considerably larger than either, and may represent an undescribed species. However, all the specimens are poorly preserved, missing many parts, and are either female or lack genitalia (some genitalia were lost prior to mounting, and their sex is unknown). So we refrain from recognizing an additional species until better preserved material leads to a more conclusive assessment.

Discussion

Megalocraerus has long represented an enigmatic lineage of rare beetles with unusual and confusing morphological attributes. One recent study (Caterino and Tishechkin 2015) has helped to clarify its phylogenetic position (although access to molecular-quality samples would be very useful), and the current study helps to better characterize its morphology and diversity. However, much remains unknown, particularly any hints as to its biology. Its rarity and unusual characters suggest something atypical for Exosternini, and we hope that microhabitat-focused collecting in areas of high diversity (esp. French Guiana, where 2 or 3 species are known to exist) will soon reveal more about these species' life histories.

Acknowledgments

For providing specimen material, assistance in the field, and assistance with permitting, we would like to thank Luciana Masutti de Almeida, Daniel Moura, Fernando Leivas, and Kleber Mise (UFPR), Max Barclay and Roger Booth (BMNH), Angel Solis (INBIO), Paul Skelley (Florida State Collection of Arthropods), Tiputini Biodiversity Station, Zack Falin (Snow Entomological Collection, University of Kansas), Nicolas Degallier, and Al Allen. We also thank the National Science Foundation for financial support (DEB-0949790).

References

Bickhardt H (1917) Histeridae. In: Wytzman P (Ed.) *Genera Insectorum*, 166a, b. La Haye, 1–112, 113–302.

- Caterino MS, Tishechkin AK (2015) Phylogeny and generic limits in New World Exosternini (Coleoptera: Histeridae: Histerinae). *Systematic Entomology* 40: 109–142. doi: 10.1111/syen.12095
- Helava JVT, Howden HF, Ritchie AJ (1985) A review of the New World genera of the myrmecophilous and termitophilous subfamily Hetaeriinae (Coleoptera: Histeridae). *Sociobiology* 10(2): 127–382.
- Lawrence JF, Ślipiński A, Seago AE, Thayer MK, Newton AF, Marvaldi AE (2011) Phylogeny of the Coleoptera based on morphological characters of adults and larvae. *Annales Zoologici* 61(1): 1–217. doi: 10.3161/000345411X576725
- Leivas FWT, Bicho CL, Almeida LM (2015) Cladistic analysis of Omalodini Kryzhanovskij. *Systematic Entomology* 40: 433–455. doi: 10.1111/syen.12112
- Lewis GL (1902) On new species of Histeridae and notices of others. *Annals and Magazine of Natural History* (7) 10: 223–239. doi: 10.1080/00222930208678661
- Mazur S (1984) A World Catalogue of Histeridae (Coleoptera). *Polskie Pismo Entomologiczne - Bulletin Entomologique de Pologne* 54(3-4): 1–376.
- Mazur S (1990) Notes on Oriental and Australian Histeridae. *Polskie Pismo Entomologiczne - Bulletin Entomologique de Pologne* 59: 743–759.
- Mazur S (1997) A world catalogue of the Histeridae (Coleoptera: Histeroidea). *Genus International Journal of invertebrate Taxonomy*, supplement: 1–373.
- Mazur S (2011) A concise catalogue of the Histeridae (Coleoptera). Warsaw University of Life Sciences - SGGW Press, Warsaw, 332 pp.
- Ôhara M (1994) A revision of the superfamily Histeroidea of Japan (Coleoptera). *Insecta Matsumurana*, New Series 51: 1–283.
- Wenzel RL, Dybas HS (1941) New and little known neotropical Histeridae (Coleoptera). *Fieldiana, Zoology* 22(7): 433–472.

A new species of *Eutettix* (Hemiptera, Cicadellidae, Deltocephalinae) from Wisconsin

Stuart H. McKamey¹

¹ USDA Agricultural Research Service, Systematic Entomology Laboratory, c/o NMNH, MRC-168, Smithsonian Institution, P.O. Box 37012, Washington, DC, 20013-7012, U.S.A.

Corresponding author: *Stuart H. McKamey* (stuart.mckamey@ars.usda.gov)

Academic editor: *M. Webb* | Received 13 September 2013 | Accepted 24 October 2013 | Published 28 January 2016

<http://zoobank.org/53FC4109-87CA-4CA2-ADD9-D8999ACAB229>

Citation: McKamey SH (2016) A new species of *Eutettix* (Hemiptera, Cicadellidae, Deltocephalinae) from Wisconsin. *ZooKeys* 557: 79–83. doi: 10.3897/zookeys.557.5939

Abstract

Eutettix latoides sp. n., is described from central Wisconsin. It most closely resembles the Californian species *E. latus* Hepner, and was collected from *Quercus ellipsoidalis*.

Keywords

Leafhopper, new species, Athysanini, Nearctic, Wisconsin, *Quercus*

Introduction

The genus *Eutettix* Van Duzee pertains to the deltocephaline tribe Athysanini, the largest tribe of the family, which defies easy diagnosis. The tribe generally consists of a diverse assortment of 228 genera with Y-shaped connectives in the male genitalia that lack characteristics that would place them in other tribes (Zahniser and Dietrich 2013).

As with many athysanine genera, *Eutettix* itself is more readily distinguished than its tribe. They are robust, somewhat flattened leafhoppers with the head in dorsal view slightly broader than the pronotum, with a faint transverse furrow just behind the rounded anterior margin, and the anterior margin with several to many transverse striations or irregular carinae. The ocelli are located on the anterior margin close to the eyes. The pronotum has very short lateral margins and bears transverse striae. The forewing has the appendix restricted to the anal vein area, with flat (non-carinate) veins, and three antepical cells. The abdominal tergum X is sclerotized. The male pygofer is

setose with a large single or double hooklike spine within it. The subgenital plates are triangular with uniseriate macrosetae.

Although 127 species were originally described in *Eutettix*, it is currently considered a coast-to-coast Nearctic genus containing 56 valid species and subspecies, 31 of which are endemic to the United States, 15 endemic to Mexico, and three species are shared between the two countries. There are seven species left over from the out-dated, wider interpretation of the genus that are still waiting for proper generic placement: *E. botelensis* Matsumura from Taiwan; *E. elongatus* Melichar from the Republic of the Congo; *E. fulminans* Melichar from Indonesia; *E. marquezii* Merino from the Philippines; *E. mimicus* Osborn from Bolivia; *E. quadripunctatus* Melichar from Somalia; and *E. ramosus* Melichar from Tanzania.

Hepner (1942) provided the first and only revision of the species of the United States, describing 18 new species, three new subspecies, three new synonyms, and descriptions and genitalic photographs of all species. He also listed five species that did not belong to *Eutettix* but retained them in the genus for convenience until their generic affinities were better understood – all have since been reassigned to other genera, including one to the genus *Ollarianus* Ball, under which one current *Eutettix* species (*E. rubianus* [Ball]) was originally described. Sixteen Mexican species were added by DeLong and Harlan (1968) and DeLong (1980). No subsequent species have been described from anywhere in the last 33 years. In the current work a new species of *Eutettix* is described, bringing the total number of Nearctic species to 50.

Methods

Multiple images per view were captured using a Microvision System with an AT-200GE videocamera mounted on a Leica 10447176 Planapo 1.0x/WO 97mm lens, and compiled using Cartograph 8.0.6 software. The resulting images were cleaned using Adobe Photoshop CS 3 version 10.0.1.

Terminology follows Zahniser and Dietrich (2013), also available online in Zahniser's interactive key to deltocephaline tribes (<http://imperialis.inhs.illinois.edu/zahniser/JZKeys.asp>).

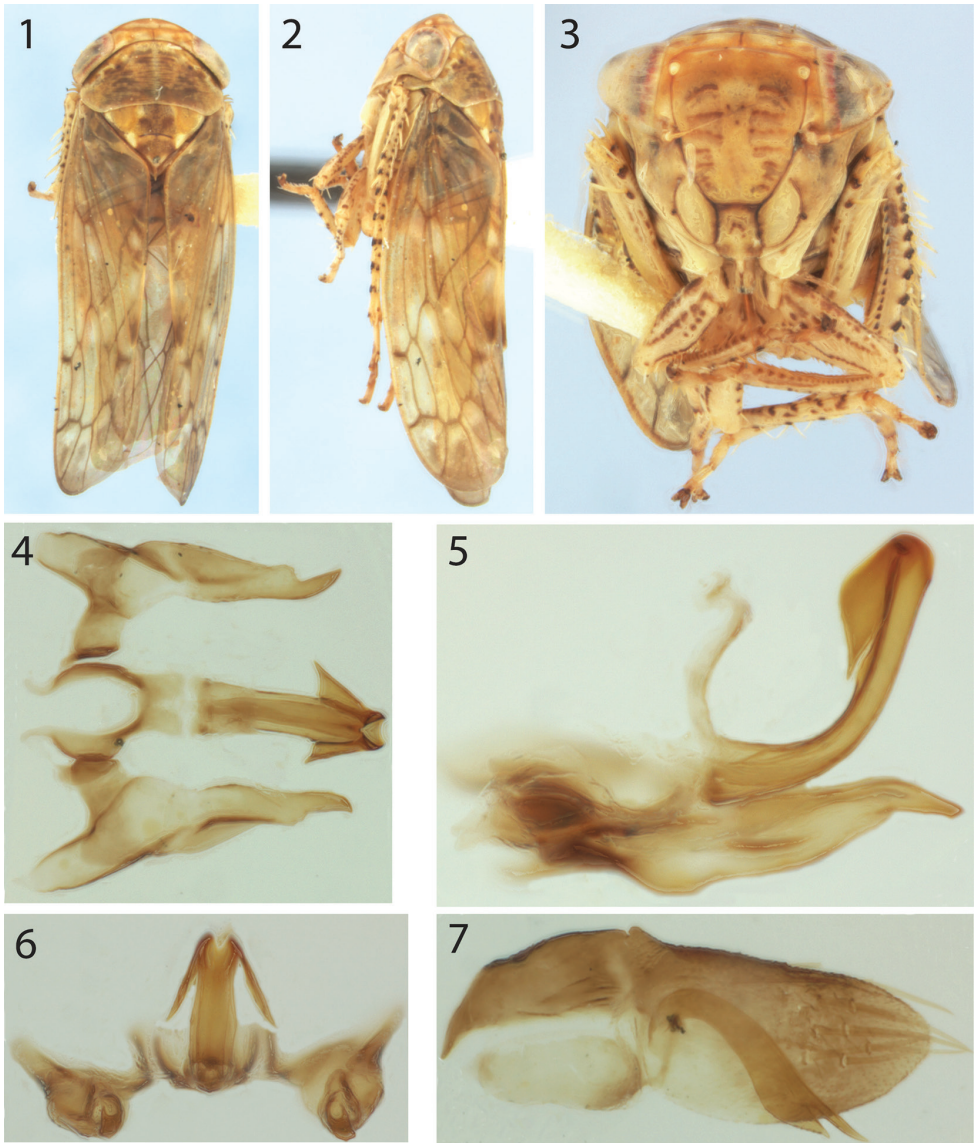
The holotype is deposited in the United States National Museum of Natural History in Washington, DC (USNM).

Results

Eutettix latoides sp. n.

<http://zoobank.org/45B41234-5AEC-411A-AD44-398D5C5CD0D7>

Diagnosis. male with internal pygofer hook bifurcate distally, its ventral branch approximately five times wider than its dorsal branch.



Figures 1–7. *Eutettix latoides* sp. n., holotype. **1–3** habitus from dorsal, lateral, and anterior views, respectively **4–6** aedeagus, styles, and connective from dorsal, lateral, and posterior views, respectively **7** Right side of pygofer, internal view, showing its diagnostic pygofer hook (left side removed).

Measurements. Length of male with forewings in repose 4.4 mm, maximum width of pronotum 1.4 mm.

Description. Head. Slightly wider than pronotum, anterior margin rounded in lateral view, with transverse striations between ocelli in anterior view, and, in dorsal view (Fig. 1) parallel margined, vertex with shallow furrow just behind anterior margin; frontoclypeal suture distinct (Fig. 3), clypeus slightly wider distally, frontoclypeus

not tumid (Fig. 2); ocelli on anterior margin of head close to eyes, separated from them by nearly their width (Fig. 3). Thorax. Pronotum transversely striate, posterior margin weakly concave, lateral margin shorter than basal width of eye (Fig. 1); forewing macropterous with veins not raised, distinct appendix limited to anal margin, three antepical cells, 2nd slightly constricted medially, venation not reticulate distally, A1–A2 crossvein absent; prothoracic femur (Fig. 3) with many small setae in row AV and intercalary row, AM1 seta present, dorsal surface rounded, not sharply carinate along AD and PD margins; metathoracic femoral apex macrosetal formula 2+2+1.

Male terminalia. Pygofer in lateral view bluntly pointed; pygofer hook (Fig. 7) arising basoventrally within pygofer, curving gradually dorsoposteriorly then abruptly ventroposteriorly, bifurcate apically, ventral branch finely serrate and gradually acuminate, approximately 5× wider than dorsal branch, which has subparallel sides until acute apex. Aedeagus (Figs 4–6) in lateral view narrow throughout, lacking basal or median processes, bearing a pair of anterior apical leaflike processes slightly longer than half of aedeagal shaft, directed ventrolaterally, gonopore apical. Style with small basal lobe, pointed apex directed posteriorly. Connective basally broad, articulated with aedeagus, in dorsal view Y-shaped.

Color. Irregularly fuscous throughout, darker along transverse furrow on head frontoclypeal suture and vertex, on forewing cubitus apex and both r-c crossveins, and on legs setal bases.

Female. Unknown.

Distribution. United States: central Wisconsin.

Probable host. *Quercus ellipsoidalis* E.J. Hill (Northern pin oak or Hill's oak). Because the label does not indicate how the specimen was collected from the oak, its host must be considered tentative until further specimens are collected. Nevertheless, it may indeed feed on oak. Hepner (1942) reported three other *Eutettix* species that have been collected from oaks: *E. querci* Gillette and Baker, from *Quercus undulata* Torr. (Wavyleaf oak), and *E. querci albus* Hepner and *E. prinooides* Hepner, both from *Q. prinooides* Willd. (Dwarf Chinkapin oak).

Holotype (USNM): male, with labels “[Wisconsin Rapids,] Wood Co., Wis. / Griffith St[ate]. Nursery / VII-22-1948 / R.D. Shenefelt Ray”, “coll. from / *Q. ellipsoidalis* / normal”, and “HOLOTYPE / *Eutettix* / *latoides* / S.H. McKamey.” Brackets indicate inferred data not on labels. Georeference: 44.3408°N; -89.7349°W (DD).

Etymology. The name is a combination of “*latus*” and the Greek suffix “*-oides*,” in reference to the resemblance of the new species to *E. latus*, as discussed below.

Discussion

In Hepner's (1942) key to species, the new species would key to couplet 5 because it is less than 4.75 mm, but has features inconsistent with either portion of the couplet: the dorsal branch of the pygofer hook is not falcate, as in *E. rugosus* Hepner, but the branches are subequal in length and the ventral branch is not curved anteriorly, as in

E. subspinosus Hepner. The internal pygofer hook most resembles that of *E. latus* Hepner (USNM paratypes examined), but in that species the pygofer hook bifurcates just after its ventral curve, with both branches narrowing to equally acute apices. Another feature distinguishing *E. latooides* from *E. latus* is that the latter species has the aedeagal shaft broad with a large medial anterior projection, and its apical pair of processes are approximately one third the size of those in *E. latooides*.

Acknowledgments

I thank J. Zahniser (Illinois Natural History Survey) for helpful comments on an earlier draft of the manuscript.

References

- DeLong DM (1980) New genera and species of Mexican and South American deltocephaline leafhoppers (Homoptera, Cicadellidae, Deltocephalinae). *Revista Peruana de Entomología* 23(1): 63–71.
- DeLong DM, Harlan HJ (1968) Studies of the Mexican Deltocephalinae: New species of *Eutettix* and two allied new genera (Homoptera: Cicadellidae). *Ohio Journal of Science* 68(3): 139–152.
- Hepner LW (1942) A taxonomic revision of the genus *Eutettix* in America north of Mexico (Homoptera, Cicadellidae). *The Kansas University Science Bulletin* 28: 253–293.
- Zahniser JN, Dietrich CH (2013) A review of the tribes of Deltocephalinae (Hemiptera: Auchenorrhyncha: Cicadellidae). *European Journal of Taxonomy* 45: 1–211. doi: 10.5852/ejt.2013.45

First Immature of the New World Treehopper tribe Thuridini (Hemiptera, Membracidae, Smiliinae) with a new synonym, a new combination, and a new country record

Stuart H. McKamey¹, Mitchell J. Porter²

1 USDA/ARS Systematic Entomology Lab, c/o NMNH MRC-168, Smithsonian Institution, Washington, DC 20560, USA **2** Department of Biology, University of Maryland, College Park, MD 20742

Corresponding author: *Stuart H. McKamey* (stuart.mckamey@ars.usda.gov)

Academic editor: *M. Webb* | Received 16 September 2015 | Accepted 8 December 2015 | Published 28 January 2016

<http://zoobank.org/E3D490F4-5654-47E4-95AA-3407F41648CE>

Citation: McKamey SH, Porter MJ (2016) First Immature of the New World Treehopper tribe Thuridini (Hemiptera: Membracidae: Smiliinae) with a new synonym, a new combination, and a new country record. ZooKeys 557: 85–91. doi: 10.3897/zookeys.557.6602

Abstract

The species *Thuris depressus* Sakakibara (1975) is proposed as a **syn. n.** of *Thuris binodosus* (Goding 1926), **comb. n.** The distribution of the genus is expanded from Brazil and Peru to include Ecuador and Venezuela, and the immature is described based on 75 characters.

Keywords

Thuris, *Parantonae*, nymph, syn. n., comb. n., Ecuador, Venezuela

Introduction

Adult treehoppers (Membracidae, Aetalionidae, and Melizoderidae) are well known for the expanded, often extravagantly developed pronotum common to nearly all of the more than 400 genera and 3,000 species (McKamey 1998). The immature stages are poorly known, but in addition to the nascent enlarged pronotum, nymphs are usually covered with various arrangements of large spinelike structures (scoli) or smaller

setae with tuberculate or stalked bases (chalazae) on the head, all thoracic segments, and the abdomen (Fig. 12). These structures are usually absent in the adults. Indeed, treehopper immatures show a vast array of structures that to a large extent have evolved independently of the adult forms. The nymph of *Thuris* Funkhouser (1943), a genus containing two valid species, has never been described. The description below is based on 75 nymphal characters and 322 possible character states exhibited among members of the subfamily Smiliinae, which includes the monobasic tribe Thuridini. Because many of the characters are conditions of the scoli and enlarged chalazae (direction, size, which segments, etc.), the description below seems abbreviated but covers all characters.

Materials and methods

Late instars of Membracidae are usually sturdy enough to maintain their form when dried, so a pinned specimen was used to determine characters. The only character that would likely be affected is the length of abdominal segment IX relative to other body parts, due to contraction upon drying.

Because some form of parental care or at least aggregation of nymphs is widespread among treehoppers, for many subfamilies it is easy to associate adults, nymphs, and egg masses. In the case of solitary taxa, repeated adult-nymph-host association, rearing, and in a few cases the extrapolation of the miniature pronotum have been used to associate adults and nymphs. In the case of *Thuris*, an aggregation of four late instars and four adults was collected, suggesting that the genus is subsocial.

The voucher (INHS) has the label “Immatures Project Voucher, McKamey et al. 2015” and the species name.

Images were captured with a Microvision system and Cartograph 8.0.6 automontage software and adjusted in Adobe Photoshop.

The terminology, 75 characters and 322 potential character states are the same used for Amastrini (McKamey et al. 2015). The character descriptions and data are posted online on the USDA/ARS Systematic Entomology Laboratory website (McKamey 2015).

Specimen repositories are as follows

- DZUP** Brazil, Paraná, Curitiba, Universidade Federal do Paraná, Museo de Entomologia Pe. Jesus Santiago Moure
INHS USA, Illinois, Campaign, Illinois Natural History Survey
NCSU USA, North Carolina, Raleigh, North Carolina State University
USNM USA, District of Colombia, Washington DC, National Museum of Natural History

Results

Thuris binodosus (Goding), comb. n.

Parantonae binodosa Goding 1926: 108 (Figs 1–4, 8; holotype USNM)

Thuris depressus Sakakibara 1975: 843, **syn. n.** (Figs 5–7; holotype DZUP)

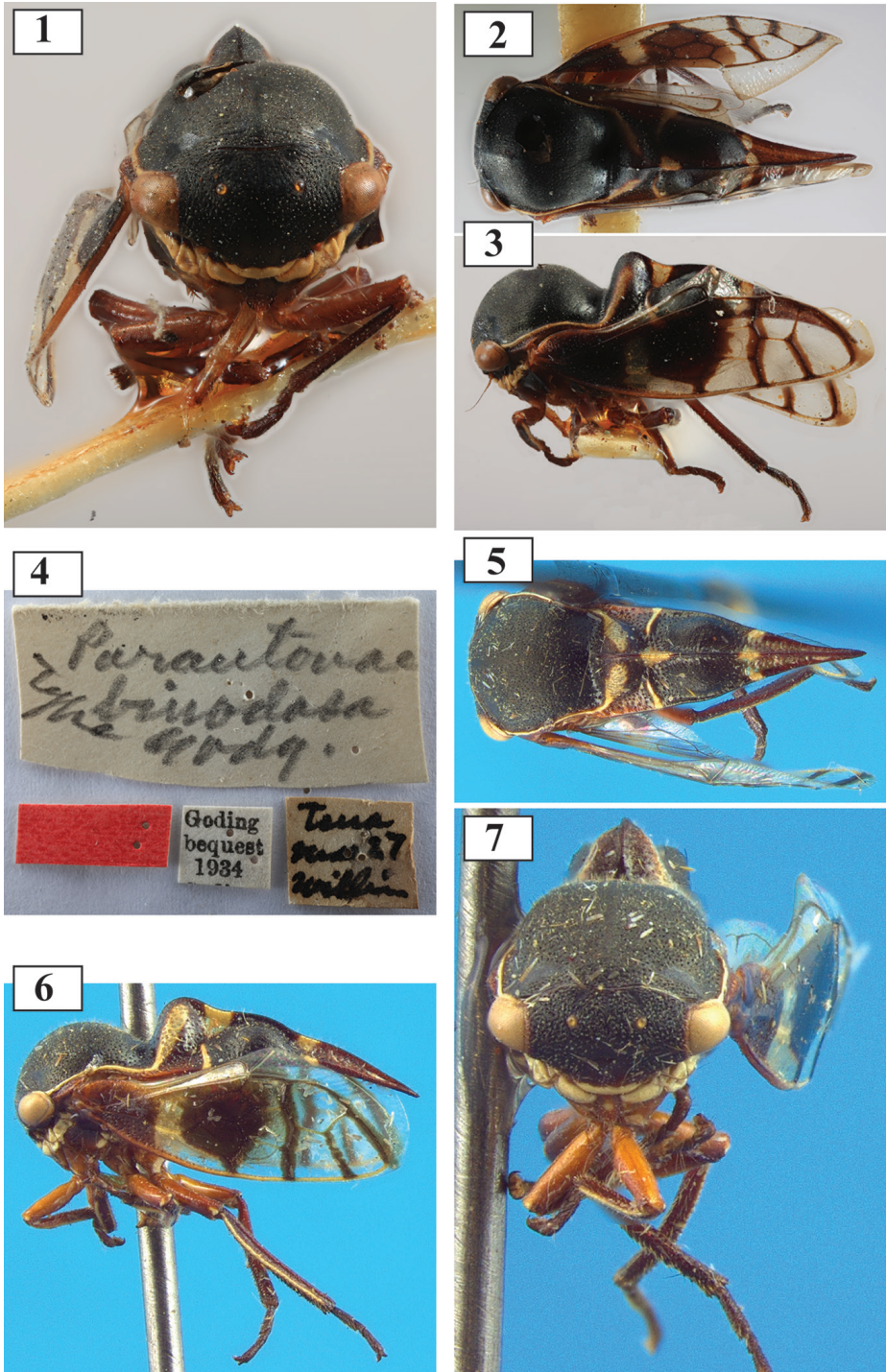
Notes and new distribution. Examination of the holotype of *Parantonae binodosa* Goding (1926), from Tena, Ecuador (Napo Province) (Figs 1–4) revealed a match with the holotype of *Thuris depressus* Sakakibara (1975) (Figs 5–7), resulting in the classification above. An aggregation of the species has also been observed in Ecuador in Coca (= Puerto Francisco de Orellana, Napo Province) and a solitary adult was found in (Fig. 8) Otoyaku, Santa Clara (Pastaza Province). The Venezuelan *Thuris* specimen (of *T. fenestratus* Funkhouser) was collected in Amazonas state.

Description of fifth instar (Figs 9–11).

Diagnosis. Body densely covered with short setae, but lacking chalazae and scoli; apex of abdominal segment IX narrowly extended ventrally far beyond dorsal extension.

Description. Overall body. Length 2.50 mm, maximum width 1.25 mm. Cross-section of abdomen subcircular; chalazae on thorax and abdomen absent; waxlike substance absent; dorsal contour of abdomen in lateral view curvilinear (Fig. 10); overall body in dorsal view elongate (distinctly longer than wide). Coloration a combination of black and brown, most pale on premetopidium, metanotum, margins of tibia, and mid dorsally from pronotum to abdominal tergum VIII. **Head.** Scoli, dorsal or anterior rounded protuberances, and chalazae absent; compound eye surface setae present; frontoclypeus not extending over central margin of eye. **Prothorax.** Premetopidium and postmetopidium scoli absent; metopidial sulcus deeply incised; posterior extension of pronotum acute, surpassing posterior margin of metanotum but not attaining abdominal apex; dorsal pronotal single medial, suprahumeral, and humeral horn buds absent; pronotal lateral margin straight. **Mesothorax.** Dorsal projections absent; forewing pad anterior costal margin form straight, surface and costal chalazae absent. **Metathorax.** Dorsal projections absent. **Legs.** Tibia without chalazae; prothoracic tibia form subcylindrical, without defined margins; metathoracic tarsal length longer than pro- and mesothoracic tarsal length; pro- and mesothoracic first tarsomeres distinctly shorter than their second tarsomeres (Fig. 9); metathoracic first tarsomere subequal in length to its second tarsomere (Fig. 10). **Abdomen.** Terga III–VIII ventrolateral margins without enlarged chalazae or other lateral extensions, lateral longitudinal rows of enlarged chalazae or scoli between mid dorsal line and ventrolateral margins not manifested. **Segment IX.** Distal half tubular in cross-section; dorsal length subequal to length of segment V–VIII; dorsal projections before and at apex absent; ventral extension narrow and distinctly longer than dorsal extension (Fig. 10); fused portion of segment IX distal to unfused portion; unfused portion distally not bifurcate.

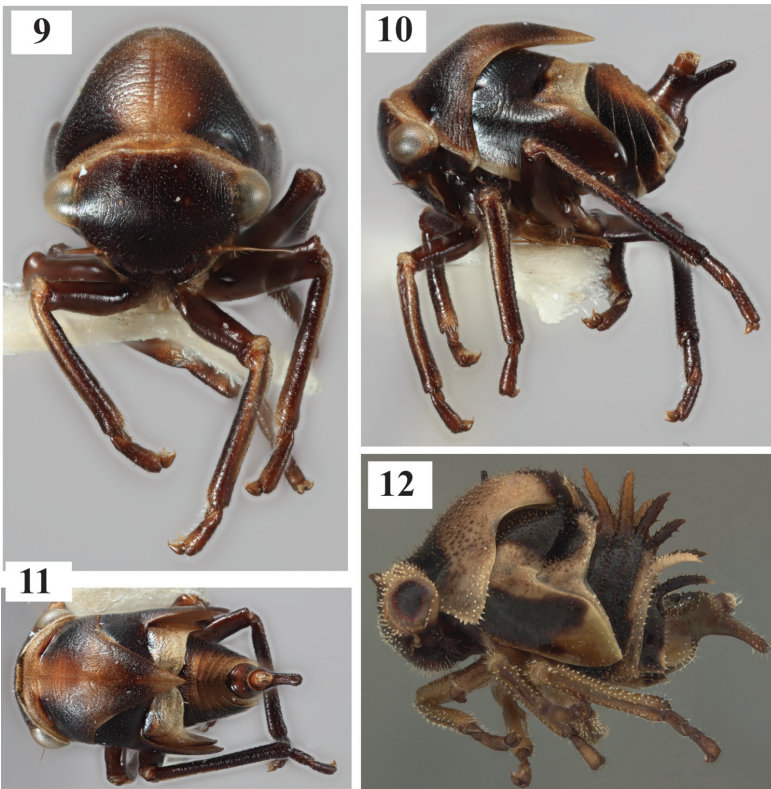
Discussion. The nymph of *Thuris binodosus* is exceptionally devoid of the chalazae and scoli that adorn most treehopper nymphs, including those of the related tribe



Figures 1–7. *Thuris binodosus* (Goding), comb. n. **1–4** *Parantoniae binodosa* holotype and labels **5–7** *Thuris depressus*, syn. n., holotype.



Figure 8. *Thuris binodosus*, live shot, Ecuador. Photo Milan Kozánek, with permission (<http://www.kozanek.com/en/insects/18/?slide=559>).



Figures 9–12. 9–11 Fifth instar of *Thuris binodosus* (Goding) 12 Fifth instar of *Neotynelia* sp., which also exhibits a ventrally extended abdominal segment IX.

Tragopini, and that is in itself distinctive. Another diagnostic feature is the ventrally extended abdominal tergum IX, which among other membracid immatures only occurs in a few taxa. Although the ventral extension is distinctly longer than the dorsal extension in *Todea cimicoides* (Coquebert) and *Colisicostata albata* (Tode) of Tragopini, *Phormophora maura* (Fabricius) of Polyglyptini, and most Aetalionidae, only in *Neotynelia* Creão-Duarte & Sakakibara (2000; Amastrini) is the extension digitiform as in *Thuris binodosus*. This digitiform ventral extension feature was not used in the phylogenetic study by Dietrich et al. (2001) and, perhaps because of this, *Thuris* did not form a clade with Amastrini. *Neotynelia* differs in always bearing large scoli on the abdomen at least (Fig. 12). Deitz (1975) established Thuridini as a tribe based in large part on the absence of cucullate setae in metathoracic tibial row I. Unfortunately, these basally covered setae so ubiquitous among membracid adults are absent in the nymphs. The subequal lengths of the metathoracic first and second tarsomeres, due to an extraordinarily long first tarsomere, is unusual but shared with other taxa such as Tragopini (McKamey et al., in prep) and is reflected in the similarly long first tarsomere (of three total) in *Thuris* adults.

Specimens examined. *Parantonae binodosa* holotype (USNM). *Thuris fenestratus* Funkhouser holotype (USNM). Additional material of *T. binodosus*: 1 nymph. ECUADOR: Napo, Coca 24-VIII-1988, C. H. Dietrich #86, INHS Insect Collection 776, 690 (INHS). Not examined but same collection lot as examined nymph: 1 nymph, 1 adult (INHS), 2 nymphs, 3 adults (NSCU). Specimens of *T. fenestratus*: 1 adult. VENEZUELA: T. F. Amazonas, San Carlos de Rio Negro, 24-I-1985, P. & P. Spangler, R. Faitoute, W. Steiner (USNM).

Acknowledgments

We thank O. Evangelista for providing images of the *T. depressus* holotype, M. Kozánek for providing the live shot, and G. Ouellette and T. Litwack for capturing the images of the nymphs of *T. binodosus* and *Neotynelia*, respectively. L. Deitz, C. H. Dietrich, M. S. Wallace, and an anonymous reviewer provided helpful comments on an earlier draft of this manuscript.

References

- Creão-Duarte AJ, Sakakibara AM (2000) Revisão do gênero *Tynelia* Stål e descrição de um novo gênero correlato (Hemiptera, Membracidae, Smiliinae). Revista Brasileira de Zoologia 17(3): 561–572. doi: 10.1590/S0101-81752000000300001
- Deitz LL (1975) Classification of the higher categories of the New World treehoppers (Homoptera: Membracidae). North Carolina Agricultural Experiment Station Technical Bulletin 225, 177 pp.

- Dietrich CH, McKamey SH, Deitz LL (2001) Morphology-based phylogeny of the treehopper family Membracidae (Hemiptera: Cicadomorpha: Membracoidea). *Systematic Entomology* 26: 213–239. doi: 10.1046/j.1365-3113.2001.00140.x
- Funkhouser WD (1943) A new membracid genus from Peru (Homoptera). *Entomological News* 54: 229–232.
- Goding FW (1926) New genera and species of Membracidae. *Transactions of the American Entomological Society* 52: 103–110.
- McKamey SH (1998) Taxonomic catalogue of the Membracoidea (exclusive of leafhoppers): second supplement to Fascicle 1 -- Membracidae of the General Catalogue of the Hemiptera. *Memoirs of the American Entomological Institute* 60: 1–377.
- McKamey SH (2015) Treehopper immatures project. <https://www.ars.usda.gov/Main/docs.htm?docid=25448> [last accessed December 4, 2015]
- McKamey SH, Wallner AM, Porter MJ (2015) Immatures of the New World treehopper tribe Amastrini (Hemiptera: Membracidae: Smiliinae) with a key to genera. *ZooKeys* 524: 65–87. doi: 10.3897/zookeys.524.5951
- Sakakibara AM (1975) Sobre o gênero *Thuris* Funkhouser, 1943, com descrição de uma nova espécie. *Revista Brasileira de Biologia* 35(4): 843–846.

Descriptions of new species of the genera *Sarima* Melichar and *Sarimodes* Matsumura from southern China (Hemiptera, Fulgoromorpha, Issidae)

Rui Meng¹, Yinglun Wang¹

¹ Key Laboratory of Plant Protection Resources and Pest Management of the Ministry of Education; Entomological Museum, Northwest A&F University, Yangling, Shaanxi 712100, China

Corresponding author: Yinglun Wang (yinglunw@nwsuaf.edu.cn)

Academic editor: M. Wilson | Received 6 August 2015 | Accepted 14 December 2015 | Published 28 January 2016

<http://zoobank.org/9AA2A48B-9772-442F-A6D4-A526FA612EDD>

Citation: Meng R, Wang Y-L (2016) Descriptions of new species of the genera *Sarima* Melichar and *Sarimodes* Matsumura from southern China (Hemiptera, Fulgoromorpha, Issidae). ZooKeys 557: 93–109. doi: 10.3897/zookeys.557.6166

Abstract

Two Issini genera, *Sarima* Melichar, 1903 and *Sarimodes* Matsumura, 1916, are examined. One new *Sarima* species: *S. bifurcus* **sp. n.** and two new *Sarimodes* species *S. clavatus* **sp. n.** and *S. parallelus* **sp. n.** are added from South China. A checklist of species in the genus *Sarima* with data on distribution is provided. The distribution and morphological peculiarities of the genera *Sarima* and *Sarimodes* are briefly discussed.

Keywords

Fulgoroidea, morphology, taxonomy, checklist, Hainan Island, Yunnan

Introduction

The genus *Sarima* belongs to the Issini Spinola, 1839 and was erected by Melichar (1903) for two species from Sri Lanka: *S. illibata* Melichar, 1903 (type species) and *S. elongata* Melichar, 1903. Subsequently, Distant (1906) recognized the genus and described one species *S. cretata* from Sri Lanka. Meanwhile, Melichar (1906) described

eight species (*S. castanea*, *S. nigrochlypeata*, *S. separata*, *S. solia*, *S. amagisana*, *S. notata*, *S. bimaculata* and *S. clathrata*), and two other species: *Hysteropterum subsfasciata* Melichar, 1903 and *H. fuscula* Melichar, 1903 were transferred to this genus. Distant (1909), Schmidt (1910, 1928), Schumacher (1915), Jacobi (1928, 1944), Esaki (1931), Kato (1933), Matsumura (1916, 1936), and Fennah (1950) subsequently added 16 species to the genus (Metcalf 1958). Three more species were described by Hori (1970, 1971) respectively from Japan and the Philippines. *S. yobennai* Matsumura 1936 was regarded as a junior synonym of *S. satsumana* Matsumura 1916 by Hori (1970). Chan and Yang (1994) transferred *S. matsumurai* Esaki, 1931 and *S. rubricans* Matsumura, 1916 to *Eusarima* Yang, 1994. Recently, Gnezdilov (2013a) erected a genus *Pavelauterum* for the species *S. fuscula* (Melichar, 1903). Gnezdilov (2013b) transferred six species to the genus *Eusarima* Yang: *S. formosana* Schumacher, 1915, *S. koshunensis* Matsumura, 1916, *S. kuyaniana* Matsumura, 1916, *S. rinkihonis* Matsumura, 1916, *S. satsumana* Matsumura, 1916, and *S. versicolor* Kato, 1933. Currently, 22 species are included in the genus *Sarima* from the Eastern Palaearctic, Oriental, and Australian Regions (Metcalf 1958, Hori 1970, 1971, Gnezdilov 2013a, 2013b, Bourgoïn 2015).

The Issini genus *Sarimodes* was erected by Matsumura (1916) for the single species *S. taimokko* from Taiwan. Recently, Gnezdilov and Hayashi (2013) suggested *Paravindilis* Yang, 1994 as a junior synonym of *Sarimodes* Matsumura based on photos of the holotype female of *S. taimokko* (Gnezdilov and Hayashi 2013) available on the web-site of the Hokkaido University as well as the illustration of Chan and Yang (1994). Meanwhile, *Pterilia formosana* and *Paravindilis taiwana* Yang, 1994 were both designated as junior synonyms of *S. taimokko*, and *P. taiwanensis* was proven to be an invalid name (Gnezdilov and Hayashi 2013). So far, the genus *Sarimodes* has only one known species distributed in Taiwan.

In this paper, one new species of *Sarima* and two new species of *Sarimodes* are described. A checklist of *Sarima* species with data on their distribution is provided below.

Materials and methods

External morphology was observed under a Leica MZ 125 microscope. All measurements are given in millimeters (mm). Terminology used for the external morphology and the male genitalia mainly follows Chan and Yang (1994). The description of the female genitalia follows Bourgoïn (1993) and Gnezdilov et al. (2014), and forewing venation pattern follows Bourgoïn et al. (2015). The genital segments of the examined specimens were dissected and macerated in hot 10% NaOH solution for approximately 2–3 minutes, and subsequently transferred into glycerin. Photographs of the specimens were made using a Leica M205A microscope with a Leica DFC Camera. Images were produced using the software version LAS (Leica Application Suite) V3.7. All specimens studied are deposited in the Entomological Museum of Northwest Agriculture and Forestry University (NWAUFU), Yangling, China.

Taxonomy

Family Issidae Spinola, 1839

Subfamily Issinae Spinola, 1839

Tribe Issini Spinola, 1839

Sarima Melichar, 1903

Sarima Melichar, 1903: 78. Type species: *Sarima illibata* Melichar, 1903, by original designation.

Diagnostic characters. The genus *Sarima* was originally described by Melichar (1903), subsequently designated by Distant (1906) and recently redescribed by Gnezdilov (2013a). It can be distinguished from other genera in the tribe Issini by frons enlarged above clypeus, sublateral carinae distinct only in upper half of frons; ocelli present; tegmen elongate, with hypocostal plate, veins ScP + R dividing near to the basal cell, ScP short and fusing with R and forming a loop (Fig. 3, see the arrow), MP with three branches (MP dividing beyond middle of tegmen, and MP1 dividing in distal half of wing), CuA bifurcate (dividing near wing mid-point); clavus as long as nearly 4/5 of wing length; Pcu and A1 joint at mid-point of clavus. Hind wing three-lobed. Hind tibia with two lateral spines in its distal half and with 6–7 apical spines.

Checklist of *Sarima* species

- S. amagisana* Melichar, 1906 – Indonesia (Sumatra, Java), Japan
- S. bifurcus* sp. n. – China (Yunnan)
- S. bimaclata* Melichar, 1906 – New Guinea
- S. carinata* Schmidt, 1910 – Indonesia (Sumatra)
- S. castanea* Melichar, 1906 – Philippines (Luzon)
- S. clathrata* Melichar, 1906 – Malaysia
- S. cretata* Distant, 1906 – Sri Lanka
- S. elongata* Melichar, 1903 – Sri Lanka (Gnezdilov 2013a: figs 6, 10, 11)
- S. erythrocyclus* Fennah, 1950 – Fiji
- S. illibata* Melichar, 1903 (type species) – Sri Lanka (Melichar 1906: fig. 73, Distant 1906: fig. 174, Gnezdilov 2013a: figs 1, 3, 5, 8, 9)
- S. miyatakei* Hori, 1971 – Philippines (Hori 1971: figs 10–15)
- S. nigrifacies* Jacobi, 1944 – China (Fujian)
- S. nigriventris* Schmidt, 1928 – Indonesia (Java)
- S. nigrochypeata* Melichar, 1906 – India
- S. notata* Melichar, 1906 – New Guinea
- S. novaehollandiae* Jacobi, 1928 – Australia (Queensland) (Gnezdilov and Fletcher 2010: fig. 13)
- S. palawana* Hori, 1971 – Philippines (Hori 1971: figs 1–9)

- S. ryukyuana* Hori, 1970 – Japan (Ryukyus) (Hori 1970: figs 11–17)
S. separata Melichar, 1906 – Indonesia (Mentawai, Sipora)
S. sinensis (Walker, 1851) – China (Hong Kong)
S. solita Melichar, 1906 – Malaysia
S. subfasciata (Melichar, 1903) – Sri Lanka
S. tappana Matsumura, 1916 – China (Taiwan), Japan

***Sarima bifurcus* sp. n.**

<http://zoobank.org/DFDB3CAE-384E-4514-9102-BEE03F333763>

Figs 1–16

Type material. Holotype: male, China: Yunnan, Mengla County, Yaoqu Town, 6 May 1991, coll. Yinglun Wang, Wanzhi Cai; Paratypes: 1 female, same data as holotype; 1 female, China: Yunnan, Menghai County, 25 October 1987, coll. Jinian Feng, Yonghui Cai.

Diagnosis. This species is similar to *S. ryukyuana* (Hori 1970: Figs 11–17) but differs from the latter by: 1) generally dark brown alternated with green, in *S. ryukyuana*, general coloration brown with dark patches; 2) pygofer with hind margin strongly convex, in *S. ryukyuana*, pygofer with hind margin faintly rounded; 3) aedeagus with long process reaching to basal 1/3, the process bifurcated apically in ventral view, in *S. ryukyuana*, aedeagus with long process reaching to base, the process bifurcated basally in lateral view.

Description. Male length (n = 1) (including tegmen): 6.2 mm, length of tegmen: 4.8–4.9 mm; female length (n = 2) (including tegmen): 6.3–6.5 mm, length of tegmen: 5.5–4.6 mm.

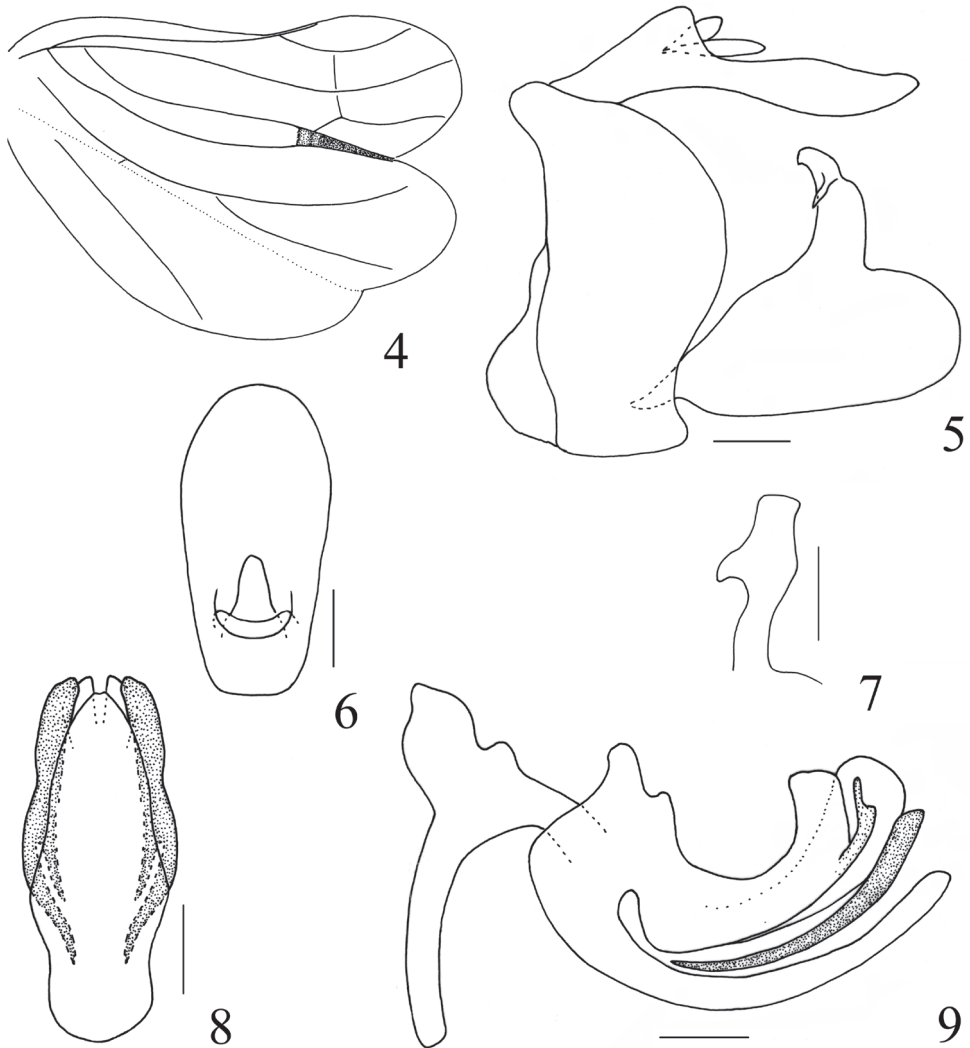
Coloration. Generally dark brown alternated with green. Eyes dark brown. Frons pale brown with yellow brown tubercles, and green near lateral margins. Clypeus brown with median carina and lateral sides yellowish brown. Ocelli brown. Gena yellow with inconspicuous dark speckles. Tegmen dark brown, longitudinal and transverse veins green. Hind wing pale brown with brown to black veins. Leg brown, apex of fore femora and base of fore tibia with dark brown. Abdomen ventrally pale yellowish green and dorsally dark brown, apex of each segment slightly pale yellowish green (Figs 1–3).

Head and thorax. Vertex nearly hexagonal, disc distinctly depressed, with median carina and two round depressions at disc, anterior margin angularly convex and hind margin concave, margins carinated, 1.8 times wider at apex than length in midline (Fig. 1). Frons coarse with small punctures, disc slightly elevated and distinctly expanding below antennae, with median carina and lateral carinae only distinct at upper half of frons; frons with tubercles along lateral margins and upper margin, 0.8 times longer than widest part, 1.8 times wider at widest part than at base (Fig. 2). Frontoclypeal suture distinctly curved. Clypeus smooth with median carina (Fig. 2). Pronotum with anterior margin strongly acutely convex, hind margin nearly straight, disc with median carina and two small pits (Fig. 1); paranotal lobe relatively small,



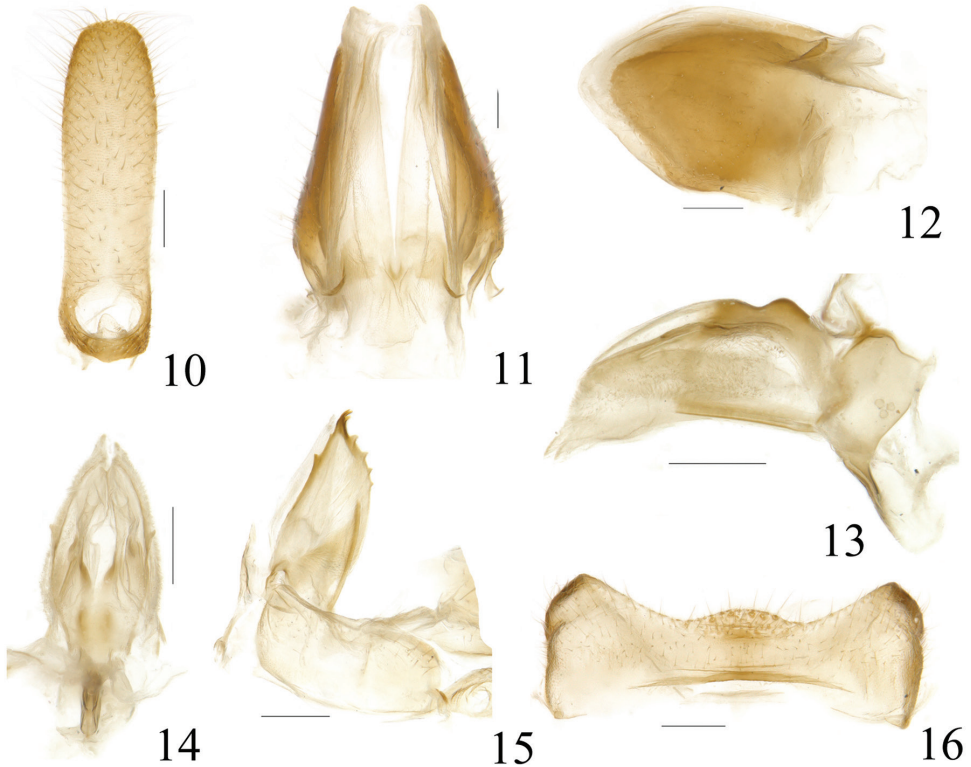
Figures 1–3. *Sarima bifurcus* sp. n. **1** adult, dorsal view **2** frons and clypeus **3** adult, lateral view. Scale bars: 1 mm.

lateroventral angle rounded (Fig. 2). Mesonotum subtriangular with median carina, two small depressions along lateral margin, 2.3 times wider at widest part than long in midline (Fig. 1). Tegmen subquadrate, anterior margin nearly parallel to sutural margin, longer than wide, 2.4 times longer than widest part (Fig. 3). Hind wing with R bifurcate, M, CuP, Pcu, A1 and A2 simple, CuA trifurcate; R2 and M and between M and CuA1 both with single transverse vein almost in a straight line, CuA3 and CuP fused and thickened (Fig. 4). Metatibiotarsal formula 2+7/9/2.



Figures 4–9. *Sarima bifurcus* sp. n. **4** hind wing **5** male genitalia, lateral view **6** male anal segment, dorsal view **7** capitulum, dorsal view **8** phallus, ventral view **9** phallus, left view. Scale bars: 0.2 mm.

Male terminalia. Anal segment in dorsal view nearly oval, widest near apex, apical margin obtusely convex; anus situated at basal part (Fig. 6). Pygofer with hind margin obtusely produced at dorsal half, and slightly concave near ventral margin (Fig. 5). Phallobase with dorsolateral lobe split near apex, lateral lobe forming a small short process near apex, abruptly tapered apically; ventral lobe split from dorsolateral lobe at base, gradually narrowing to apex, apical margin weakly concave at middle in ventral view; aedeagus with long process arising from apex to basal 1/3, the process bifurcated near its apex in ventral view, the inside branch slightly shorter than half length of the outside one (Figs 8, 9). Genital style in lateral view subtriangular, with hind margin



Figures 10–16. *Sarima bifurcus* sp. n. **10** female anal segment, dorsal view **11** gonoplac, dorsal view **12** gonoplac, right view **13** gonapophyses IX and gonaspiculum bridge, right view **14** gonapophyses IX and gonaspiculum bridge, dorsal view **15** gonocoxa VIII and gonapophysis VIII, right view **16** sternum VII, ventral view. Scale bars: 0.2 mm.

strongly concave, caudoventral angle roundly convex (Fig. 5). Capitulum elongate, basal half thin and widened at middle, with a small lateral tooth (Fig. 7).

Female terminalia. Anal segment in dorsal view suboblong, elongate, lateral margins nearly parallel, weakly widened at subapex, apical margin slightly convex; anus short, situated at base (Fig. 10). Gonoplac elongate, with wide membranes near apex, apical margin strongly convex at dorsal half, disc elevated near base in dorsal view, in dorsal view fork faintly pigmented (Figs 11, 12). Proximal part of posterior connective lamina of gonapophyses IX strongly convex in lateral view, median field bifurcate at apex in dorsal view, lateral fields with a pair of short teeth near middle, with the surface bearing numerous microvilli (Figs 13, 14). Anterior connective laminae of gonapophysis VIII broad, ventral margin straight, bearing two small teeth near apex, apical group with three small similar-sized of teeth, with four teeth in lateral group (Fig. 15). Sternum VII with apical margin distinctly arcuately convex at middle (Fig. 16).

Etymology. The specific epithet is derived from the Latin word “*bifurcus*”, referring to the bifurcated process of the aedeagus in ventral view.

***Sarimodes* Matsumura, 1916**

Sarimodes Matsumura, 1916: 115. Type species: *Sarimodes taimokko* Matsumura, 1916. *Paravindilis* Yang, 1994: 94 (in Chan and Yang 1994). Type species: *Paravindilis taiwana* Yang, 1994. Synonymised by Gnezdilov and Hayashi 2013.

Diagnostic characters. The distinctive characters used by Matsumura (1916) are modified as follows.

Head with eyes slightly narrower than pronotum. Vertex hexagonal, all margins ridged, with weak median carina, disc moderately depressed (Figs 17, 33). Frons slightly longer than wide, upper margin distinctly concave, lateral margins ridged and diverging to below level of antennae thence incurved to frontoclypeal suture, disc convex in upper half, with a row of submarginal tubercles laterally, with short median carina, sublateral carina indistinct (Figs 18, 34). Ocelli present. Frontoclypeal suture arcuately curved upward (Figs 18, 34). Clypeus with disc slightly convex. Rostrum reaching post-trochanter. Pronotum almost as long as vertex, with anterior margin acutely convex, posterior margin nearly straight, median carina present, with two central pits (Figs 17, 33). Mesonotum moderately shorter than pronotum and vertex combined in middle line, with three carinae (Figs 17, 33). Tegmen without hypocostal plate, costal margin convex near basal one-fourth of tegmen, narrowing to obtuse apical margin, longitudinal veins distinctly prominent and transverse veins relatively weak, ScP+R forking near basal cell, ScP just reaching or a little beyond midlength of tegmen, MP forked near distal one-third of tegmen, MP1 bifurcate near apex, CuA forked near middle, almost at the same point as the union of claval veins; clavus almost extended to apical margin (Figs 19, 35). Hind wing well developed, trilobed, veins R, M, CuP, Pcu, A1 and A2 simple, CuA bifurcate, CuA2 and CuP fused and thickened (Figs 20, 36). Hind tibia with two lateral teeth and seven spines apically.

Male terminalia. Anal segment relatively long, anus stubbed, located near base of anal segment (Figs 25, 37). Pygofer in lateral view with hind margin oblique, produced near ventral margin (Figs 22, 38). Phallobase with dorsolateral lobe bearing a pair of strong and long processes near apex, directing cephalad, ventral lobe separate from dorsolateral lobe at base, narrowing to apex; aedeagus with a pair of long hooks at middle (Figs 23, 24, 40, 41).

Distribution. China (Taiwan, Hainan)

***Sarimodes clavatus* sp. n.**

<http://zoobank.org/974ADF4E-9EE5-4D0E-84A4-1F27041D9DEF>

Figs 17–32

Type material. Holotype: male, China, Hainan Province, Jianfengling Mountain, 14 December 1974, coll. Fasheng Li. Paratypes: 1 male, China, Hainan Province,



17



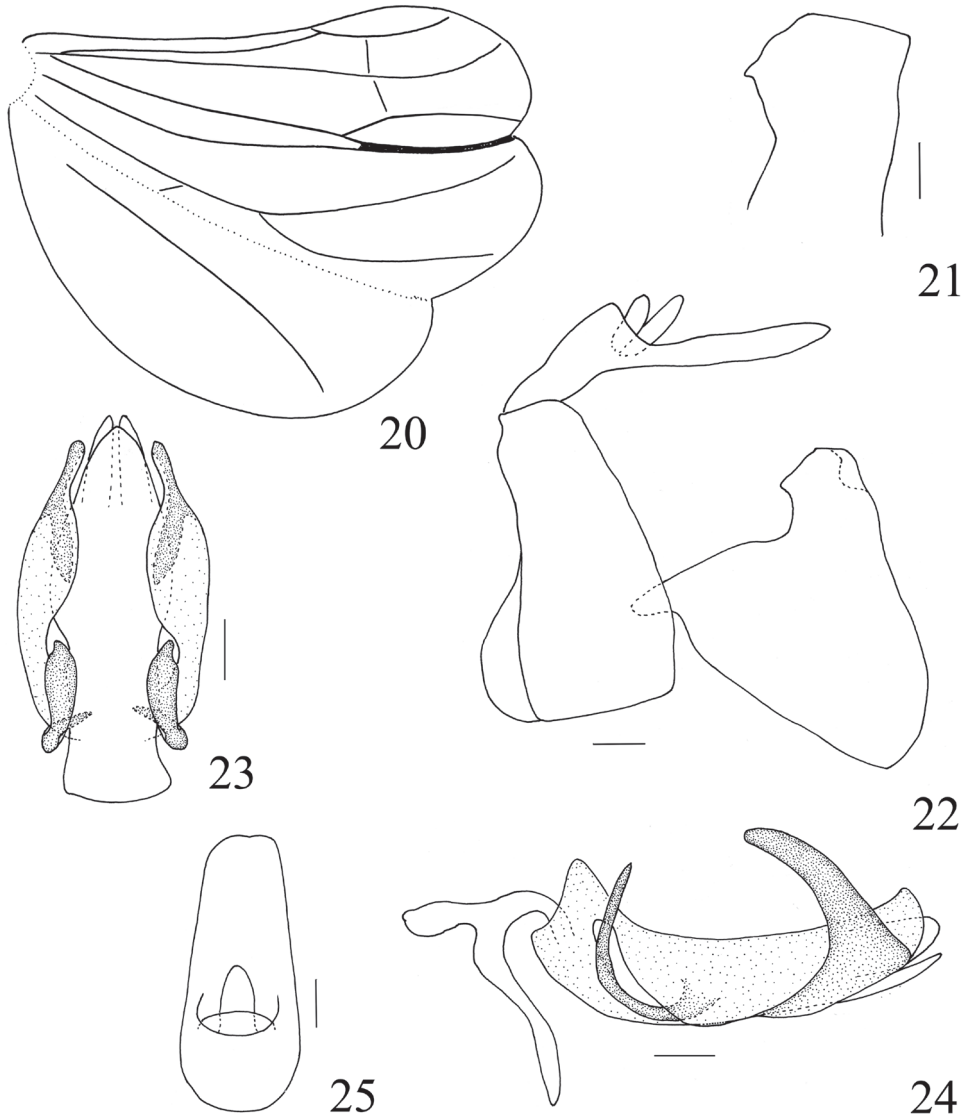
18



19

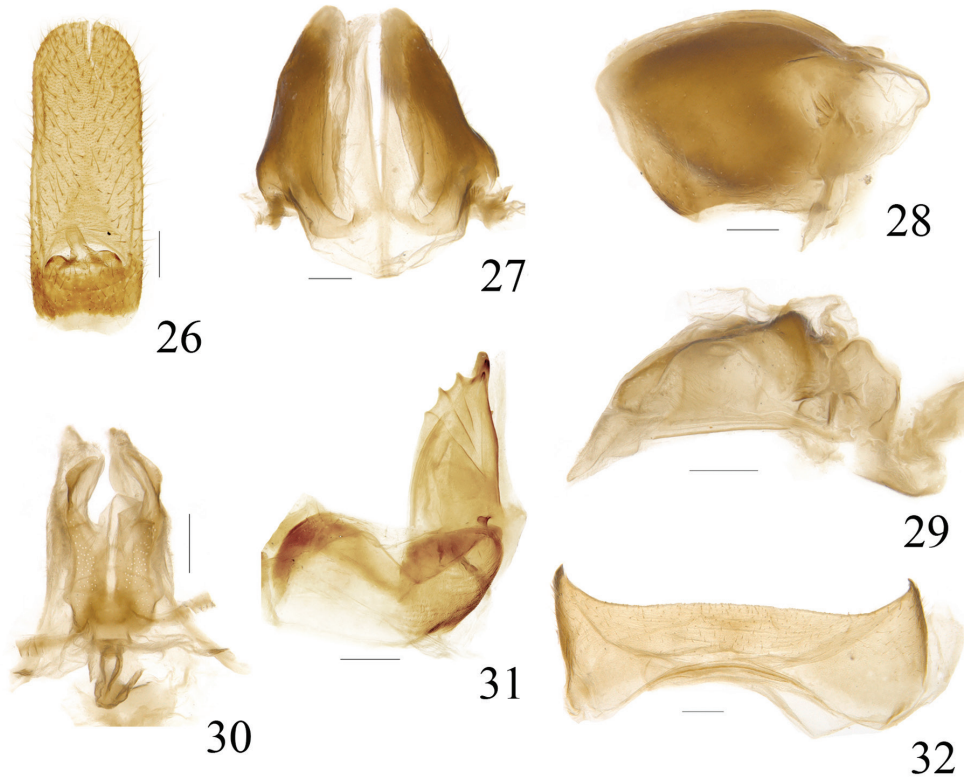
Figures 17–19. *Sarimodes clavatus* sp. n. **17** adult, dorsal view **18** frons and clypeus **19** adult, lateral view. Scale bars: 1 mm.

Jianfengling Mountain, 15 June 1982, coll. Youdong Lin; 1 male, Hainan Province, Jianfengling Mountain, 24 November 1981, coll. Zhenyao Chen; 1 male, Hainan Province, Jianfengling Mountain, 900m, 10 April 1980, coll. Jiang Xiong; 1 female, Hainan Province, Jianfengling Mountain, 18 March 1982, coll. Yuanfu Liu; 1 female, Hainan Province, Jianfengling Mountain, 31 March 1984, coll. Zhiqing Chen; 1 female, Hainan Province, Limu Mountain, 27 May 1984, coll. Maobin Gu.



Figures 20–25. *Sarimodes clavatus* sp. n. **20** hind wing **21** capitulum, dorsal view **22** male genitalia, lateral view **23** phallus, ventral view **24** phallus, left view **25** male anal segment, dorsal view. Scale bars: 0.2 mm.

Diagnosis. This new species resembles *S. taimokko* Mastumura, but differs from the latter by 1) frons with median carina distinct at upper half, in *S. taimokko*, frons with median carina distinct at basal third; 2) genital style with hind margin almost straight, in *S. taimokko*, genital style with hind margin weakly concave near middle; 3) phallobase with dorsolateral lobe bearing a pair of long clavate processes near apex, aedeagus with a pair of curved hooks at middle, in *S. taimokko*, phallobase with dorso-



Figures 26–32. *Sarimodes clavatus* sp. n. **26** female anal segment, dorsal view; **27** gonoplac, dorsal view **28** gonoplac, right view **29** gonapophyses IX and gonaspiculum bridge, right view **30** gonapophyses IX and gonaspiculum bridge, dorsal view **31** gonocoxa VIII and gonapophysis VIII, left view **32** sternum VII, ventral view. Scale bars: 0.2 mm.

lateral lobe bearing a pair of short triangular processes, aedeagus each with two processes, inner one slightly short.

Description. Male length (n = 4) (including tegmen): 7.6–7.9 mm, length of tegmen: 6.6–6.9 mm; female length (n = 3) (including tegmen): 8.8–9.5 mm, length of tegmen: 7.8–9.5 mm.

Coloration. Body fulvous with fuscous maculae. Vertex yellowish brown. Eyes black brown. Frons fuscous with pale tubercles at black lateral area. Clypeus brown with two dark lateral fascia. Rostrum dark brown and black at apex. Ocelli yellowish brown. Pronotum and mesonotum yellowish brown. Tegmen fulvous with fuscous and yellow speckles. Hind wing brown, veins fuscous. Leg fulvous with fuscous transverse stripes, tips of teeth black (Figs 17–19). Abdomen fulvous and fuscous medially.

Head and thorax. Vertex hexagonal, 1.2 times longer than wide in middle line, anterior margin angulately convex at middle, posterior margin deeply angulately excavate (Fig. 17). Frons slightly longer than wide, upper margin distinctly concave, with

median and sublateral carinae present at upper half of frons (Fig. 18). Clypeus smooth with disc slightly convex. Rostrum reaching post-trochanter. Pronotum almost as long as vertex, with anterior margin acutely convex, posterior margin nearly straight, only shallowly emarginate at middle, median carina distinct (Fig. 17), paranotal lobe smooth, ventral margin oblique and straight, lateroventral angle subacute (Fig. 18). Tegmen elongate, 3.1 times longer than wide at widest part at basal third (Fig. 19). Hind wing with single transverse vein in between R and M and between M and CuA1 respectively; CuA2 and CuP fused from one third of CuA2 to apex, the fused part relatively thin and long (Fig. 20). Metatibiotarsal formula 2+7/9/2.

Male terminalia. Anal segment cyathiform in dorsal view, 2.1 times longer than widest part, lateral margin weakly widened at base, apical margin weakly concave at middle (Fig. 25). Phallobase with dorsolateral lobe bearing a pair of long clavate processes near apex, ventral lobe with apical margin acutely convex; aedeagus with a pair of curved hooks at middle (Figs 23, 24). Genital style in lateral view subtriangular, hind margin almost straight, caudo-ventral angle slightly convex (Fig. 22). Capitulum short and wide, with a very small lateral tooth (Fig. 21).

Female terminalia. Anal segment elongate, nearly oblong in dorsal view, 2.5 times longer than widest part, apical margin slightly convex; anus short, situated at base of anal segment (Fig. 26). Gonoplac with apical margin oblique and convex at dorsal half, disc elevated near base in dorsal view, fork faintly pigmented (Figs 27, 28). Proximal part of posterior connective lamina of gonapophyses IX strongly convex in lateral view, median field single lobed, lateral fields obtusely bent at distal part (Figs 29, 30). Anterior connective laminae of gonapophysis VIII broad, ventral margin straight, bearing one tiny tooth near apex, apical group with three short stout teeth, with three keeled teeth in lateral group (Fig. 31). Sternum VII with posterior margin nearly straight at middle (Fig. 32).

Etymology. The specific epithet is derived from the Latin word “clavatus”, referring to dorso-lateral lobe of phallobase having a clavate process in lateral view.

Distribution. China (Hainan).

***Sarimodes parallelus* sp. n.**

<http://zoobank.org/40B74FF0-51AE-43F8-8583-9911A2C885D3>

Figs 33–41

Type material. Holotype: male, China, Hainan Province, Jianfengling Mountain, 27 May 1983, coll. Maobin Gu.

Diagnosis. This new species resembles *S. clavatus* sp. n. in the present paper, but differs from the latter by 1) frons approximately 1.25 times wider than long in middle line, in *S. clavatus*, frons slightly longer than wide; 2) genital style with hind margin produced near apex, caudo-ventral angle strongly convex, in *S. clavatus*, genital style with hind margin almost straight, caudo-ventral angle slightly convex; 3) aedeagus with a pair of hooks semicircularly curved, in *S. clavatus*, aedeagus with hooks almost straight, slightly curved dorsally at apex.



33



34

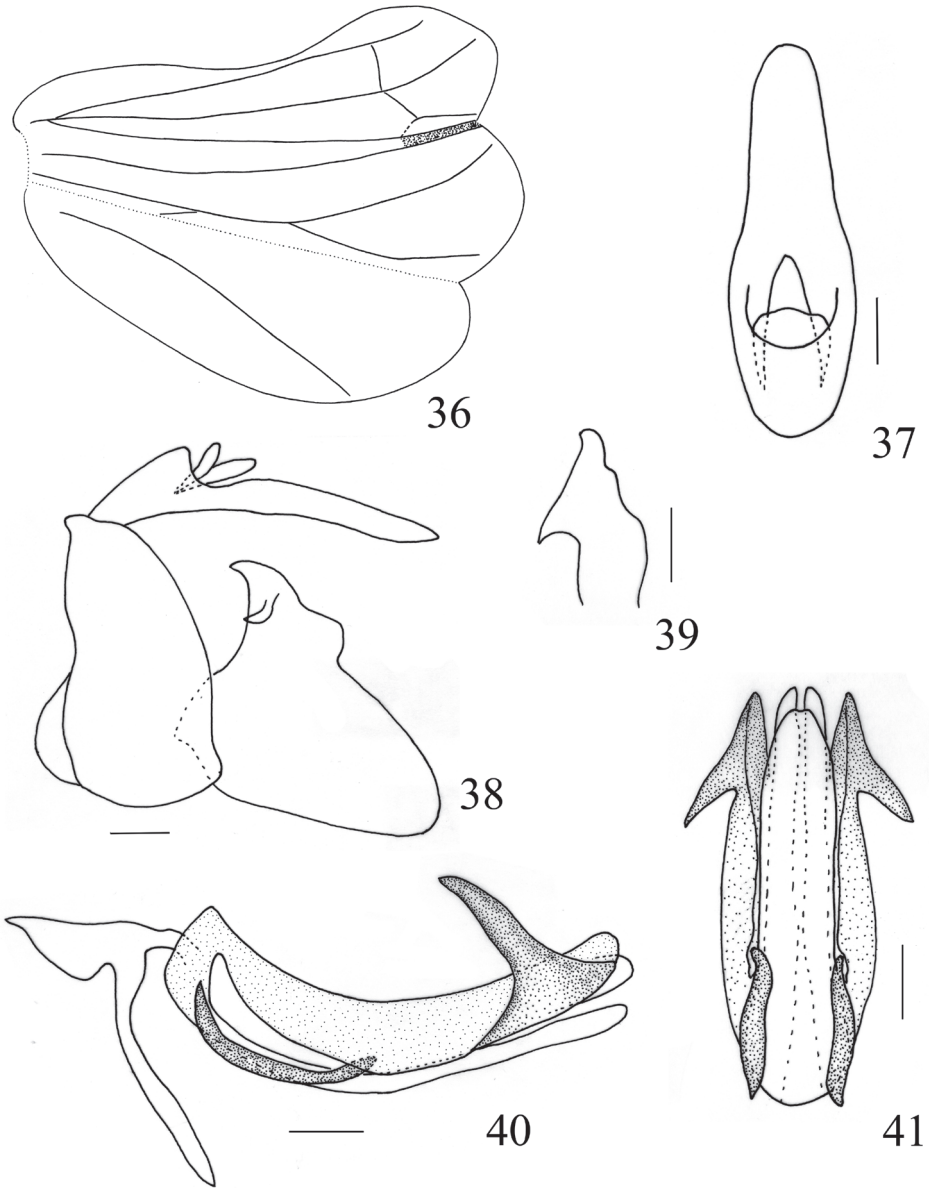


35

Figures 33–35. *Sarimodes parallelus* sp. n. **33** adult, dorsal view **34** frons and clypeus **35** adult, lateral view. Scale bars: 1 mm.

Description. Male length (n = 1) (including tegmen): 6.8 mm, length of tegmen: 5.8 mm.

Coloration. Generally brown with pale brown carinae and dark brown maculae. Vertex yellowish brown with black brown spots. Eyes dark brown. Frons dark brown with pale brown tubercles, near lateral and apical margins black. Gena yellowish brown with dark macula in front of eyes. Antenna with scape pale brown, pedicel brown with pale sensory pits. Clypeus yellowish brown with dark brown longitudinal stripes. Tegmen brown. Hind wing yellowish brown. Leg brown, base and apex of fore and mid femora and tibiae with dark brown band, and base of hind femora dark



Figures 36–41. *Sarimodes parallelus* sp. n. **36** hind wing **37** male anal segment, dorsal view **38** male genitalia, lateral view **39** capitulum, dorsal view **40** phallus, left view **41** phallus, ventral view. Scale bars: 0.2 mm.

brown, tips of teeth black. Abdomen ventrally and dorsally brown, disc dark brown (Figs 33–35).

Head and thorax. Vertex nearly hexagonal, approximately 2 times wider than long in middle line, anterior margin weakly angulately convex at middle, posterior margin

distinctly obtusely concave (Fig. 33). Frons approximately 1.25 times wider than long in middle line, upper margin moderately concave, with median carina present at basal half, with a row of submarginal tubercles (Fig. 34). Pronotum narrower than head combined with eyes, longer in middle line than vertex, median carina distinct, with several small tubercles at lateral area (Fig. 33); paranotal lobes lamelliferous, with three small tubercles along posterior margin, ventral margin moderately oblique (Fig. 34). Tegmen approximately 3.2 times longer than widest part (Fig. 35). Hind wing with single transverse vein in between R and M and between M and CuA1 respectively; CuA2 thoroughly fused with CuP, the fused part relatively thick and short (Fig. 36). Metatibiotarsal formula 2+7/8/2.

Male terminalia. Anal segment elliptical, 2.9 times longer than widest part near base, apical margin obtusely convex (Fig. 37). Phallobase with dorsolateral lobe bearing a pair of spiniform processes near apex, directing cephalad, ventral lobe with apical margin weakly concave medially; aedeagus with a pair of almost straight hooks at middle (Figs 40, 41). Genital style with hind margin obtusely convex near apex, caudo-ventral angle strongly convex (Fig. 38). Capitulum short, with posterior margin sinuate, apex pointed, with triangular lateral tooth (Fig. 39).

Etymology. The specific epithet is derived from the Latin word “parallelus”, referring to the pair of ventral hooks of aedeagus being nearly parallel in ventral view.

Distribution. China (Hainan).

Discussion

The genus *Sarima* currently comprises 23 species including *Sarima bifurcus* sp. n., widely distributed in Oriental region, and also extending into the Eastern Palearctic and Australian regions. Gnezdilov (2013a) proposed that the genus *Sarima sensu stricto* apparently endemic to Sri Lanka and that the generic position of other species described in this genus from other regions needed to be revised. However, the discovery of the new species *Sarima bifurcus* sp. n. from China (Yunnan) in the present paper shows the genus *Sarima* is not an endemic taxon of Sri Lanka. The genus *Sarima* appears to be a large group mainly widely distributed in the Oriental Region. Of course, some species of *Sarima* (*S. amagisana*, *S. ryukyuana*, *S. tappana*) need further study (Gnezdilov 2013b) and the genus *Sarima* needs to be revised.

The genus *Sarima* is very close to the genus *Eusarima* according to the similar structure of phallus, phallobase with dorsolateral lobe split near apex, lateral lobe forming a small short process directing caudad, and aedeagus with long process arising from subapex. But *Eusarima* in contrast to the *Sarima* has the frons with clear sublateral carinae, tegmen without hypocostal plate and vein MP branched at middle. The genus *Sarima* is also close to the genus *Sarimodes* by the similar veins on tegmen. But the genus *Sarimodes* has the frons with short median carina, tegmen without hypocostal plate, and phallobase with dorsolateral lobe bearing a process directing cephalad laterally. The phylogenetic relationships of these close genera needs further study.

Acknowledgements

We are sincerely grateful to Prof. John Richard Schrock (Department of Biological Sciences, Emporia State University, USA) for proof-reading the manuscript. This study is supported by the National Natural Science Foundation of China (31372234, 30970388) and Fauna Sinica (2006FY120100, 2015FY210300) under the Ministry of Science and Technology of China.

References

- Bourgoin T (1993) Female genitalia in Hemiptera Fulgoromorpha, morphological and phylogenetic data. *Annales de la Société Entomologique de France* 29(3): 225–244.
- Bourgoin T, Wang R-R, Asche M, Hoch H, Soulier-Perkins A, Stroiński A, Yap S, Szwed J (2015) From micropterism to hyperpterism: recognition strategy and standardized homology-driven terminology of the forewing venation patterns in planthoppers (Hemiptera: Fulgoromorpha). *Zoomorphology* 134(1): 63–77. doi: 10.1007/s00435-014-0243-6
- Bourgoin T (2015) FLOW (Fulgoromorpha Lists On the Web): a world knowledge base dedicated to Fulgoromorpha. Version 8, updated [2015.11.13]. <http://hemiptera-databases.org/flow/>
- Chan M-L, Yang C-T (1994) Issidae of Taiwan (Homoptera: Fulgoroidea). Chen Chung Book Press, Taichung, 168 pp.
- Distant WL (1906) The fauna of British India, Ceylon and Burma. Rhynchota (Heteroptera-Homoptera) 3. Taylor and Francis, London, 503 pp.
- Distant WL (1909) Rhynchotal notes—XLVIII. *Annals and Magazine of Natural History* (8)4: 73–87. doi: 10.1080/00222930908692643
- Esaki T (1931) Undescribed Hemiptera from Japan and Formosa. *Annotationes Zoologicae Japonenses* 13: 259–269.
- Fennah RG (1950) Fulgoroidea of Fiji. *Bulletin Bernice P. Bishop Museum* 202: 1–122.
- Gnezdilov VM (2013a) Notes on the genus *Sarima* (Hemiptera: Fulgoroidea: Issidae) with description of a new genus from Sri Lanka. *Acta Musei Moraviae, Scientiae Biologicae (Brno)* 98(2): 175–182.
- Gnezdilov VM (2013b) New synonyms and combinations for the planthopper genus *Eusarima* (Hemiptera: Fulgoroidea: Issidae). *Acta Entomologica Musei Nationalis Pragae* 53(2): 485–492.
- Gnezdilov VM, Fletcher MJ (2010) A review of the Australian genera of the planthopper family Issidae (Hemiptera: Fulgoromorpha) with description of an unusual new species of *Chlamydopteryx* Kirkaldy. *Zootaxa* 2366: 35–45.
- Gnezdilov VM, Hayashi M (2013) New Synonyms of *Sarimodes taimokko* Matsumura, 1916 (Hemiptera, Fulgoroidea, Issidae). *Formosan Entomology* 33: 161–165.
- Gnezdilov VM, Holzinger WE, Wilson MR (2014) The Western Palaearctic Issidae (Hemiptera, Fulgoroidea): an illustrated checklist and key to genera and subgenera. *Proceedings of the Zoological Institute RAS* 318 (Supplement 1): 1–124.

- Hori Y (1970) Genus *Sarima* Melichar of Japan, with the description of a new Ryukyu species (Hemiptera: Issidae). Transactions of Shikoku Entomological Society 10(3–4): 79–83.
- Hori Y (1971) Notes on some Philippine Issidae (Hemiptera). Transactions of Shikoku Entomological Society 11(2): 60–70.
- Jacobi A (1928) Results of Dr. E. Mjöberg's Swedish Scientific Expeditions to Australia 1910–1913. Rhynchota Homoptera. 1. Fulgoridae und Cercopidae. Arkiv för Zoologi 19A: 1–50.
- Jacobi A (1944) Die Zikadenfauna der Provinz Fukien in Südchina und ihre tiergeographischen Beziehungen. Mitteilungen der Münchener Entomologischen Gesellschaft München 34: 5–66.
- Kato M (1933) Notes on Japanese Homoptera, with descriptions of one new genus and some new species. Entomological World 1: 452–471.
- Matsumura S (1916) Synopsis der Issiden (Fulgoriden) Japans. Transactions of the Shikoku Entomological Society 6(2): 85–118.
- Matsumura S (1936) Six new species of Homoptera collected at Okinawa by Mr. Chiro Yohena. Insecta Matsumurana 10(3): 81–84.
- Melichar DL (1903) Homopteren-Fauna von Ceylon. F.L. Dames, Berlin, 72–81.
- Melichar DL (1906) Monographie der Issiden (Homoptera). Abhandlungen der k. k. Zoologisch-botanischen Gesellschaft in Wien 3: 1–327.
- Metcalf ZP (1958) General Catalogue of the Homoptera, Fascicle IV Fulgoroidea, Part 15 Issidae. North Carolina State College, Raleigh, 561 pp.
- Schmidt E (1910) Die Issinen des Stettiner Museums (Hemiptera-Homoptera). Stettin Entomologische Zeitung 71: 146–220.
- Schmidt E (1928) Die Zikaden des Buitenzorgen Museums (Hemiptera-Homoptera) I. Treubia 10: 107–144.
- Schumacher F (1915) Homoptera in H. Sauter's Formosa-Ausbeute. Supplementa Entomologica 4: 108–142.
- Spinola M (1839) Sur les Fulgorelles, sous-tribu de la tribu des Cicadaïres, ordre des Rhyngotes (Suite). Annales de la Société Entomologique de France 8: 339–454.

One new species and two new records of the genus *Aeolothrips* from Iran (Insecta, Thysanoptera, Aeolothripidae)

Jalil Alavi¹, Mehdi Modarres Awal¹, Lida Fekrat¹, Kambiz Minaei², Shahab Manzari³

1 Department of Plant Protection, College of Agriculture, Ferdowsi University of Mashhad, Iran **2** Department of Plant Protection, College of Agriculture, Shiraz University, Iran **3** Insect Taxonomy Research Department, Iranian Research Institute of Plant Protection, Agricultural Research, Education and Extension Organization (AREEO), Tehran, Iran

Corresponding author: Lida Fekrat (fekrat@ferdowsi.um.ac.ir)

Academic editor: L. Mound | Received 26 November 2015 | Accepted 2 December 2015 | Published 28 January 2016

<http://zoobank.org/38F4436A-04F9-4CF4-86AD-DC402EAD165C>

Citation: Alavi J, Modarres Awal M, Fekrat L, Minaei K, Manzari S (2016) One new species and two new records of the genus *Aeolothrips* from Iran (Insecta, Thysanoptera, Aeolothripidae). ZooKeys 557: 111–120. doi: 10.3897/zookeys.557.7046

Abstract

Aeolothrips gundeliae sp. n. is described, and two bicolored species of the same genus, *A. ericae* Bagnall and *A. albithorax* Pelikan are newly reported from northeast of Iran. Diagnostic characters are provided for each species as well as illustrations to distinguish these species.

Keywords

Aeolothrips, Iran, new record, new species

Introduction

Most species in the order Thysanoptera are placed in one of the two families, Phlaeothripidae or Thripidae. Aeolothripidae, with more than 202 extant species and 23 genera, is ranked as the second largest family of suborder Terebrantia after Thripidae (ThripsWiki 2015). Aeolothripids are mainly distributed in the temperate parts of the world, although members of several genera are restricted to the tropics. Those are mainly flower living phytophagous species, or facultative predators of other arthropods (Reynaud 2010). A few species can be found living at ground level as obligate

predators (ThripsWiki 2015). Approximately 60% of the described species in this family are placed either in the Holarctic genus *Aeolothrips* Haliday or in the Australian genus *Desmothrips* Hood, with 103 and 20 species respectively (ThripsWiki 2015). The remaining known species of this family are distributed between 21 genera.

In Iran, the main aeolothripid genus, *Aeolothrips*, comprises many species (Minaei 2013a). There has recently been a remarkable increase in the number of taxonomic studies on this genus, with the number of species known from Iran increasing from 12 (Bhatti et al. 2009) to 17 (Minaei 2013b), and with four new species in the most recent studies (Minaei 2014, 2015; Alavi et al. 2015). In this paper one further new species of *Aeolothrips* is described from Iran.

Material and methods

The specimens were collected from various places of the northeastern province of Iran, Khorasan-e shomali, during spring of 2014, by shaking or beating flowers onto a white plastic tray. The fallen thrips were then removed from tray surface into the vials containing 95% alcohol using a fine brush. Thrips specimens were mounted onto slides in Canada balsam by minor changes in protocol given by Bisevac (1997). Morphological terminology follows that of Mound and Marullo (1998) and zur Strassen (2003). All measurements were made with a Micros MCX100 microscope; measurements in descriptions are given in micrometers. Photomicrographs were captured using a Motic BA310 microscope with Motic Image Plus 2.0ML software.

Type deposition. The female holotype and one male paratype of *A. gundeliae* sp. n., one female and one male of *A. albithorax*, and two females of *A. ericae* are deposited in Hayk Mirzayans Insect Museum (HMIM), Iranian Research Institute of Plant Protection (IRIPP), Tehran. Furthermore, one paratype female and one paratype male of the new species are deposited in the Senckenberg Natural History Museum, Frankfurt.

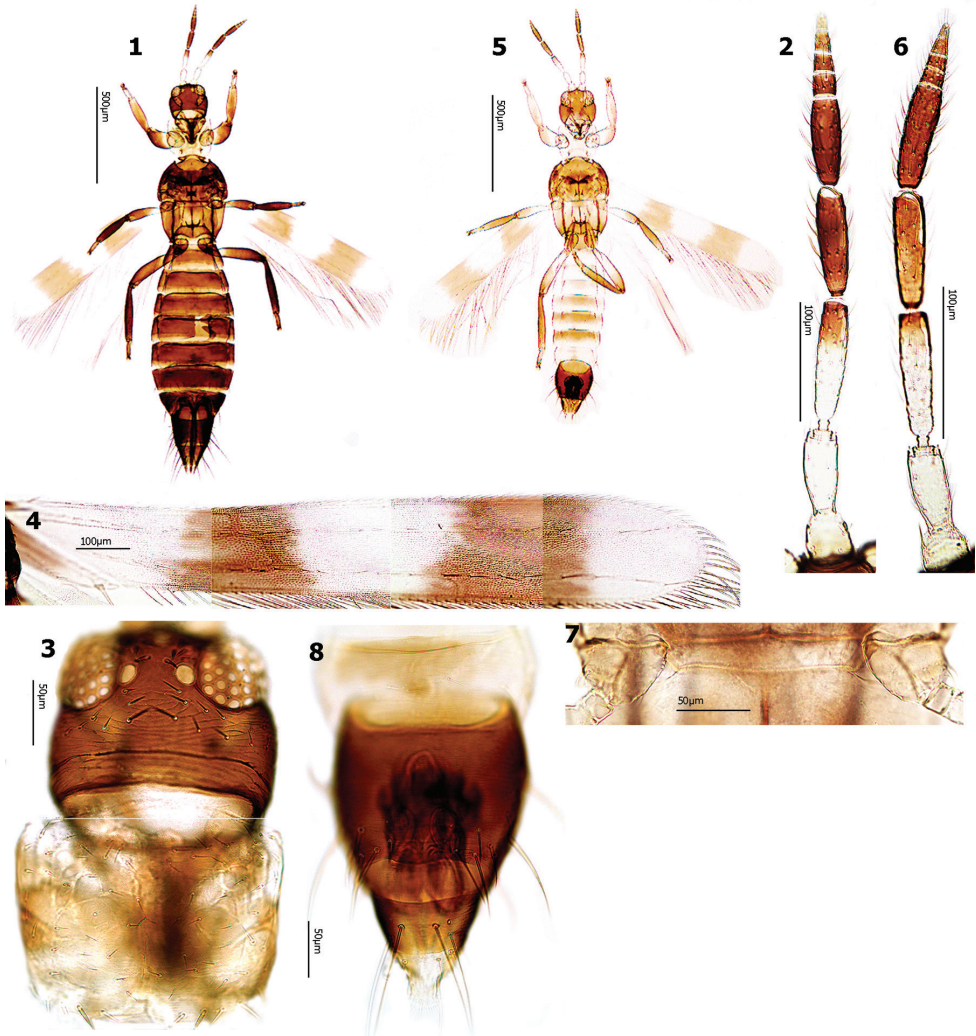
Taxonomy

Aeolothrips albithorax Pelikan, 1964

Figs 1–8

Note. Described from Tajikistan (central Asia), this is the first report of this species outside its type locality. Collected originally from “low herbages” and “*Rumex* sp.” (Pelikan 1964), we collected it only on *Crambe cordifolia*.

Material examined. IRAN, Khorasan-e shomali province, from flowers of *Crambe cordifolia* (Brassicaceae), all collected by J. Alavi: 11 females, 3 males, Bojnourd, Ghuch-ghaleh village, 16 April 2014; 1 male, Bojnourd, Rakhthian village, 21 April 2014; 1 female, Esfarayen, Pelmis spring, 27 April 2014; 1 female, Bojnourd, Chaharkharvar village, 4 May 2014.



Figures 1–8. *Aeolothrips albithorax*. Female: (1–4): 1 Body 2 Antenn 3 Head & pronotum 4 Fore wing. Male (5–8): 5 Body 6 Antenna 7 Middle coxae 8 Abdominal tergites VIII–X.

Diagnosis. Female distinctly bicolored, lemon yellow prothorax in sharp contrast to the rest of the dark brown body (Fig. 1); legs brown. Antennal segment I yellowish grey, II and III yellow, III rather abruptly brown in distal half (Fig. 2). Submedian pair of posteromarginal setae on pronotum longer and stouter than others (Fig. 3). Fore wings with two brown cross bands, connected with dark posteromarginal vein between them (Fig. 4).

Males generally similar to females but paler and smaller (Figs 5–6). Middle coxae without stridulatory structure (Fig. 7). Abdominal tergites IV–VI without dorsal tubercles. Segment IX without claspers, posterior margin of tergite IX convex medially (Fig. 8).

***Aeolothrips ericae* Bagnall, 1920**

Figs 9–18

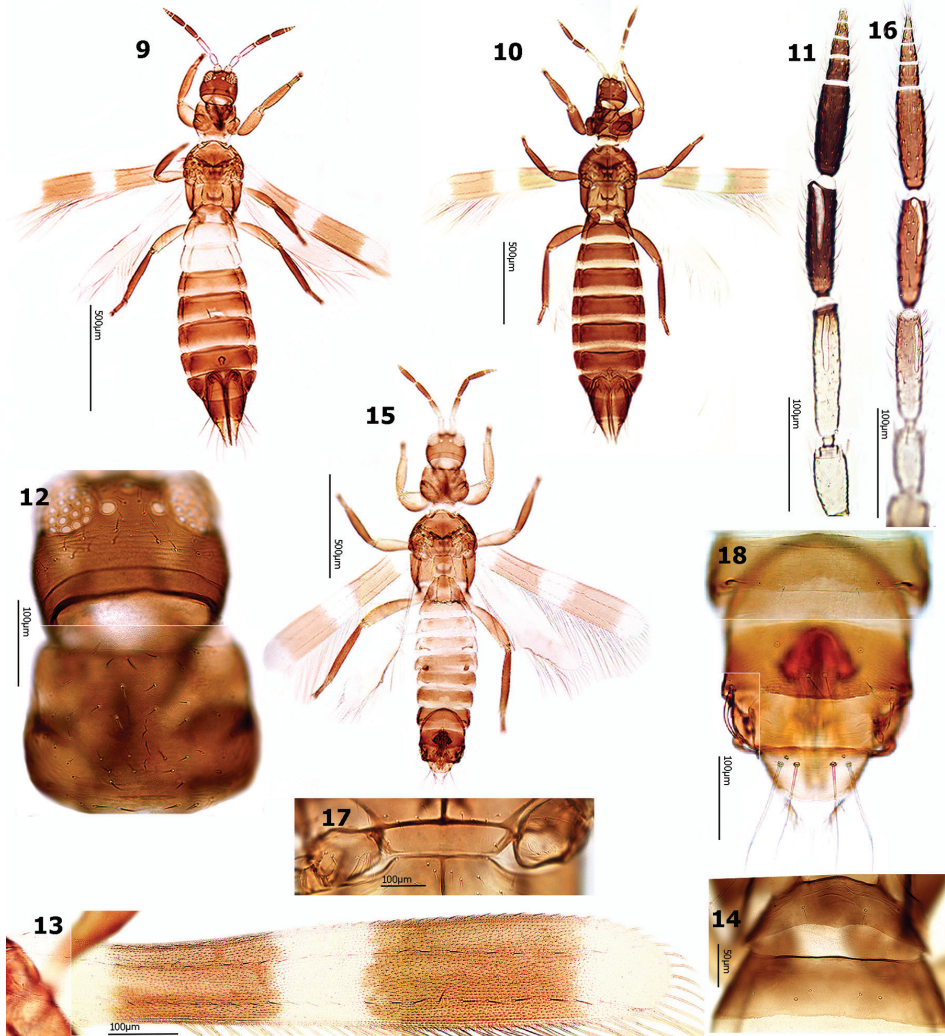
Note. Described from England on flowers of *Erica tetralix*, this species is widespread across western Eurasia, and introduced to North America (zur Strassen 2003, Hoddle et al. 2015). It is usually found on flowering Ericaceae (*Erica* and *Calluna*) but also on various Fabaceae (zur Strassen 2003, Hoddle et al. 2015). This is the first record of this species from Iran.

Material examined. IRAN, Khorasan-e shomali province, all collected by J. Alavi: 1 female, Bojnourd, Oter-abad village, from flowering *Paliurus spina-christi* (Rhamnaceae), 12 May 2014; 1 female, Ashkhaneh, Biyar falls, from flowering *Glycyrrhiza glabra* (Fabaceae), 30 May 2014; 1 female, same location and date, from flowering *Contium maculatum* (Apiaceae). 4 females, Ashkhaneh, Darkesh village, from flowering *Rorippa officinale* (Brassicaceae), 30 May 2014; 2 females, same location and date, from flowering *P. spina-christi*; 1 female, Ashkhaneh, Hawer village, from flowering *Cornus sanguinea* (Cornaceae), 30 May 20; 3 females, same location and date, from flowering *Melilotus officinalis* (Fabaceae). GERMANY, 1 female, Baden-Württemberg, Reichenbach, from herbs and grasses, 1 June 2012, collected by M. Ulitzaka. NORWAY, all collected by S. Kobro: 1 female and 1 male, Haoya, from *Lathyrus pratensis* (Fabaceae), 29 June 1996; 1 female, Aurland, from *Galium verum* (Rubiaceae), 30 June 1998; 1 female, Aurland, from *L. pratensis*, 30 June 1998; 1 female, Fagerstrand, from *L. pratensis*, 5 July 1998; 1 male, Eidfjord, from *Lotus corniculatus* (Fabaceae), 31 May 1999; 1 female, Steigen, from *Vicia cracca* (Fabaceae), 14 July 1999; 1 male, Horten, from *V. cracca*, 2 July 1999.

Diagnosis. Female distinctly bicolored, generally brown with abdominal segment II and/or III yellow to yellowish brown (Fig. 9), sometimes (in European specimens) all abdominal segments uniformly brown (Fig. 10), segment X orange-yellow, much paler than VIII–IX (Figs 9–10); Antennal segment I greyish yellow, II–III yellow, III brown in distal one third (Fig. 11). Pronotum with about 40 discal setae (Fig. 12). Fore wings with two separate long brown cross bands, 2–3 times as long as intervening white area (Fig. 13). Abdominal tergite I without campaniform sensilla (Fig. 14).

Males paler and smaller than females (Fig. 15–16). Middle coxae with stridulatory structure (Fig. 17). Abdominal tergites III–VIII with dorsal tubercles. Segment IX with bifurcate claspers and sickle-shaped setae laterally (Fig. 18).

Remarks. The bicolored body pattern in some specimens of *A. ericae* makes the species resemble only *A. albicinctus* Haliday, but it is distinguished from that antimimic species by its well-developed wings (*versus* usually short wings) and shorter and stouter antenna. Moreover, males of *A. ericae* with bifurcate claspers are readily distinguishable from *A. albicinctus* males. The male of *A. ericae* is also similar in color and structure to *A. collaris*, but it is distinguished from the latter by having distinctly longer cross-bands on fore wings and also shorter distance of median setae S1 from each other.



Figures 9–18. *Aeolothrips ericae*. Female (9–14): 9–10 Body 11 Antennal segments II–XI 12 Head & pronotum 13 Wing 14 Abdominal tergites I–II. Male (15–17): 15 Body 16 Antenna 17 Middle coxae 18 Abdominal tergites VIII–X.

***Aeolothrips gundeliae* sp. n.**

<http://zoobank.org/25D34F9B-C959-4C5F-80A6-42EFA834E136>

Figs 19–33

Material examined. Holotype female: IRAN, Khorasan-e shomalii province, Bojnour, Sar-cheshmeh village, from flowering *Gundelia tournefortii* (Asteraceae), 26 April 2014, collected by J. Alavi.

Paratypes: (all from IRAN, Khorasan-e shomalii province, from flowering *G. tournefortii*, collected by J. Alavi): 25 females, 7 males, same data as holotype; 1 female, Raz, Kargaz village, 10 May 2014; 1 female, Bojnourd, Tatar village, 12 May 2014; 2 females, Shirvan, 20 km after Lojali village, 7 June 2014.

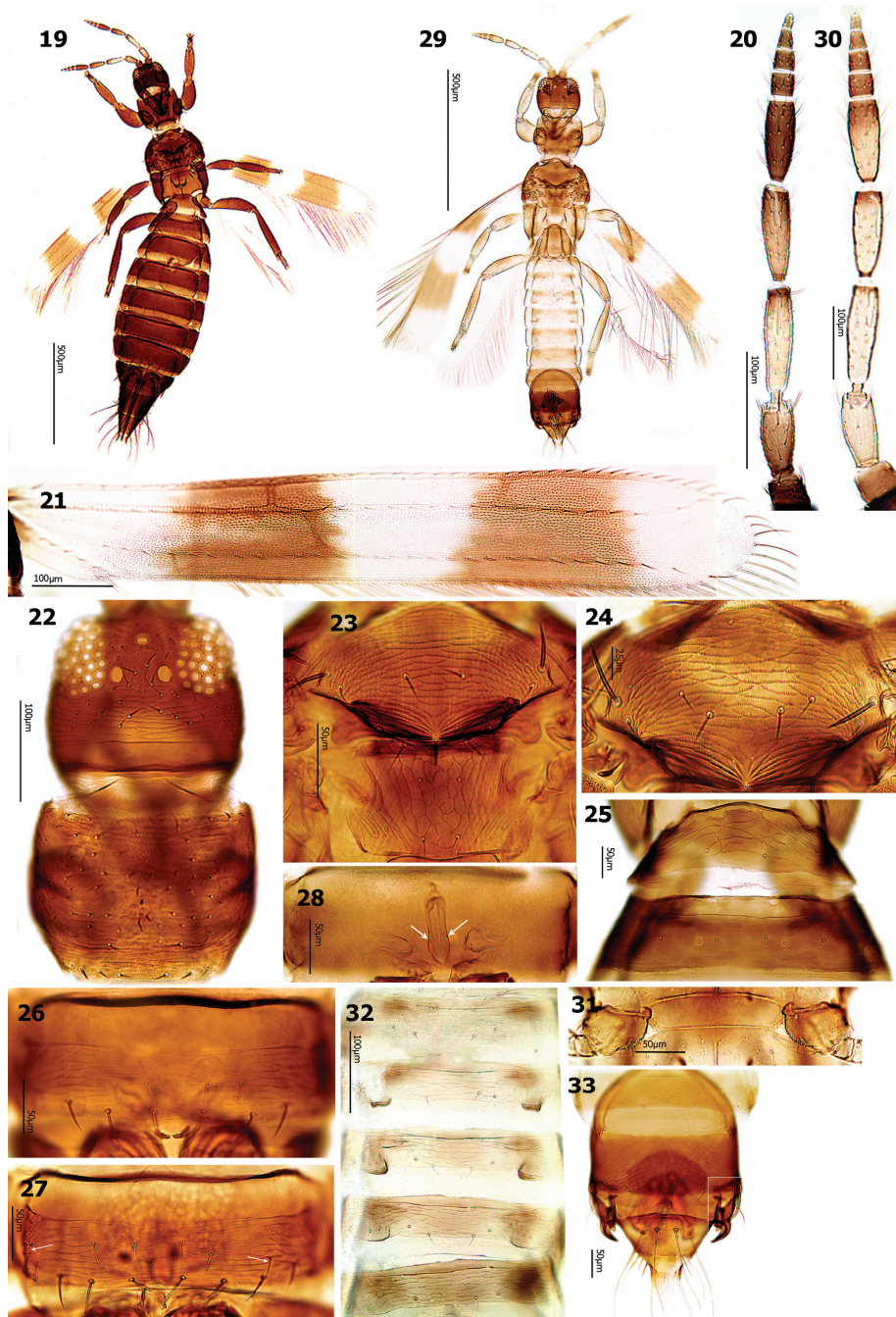
Description. *Female macroptera.* Head wider than long, cheeks convex (Fig. 22); vertex with 6–7 pairs of preocellar setae in front of ocellar triangle; postocular area with 8–9 pairs of setae in 2–3 transverse rows. Antennal segment III with straight liner sensorium, extending to apical third of segment (or more), not reaching to half length of the segment; IV with sensorium curved at apex, extending at most to basal half of the segments, surpassing extreme distal tip of segment (Fig. 20).

Pronotum distinctly sculptured, with about 50 small setae, with 5–6 pairs of post-romarginal setae (Fig. 22). Mesonotum with 1 pair of median setae (Fig. 23), in a few paratypes with 3–4 median setae (Fig. 24). Metanotum with equiangular reticulation medially, without internal markings (Fig. 23). Forewing first cross vein situated in the middle of the first cross band, second cross vein at the basal part of the second cross band (Fig. 21); scale with 6–10 (usually 8) veinal setae.

Abdominal tergite I with distinct transverse striations medially and laterally (Fig. 25); . Abdominal sternites with distinct transverse striations; sternite II with 3 pairs of posteromarginal setae, median pair far from posterior margin; III–VI with 4 pairs; VII with 4 pairs of which the last lateral pair is far from posterior margin, the distance of S1 setae from each other usually approximately equals to that of S1 from S2 (Figs 26–27); sternites II–VI each with 0–3 median discal setae (in holotype, II–V each with 1 seta, and VI with 2 setae); sternite VII with 2 pairs of accessory setae, arranged besides each other, far from posterior margin (Fig. 27–28). In two paratypes sternite VII with 1 or 2 (one seta in each side) discal setae laterally in addition to 2 pairs of accessory setae submedially (Fig. 27). Spermatheca structurally very similar to that of *tenuicornis* (see: Bhatti 1988), but slightly smaller and thinner, with fewer number of spiniform chitinous processes (Fig. 28).

Measurements (holotype female in microns). Body distended length 1900. Head length (width across cheeks) 135 (171). Antenna length 420; segments I–IX length (width): 32 (22), 54 (27), 88 (24), 76 (25), 66 (25), 20 (20), 17 (17), 16 (12), 15 (7). Pronotal median length (width) 140 (220), Pterothorax ventral length (width) 350 (300). Mesonotum median setae length (interval) 17 (42), strong lateral setae length 37. Metanotum anteromarginal setae length (interval) 25 (44), posterior setae length (interval) 15 (25). Fore wings length 940, width across 1st anterior cross vein 122, across second cross vein 135, the cross bands length along the anterior margin 270 and 230–250, the intervening white area length 150. Tibia length: 165, 150, and 250. Tergite IX median length 105, S1 length 159, S2 length 171. Ovipositor length 390.

Male macroptera. Body pale brown (Fig. 29), sometimes seems bicolor; head prothorax and mesothorax brown, metathorax pale brown, abdominal segment I pale brown, II–VI pale brown to yellowish brown, VII–X brown. Legs yellowish brown, fore tibiae yellow, all tarsi yellow. Antennal segments I pale brown; II–IV yellow; III–IV with apical margins light brown; V–IX light brown; V lighter in distal two thirds



Figures 19–33. *Aeolothrips gundeliae* sp. n. Female (19–33): 19 Body 20 Antenna 21 Fore wing 22 Head & pronotum 23 Meso- and metanotum (Holotype) 24 Mesonotum (Paratype) 25 Abdominal tergites I–II 26 Abdominal sternite VII (Holotype) 27 Abdominal sternite VII (Paratype, arrows indicate lateral discal seta) 28 Spermatheca (arrows indicate spiniform chitinous processes). Male (29–33): 29 Body 30 Antenna 31 Middle coxae 32 Abdominal tergites III–VI 33 Abdominal tergites VIII–X.

(Fig. 30). Mesonotum with 1–3 pairs of median setae. Middle coxae with stridulatory structure (Fig. 31). Abdominal tergites IV–VI with dorsal tubercles (Fig. 32). Sternites III with 0–6; IV with 3–6; V with 3–6; VI with 2–7 and VII with 2–5 discal setae. Segment IX with bifurcate claspers, and with sickle-shaped setae laterally (Fig. 33), with dark dorsal plate rounded anteriorly, campaniform sensilla situated out of dorsal dark plate, posterior margin concave medially, semilateral setae short, only slightly surpassing the dorsal furcate claspers, two median setae S1 rather long and curved (Fig. 33).

Measurements (paratype male, in microns). Body distended length 1350. Head length (width across cheeks) 118 (157). Antenna length 360, segments I–IX length (width): 27 (28), 51 (20), 71–76 (20), 60 (22), 56 (23), 13 (18), 12 (15), 12 (12), 10 (6). Mesonotum median setae length (interval) 17 (26–36), strong lateral setae length 27. Fore wings length 780–840, width across 1st anterior cross vein 100, across second cross vein 115, the cross bands length along the anterior margin 120 and 160, the interval white area length 140. Abdominal tergite I length 120–127. Tergite IX median length 76, semilateral setae length (interval) 41–46 (137), length of dorsal setae S1 49, S2 25.

Etymology. This species is named after the genus of plant from which it was collected.

Remarks. Possession of discal setae on sternites is not usual in the genus *Aeolothrips*. This condition can be seen at least in two other aberrant species, the Indian species, *A. moundi* Kulshrestha & Vijay Veer, which has one pair of discal setae laterally on sternite VII in female (Kulshrestha and Vijay Veer 1984), and the African species *A. scabiosatibia* Moulton, with 2–3 pairs of discal setae laterally on sternites VI–VII in female.

Female of *A. gundeliae* sp. n. is distinguished from *A. moundi* by presence of discal setae on sternites II–VI (0–3) and in the same time there is no discal seta on sternite VII (except two paratypes as explained above). Moreover, they are different in mesonotal median setae (1–2 pairs *versus* 1 pair) and color of fore wing apex (white *versus* shaded). Female of *A. scabiosatibia* especially characterized by the spiny fore tibia on dorsal side, and long pronotal posteromarginal seta. Male of the new species is distinguished from *A. moundi* and *A. scabiosatibia* by having claspers and having several discal setae on sternites.

The new species shares some characters with the Australian genus *Desmothrips* Hood, such as presence of discal setae on sternites as well as presence of more than one pair of mesonotal setae in some specimens. But in *A. gundeliae* sp. n., sternal discal setae III–VI are placed medially (*versus* laterally in *Desmothrips*). Additionally, sternite VII has 2 pairs of accessory setae submedially between marginal setae S1 and S2, whereas in *Desmothrips* in addition to the marginal setae, sternite VII has discal setae laterally and sometimes medially, as well as 2 pairs of accessory setae submarginally between marginal setae S1 and S2 (Mound and Marullo 1998, Mound 1972). Finally, apex of fore wing of the new species is not shaded in contrast to *Desmothrips* species (except *D. marilynae* Mound & Marullo, 1998).

Aeolothrips gundeliae sp. n. was collected only on *G. tournefortii* from various areas of the province. Furthermore, this species was observed in 6 of 10 samplings on this plant; so, it seems likely to be a monophagous species on this plant.

Acknowledgments

We would like to express our cordial thanks to Manfred R. Ulitzka (Offenburg, Germany) and Sverre Kobro (Ås, Norway) for the loan of thrips material. We are most grateful to Laurence A. Mound (Canberra, Australia) for his editorial help. Three anonymous referees are much appreciated for their comments on the manuscript. The senior author thanks Majid Gholizadeh and Behzad Yazdani for their generous assistance during collecting trips, and Mehdi Imani for his assistance with determination of plant species.

References

- Alavi J, Modarres Awal M, Fekrat L, Minaei K (2015) The Holarctic genus *Aeolothrips* (Thysanoptera: Aeolothripidae) from Iran, with description two new species. *Zootaxa* 3972(1): 93–100. doi: 10.11646/zootaxa.3972.1.7
- Bagnall RS (1920) Preliminary notes and descriptions of some European species of *Aeolothrips*. *Entomologist's monthly Magazine* 56: 60–62.
- Bhatti JS (1988) The spermatheca as a useful character for species differentiation in *Coleothrips* Haliday (Insecta: Terebrantia: Aeolothripidae). *Zoology (Journal of Pure and Applied Zoology)* 1(2): 111–116.
- Bhatti JS, Alavi J, zur Strassen R, Telmadarraiy Z (2009) Thysanoptera in Iran 1938–2007. An Overview. *Thrips* 7–8: 1–373.
- Bisevac L (1997) A new method for mounting Thrips (Thysanoptera) on slides. *Australian Journal of Entomology* 36(3): 220–220. doi: 10.1111/j.1440-6055.1997.tb01457.x
- Hoddle MS, Mound LA, Paris D (2015) Thrips of California 2012. http://keys.lucidcentral.org/keys/v3/thrips_of_california/Thrips_of_California.html [accessed 18 June 2015]
- Kulshrestha SK, Vijay Veer (1984) Two new species of Thysanoptera (Insecta) from India. *Bulletin of Entomology* 25(1): 33–37.
- Minaei K (2013a) The genus *Aeolothrips* in Iran (Thysanoptera: Aeolothripidae) with one new species. *Zootaxa* 3630(3): 594–600. doi: 10.11646/zootaxa.3630.3.14
- Minaei K (2013b) Thrips (Insecta, Thysanoptera) of Iran: a revised and updated checklist. *Zookeys* 330: 53–74. doi: 10.3897/zookeys.330.5939
- Minaei K (2014) New record of predatory thrips, *Aeolothrips melaleucus* (Thysanoptera, Aeolothripidae) from Iran. *Linzer biologische Beiträge* 46(1): 637–642.
- Minaei K (2015) A new species of the genus *Aeolothrips* (Thysanoptera: Aeolothripidae) from Iran. *Biologia* 70(10): 1401–1405. doi: 10.1515/biolog-2015-0158
- Mound LA (1972) Further studies on Australian Aeolothripidae (Thysanoptera). *Journal of the Australian Entomological Society* 11(1): 37–54. doi: 10.1111/j.1440-6055.1972.tb01603.x
- Mound LA, Marullo R (1998) Biology and identification of Aeolothripidae (Thysanoptera) in Australia. *Invertebrate Taxonomy* 12: 929–950. doi: 10.1071/IT97014

- Pelikan J (1964) Five new Thysanoptera from Soviet Central Asia. *Časopis Československé Společnosti Entomologické (Acta Societatis Entomologicae Cechosloveniae)* 61(3): 224–237.
- Reynaud P (2010) Thrips (Thysanoptera). In: Roques A et al. (Eds) Alien terrestrial arthropods of Europe. *BioRisk* 4(2): 767–791. doi: 10.3897/biorisk.4.59
- ThripsWiki (2015) ThripsWiki-providing information on the World's thrips. <http://thrips.info/wiki/> [accessed 18 June 2015]
- zur Strassen R (2003) Die terebranten Thysanopteren Europas und des Mittelmeer-Gebietes. *Die Tierwelt Deutschlands* 74: 1–271.

Systematic revision of the Taiwanese genus *Kurixalus* members with a description of two new endemic species (Anura, Rhacophoridae)

Shu-Ping Wu¹, Chuan-Chin Huang², Chi-Li Tsai³,
Te-En Lin³, Jhih-Jia Jhang³, Sheng-Hai Wu⁴

1 Department of Earth and Life Science, University of Taipei, No. 1, Ai-Guo West Road, Taipei, 10048 Taiwan

2 Department of Anesthesiology, Perioperative and Pain Medicine at Brigham and Women's Hospital, Boston, 02115, USA **3** Taiwan Endemic Species Research Institute, 1, Ming-shen East Road, Chichi Township, Nantou County 55244, Taiwan **4** Department of Life Sciences, National Chung-Hsing University, No. 250, Guo-Guang Road, Taichung City, 40227 Taiwan

Corresponding author: *Shu-Ping Wu* (shupingwu@ntu.edu.tw)

Academic editor: *F. Andreone* | Received 21 July 2015 | Accepted 25 November 2015 | Published 28 January 2016

<http://zoobank.org/139FC028-8FA9-4E42-949F-2D6B29AA649D>

Citation: Wu S-P, Huang C-C, Tsai C-L, Lin T-E, Jhang J-J, Wu S-H (2016) Systematic revision of the Taiwanese genus *Kurixalus* members with a description of two new endemic species (Anura, Rhacophoridae). *ZooKeys* 557: 121–153. doi: 10.3897/zookeys.557.6131

Abstract

Two new species of rhacophorid tree frog were identified in Taiwan. In both new taxa, derived reproductive characteristics of laying eggs in tree holes and oophagous tadpoles are shared with *Kurixalus eiffingeri*, but they are divergent from each other in molecular genetics, mating calls, and tadpole and adult morphology. The morphological characteristics and the molecular phylogenetic evidence support the hypothesis that the two new species, *Kurixalus berylliniris* **sp. n.** and *Kurixalus wangi* **sp. n.**, are both monophyletic lineages.

Keywords

Kurixalus berylliniris sp. n., *Kurixalus wangi* sp. n., oophagous tadpoles

Introduction

There are four genera (*Buergeria*, Tschudi, 1838, *Kurixalus*, Ye, Fei, and Dubois In Fei, 1999, *Polypedates*, Tschudi, 1838, and *Rhacophorus*, Kuhl and Van Hasselt, 1822) and eleven species of rhacophorid tree frogs on the island of Taiwan (Lue et al. 1999, Shang 2010). In 1999, Ye et al. described the monotypic genus of *Kurixalus*, which only contained *Kurixalus eiffingeri* (Fei 1999). Subsequently, new species attributed to the genus *Kurixalus* were identified and characterized in southern Asia and China (Wilkinson et al. 2002, Frost et al. 2006, Li et al. 2008, Li et al. 2009, Hertwig et al. 2013, Yu et al. 2013, Frost 2014, Nguyen et al. 2014a, Nguyen et al. 2014b) mainly based on molecular analyses. *Rana eiffingeri* was originally described by Boettger (1895), based on specimens collected from the “Liukiu -Inseln” (Boettger 1895). At present, this species is distributed on the two isles Iriomote and Ishigaki in the Yaeyama Archipaleago of Ryukyu Islands, Japan (Maeda and Matsui 1989) and the lowland to the medium elevations forests of Taiwan (Lue et al. 1999).

Kurixalus eiffingeri, a native species in the island of Taiwan, is the only rhacophorid within the genus *Kurixalus* that has a tree-hole breeding reproductive mode and oophagous tadpoles (Ueda 1986, Lehtinen and Nussbaum 2003, Wells 2007). *Kurixalus idiootocus*, a species endemic to Taiwan, has a lentic feeding tadpole type, which is similar to most species in the genus *Kurixalus* (Inger 1966, Inger et al. 1999, Kuramoto and Wang 1987). In previous molecular phylogenetic studies, *K. eiffingeri* and *K. idiootocus* have been recovered as sister taxa (Abraham et al. 2013, Yu et al 2013, Nguyen et al. 2014a, b). Since *K. eiffingeri* and *K. idiootocus* are the only two species that have been described from the island of Taiwan, rhacophorid frogs with similar life history to *K. idiootocus* (but see Abraham et al 2013), specifically any rhacophorid frogs with tree-hole breeding reproductive mode or lentic feeding tadpole type would be assigned to either of the two species.

In our study, *Kurixalus* treefrog specimens were collected from the island of Taiwan. Additionally, the specimens of *Kurixalus eiffingeri* were collected from the type localities, Iriomote and Ishigaki isles. In the field, we noticed that some of the *Kurixalus* populations in eastern and southern Taiwan resembled *K. eiffingeri* in external morphology but differed in their reproductive season (November to February) from *K. eiffingeri* (from February to August). One group has an extraordinarily small body size, and the other group has green irises. Further examination of the samples from the two populations and *K. eiffingeri* revealed the differences in external morphology, tadpole morphology, comparative anatomy, mating call analysis, and molecular genetic evidence. From these results, the two populations of rhacophorid frogs are describe as new species.

Materials and methods

Sampling

The type specimens of frogs and tadpoles of the two new *Kurixalus* species were collected by hand, euthanized using a dilute chloretone solution, and fixed in 10% buffered formalin. Frogs were later transferred to 70% ethanol, and tadpoles were stored in 10% buffered formalin. In addition to the type specimens described in this study, 343 samples that consisted of *Kurixalus eiffingeri* and related taxa were collected from 22 locations throughout the island of Taiwan. Furthermore, three specimen of *Kurixalus eiffingeri* were collected from the type locality. One was from Iriomote isle and the other two were from Ishigaki isle (Fig. 1). Based on body size, mating call differences, and iris color, the samples were subdivided into three groups: *Kurixalus eiffingeri*, Taxon 1, and Taxon 2 (Fig. 1).

Morphometric characteristics of adult specimens: snout-vent length (SVL), head width (HW), head length (HL), internarial distance (IN), eye-narial distance (EN), horizontal eye diameter (ED), distance between the anterior margins of eyes (DFE), distance between the posterior margins of eyes (DBE), upper eyelid width (UEW), interorbital distance (IO), tympanic annulus diameter (TAD), distance between the axillae, between posterior margins of the upper arm (AXI), axilla-groin distance (AGD), forearm length (UAW), manus length (PAL), length of first finger from base of palmar tubercle to tip of third finger disc (F1L), width of third finger disc (D3L), femur length (FEL), tibia length (TBL), tarsus length (TSL), foot length from proximal margin of inner metatarsal tubercle to tip of fourth toe (FOL), first toe length (TL), inner metatarsal tubercle length (IML), and disc width of fourth toe (T4D) (Table S1). The abbreviations listed above were chosen to be consistent with Manamendra-Arachchi and Pethiyagoda (2005).

In addition, the eggs and tadpole morphometric characteristics were measured comprising total length (TL), body length (BL), tail length (CL), tail height (TH), tail muscle height (TM), internarial distance (NA), distance between eyes (IN), and tail muscle width (MW) (Altig and McDiarmid 1999a, b). Except for TL, BL, and CL, which were measured using dial calipers, tadpoles and eggs were measured under a dissecting microscope with a stage micrometer. Developmental stages of tadpoles were as defined by Gosner (1960). Drawings of the tadpoles were done by SHW using a dissecting microscope with a *camera lucida* attachment.

All measurements of morphometric characteristics were taken using a dial caliper under a dissecting microscope, and measurements were rounded to 0.1 mm. Digital webbing of the adults was recorded using Savage and Heyer's formula (1997).

T-tests were used to examine whether body size varied by gender within each taxon. An analysis of covariance (ANCOVA) method was used to compare the size-adjusted means of morphometric characteristics. Morphometric characteristics that satisfied the normality assumption were included in a multivariate principal component analysis (PCA) based on the correlation matrix of size-standardized measurements (all

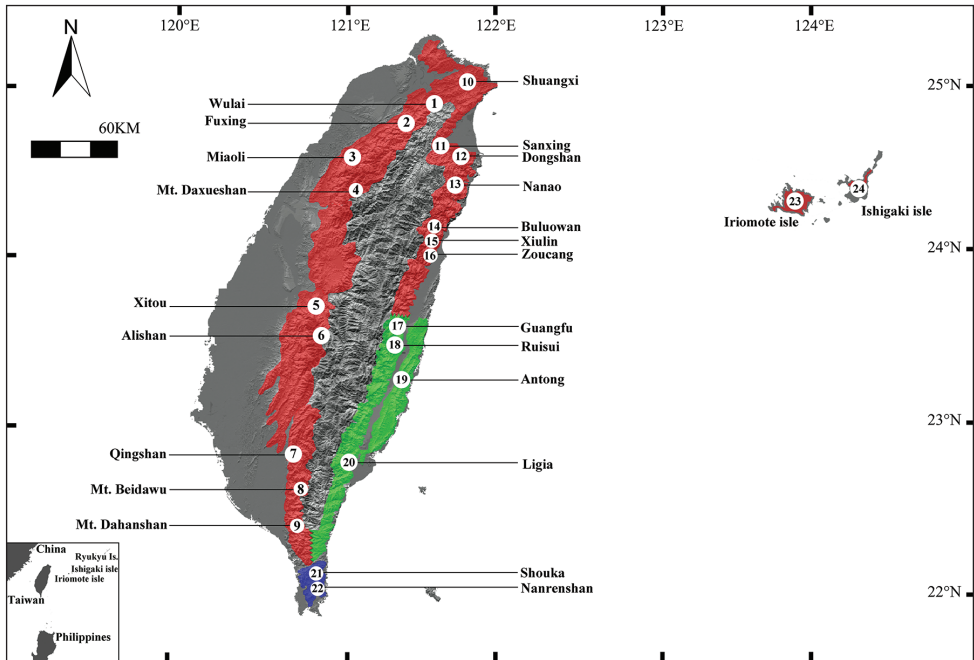


Figure 1. Sampling localities of this study. Localities 1 through 22 are around Taiwan island, locality 23 from Iriomote isle, locality 24 from Ishigaki isle. The two isles belong to the southern end of Ryukyu archipelago. Color refers to the geographical distribution of the three *Kurixalus* species. Red: *K. eiffingeri*; Green: *K. berylliniris* sp. n. (Taxon 1); B: *K. wangi* sp. n. (Taxon 2). Loc. 20: Ligia, type locality of *K. berylliniris* sp. n.; Loc. 21: Shouka, type locality of *K. wangi* sp. n.

measurements divided by SVL). Scatter plots of the scores of the first three factors of PCA were used to examine the differentiation among specimens. All of these tests and analyses were applied separately to male and female specimens. The statistical analyses were performed using SigmaPlot 12 (Systat Software, Inc.).

Mating calls study

Frog mating calls were recorded using a digital recorder (Fostex FR-2LE) and a microphone (Sennheiser ME 67/k6). Calls were recorded in the native habitats of these tree frogs, and environmental parameters including temperature and humidity were also recorded. Avisoft SASLab Pro 5.2.08 (Avisoft Bioacoustics) was used to extract the maximum and minimum frequencies, as well as the width of frequency, the single note duration, and the time interval between notes of the mating calls. A rapid call and a slow call were identified. Slow mating calls were compared among the subtypes in a pair-wise manner using Wilcoxon-Mann-Whitney odds (WMWodds) calculations (Divine et al. 2013). A bootstrap method was used to calculate the Bonferroni corrected confidence intervals of the WMWodds.

Molecular study

Whole genomic DNA was extracted from muscle tissue of fresh or ethanol-preserved specimens using the procedure originally described by Truett et al. (2000). We selected the mitochondrial DNA cytochrome *c* oxidase subunit 1 (CO1) and the 16S rRNA genes to examine the phylogenetic relationships among the three subtypes (S2 and Table S3). The fragments of partial CO1 (658 base pairs) and 16S rRNA (549 base pairs) genes were amplified using the primer pairs LCO1491/HCO2198 (Folmer et al. 1994) and 16Sar/16Sbr (Palumbi 1996, Vences et al. 2005, Vences et al. 2005). Each 50 μ l PCR mixture consisted of 5 μ l 10X reaction buffer containing 15 mM MgCl₂, 4 μ l dNTP (2.5 mM), 0.05 units of *Taq* polymerase (Super-Therm), 0.5 μ l of each primer (10 pm/ λ), 1 μ l template DNA and ddH₂O. Thermal cycling was performed on a GeneAmp 9700 with 5 minutes at 95 °C for pre-denaturing, 35 cycles of 1 minute at 95 °C, 1 minute at 50 °C, 1 minute at 72 °C, and a final extension for 7 minutes at 72°C for both of the CO1 and the 16S rRNA genes. The amplicons were examined on a 2% agarose gel for quality and fragment size. Then they were purified using a Geneaid PCR Extraction Kit and sequenced on an ABI 3730 automated sequencer. Estimates of genetic divergence among taxa were calculated using the Kimura two-parameter model of correction for multiple substitutions at a site (Kimura 1980). The transition / transversion ratio was set as 2:1. Chromatographs and sequences were examined and edited in BIOEDIT 7.0.1. (Hall 1999) and were aligned using CLUSTAL W (Thompson et al. 1994). The homogeneity of the two datasets was analyzed by the ILD procedure (Farris 1995) as implemented in PAUP (Swofford 2002) using the branch-and-bound search algorithm with 1000 permutation replicates to generate the null distribution. The fraction of ILD null replicates with a significance value greater than the significance value of the ILD was recorded. The sequences of the two gene segments were combined into one data set for subsequent analyses. DnaSP 5.10 (Rozas and Rozas 1999) was used to compute the population divergence conditions. TCS 1.21 (Clement et al. 2000) was used to reconstruct the minimum spanning network of haplotypes from each genetic population or species. A consensus ML tree was reconstructed by Mega 6 (Kumar et al. 2008, Tamura et al. 2013) to understand the genetic variation among the haplotypes. Three taxa, *K. idiotocus*, *Feihyla palpebralis*, and *Rhacophorus moltrechti* were used as outgroups in the phylogenetic analysis.

A general time reversible model with a proportion of invariable sites and a gamma shaped distribution of rates across sites (GTR + I + G, I = 0.4402, G = 0.4519) was determined as the best-fitting model for the aligned sequences of the combined dataset using a hierarchical likelihood ratio test performed with the program MrModeltest 2.2 (Nylander 2004). The selected substitution model then was adopted in the reconstruction of the phylogeny by Bayesian analysis and neighbor-joining (NJ) analysis (Saito and Nei 1987).

The Bayesian tree and the posterior probability distribution were determined using the program MrBayes 3.1 (Huelsenbeck and Ronquist 2001, Ronquist and Huelsenbeck 2003). Two independent Monte Carlo Markov Chain (MCMC) analyses were

run simultaneously for 200,000 generations and sampled every 100 generations. To summarize the parameters and trees, the first 500 (25%) parameter values and trees were discarded. The NJ analysis was conducted in PAUP using ML distance. Gaps within the alignment were considered as missing values. The MP (Maximum Parsimony) analysis was performed with a heuristic search using 10 random stepwise steps followed by tree bisection reconnection (TBR) branch swapping. Support for nodes was evaluated by bootstrap analysis (Felsenstein 1985) with 1000 replicates of the NJ and the MP methods.

Partial sequences of mtDNA CO1 gene were used as haplotypes to examine the genetic structures of the three subtypes. We calculated the *Fst*, *Nm* (number of immigrants per generation, $Nm = ((1/Fst) - 1) / 4$), nucleotide diversity (*Pi*), and haplotype diversity (*Hd*). These calculations were made to comprehend the divergence and the intensity of gene flow among these taxa and to infer the evolutionary histories experienced by these taxa or their populations (Wright 1965, Avise 1994).

Results

Systematics

Kurixalus berylliniris sp. n.

<http://zoobank.org/837AE8BF-FF6F-4E27-8849-20EF9E89CA0C>

Figs 2, 3A, C, D, 4A, 5A, 6A, 7A, 7B, 8B; Table 1, Table S5, Table S6, Table S7

Material examined. Holotype. ASIZAM 0053, an adult male (Figs 2 and 3A, Table 1), collected on Ligia timber trail, 1250 m elevation, Taitung County, Taiwan (Fig 1, Loc. 20, 22°49'26.79"N, 121°00'35.45"E), 15 September 2005 by Shu-Ping Wu.

Paratypes. NCHUZOOL 11311-13 collected on 2 August 2005 by Hui-Ming Huang at the type locality; NCHUZOOL 11431, ASIZAM 0054 collected on 15 September 2005 by Shu-Ping Wu at the type locality; NCHUZOOL 11442 (eggs and tadpoles), collected on 7 February 2006 by Shu-Ping Wu at the type locality; NCHUZOOL 11448, collected on 16 February 2006 by Shu-Ping Wu at 425 meters above sea level, at Antong, Hualien County (Fig. 1, Loc. 19, 23°17'06.62"N, 121°21'44.82"E).

Type locality. Ligia timber trail, 1250 meters above sea level, Taitung County, Taiwan, Republic of China (Fig. 1, Loc. 20, 22°49'26.79"N, 121°00'35.45"E).

Diagnosis. A moderate-sized *Kurixalus*. Females average about 41 mm snout-vent length (range: 27.6–46.3 mm); males average about 35 mm (range: 29.0–42.3 mm). Iris emerald to light green. Two dark brown spots on eyelids, separated from each other and from X-shaped blotch on dorsum. Subarticular tubercles on foot rounded and flat. Belly and throat white or faintly-speckled. Prepollex in males squarish, compressed and expanded. About half-webbed between two outer toes. Anterior margin of tadpole dorsal fin extending to body. Tadpole heavily dark brown to black pigmented

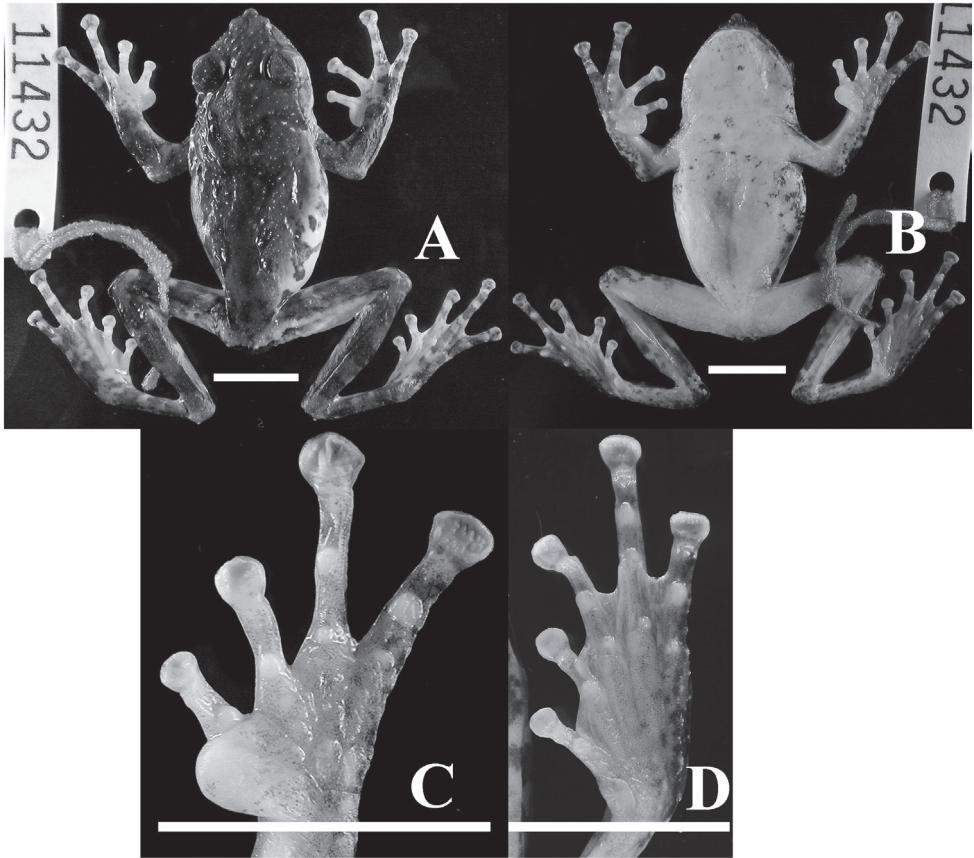


Figure 2. Holotype of *Kurixalus berylliniris* sp. n. Dorsal (A), ventral (B), and ventral view of hand (C) and foot (D). Scale bars: 10 mm.

in gular region and on tail muscle. Upper lip of tadpole with deep transverse furrow, and prominent ridge extending from upper lip to anterior margin of nostril (key of tadpole, 3).

Etymology. The epithet *berylliniris* is a compound word formed from *beryllin* (L.), green-colored, and from *iris* (L.), iris of the eye, and is treated as a noun in nominative singular in opposition to the generic name.

Description of holotype. Habitus moderately slender and somewhat flattened, size moderate (SVL 40.1 mm); head wider than long; tip of snout pointed; snout obtuse in lateral view; nostril barely visible from above; canthus rostralis curved, prominent; loreal region concave, oblique; interorbital distance 1.5 times wider than upper eyelid width; nostril oval, oblique, closer to tip of snout than to eye; internarial distance slightly longer than nostril-eye distance; eye diameter larger than nostril-eye distance; pupil horizontal; tympanic region oblique; diameter of tympanum approximately half of eye diameter; tympanum distinct, round; tympanum to eye distance smaller than half tympanum diameter; supratympanic fold from posterior tip of eye to base of arm;

Table 1. Measurements (in mm) of type series and other specimens of *Kurixalus berylliniris* sp. n. and *K. wangi* sp. n. Abbreviations as in Materials and methods.

no.	<i>K. berylliniris</i> sp. n.			<i>K. wangi</i> sp. n.		
	male		female	male		female
	ASIZAM 53 holotype	Mean±SD ^a (n=13)	range	ASIZAM 55 holotype	Mean±SD ^a (n=17)	range
SVL	40.0	34.4±4.1	29.0–42.3	29.3	30.0±0.9	28.6–31.6
HW	13.1	11.7±1.3	7.4–13.7	11.3	11.2±0.6	10.1–12.2
HL	9.9	9.0±1.1	7.8–12.0	8.6	7.9±0.5	6.7–8.6
IN	4.5	3.6±0.5	3.0–4.5	3.5	3.3±0.2	2.9–3.7
EN	4.5	3.5±0.5	2.9–4.5	3.7	3.2±0.3	2.6–3.7
ED	5.2	4.3±0.5	3.5–5.2	3.5	4.1±0.3	3.5–4.8
UEW	2.9	3.1±0.4	2.8–4.1	3.6	3.0±0.4	2.2–3.6
DFE	7.9	6.7±0.6	6.0–7.9	6.7	6.4±0.5	5.5–7.2
DBE	11.6	10.4±1.0	8.7–12.8	11.0	9.9±0.5	9.1–11.0
IO	5.2	4.1±0.6	3.4–5.2	3.6	4.0±0.2	3.6–4.3
TAD	2.5	2.1±0.2	1.7–2.5	1.9	1.9±0.2	1.5–2.1
AXI	13.8	10.8±1.4	8.9–13.8	10.3	9.9±0.9	7.4–11.0
AGD	19.4	17.4±1.6	15.6–20.6	14.1	13.3±1.6	10.4–16.4
UAW	7.5	6.8±0.9	5.6–8.2	4.5	5.6±0.5	4.5–6.6
PAL	13.9	10.7±1.5	9.2–13.9	9.2	9.0±0.6	8.1–10.3
FIL	6.8	5.5±0.8	4.6–6.8	4.6	4.6±0.4	3.7–5.2
D3L	2.4	1.6±0.4	1.1–2.4	1.8	1.5±0.2	1.1–1.9
FEL	18.8	16.1±2.1	13.0–18.8	14.6	14.6±0.8	13.0–16.0
TBL	19.9	17.0±2.1	14.6–19.9	14.4	14.6±0.8	13.3–16.2
TSL	9.6	8.1±0.8	6.9–9.6	5.9	6.9±0.6	5.9–7.9
FOL	17.9	15.4±2.0	13.0–18.5	12.9	12.4±0.7	11.4–13.9
TL	6.7	5.7±1.0	4.5–7.2	4.2	4.3±0.2	3.8–4.6
T4D	1.7	1.2±0.3	0.8–1.7	1.1	1.3±0.2	1.0–1.6
IML	1.9	1.4±0.3	1.0–1.9	1.3	1.2±0.2	0.9–1.8
					Mean±SD (n=8)	range
					34.3±1.8	30.8–37.1
					12.5±0.6	11.4–13.2
					9.3±1.0	8.3–11.2
					3.7±0.3	3.2–4.2
					3.4±0.2	3.2–3.8
					4.5±0.4	4.0–5.0
					3.3±0.1	3.0–3.4
					6.9±0.5	6.2–7.7
					11.1±0.8	9.6–12.1
					4.2±0.3	3.8–4.8
					2.0±0.1	1.9–2.2
					11.0±1.1	8.9–12.4
					15.0±2.0	12.6–17.8
					6.2±0.4	5.7–7.0
					9.5±0.5	8.8–10.3
					4.8±0.4	4.5–5.7
					1.7±0.1	1.5–1.8
					16.3±0.4	15.4–16.8
					16.4±0.7	15.1–17.1
					7.7±0.5	7.2–8.8
					13.8±0.7	12.6–14.9
					4.8±0.4	4.3–5.3
					1.4±0.3	1.0–1.7
					1.4±0.1	1.2–1.5

^aincluding the holotype.

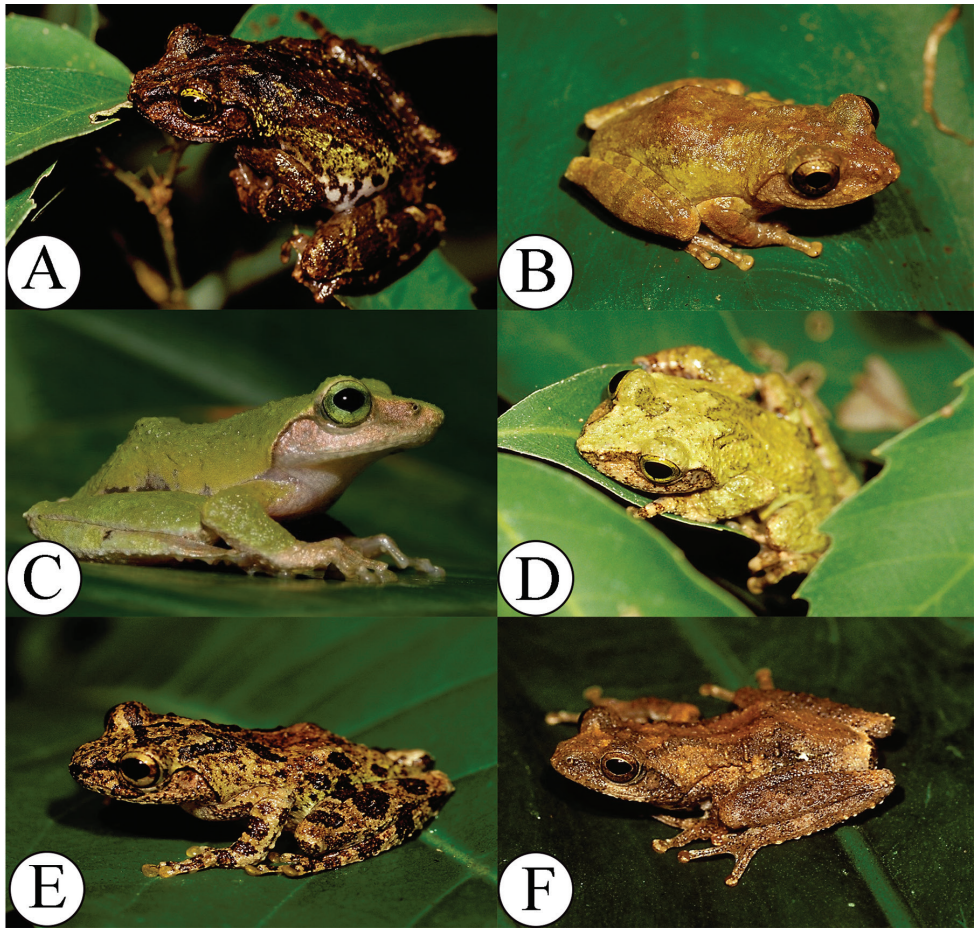


Figure 3. Four *Kurixalus* species of Taiwan. **A** *K. berylliniris* sp. n. (holotype, adult, dark morph) **B** *K. wangi* sp. n. (holotype) **C** *K. berylliniris* sp. n. (sub-adult) **D** *K. berylliniris* sp. n. (adult, light morph) **E** *K. eiffingeri* **F** *K. idiototocus*.

jaw angle almost to posterior rim of tympanum; premaxillary and maxillary teeth present; choana exposed; vomerine teeth present only on left side; tooth patch oval, about half of choana diameter. Vocal slits near commissure of jaw, slit-like.

Limbs slender; tips of all four fingers expanded into discs with ventro-marginal and transverse grooves; disc of finger III about 67% of tympanum diameter; relative finger lengths: I<II<IV<III; relative disc widths I<II<III<IV; disc on finger I small, slightly wider than phalanx width. Webbing more extensive on right hand; only trace of webbing on left hand between fingers III and IV; webbing formula on right hand: I(1.5)–(1.5)II(2)–(2)III(1)–(1.5)IV; subarticular tubercles rounded, elevated, larger under phalanges than at base of fingers; supranumerary tubercles present, smaller than subarticular tubercles; two palmar tubercles, outer longer but narrower than inner. Nuptial pad greatly expanded, proximal edge more flattened than at base; epidermal

glands discontinuous, on lateral margin of nuptial pad, and on internal margin of finger I; outer margin of hand with series of longitudinal tubercles somewhat connected to weak skin folds.

Heels overlapping when adpressed; tips of toes expanded into discs with ventromarginal and transverse grooves; relative length of toes: I<II<V<III<IV; relative width of toe discs: I<II<III<IV<V; disc on toe I small, truncated; disc widest on toe V, less than twice of width of phalanx; webbing formula: I(0.5)–(1)II(0.5)–(1.5)III(1)–(2)IV(1)–(0.5)V; subarticular tubercles rounded, elevated, those at base of toes III, IV, and V smaller than supernumerary tubercles; inner metatarsal tubercle flat, oval, median margin free; outer metatarsal tubercle absent; a series of tubercles on outer surface of tarsus to outer margin of toe V.

Dorsum granular with small tubercles; palpebral tubercles absent; flank and venter smooth or slightly shagreened.

Color. In preservative, two dark brown spots on eyelids; dorsum at shoulder region with a large irregular X-shaped blotch; anterior horn of blotch not continuous with spots on eyelids; two brown blotches on lower back in groin region; flank white with large irregular blotches; dark blotches at cloacal opening, surrounded ventrally by white tubercles; loreal region with dark brown irregular spot; dark spots also present under eye, on posterior part of upper lip near jaw joint, and on supratympanic fold; arm with one thick cross bar on upper arm, two on forearm, one on outer palm; three transverse bars on thigh and on tibia; medial palm and foot white on dorsal surface; venter white; few irregular brown spots on chest, faintly maculated on gular region (Figs 2 and 3A).

Color in life. iris emerald to light green; dorsum dark green to deep tan with a black X-shaped and irregular blotches; tympanum light yellowish-brown with small dark spots; medial surface of hand and foot creamy white; venter cream sprinkled with minute black spots in gular region (Fig. 3A, C, D).

Variation. Sexual dimorphism was evident in the possession of nuptial pads and the hypertrophied upper and lower arms in males. Females were 10% larger than males (t-test, $p > 0.05$). Females possess a supra-cloacal flap (absent in males). The species has dark and white morphs. The dark morph is similar to the holotype (Fig. 3A). In the white morph, the dorsum is light emerald green, and the dorsal X pattern is obscured (Fig. 3C, D). Measurements of the holotype and paratypes are shown in Table 1.

Description of eggs and tadpoles. Average diameter of the eggs was 4.55 (± 0.25) mm ($n = 5$) with capsule and 1.79 (± 0.09) mm ($n = 8$) without capsule. The eggs were creamy yellow with developing embryos. The range of total length of five preserved tadpoles between stages 26–33 was 17.64–30.00 mm (Fig. 5A; Table S4).

Dorsal surface of tadpoles dark brown; ventral surface white; tail fins almost transparent with many faint black flecks; region of tail muscle heavily pigmented, especially anteriorly; body ovoid in lateral view, compressed above, more rounded below; eyes dorsal, not visible from below; eyes on anterior 1/3 of body; nostril lateral, about half way between upper lip and eye; internarial distance 105% of interorbital distance; eye-nostril distance smaller than interorbital distance; a very prominent and elevated

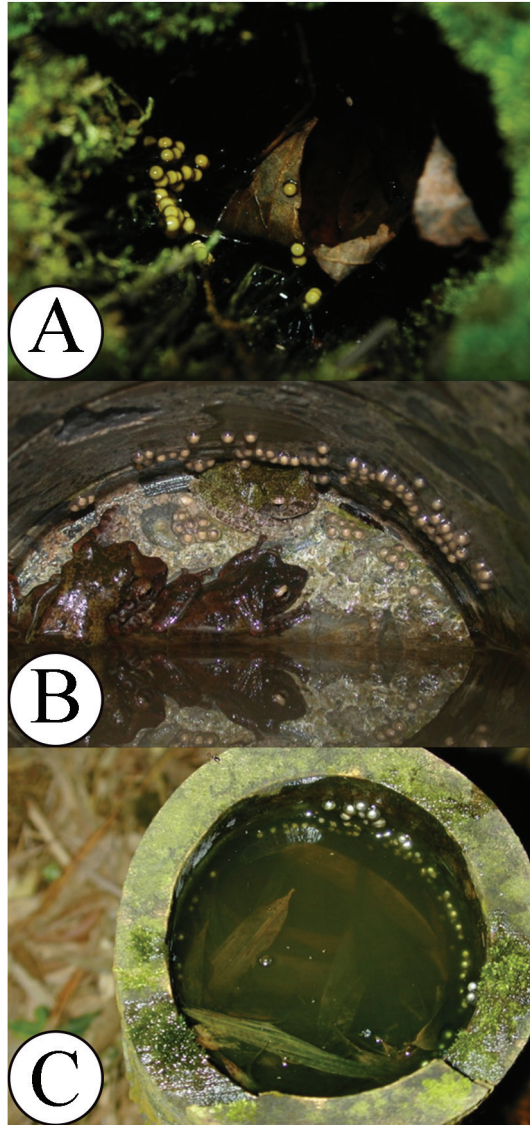


Figure 4. Nesting sites of three tree-hole breeding *Kurixalus* species (a nest is made by the animal). **A** eggs of *K. berylliniris* sp. n. **B** eggs of *K. wangi* sp. n.; note that the parents were present with eggs **C** eggs of *K. eiffingeri*.

ridge extending from nostril to upper lip; a deep transverse groove present in posterior to upper lip; a longitudinal groove on either side of head from lateral rim of upper lip to level between nostril and eye (Fig. 5A). Oral disc terminal, opening anterodorsally; lateral half of upper lip with a single row of papillae; lower lip slightly protruding; a single row of short papillae on lower lip without median interruption. Tooth row formula 3(3)/1(1) or 3(3)/0 or 3(3)/1; the first and second tooth rows on upper lip

Table 2. Measurements of advertisement calls of *Kurixalus* species.

Species	MAX (Hz)	MIN (Hz)	WID (Hz)	DUR (msec)	INT (msec)	DF (Hz)
<i>K. berylliniris</i> sp. n. (slow)	2901 (89)	2517(106)	384 (80)	158 (56)	3195(1060)	2704(35)
<i>K. berylliniris</i> sp. n. (rapid)	2961 (71)	2518 (124)	443 (97)	103 (42)	1562(1442)	2772(360)
<i>K. wangi</i> sp. n. (slow)	3185(194)	2399 (122)	786 (192)	99 (19)	1122 (230)	2841(145)
<i>K. wangi</i> sp. n. (rapid)	3072 (47)	2565 (62)	507 (62)	57 (15)	115 (22)	2848(59)
<i>K. eiffingeri</i>	3034 (59)	2550 (54)	484 (90)	154 (27)	2063 (121)	2772(260)
<i>K. idiootocus</i>	2889 (46)	2412 (64)	477 (80)	48 (16)	1900 (40)	2647(62)

MAX: maximum frequency; MIN: minimum frequency; WID: width of frequency (MAX-MIN); DUR: single note duration; INT: time interval between notes; DF: dominant frequency; all data shown are mean and standard deviation (in parentheses) based on 30 advertisement calls recorded in the field under natural conditions. Environmental parameters: 1) *K. berylliniris* sp. n.: 18 °C, 93% RH. 2) *K. wangi* sp. n.: 25 °C, 84% RH. 3) *K. eiffingeri*: 19 °C, 91% RH. 4) *K. idiootocus*: 24 °C, 80% RH.

long, traverse entire width of upper labium; the third upper tooth row only visible when entire upper lip is upturned, very short, abutting lateral-most edge of second row; lower labium teeth lost in most specimens. Upper and lower beak black; upper beak straight, with median notch and moderately long lateral process, upper beak with medial transverse ridge; lower beak serrated on inner surface. Spiracle sinistral, not tubular; opening at center of body, visible in ventral aspect.

Vent dextral, opening at proximal edge of ventral fin; tail moderately strong, deeper than body; dorsal and ventral fin depth equal, almost symmetrical (or slightly deeper on dorsal fin); origin of dorsal fin anterior to that of ventral fin, on posterior 1/5 of body (Figs 5A and 6A; Table S4).

Distribution and ecological notes. *Kurixalus berylliniris* sp. n. occurs in eastern Taiwan (at 225 to 1250 meters above sea level). The highest recorded elevation was on the eastern slope of the Central Mountain Range (Taitung County, 1250 meters above sea level), and the lowest recorded elevation was on the western slope of the Coastal Range (Hualien County, 225 meters above sea level). Specimens were collected near the canopy level in moist broad-leaf forests in Taitung and on forest edges in Hualien. The northern border of the specimen's distribution was near the Guangfu township of the central Hualien County (Fig. 1, Green stain).

Mating calls. Mating calls were heard during the winter months from November through February. Both a slow call and a rapid call consisted of a single beeping sound. Slow calls recorded in the field had an average duration of 158 (\pm 56) ms ($n = 30$, equivalent thereafter); rapid calls had an average duration of 103 (\pm 42) ms. Intervals between notes were 3195 (\pm 1060) ms (slow calls) and 1562 (\pm 1442) ms (rapid calls). For the slow and rapid calls, the maximum frequencies of calls were 2901 (\pm 89) Hz (slow calls) and 2961 (\pm 71) Hz (rapid calls); the minimum frequencies of calls were 2517 (\pm 106) Hz (slow calls) and 2518 (\pm 124) Hz (rapid calls). (Fig. 7A B; Table 2).

Eggs and tadpoles were found in the pooled water in decaying trunks of tree ferns, *Cyathea spinulosa*. The eggs were adhered together in a single layer by colloidal gel and

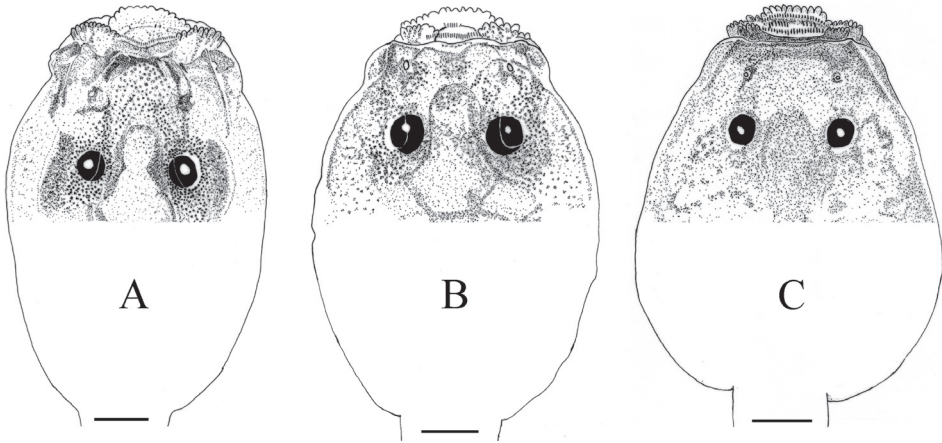


Figure 5. Dorsal view of tadpole head region of three oophagus *Kurixalus* species. **A** *K. berylliniris* sp. n. **B** *K. wangi* sp. n. **C** *K. eiffingeri*. Scale bars 1 mm.

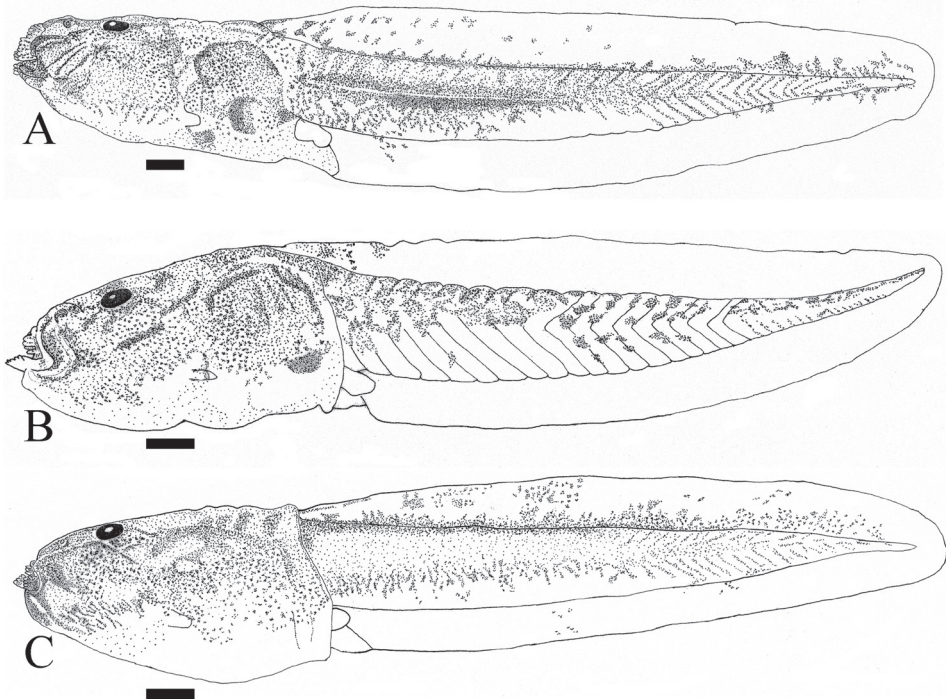


Figure 6. Lateral view of tadpoles of three oophagus *Kurixalus* species. **A** *K. berylliniris* sp. n. **B** *K. wangi* sp. n. **C** *K. eiffingeri*. Scale bars 1 mm.

attached to the inner roof and wall above the water. A total of 62 eggs were counted in one tree hole (Fig. 4A). Tadpoles collected at stages 31 and 33 had a creamy yellow stomach, suggesting the tadpoles might have ingested eggs recently.

***Kurixalus wangi* sp. n.**

<http://zoobank.org/FED9C27A-95D9-43B5-A789-351F1F208953>

Figs 3B, 4B, 5B, 6B, 7C, D, 8; Table 1, Table S5, Table S6, Table S7

Material examined. Holotype. ASIZAM 0055 (Figs 3B, 9, Table 1), adult male collected on Shouka timber trail, 400 meters above sea level, Pingtung County, Taiwan (Fig 1, Blue dots, 22°14'41.12"N, 120°49'50.14"E), 9 February 2005 by Shu-Ping Wu.

Paratypes. NCHUZOO 11161–62, collected on 13 September 2005 by Sheng-Hai Wu at Shuan-Liu, Pingtung County (22°13'15.58"N, 120°49'21.92"E); NCHUZOO 11314, 11318, 11321–32, collected on 20 October 2005 by Shu-Ping Wu, on Shouka timber trail, Pingtung County, NCHUZOO 11315, collected on 8 December 2005 by Shu-Ping Wu at Nanjenshan, Pingtung County (22°05'08.32"N, 120°51'24.04"E); NCHUZOO 11316–17, 11319, collected on 20 December 2005 on Shouka timber trail, Pingtung County; NCHUZOO 11334–35, collected on 7 December 2005 by Shu-Ping Wu, on Shouka timber trail, Pingtung County; NCHUZOO 11441 (tadpoles and eggs), ASIZAM 0056 and NCHUZOO 11445–47, collected on 9–12 February 2006 by Shu-Ping Wu, on Shouka timber trail, Pingtung County.

Type locality. Shouka timber trail, 400 meters above sea level, Pingtung County, Taiwan, Republic of China (Fig 1, Loc. 21, 22°13'15.58"N, 120°49'21.92"E).

Diagnosis. A small to moderate-sized *Kurixalus*. Females snout-vent length averaging about 34 mm (range: 30.8–37.1 mm); males averaging 30 mm (range: 28.6–31.6 mm). Iris golden-yellow. Two anterior horns of the X-shaped marking on back extending to eyelid. Webbing extensive on toes, extending to the toe disc on the inner margin of toe V. Belly and throat whitish. Anterior margin of tadpole dorsal fin extending to posterior body. Tadpole with almost no pigment on region of tail muscle. Upper lip of tadpole with shallow transverse furrow.

Etymology. The epithet is named and dedicated to Mr. Ching-Shong Wang for his pioneering work and contributions to the herpetology of Taiwan (Wang 1962). Mr. Wang discovered two rhacophorid frogs (*Rhacophorus taipeianus* and *K. idiootocus*) (Liang and Wang 1963, Kuramoto and Wang 1987) in Taiwan and suggested, in the early 1980s, that some *Kurixalus* specimens collected near the type locality of this new species might be different from *K. eiffingeri* (personal communication). The name is used in the genitive case.

Description of holotype. Habitus slender, body flat, small (SVL 29.3 mm), head wider than long, snout shape in dorsal view subovoid with pointed tip; profile acuminate, slightly protruding; canthus rostralis distinct, rounded; loreal region oblique, slightly concave; nostril oval and oblique; nostril closer to tip of snout than to eye; internarial distance equals nostril to eye distance; nostril to eye distance smaller than eye diameter; interorbital distance subequal to internarial distance and eyelid width; pupil horizontally oval; tympanum distinct, round, upper margin covered by curved supratympanic fold, which runs from posterior angle of eye to arm; angle of jaw at level of middle of tympanic ring; tympanum less than half of eye diameter; tympanum to

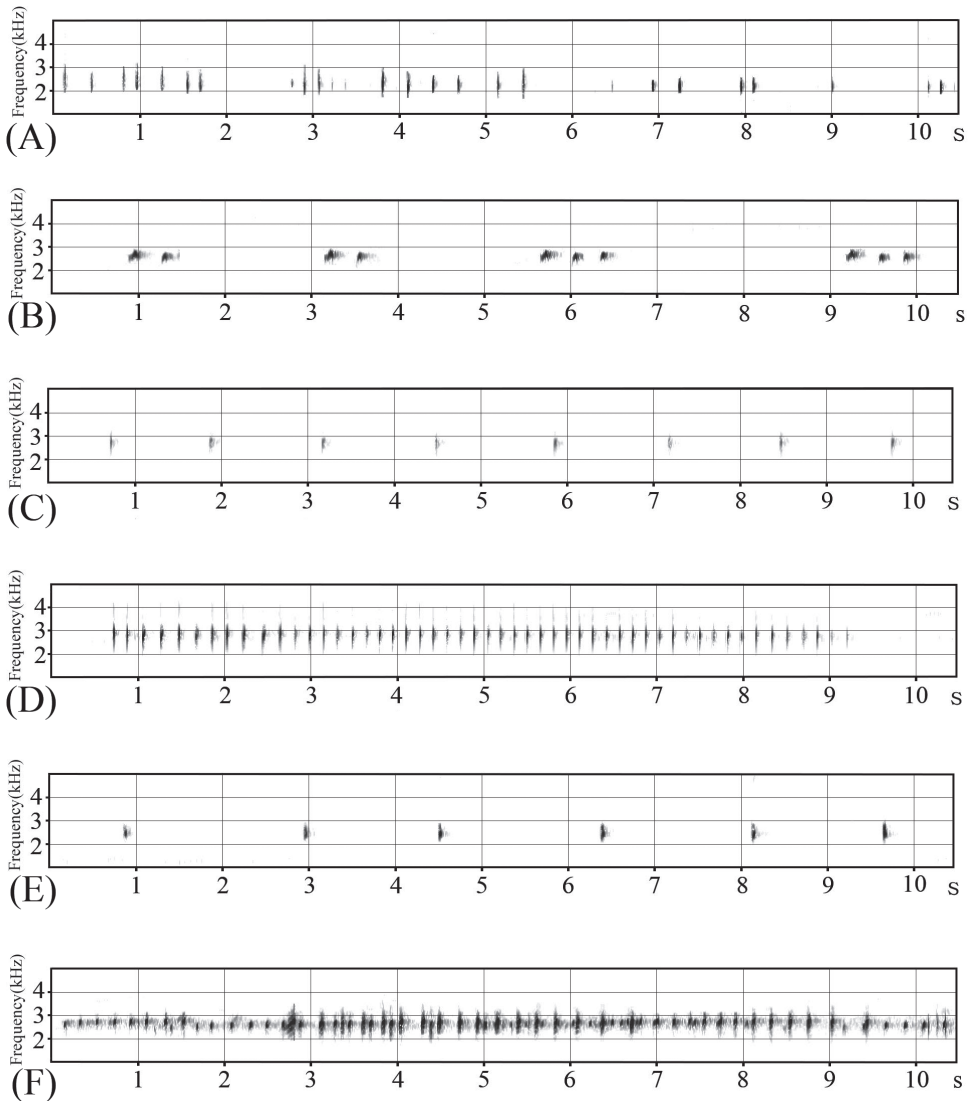


Figure 7. Advertisement calls of four *Kurixalus* species from Taiwan. **A.** *K. berylliniris* sp. n. “slow call” **B.** *K. berylliniris* sp. n. “rapid call” **C.** *K. wangi* sp. n. “slow call” **D.** *K. wangi* sp. n. “rapid call” **E.** *K. eiffingeri* **F.** *K. idiotocus*.

eye distance greater than half tympanum diameter; premaxillary and maxillary teeth present; choana exposed; vomerine odontoid in oval patch, equal in diameter to choana; vomerine teeth present; tongue large, forked and shallowly emarginate; no lingual papilla; vocal slits long, near commissure of jaw on floor of mouth.

Limbs moderately robust; forearm shorter than hand; tips of fingers expanded into discs with ventro-marginal and transverse grooves; disc of finger III about 2/3 of

tympanum diameter; finger length I<II<IV<III; disc even, truncate, with indistinct transverse groove; size of disc I<II<III<IV; disc of finger I small, same width as phalanx width; phalanges emarginate with trace of webbing; subarticular tubercles prominent, rounded, globular; prepollex expanded, rounded; glandular skin associated with nuptial pad from base of disc I on medial and dorsal side of pollex; palmar tubercle double, oval, subequal in size; supernumerary tubercles small; outer margin of fourth finger with longitudinal flat tubercles connected into a weak flap.

Heels overlapping when adpressed; hind limb moderate in length; shank shorter than thigh and longer than foot; tips of toes expanded into discs with ventro-marginal and transverse grooves; relative length of toes I<II<III<V<IV; relative size of discs I<II<III<IV<V; disc on toe I same width as phalanx width; discs truncate and with indistinct transverse grooves. Webbing moderate on all toes; webbing formula I(1)–(trace)II(0.5)–(1.5)III(1)–(2)IV(1)–(0.2)V; weak dermal fringe on outer side of toe V, from posterior tarsus to base of disc V, formed by continuous elongated papilla; subarticular tubercles rounded, slightly conical; subarticular tubercle on proximal joint on toe IV smaller than the others; inner metatarsal tubercle oval, small; outer metatarsal tubercle absent; supernumerary tubercle absent; small white-tipped tubercle on heel.

Skin shagreen, tubercles not present on back; ventral surface slightly granular, white tipped dermal tubercles on posterior thigh. Series of tubercles near lateral margin of upper eyelids; skin smooth on flank; white tipped tubercles on lateral lower arm in ventral view.

Color. In preservative, dorsum grayish with black irregular spots; patches of dark brown markings on median eyelid, forming triangular X-shaped blotch; two posterior branches of the X marking terminated at middle of dorsum; two dark blotches on posterior back; flank with dark oblique irregular band demarcating grayish dorsum and whitish venter; dark irregular blotches on loreal region, antero-ventral corner of eye, and tympanum; black band from anterior eye angle, through nostril to tip of snout; gular region sprinkled with black spots; upper arm with three wide bands, thigh and shank with three bands; ventral surface orange, speckled with brown spots on gular region; vent with large dark brown blotch over cloacal opening, surrounded ventrally and dorsally by white tubercles (Figs 3B and 8).

Color in life, iris golden-yellow; dorsum dark brownish-green scattered with deep brown and black spots, with dark X marking on anterior half of dorsal surface; tympanic membrane light brown to milk-white; white and rounded tubercle located on outer fringe of heel (Fig. 3B).

Variation. Females were 14% larger than males (Table 1) (t-test, $p < 0.01$). Males had longer hands than females. Sexual dimorphism is evident in the possession of nuptial pads and the hypertrophied upper and lower arms in males. Females possess supracloacal dermal flaps (absent in males). The dorsum color of both genders ranges from light brown with distinctly dark markings to almost uniformly light green. Webbing patterns between the two outer metatarsals vary. Among the 69 specimens examined, one was not webbed, and two were 2/3 webbed, and the rest of the specimens were half-webbed or less. Measurements of holotype and other type specimens are shown in Table 1.

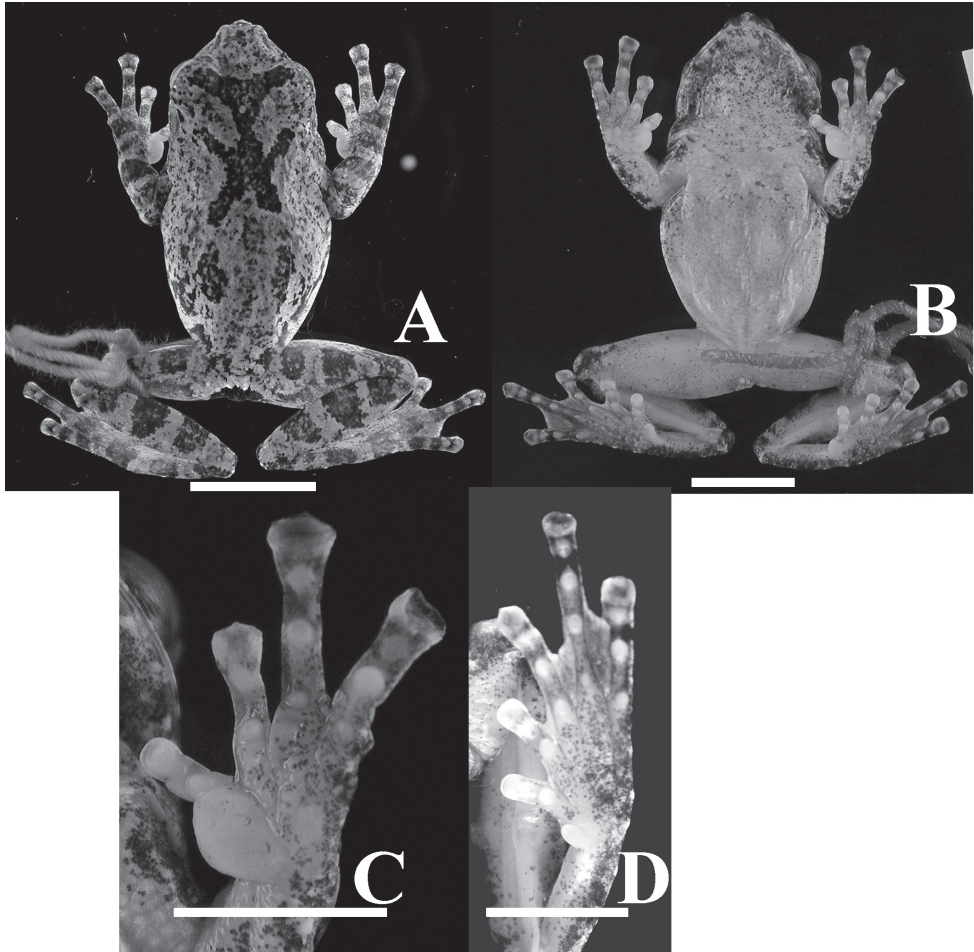


Figure 8. Holotype of *Kurixalus wangi* sp. n. Dorsal (A), ventral (B), and ventral view of hand (C) and foot (D). Scale bars 10 mm in (A) and (B); 5 mm in (C) and (D).

Description of eggs and tadpoles. Average diameter of eggs from 4 clutches was $3.37 (\pm 0.27)$ mm with capsule ($n = 38$) and $1.74 (\pm 0.09)$ mm without capsules; eggs were creamy yellow with developing embryos. The range of total length of ten tadpoles between stages 27–32 was 13.19–22.64 mm (Fig. 4B; Table S4).

Dorsal surface of tadpoles dark brown; ventral surface white; pigment on tail confined mostly to upper half of tail muscle; tail fins transparent; body ovoid in lateral view, flat and sloping above, rounded below; eye dorsal, not visible from below, located on anterior 1/3 of body; nostril lateral; distance from nostril to upper lip much shorter than to eye; internarial distance subequal to interorbital distance; eye-nostril distance less than internarial distance. Face with slightly elevated ridge, from rostrum to upper lip (Fig. 5B). Oral disc terminal, opening anteriorly; lower lip slightly protruding; lateral half of upper lip with a single row of papilla; a single row of short papil-

lae on lower lip without median interruption. Tooth row formula 3(3)/2(1); the first and second rows on upper lip long, traverse entire width of upper labium; the third upper tooth row only visible when the entire upper lip is upturned, very short, confined to the lateral-most edge of the upper labium. The first tooth row on lower labium interrupted medially by a gap half the width of the lower jaw, the second tooth row short, less than half of oral disc width. Lower beak visible only in youngest tadpoles, black in color, upper beak straight, with very short lateral processes, upper beak ridged in middle; lower beak serrated on inner surface; older tadpoles all have broken upper beaks, lower beak white; spiracle sinistral, not tubular; opens at center of body, visible in ventral aspect. Vent dextral, opening at lower edge of ventral fin; tail deeper than body at center; dorsal and ventral fin equal in depth, tail muscle moderately strong. Dorsal fin origin on posterior body (Figs 5B and 6B).

Distribution and ecological notes. *Kurixalus wangi* sp. n. is distributed in the southern part of Pingtung County in southern Taiwan below 500 meters above sea level (Fig. 1, Blue dots). All specimens were collected in the shrubs of secondary forests or lowland broad-leaved forests at low altitudes.

Mating calls. Mating calls were heard in bushes or on tree branches up to 3 m above the ground between September and March, peaking in December. A slow call and a rapid call were identified. Both types of call consisted of a single beeping sound. Slow calls recorded in the field had an average duration of 99 (\pm 19) ms ($n = 30$, equivalent hereafter) and rapid calls had an average duration of 57 (\pm 15) ms. Intervals between notes were 1122 (\pm 230) ms (slow calls) and 115 (\pm 22) ms (rapid calls). For the slow and rapid calls, the maximum frequencies of calls were 3185 (\pm 194) Hz (slow calls) and 3072 (\pm 47) Hz (rapid calls); the minimum frequencies of calls were 2399 (\pm 122) Hz (slow calls) and 2565 (\pm 62) Hz (rapid calls). (Fig. 7C, D; Table 2). The diagrams of all *Kurixalus* species' calls from Taiwan are illustrated in Fig. 7 and detailed in Table 2.

Eggs were discovered in tree hollows, plastic pipes embedded in retaining walls on slopes (Fig 4B), and discarded plastic cups on the forest floor. Eggs of some clutches adhered in a single layer to the walls above water; others were submerged in water. The average clutch size was 70 ($n = 7$, range: 56–104). Tadpole stomachs contained yellow yolk substances, suggesting that the tadpoles might have ingested eggs recently.

Morphological comparisons. Within-species comparisons showed that the body size was differentiated by sex in *Kurixalus eiffingeri* and *K. wangi* sp. n., but not in *K. berylliniris* sp. n. (Table 1, Table S5). Among-species comparisons indicated that males were significantly different in body size ($p < 0.001$, Table S5). ANCOVA tests showed that the three species were significantly different in all morphometric characteristics. For the ANCOVA of male morphometric data, all characters differed significantly, and 17 characteristics exhibited significant variation in size-adjusted means (Table S6). In females, all characteristics also differed in slopes, and eight characteristics exhibited significant variation in size-adjusted means. A repeated ANOVA comparing the two new species and *K. eiffingeri* showed that all morphometric characteristics differed significantly among species between males and females (Table S6).

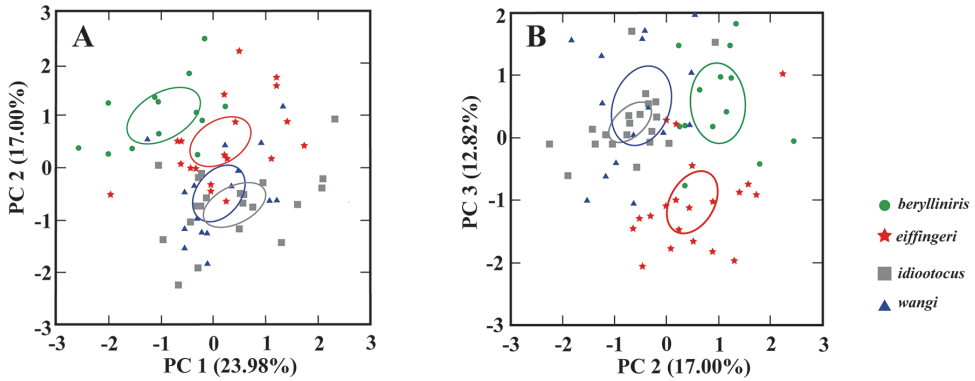


Figure 9. PCA morphometric comparisons of four *Kurixalus* species from Taiwan. Scatterplots of (A) principal components 1 and 2, and (B) principal components 2 and 3 of size-adjusted morphometric data for male frogs of the four *Kurixalus* species. The 95% confidence ellipses for each population (ELM) are shown.

Table 3. Comparisons of the characteristics of slow mating calls among *K. eiffingeri*, *K. berylliniris* sp. n. and *K. wangi* sp. n.

Characteristics	<i>K. eiffingeri</i> vs. <i>K. berylliniris</i> *	<i>K. berylliniris</i> * vs. <i>K. wangi</i> *	<i>K. eiffingeri</i> vs. <i>K. wangi</i> *
	WMWODDS (95% CI)	WMWODDS (95% CI)	WMWODDS (95% CI)
Maximum frequency	3.4 (1.59–10)	Inf (Inf-Inf)	2.67 (1.391–5.88)
Minimum frequency	1.2 (0.571–2.67)	0.18 (0–0.54)	0.53 (0.25–1.04)
Single note duration	0.63 (0.29–1.32)	0 (0–0)	0.37 (0.17–0.72)
Time interval between notes of mating	0.07 (0–0.22)	0 (0–0)	0 (0–0)
Width of frequency	13.67 (4.5-Inf)	Inf (Inf-Inf)	12.75 (5.11-Inf)
Dominant frequency	2.38 (1.2–6.33)	3 (1–9)	1.5 (0.77–3.23)

*slow call

In the PCA, after eliminating the effect of size by using a normalizing ratio (measurements divided by SVL) and omitting the five non-normal morphometric characteristics (HL, EN, TAD, D3L, TL), 23.98% of the variation was associated with body size (Table S7). The large-sized *K. berylliniris* sp. n. was separated from the other three species, while *K. idiototocus* and *K. wangi* sp. n. overlapped considerably (Fig 9A). In the plot of two shape components (Fig. 9B, Table S7), *K. berylliniris* sp. n. and *K. eiffingeri* are clearly differentiated from the other two species *K. idiototocus* and *K. wangi* sp. n.

Mating call comparisons. The calls of the two new species and of *K. eiffingeri* were found to be different in maximum frequency, single note duration, and time interval between notes of mating calls. The minimum frequency among the three species was not different (Table 3).

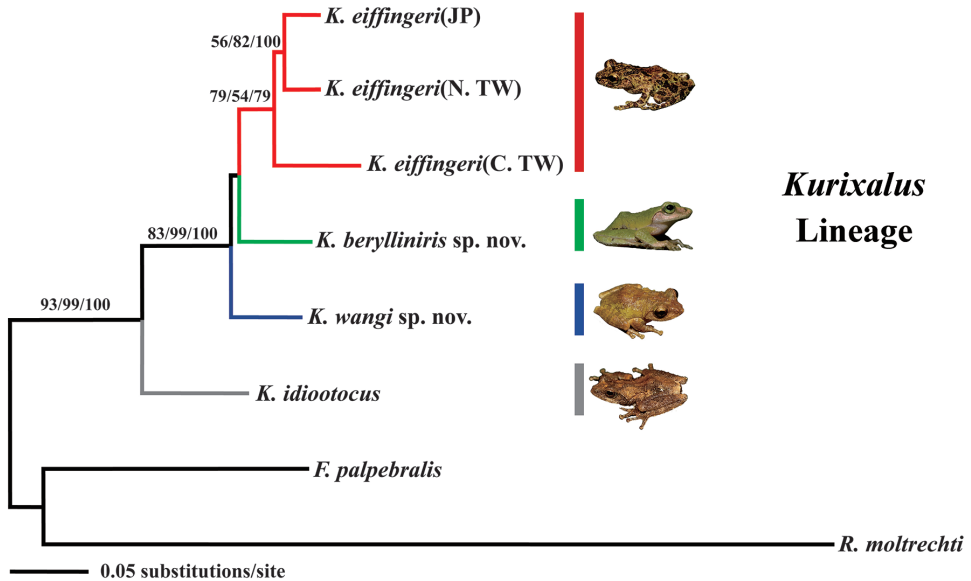


Figure 10. Phylogenetic relationship of all *Kurixalus* species from Taiwan. A phylogram showing the phylogenetic relationships of the four *Kurixalus* species, obtained by a maximum likelihood search based on 1207 nucleotides from mtDNA CO1 and 16S rRNA genes. *Feihyla palpebralis* and *Rhacophorus moltrechti* were used as outgroups. The three values on each branch are maximum likelihood (ML), maximum parsimony (MP), and neighbor-joining (NJ) analyses with bootstrapping support based on 2000 replicates. Bootstrapping values below 50% are not shown. (JP: Ryukyu Islands of Japan; N. TW: northern Taiwan; C. TW: central Taiwan).

Phylogenetic relationships

As demonstrated by the high bootstrap support, the robustness of the phylogenetic relationship of the three rhacophorid genera is strong. Based on this robust phylogenetic tree, we found that the among-genera genetic distances were greater than the within-genus genetic distance (Fig. 10). Using the partial sequence of mtDNA CO1 gene as a molecular marker (Table S2), the genetic distances of the all pair-wise comparisons of the four *Kurixalus* species were all larger than 10% (Table S3). The phylogenetic trees constructed by Bayesian inference, NJ analysis, and MP methods showed the same topology (Fig. 10). The topology of branches was sufficiently supported by the posterior probabilities, bootstrap values, and branch lengths. The four *Kurixalus* species of Taiwan formed a well-structured monophyletic group with distinguishable branch length. Samples of *K. eiffingeri* collected from Iriomote Island, northern Taiwan, and central Taiwan were embedded in the same lineage and formed a monophyletic group (Fig. 11 below). Individuals from southern (*Kurixalus wangi* sp. n.) and eastern Taiwan (*K. berylliniris* sp. n.) were sister taxa of *K. eiffingeri*. *Kurixalus idiotoocus* was phylogenetically distinct from the three *Kurixalus* species (Figs 10 and 11 below).

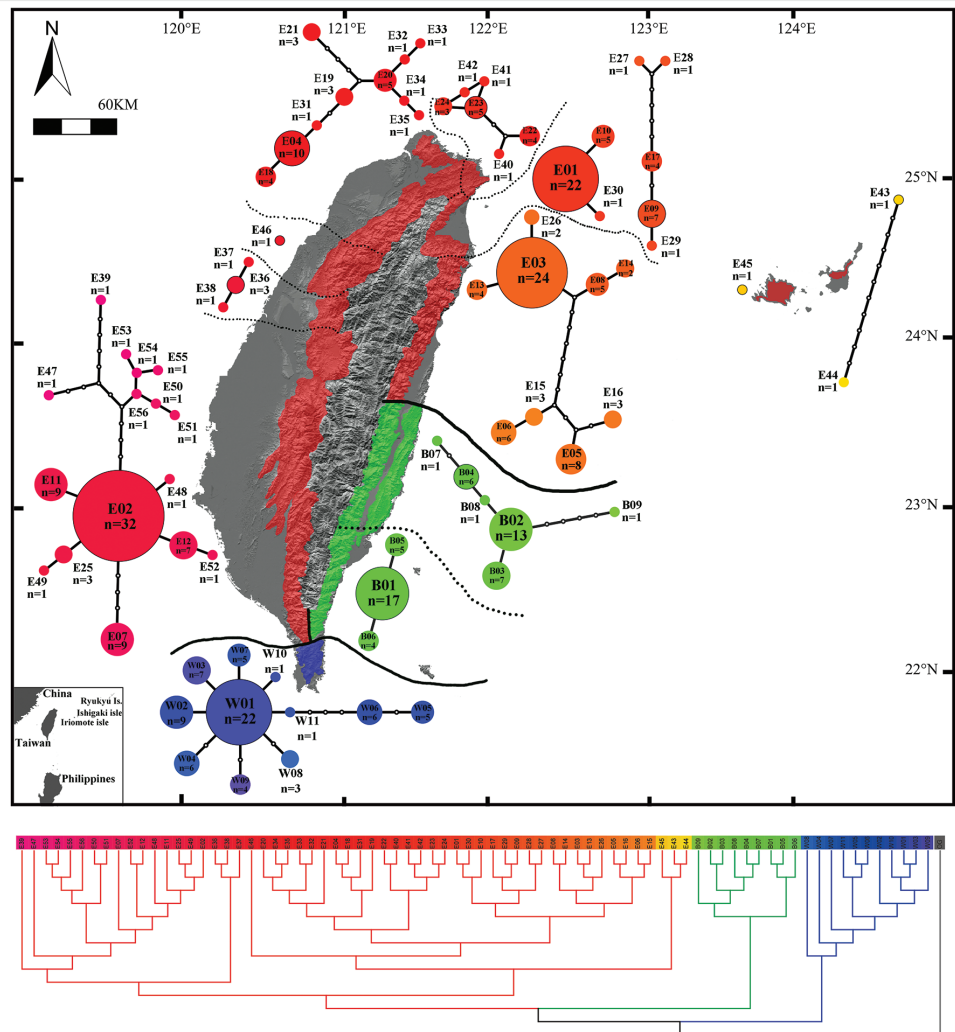


Figure 11. Geographic distribution and genetic structures of *K. eiffingeri* and the two newly discovered cryptic species from Taiwan and its two adjacent islands. Red: *K. eiffingeri*; Green: *K. berylliniris* sp. n.; B: *K. wangi* sp. n. Bold lines mark the boundaries of each species' distribution, dotted lines discriminate different genetic groups intra species. Below: a consensus ML tree to show the variation between haplotypes. GenBank number accession numbers KT259055–KT259131.

The phylogenetic consensus tree of *K. wangi* sp. n. presented a star-like haplotype minimum spanning network with a core ancestral haplotype (W01) and ten derivative haplotypes (W02–W11) (Fig. 11, blue haplotypes, above; blue clade, below; GenBank accession numbers KT259064–KT259074). The within-species haplotypes of *K. berylliniris* sp. n. and *K. eiffingeri* showed a transitional variation pattern. *K. berylliniris* presented two genetic groups that showed two genetic subgroups (Fig. 11, green haplotypes, above; green

clade, below; GenBank accession numbers KT259055–KT259063). *Kurixalus eiffingeri* (including the populations in Taiwan and Ryukyu islands) revealed several subgroups based on genetic structures (Fig. 11, red haplotypes, above; red clade, below; GenBank accession numbers KT259075–KT259130). The topology of the phylogenetic tree matched the geographic distributions of the populations. The monophyletic lineage coincided with the phylogenetic tree, and the genetic divisions are shown in Figs 10, 11 and Table S3.

The indicators of genetic diversity – haplotype diversity (Hd), nucleotide diversity (Pi), and number of haplotypes of each population – are shown in Table S8 and Fig 11. Pairwise comparisons of *Fst* and *Nm* in three *Kurixalus* species (Table S9) demonstrated extremely low gene flow among the three species.

Key to the species of *Kurixalus* from Taiwan

- 1 Dorsum with a brown “) (“ saddle-shaped marking, two arms of the marking not touching each other at mid-dorsum; venter with two large brownish rounded blotches in axilla region; males with very weak nuptial pad; iris golden speckled with brown; cloacal opening of female without supracloacal flap ***K. idiootocus***
- Dorsum with a X- or Y-shaped marking, two arms of the marking touching each other at mid-dorsum; venter without blotches; males with greatly expanded nuptial pad; cloacal opening in females with supracloacal flap..... **2**
- 2 Belly smooth; two spots present on upper eyelids, separated from each other, not in contact with marking on back; medial palmar tubercle larger than lateral one; iris emerald to light green ***K. berylliniris* sp. n.**
- Belly granular or shagreened; spots on upper eyelids in contact each other, forming a dark bar or connecting with the X-marking on back; two palmar tubercles equal in width; iris golden..... **3**
- 3 Tubercles on lateral margin of finger IV connected with dermal fringe; venter whitish with very little pigmentation; loreal region oblique; canthus rostralis curved..... ***K. wangi* sp. n.**
- Tubercles on lateral margin of finger IV separated from each other; venter with numerous fine brownish dots, especially in the gular region; loreal region vertical; canthus rostralis straight ***K. eiffingeri***

Key to the tadpoles of the genus *Kurixalus* species from Taiwan

- 1 Lentic tadpole, mouth antero-ventral, tooth formula 5(3-5)/3 or 5(2-5)/3 ***K. idiootocus***
- Oophagous tadpole, mouth terminal or antero-dorsal, tooth row three or less on upper lip, two or less in lower lip..... **2**
- 2 Dorsal fin originates at base of tail muscle..... ***K. eiffingeri***

- Dorsal fin originates on posterior body **3**
- 3 Dorsum flat in profile; nostril equidistant between upper lip and eye; deep transverse groove on upper lip; a ridge present from lateral margin of upper lip to nostril; gular region and tail muscle heavily pigmented.....
..... ***K. berylliniris* sp. n.**
- Dorsum sloping in profile; nostril closer to upper lip than to eye; inconspicuous transverse groove on upper lip; no ridge from lateral margin of upper lip to nostril; gular region and tail muscle without pigmentation, or with only small scattered spots.....***K. wangi* sp. n.**

Discussion

Based on the 1) different mating call characteristics, 2) different timing of mating calls, 3) diversified morphological characteristics and genetic composition, 4) no interspecies gene flow indicated by extremely high *Fst* and low *Nm*, and 5) sufficient genetic divergences among species (Vences et al. 2005a, b, Table S3), we concluded that the two *Kurixalus* taxa (*K. berylliniris* sp. n. and *K. wangi* sp. n.) from eastern and southern Taiwan are two distinct species. In contrast, with our re-evaluation of the taxonomic status of *K. eiffingeri* we confirmed that the *K. eiffingeri* populations in northwestern Taiwan, central Taiwan, and the Iriomote and Ishigaki isles (Ryukyu islands) are a robust genetic monophyletic group (Figs 10 and 11, Red clade). The two new species resemble *K. eiffingeri* in breeding habits, tadpole morphology, and clutch size. Therefore, *K. berylliniris* sp. n. and *K. wangi* sp. n. were cryptic members of the *K. eiffingeri* complex before our study.

Unlike previous researchers who did not note the within-species variation of mating calls (Kuramoto 1974, Kuramoto and Wang 1987), using an advanced voice recording system we identified that the mating calls of these three species were different in maximum frequency, width of frequency, single note duration, and time interval between notes of the mating calls. The divergence of mating calls plays a major role in pre-zygotic isolation—an important component of speciation (Mayr and Ashlock 1991). Speciation is further promoted by the two new species having different reproductive seasons (Mayr 1942, Mayr and Ashlock 1991, Coyne and Orr 2004)

The guts of tadpoles of the two new species contained a yellow ‘yolky’ substance. When the same characteristic was observed in *K. eiffingeri* it was confirmed as tadpole oophagy (Ueda 1986, Liang et al. 2002). Therefore, it is likely that the tadpole oophagy is a synapomorphy for the two new species and *K. eiffingeri*. Interestingly, *K. idiootocus*, as well as all known *Kurixalus* species from mainland China and Southern Asia lack this particular reproductive behavior. Therefore, the oophagy reproductive behavior could also support the phylogenetic positions of *K. eiffingeri*, *K. berylliniris* sp. n., and *K. wangi* sp. n. within the *Kurixalus* genus.

Previous reports estimated the distribution of *K. eiffingeri* to be up to 2000 m in mountain forests all over the island of Taiwan. These records were problematic in

that they primarily relied on mating call surveys. Our study not only demonstrated the usefulness of advanced voice recording systems in identifying the new species but also highlighted the importance of collecting voucher specimens. In addition to the two newly described species and *K. eiffingeri*, there is one further species in this genus, *K. idiootocus*. Until 1987, *K. idiootocus* was treated as a subgroup within *K. eiffingeri* (Kuramoto and Wang 1987, Liang and Wang 1963). This species is found in low hill habitats up to 1000 meters above sea level throughout the island of Taiwan except the eastern part. In our study, we assessed the morphological characteristics and genetic structure of the four species within the genus *Kurixalus* and confirmed the four Taiwanese *Kurixalus* species are phylogenetic monophyly. To our knowledge, this is the first comprehensive report of the genus *Kurixalus* on the island of Taiwan. The actual amphibian species diversity on the island of Taiwan is likely higher than currently thought, given the diverse habitats and the dynamic history of geographic events. Although Taiwan is a highly developed island with significant alterations to the natural landscape and destruction of critical habitats for amphibians, it is noteworthy that during the last fifty years, six of the seven newly described frog species in Taiwan were treefrogs inhabiting forested areas.

Author contributions

SP Wu envisioned the original idea, executed this study and wrote the manuscript; CC Huang helped with the statistical methods, data analysis, and paper writing; CL Tsai and TE Lin performed the data analyses; JJ Jhang measured and analyzed the mating call data; SH Wu described adult and tadpole morphology, performed anatomical studies, morphometric analyses and proofread the paper. All the authors contributed to this paper sufficiently.

Acknowledgments

We would like to show our gratitude to HM Huang for collecting the first specimen of *K. berylliniris* sp. n.; to JH Chu, CC Hwang, HJ Su and SM Lin for advice on molecular analysis; to H Masaki for providing specimens of *K. eiffingeri* from the Ryukyu islands, to CY Hsiao for photographs; to YT Chung for his dedicated fieldwork; to CC Wu for performing bench work; and to CF Lin for providing *K. eiffingeri* tadpoles. Thanks are extended to CJ Huang, CH Chang, CW Lin and YC Liu for assistance with the fieldwork. We appreciate the help of SF Chan with vocal analysis and YH Chen for partial sample contribution. The map of Taiwan was kindly prepared by PF Lee. This study was partially supported by the Council of Agriculture Grant (94-admin-4.1-conserv-03(2)), by Shei-Pa National Park, Ministry of Interior Grant (094-301020500G1-005), and a support from Mr. CC Chen. RE Brown greatly improved an early draft of the manuscript.

References

- Abraham RK, Pyron RA, Ansil BR, Zachariah A, Zachariah A (2013) Two novel genera and one new species of treefrog (Anura: Rhacophoridae) highlight cryptic diversity in the Western Ghats of India. *Zootaxa* 3640: 177–199. doi: 10.11646/zootaxa.3640.2.3
- Altig R, McDiarmid RW (1999) Body plan: development and morphology. In: McDiarmid RW, Altig R (Eds) *Tadpoles: The biology of anuran larvae*. Univ of Chicago Press, Chicago, 24–51.
- Altig R, McDiarmid RW (1999) Diversity: familial and generic characterizations. In: McDiarmid RW, Altig R (Eds) *Tadpoles: The biology of anuran larvae*. Univ of Chicago Press, Chicago, 295–337.
- Avise JC (1994) *Molecular markers, natural history and evolution*. Chapman and Hall, New York, 511 pp. doi: 10.1007/978-1-4615-2381-9
- Boettger O (1895) Neue Frösche und Schlangen von den Liu-Kiu Inseln. *Zoologischer Anzeiger* 18: 266–270.
- Clement M, Posada D, Crandall K (2000) TCS: a computer program to estimate gene genealogies. *Molecular Ecology* 9: 1657–1660. doi: 10.1046/j.1365-294x.2000.01020.x
- Coyne JA, Orr HA (2004) *Speciation*. Sinauer Associates Inc., Sunderland, MA, USA, 545 pp.
- Divine G, Norton HJ, Hunt RMD, Dienemann J (2013) A review of analysis and sample size calculation considerations for Wilcoxon tests. *Anesthesia and Analgesia* 117: 699–710. doi: 10.1213/ANE.0b013e31827f53d7
- Farris JS, Källersjö M, Kluge AG, Bult C (1995) Testing significance of incongruence. *Cladistics* 10: 315–319. doi: 10.1111/j.1096-0031.1994.tb00181.x
- Fei L (Ed.) (1999) *Atlas of Amphibians of China*. Henan Science and Technology Press, Zhengzhou, 432 pp. [In Chinese]
- Felsenstein J (1985) Confidence limits on phylogenies: an approach using the bootstrap. *Evolution* 39: 783–791. doi: 10.2307/2408678
- Folmer O, Hoeh MBW, Lutz R, Vrijenhoek R (1994) DNA primers for amplification of mitochondrial cytochrome c oxidase subunit I from diverse metazoan invertebrates. *Molecular Marine Biology and Biotechnology* 3: 294–299.
- Frost DR, Grant T, Faivovich JN, Bain RH, Haas A, Haddad CFB (2006) The amphibian tree of life. *Bulletin of the American Museum of Natural History* 297: 1–370. doi: 10.1206/0003-0090(2006)297[0001:TATOL]2.0.CO;2
- Frost DR (2014) *Amphibian species of the world: an Online Reference*. Version 6.0. American Museum of Natural History, New York, USA. Electronic Database accessible: <http://research.amnh.org/herpetology/amphibia/index.html>
- Gosner KL (1960) A simplified table for staging anuran embryos and larvae, with notes of identification. *Herpetologica* 16: 183–190.
- Hall TA (1999) BioEdit: a user-friendly biological sequence alignment editor and analysis program for Windows 95/98/NT. *Nucleic Acids Symposium Series* 41: 95–98.
- Hertwig ST, Schweizer M, Das I, Haas A (2013) Diversification in a biodiversity hotspot – The evolution of Southeast Asian rhacophorid tree frogs on Borneo (Amphibia: Anura: Rhacophoridae). *Molecular Phylogenetics and Evolution* 68: 567–581. doi: 10.1016/j.ympev.2013.04.001

- Huelsenbeck JP, Ronquist F (2001) MRBAYES: Bayesian inference of phylogeny. *Bioinformatics* 17: 754–755. doi: 10.1093/bioinformatics/17.8.754
- Inger RF (1966) The Systematics and Zoogeography of the Amphibia of Borneo. *Fieldiana: Zoology. New Series* 52: 1–402. doi: 10.5962/bhl.title.3147
- Inger RF, Orlov NL, Darevsky IS (1999) Frogs of Vietnam: A report on new collections. *Fieldiana. Zoology. New Series* 92: 1–46.
- Kimura M (1980) A simple method for estimating the evolutionary rate of base substitution through comparative studies of nucleotide sequences. *Journal of Molecular Evolution* 16: 111–120. doi: 10.1007/BF01731581
- Kuhl H, Van Hasselt JC (1822) *Algemeene Konst-en Letter-Bode* 7: 104.
- Kumar S, Dudley J, Nei M, Tamura K (2008) MEGA: A biologist-centric software for evolutionary analysis of DNA and protein sequences. *Briefings in Bioinformatics* 9: 299–306. doi: 10.1093/bib/bbn017
- Kuramoto M (1974) Mating calls of Japanese tree frogs (Rhacophoridae). *Bulletin of Fukuoka University of Education* 24: 67–77.
- Kuramoto M, Wang CS (1987) A new rhacophorid tree frog from Taiwan, with comparisons to *Chirixalus eiffingeri* (Anura: Rhacophoridae). *Copeia* 1987: 31–42. doi: 10.2307/1445556
- Lehtinen RM, Nussbaum RA (2003) Parental care: a phylogenetic perspective. In: Jamieson BGM (Ed.) Chapter 8, *Reproductive Biology and Phylogeny of Anura*. Science Publishers, Inc., Plymouth.
- Li JT, Jing C, Bain RH, Zhao EM, Zhang YP (2008) Molecular phylogeny of Rhacophoridae (Anura): A framework of taxonomic reassignment of species within the genera *Aquixalus*, *Chiromantis*, *Rhacophorus*, and *Philautus*. *Molecular Phylogenetics and Evolution* 48: 302–312. doi: 10.1016/j.ympev.2008.03.023
- Li JT, Che J, Murphy RW, Zhao H, Zhao EM, Rao DQ, Zhang YP (2009) New insights to the molecular phylogenetics and generic assessment in the Rhacophoridae (Amphibia: Anura) based on five nuclear and three mitochondrial genes, with comments on the evolution of reproduction. *Molecular Phylogenetics and Evolution* 53: 509–522. doi: 10.1016/j.ympev.2009.06.023
- Liang MF, Huang CH, Kam YC (2002) Effects of intermittent feeding on the growth of oophagous (*Chirixalus eiffingeri*) and herbivorous (*Chirixalus idiotocous*) tadpoles from Taiwan. *Journal of Zoological Research London* 256: 207–213. doi: 10.1017/S0952836902000249
- Liang YS, Wang CS (1963) A new tree frog, *Rhacophorus taipeianus* (Anura, Rhacophoridae) from Taiwan (Formosa). *Quarterly journal of the Taiwan Museum* 16: 185–202.
- Lue KY, Tu MC, Shang G (1999) *Atlas of Taiwan Amphibians and Reptiles*. Nature Press, Taipei, 343 pp. [In Chinese]
- Maeda M, Matsui M (1989) *Frogs and Toads of Japan*. Bun-Ichi Sōgō Shuppan Co., Ltd., Tokyo, 206 pp.
- Manamendra-Arachchi K, Pethiyagoda R (2005) The Sri Lankan shrub-frogs of the genus *Philautus* Gistel, 1848 (Ranidae: Rhacophorinae), with description of 27 new species. *The Raffles Bulletin of Zoology* 12: 163–303.
- Mayr EW (1942) *Systematics and the Origin of Species*. Columbia University Press, 334 pp.

- Mayr EW, Ashlock PD (1991) Principles of systematic zoology. McGraw-Hill Book, New York, 416 pp.
- Nguyen TT, Matsui M, Duc HM (2014a) A New Tree Frog of the Genus *Kurixalus* (Anura: Rhacophoridae) from Vietnam. *Current Herpetology* 33(2): 101–111. doi: 10.5358/hsj.33.101
- Nguyen TT, Matsui M, Eto K (2014b) A new cryptic tree frog species allied to *Kurixalus banaensis* (Anura: Rhacophoridae) from Vietnam. *Russian Journal of Herpetology* 21: 295–302.
- Nylander JAA (2004) MrModeltest v2. Program distributed by the author. Evolutionary Biology Centre, Uppsala University.
- Palumbi SR (1996) What can molecular genetics contribute to marine biogeography. An urchin's tale. *Journal of Experimental Marine Biology and Ecology* 203: 75–92. doi: 10.1016/0022-0981(96)02571-3
- Ronquist F, Huelsenbeck JP (2003) MRBAYES 3: Bayesian phylogenetic inference under mixed models. *Bioinformatics* 19(3): 1572–1574. doi: 10.1093/sysbio/sys029
- Rozas J, Rozas R (1999) DnaSP version 3: an integrated program for molecular population genetics and molecular evolution analysis. *Bioinformatics* 15: 174–175. doi: 10.1093/bioinformatics/15.2.174
- Saito N, Nei M (1987) The neighbor-joining method: a new method for reconstructing phylogenetic trees. *Molecular Biology and Evolution* 4: 406–425.
- Savage JM, Heyer WR (1997) Digital webbing formulae for anurans: a refinement. *Herpetological Review* 28(3): 131.
- Shang G (2010) A new environmental dilemma of Taiwan: The Spot-legged Tree frog. *The Nature Magazine* 108: 66–69. [In Chinese]
- Swofford DL (2002) PAUP*, Phylogenetic Analysis Using Parsimony (*and other methods). Vers. 4. Sinauer Associates, Sunderland.
- Tamura K, Stecher G, Peterson D, Filipski A, Kumar S (2013) MEGA6: Molecular Evolutionary Genetics Analysis Version 6.0. *Molecular Biology and Evolution* 30: 2725–2729. doi: 10.1093/molbev/mst197
- Thompson JD, Higgins DG, Gibson PJ (1994) CLUSTAL W: improving the sensitivity of progressive multiple sequence alignment through sequencing weighting, position-specific gap penalties and weight matrix choice. *Nucleic Acids Research* 22: 4673–4680. doi: 10.1093/nar/22.22.4673
- Truett GE, Heeger P, Mynatt RL, Truett AA, Walker JA, Warman ML (2000) Preparation of PCR–Quality Mouse Genomic DNA with Hot Sodium Hydroxide and Tris (HotSHOT). *Biotechniques* 29: 52–54.
- Tschudi Jv (1838) Classification der Batrachier mit Berücksichtigung der fossilen Thiere dieser Abtheilung der Reptilien, 34, 75.
- Ueda H (1986) Reproduction of *Chirixalus eiffingeri* (Boettger). *Scientific Report of the Laboratory for Amphibian Biology, Hiroshima University* 8: 109–116.
- Vences M, Thomas M, Bonett RM, Vieites DR (2005) Deciphering amphibian diversity through DNA barcoding: chances and challenges. *Philosophical Transactions of the Royal Society, B: Biological Sciences* 360: 1859–1868. doi: 10.1098/rstb.2005.1717

- Vences M, Thomas M, van der Meijden A, Chiari Y, Vieites DR (2005) Comparative performances of the 16S rRNA gene in DNA barcoding of amphibians. *Frontiers in Zoology* 2: 5. doi: 10.1186/1742-9994-2-5
- Wang CS (1962) The reptiles of Botel-Tobago. *Quarterly Journal of the Taiwan Museum* 15: 141–191.
- Wells KD (2007) *The Ecology and Behavior of Amphibians*. The University of Chicago Press, Chicago, USA, 1148 pp. doi: 10.7208/chicago/9780226893334.001.0001
- Wilkinson JA, Drewes RC, Tatum OL (2002) A molecular phylogenetic analysis of the family Rhacophoridae with an emphasis on the Asian and African genera. *Molecular Phylogenetics and Evolution* 24: 265–273. doi: 10.1016/S1055-7903(02)00212-9
- Wright S (1965) The interpretation of population structure by F-statistics with special regard to systems of mating. *Evolution* 19: 395–420. doi: 10.2307/2406450
- Yu GH, Zhang MW, Yang JX (2013) Molecular evidence for taxonomy of *Rhacophorus appendicularis* and *Kurixalus* species from northern Vietnam, with comments on systematics of *Kurixalus* and *Gracixalus* (Anura: Rhacophoridae). *Biochemical Systematics and Ecology* 47: 31–37. doi: 10.1016/j.bse.2012.09.023

Appendix

Additional specimens examined

Buergeria japonica: NCHUZOO: 4021, 4825, 4826 (Taiwan). ***B. robusta***: NCHUZOO 4025, 4027, 4831 (Taiwan). ***Kurixalus eiffingeri***: NTU 927–28, 931–32, 939, 1052, 1054–56, 1649 (Shitou, Nantou); 1058–67, 1645–46, 1769 (Wulai, Taipei); NCHUZOO: 2502–03, 2508, 2509(C/S), 2514–15, 2517–19, 2523–24, 2525(C/S), 2526–27, 2535, 2536(C/S), 2537, 2538(C/S), 2539–40, 2545–47, 2550–51, 2829, 2831, 4018(C/S), 11320, 11436–40 (Shindian, Taipei); 11333 (Shitou, Nantou). ***K. idiootocus***: NTU 929, 1005–09, 1033, 1035–37, 1038–42 (Shiding, Taipei); 1045 (Suao, Yilan); 1010 (holotype of *Chirixalus idiootocus*), 1011, 1013–29, 1657, 1695–96, (Yanminshan, Taipei); 1658 (Shindien, Taipei); 1708–09 (Juchi, Chiayi); 1770 (Wulai, Taipei); NCHUZOO 1010, 2780, 2782, 2784, 2785(C/S), 2787–88, 2792, 2795, 2796(C/S), 2805, 2845, 2847, 2954, 2956(C/S), 2959–63, 3709, 3711(C/S), 4304(C/S), 4990, 4993, 4995(C/S), 7402. ***K. wangi* sp. n.**: NTU 1043–1044, 1046, 1647–48 (Manjo, Pingtung County).

Supporting information

Table S1. Morphometric characteristics and the abbreviations in this study.

Abbreviation	Morphometric characteristic
SVL	snout-vent length
HW	head width
HL	head length
IN	internarial distance
EN	eye-narial distance
ED	horizontal eye diameter
DFE	distance between the anterior margins of eyes
DBE	distance between the posterior margins of eyes
UEW	upper eyelid width
IO	interorbital distance
TAD	tympanic annulus diameter
AXI	between posterior margins of the upper arm
AGD	axilla-groin distance
UAW	forearm length
PAL	manus length
F1L	length of first finger from base of palmar tubercle to tip of third finger disc
D3L	width of third finger disc
FEL	femur length
TBL	tibia length
TSL	tarsus length
FOL	foot length from proximal margin of inner metatarsal tubercle to tip of fourth toe
TL	first toe length
IML	inner metatarsal tubercle length
T4D	disc width of fourth toe

Table S2. DNA sequences used in this study and their GenBank accession numbers.

Species	Sampled locality	Gene sequences	No. of GenBank	Voucher specimen
<i>K. eiffingeri</i>	Ryukyu Islands, Japan	mtDNA CO 1	DQ468681	NTUMA 2427
		mtDNA 16S	DQ468673	
<i>K. eiffingeri</i>	Wulai, Taipei, northern Taiwan	mtDNA CO 1	DQ468680	NCHUZOOL 11320
		mtDNA 16S	DQ468672	
<i>K. eiffingeri</i>	Xitou, Nantou, central Taiwan	mtDNA CO 1	DQ468678	NCHUZOOL 11333
		mtDNA 16S	DQ468670	
<i>K. berylliniris</i> sp. n.	Beinan, Taitung, eastern Taiwan	mtDNA CO 1	DQ468677	ASIZAM 00053
		mtDNA 16S	DQ468669	
<i>K. wangi</i> sp. n.	Shouka, Pintung, southern Taiwan	mtDNA CO 1	DQ468679	ASIZAM 00055
		mtDNA 16S	DQ468671	
<i>K. idiootocus</i>	Wulai, Taipei, northern Taiwan	mtDNA CO 1	DQ468682	NA
		mtDNA 16S	DQ468674	
<i>Feihyla palpebralis</i>	Yunnan, China	mtDNA CO 1	DQ468683	NA
		mtDNA 16S	DQ468675	
<i>Rhacophorus moltrechti</i>	Antong, Hualien, eastern Taiwan	mtDNA CO 1	DQ468684	NA
		mtDNA 16S	DQ468676	

Table S3. Genetic distances among *Kurixalus* species and two outgroup taxa in CO 1 gene (above diagonal) and 16S rRNA gene (below diagonal). Numbers on top row refer to species shown on the left column. Genetic distances are shown as percentage.

Species	1	2	3	4	5	6	7	8
1. <i>K. eiffingeri</i> (JP)	–	6.30	9.13	11.23	10.85	15.02	21.36	24.99
2. <i>K. eiffingeri</i> (NTW)	0.92	–	9.48	9.92	10.47	16.21	20.51	25.94
3. <i>K. eiffingeri</i> (CTW)	3.41	3.21	–	10.84	13.12	14.20	20.51	24.33
4. <i>K. berylliniris</i> sp. n.	3.19	3.00	4.77	–	10.65	14.36	19.21	23.89
5. <i>K. wangi</i> sp. n.	3.80	3.60	4.19	3.98	–	14.16	21.17	25.06
6. <i>K. idiootocus</i>	5.97	5.97	5.76	6.15	6.59	–	18.18	23.06
7. <i>F. palpebralis</i>	10.68	10.90	11.56	11.34	11.13	11.61	–	23.79
8. <i>R. moltrechti</i>	14.04	13.12	14.74	14.48	14.49	14.94	15.40	–

Abbreviations: *K.* *Kurixalus*; *F.* *Feihyla*; *R.* *Rhacophorus*; JP: Ryukyu Islands of Japan; NTW: northern Taiwan; CTW: central Taiwan.

Table S4. Comparisons of measurements and ratios of tadpoles of three oophagus *Kurixalus* species from Taiwan (ANOVA significant level, *: $0.01 < p < 0.05$; **: $p < 0.01$).

species	<i>berylliniris</i>	<i>wangi</i>	<i>eiffingeri</i>	ANOVA
measurements	n=5	n=10	n=8	
TL	24.89 ± 5.21	18.60 ± 2.44	16.75 ± 2.85	**
BL	7.92 ± 1.72	6.68 ± 1.01	5.54 ± 1.01	**
CL	16.97 ± 3.51	11.92 ± 1.79	11.22 ± 1.87	*
TH	4.84 ± 1.10	4.04 ± 0.84	2.94 ± 0.66	**
TM	1.99 ± 0.39	1.86 ± 0.38	1.63 ± 0.31	
NA	1.99 ± 0.21	1.59 ± 0.23	1.30 ± 0.20	**
IN	1.89 ± 0.51	1.59 ± 0.27	1.38 ± 0.29	*
MW	1.94 ± 0.71	1.57 ± 0.38	1.37 ± 0.28	
BL / TL	0.32 ± 0.01	0.36 ± 0.04	0.33 ± 0.01	*
CL / TL	0.68 ± 0.01	0.64 ± 0.04	0.67 ± 0.01	*
TH / TL	0.19 ± 0.01	0.22 ± 0.04	0.17 ± 0.01	*
TM / TL	0.08 ± 0.00	0.10 ± 0.02	0.10 ± 0.00	*
NA / TL	0.08 ± 0.01	0.09 ± 0.04	0.08 ± 0.00	
IN / TL	0.08 ± 0.01	0.09 ± 0.01	0.08 ± 0.00	
MW / TL	0.08 ± 0.01	0.08 ± 0.01	0.08 ± 0.01	
TH / CL	0.28 ± 0.02	0.34 ± 0.08	0.26 ± 0.02	*
TM / MW	1.08 ± 0.21	1.20 ± 0.11	1.19 ± 0.11	
IN / NA	0.94 ± 0.16	0.99 ± 0.05	1.06 ± 0.08	
CL / BL	2.15 ± 0.10	1.81 ± 0.27	2.03 ± 0.11	**
TH / TM	2.42 ± 0.19	2.18 ± 0.18	1.80 ± 0.09	**

Table S5. Body size variation (SVL) in female and male *Kurixalus* species from Taiwan (mean \pm standard deviation). (**: significant level < 0.01).

Species	female	male	t-test
<i>K. berylliniris</i> sp. n.	37.8 \pm 7.1	34.4 \pm 4.1	0.178
	n = 7	n = 13	
<i>K. eiffingeri</i>	33.7 \pm 2.9	31.1 \pm 2.3	**
	n = 15	n = 20	
<i>K. wangi</i> sp. n.	34.3 \pm 1.8	30.0 \pm 0.9	**
	n = 8	n = 17	
<i>K. idiotocus</i>	36.3 \pm 2.5	26.9 \pm 1.4	**
	n = 3	n = 21	
ANOVA	F _{3,29} = 1.964	F _{3,67} = 30.227**	

Table S6. Analysis of covariance of morphometric characteristics of males and females among four *Kurixalus* species.

measurement	<i>berylliniris</i> sp. n.	<i>eiffingeri</i>	<i>idiotocus</i>	<i>wangi</i> sp. n.	equal slope	equal mean
male						
HW	10.59	10.83	10.56	11.21	**	0.001
HL	8.16	8.04	8.21	7.96	**	
IN	3.29	3.41	3.20	3.31	**	0.028
EN	3.08	2.91	2.98	3.21	**	0.004
ED	3.95	4.10	4.27	4.11	**	
UEW	2.82	3.12	3.27	3.03	**	0.019
DFE	6.28	6.23	6.25	6.38	**	
DBE	9.55	9.76	9.67	9.99	**	0.046
IO	3.69	3.81	3.95	4.00	**	0.005
TAD	1.93	1.33	1.76	1.87	**	
AXI	9.25	9.72	9.82	9.93	**	
AGD	15.47	14.48	14.91	13.42	**	0.000
UAW	6.12	5.40	5.70	5.60	**	0.000
PAL	9.56	10.10	9.21	9.06	**	0.000
FIL	4.95	5.06	4.34	4.60	**	0.000
D3L	1.30	1.86	1.78	1.56	**	0.000
FEL	14.50	14.00	13.74	14.64	**	0.010
TBL	15.51	14.59	13.99	14.62	**	0.002
TSL	7.37	6.94	6.78	6.93	**	0.028
FOL	13.76	13.66	12.94	12.48	**	0.000
TL	5.00	5.00	4.43	4.29	**	0.000
T4D	0.99	1.51	1.32	1.33	**	0.000
IML	1.27	1.36	1.39	1.23	**	
female						
HW	12.20	12.22	12.16	12.67	**	0.030
HL	9.17	9.08	8.88	9.37	**	
IN	3.77	3.75	3.73	3.74	**	
EN	3.53	3.31	3.25	3.48	**	

measurement	<i>berylliniris</i> sp. n.	<i>eiffingeri</i>	<i>idiotoocus</i>	<i>wangi</i> sp. n.	equal slope	equal mean
ED	4.25	4.56	4.05	4.52	**	
UEW	3.28	3.46	3.48	3.33	**	
DFE	7.02	7.02	6.93	7.02	**	
DBE	10.99	10.97	10.61	11.17	**	
IO	4.19	4.27	4.57	4.30	**	
TAD	2.20	2.23	2.21	2.09	**	
AXI	11.27	11.43	11.57	11.22	**	
AGD	16.49	16.94	17.55	15.36	**	
UAW	6.65	6.36	6.89	6.31	**	
PAL	11.47	11.35	10.22	9.71	**	0.000
F1L	5.52	5.52	5.08	4.92	**	0.002
D3L	1.62	2.04	1.94	1.72	**	0.005
FEL	16.51	15.60	15.93	16.53	**	0.025
TBL	17.21	16.66	16.27	16.56	**	
TSL	8.01	7.74	8.06	7.83	**	
FOL	15.83	15.35	14.93	14.08	**	0.000
TL	5.85	5.79	5.25	4.94	**	0.001
T4D	1.17	1.65	1.81	1.46	**	0.001
IML	1.48	1.49	1.60	1.43	**	

Means adjusted to SVL. * significant difference at 0.95 level, ** significant differences at the 0.99 level, exact probabilities are given only for slopes that are unequal. Sample sizes listed in Table S5.

Table S7. Factor loadings of the first three principal components of 18 size-adjusted morphometric characteristics of males of four *Kurixalus* species. Absolute values of loadings greater than 0.50 in boldface.

Character	PC 1	PC 2	PC 3
Eigenvalue	4.316	3.061	2.308
% variation	23.98	17	12.82
HW	0.609	-0.299	0.081
IN	0.615	0.147	-0.237
ED	0.590	-0.512	0.041
UEW	0.581	-0.471	-0.144
DFE	0.742	-0.292	0.198
DBE	0.739	-0.424	0.054
UEW	0.449	-0.273	0.245
AXI	0.107	0.014	-0.354
AGD	-0.156	0.162	-0.123
UAW	0.112	0.089	0.682
PAL	0.418	0.604	-0.520
F1L	0.293	0.698	-0.323
FEL	0.431	0.413	0.479
TBL	0.453	0.584	0.527
TSL	0.300	0.507	0.502
FOL	0.413	0.686	-0.150
T4D	0.533	-0.018	-0.564
IML	0.582	0.015	-0.206

Table S8. Genetic variation of three *Kurixalus* species from Taiwan according to mtDNA *COI* gene partial sequence.

	N	Number of haplotypes	Haplotype diversity (Hd)	Nucleotide diversity (Pi)
<i>K. berylliniris</i> sp. n.	55	9	0.82088	0.02271
<i>K. wangi</i> sp. n.	69	11	0.85209	0.00443
<i>K. eiffingeri</i>	219	53	0.94600	0.05524

Table S9. *Fst* (above diagonal) and *Nm* (below diagonal) between three *Kurixalus* species from Taiwan.

	<i>K. berylliniris</i> sp. n.	<i>K. wangi</i> sp. n.	<i>K. eiffingeri</i>
<i>K. berylliniris</i> sp. n.	--	0.85922	0.60226
<i>K. wangi</i> sp. n.	0.04	--	0.71956
<i>K. eiffingeri</i>	0.17	0.10	--

$F_{st} = 1 / (4Nm+1)$ whereas $Nm = ((1/F_{st})-1)/4$.

